Endogenous opioid modulation of fear learning circuits in the amygdala

Roger Wang

Sydney Pharmacy School, Faculty of Medicine and Health

The University of Sydney

A thesis submitted to fulfil the requirements for the degree of Doctor of Philosophy

March 2025

Acknowledgements

First and foremost, thank you Elena, you have been an amazing supervisor and an incredible mentor. Throughout the years, your support and guidance have been invaluable, and I wouldn't have been able to do this without your help. Your mentorship has helped me overcome many challenges and you've helped me foster some confidence in the work I do. Thank you for the patience you have given me and the time investment over these years. Your influence has been transformative and for that I am truly grateful that you were my supervisor.

To those from the lab both past and present, thank you all. Especially Sahil and Gabi for teaching me how to patch during those early days in the lab. Special thanks to Muskaan for doing most my surgeries, truly a life saver. Also special thanks to Chow, Bryony, Rakulan, Sophia, Charlie and Neda for being great company in and around the lab.

To my friends and family, thank you for supporting me throughout the years. Thank you for all the love and encouragement to keep me going. Especially to my family and in-laws your support has helped me be able to finish this thesis.

Lastly, to Samira. You are my biggest supporter and the foundation that has made all of this possible. Your unwavering belief in me, especially during these past few hard weeks, has given me the strength to persevere. Thank you for standing beside me through every step of this journey, your love and encouragement have meant more than words can express.

Statement of originality

Unless specifically noted, experiments in this thesis were designed by Professor Elena Bagley and I.

Muskaan Kalra (University of Sydney) performed the stereotaxic surgeries for experiments in chapters 3 and chapter 4

The experiment for chapter 3, Figure 3.26 was performed by Dr Joanna Yau (UNSW) and Professor Gavan McNally (UNSW).

Professor Yulong Li (Peking University) provided custom code used in chapters 3 and 4.

Professor Michael Bruchas (University of Washington) provided viral sensors used in chapter 3.

Professor Greg Neely (University of Sydney) provided viral CRISPR constructs used in chapter 3.

The Children's Medical Research Institute (CMRI) packaged viral constructs to use in chapter 3.

Dr Gabrielle Gregoriou contributed to the experiments in chapter 5

This thesis was written by myself and reviewed by Professor Elena Bagley.

This research was supported by the award of the Dorothy Blanche Chandler Scholarship

I certify that this thesis comprises only of original work towards the degree of Doctor of Philosophy, except where indicated above. Due acknowledgement has been made in text to all other material used.

I declare that generative AI has not been used in this thesis

Roger Wang

10/03/2025

Abstract

The amygdala plays a central role in emotional learning, particularly fear conditioning, where neutral stimuli are associated with threatening events. Endogenous opioids have been implicated as fear-inhibiting neuromodulators, but their specific mechanisms of action within amygdala circuits remain poorly characterised. This thesis investigates the role of endogenous opioid signalling in fear related circuits of the amygdala, examining how sensory inputs can trigger endogenous opioid release and how these opioids potentially regulate fear learning through multiple mechanisms.

Using a combination of electrophysiology, fibre photometry, and fluorescent biosensors, I demonstrated that auditory thalamic inputs form strong, functional glutamatergic synapses onto neurons in the amygdalo-striatal transition zone, triggering enkephalin release. This enkephalin acts at multiple sites within the fear circuit, including inhibiting glutamate transmission, suppressing dopamine release and modulating synaptic plasticity under specific conditions. Furthermore*, in vivo* recordings during fear conditioning revealed dynamic endogenous opioid release patterns, initially occurring in response to shock before gradually shifting to the conditioned stimulus as learning progressed.

These findings establish a circuit mechanism by which sensory inputs trigger opioid release that regulates fear learning through multiple pathways. This work provides a deeper understanding of how neuromodulator systems can potentially fine-tune emotional learning, which may inform future approaches for treating disorders characterised by dysregulated fear responses.

Table of Contents

List of Figures

List of Tables

Abbreviations

AAV	Adeno-associated virus
ACE	Angiotensin converting enzyme
Adora2a	Adenosine A2A receptor
aITC	Apical Intercalated Cells
AMPA	Alpha-amino-3-hydroxy-5-methyl-4-isooxazole-propionic acid
ANOVA	Analysis of variance
APN	Aminopeptidase N
ASt	Amygdalo-striatal transition zone
BLA	Basolateral amygdala
cAMP	Cyclic adenosine monophosphate
CeL	Central lateral amygdala
CeM	Central medial amygdala
ChR2	Channelrhodopsin 2
cpGFP	Circularly permuted green fluorescent protein
CRSPR	Clustered regularly interspaced short palindromic repeats
CS	Conditioned stimulus
EC	External capsule
EC50	Half maximal excitatory concentration
D1	Dopamine D1 receptor
D2	Dopamine D2 receptor
D3	Dopamine D3 receptor
D4	Dopamine D4 receptor
D5	Dopamine D5 receptor
DOR	δ-opioid receptor
eEPSC	evoked excitatory post synaptic current
GABA	γ-Aminobutyric acid
$GABA_A$	$GABA_A$ receptor
GFP	Green fluorescent protein
GIRK	G protein-gated inwardly rectifying potassium
GPCR	G-protein coupled receptor
HPLC	High performance liquid chromatography
IC	Internal capsule
IM	Main island intercalated cells
ITC	Intercalated cell cluster
KOR	κ-opioid receptor
LA	Lateral amygdala
lITC	Lateral intercalated cells
LTP	Long term potentiation
MGD	Medial geniculate body, dorsal
MGN	Medial geniculate nucleus
MGV	Medial geniculate body, ventral
mITC	Medial intercalated cells
MOR	μ-opioid receptor
MSN	Medium spiny neuron

NAc	Nucleus Accumbens
NEP	Neutral endopeptidase
NMDA	N-methyl-D-aspartate
oEPSC	Optical evoked excitatory post synaptic current
PBS	Phosphate buffered saline
PFA	Paraformaldehyde
PENK	Proenkephalin
PET	Positron electron tomography
PKA	Protein kinase A
PiL	Posterior intralaminar nucleus
ppENK	Preproenkephalin
PPR	Paired pulse ratio
SG	Suprageniculate nucleus
SNr	Substantia nigra
STDP	Spike timing dependent plasticity
τ	Membrane time constant
TH	Tyrosine hydroxylase
US	Unconditioned stimulus
VGlut2	Vesicular glutamate transporter 2
VTA	Ventral tegmental area

Chapter 1
Introduction

A. Fear and reward learning

Our understanding of the world is continuously reshaped by the diverse experiences we encounter throughout our lives. This dynamic process is a fundamental aspect of our adaptive mechanisms aimed at enhancing our survival. By encoding information about predictors of dangers and rewards, we better equip ourselves to guide our future actions. For instance, remembering the location of our favourite coffee shop helps us find it again, just as recalling which hiking trails were too dangerous helps us avoid them in the future. This act of avoidance, often accompanied by an innate feeling of negativity is what we know as fear. Fear is among the most extensively studied emotions, with classical Pavlovian fear conditioning being the predominant methods used to study it. This technique typically involves pairing a biologically neutral conditioned stimulus (CS), such as a tone, with an aversive unconditioned stimulus (US), typically a mild electric shock (Pavlov, 1927; Rescorla, 1973). As a result, the CS begins to elicit specific behavioural responses, most notably freezing behaviours but is also often accompanied by physiological adjustments controlled by the autonomic nervous system, including changes in heart rate, blood pressure and respiration (Bouton & Bolles, 1980; J. E. LeDoux, 2014). Fear conditioning operates by engaging a fundamental process known as associative learning, which is a central feature of nervous systems circuits in many animals and potentially extends to even single-cell organisms (Fanselow & Wassum, 2015; J. E. LeDoux, 2014). The process of associative learning extends beyond fear to encompass the acquisition of knowledge concerning rewards, as associations between cues and rewards or aversion takes place within the relevant neurocircuitry (J. E.

LeDoux, 2014). Through this process the US dynamically modifies the efficacy of the CS in activating specific circuits responsible for triggering the defensive responses in anticipation of potential harm or seeking responses in anticipation of potential rewards (DiFazio, Fanselow, & Sharpe, 2022; J. E. LeDoux, 2014). Fear conditioning is therefore a fundamental model for understanding the cellular mechanisms of learning. Its value can also be seen in several key characteristics. Firstly, fear is rapidly acquired (J. LeDoux, 2003), typically requiring only a few trials. Secondly, fear is evolutionarily conserved across both vertebrate and invertebrate species (Fanselow & Wassum, 2015) and finally, fear is reproducible in human subjects (Woodson, Farb, & Ledoux, 2000). The simplicity of this paradigm, where a neutral stimulus acquired emotional significant through pairing with an aversive outcome, provides a powerful tool for investigating the cellular basis of learning and memory.

ii. Maladaptation's in fear and reward learning

Specificity in learning plays a vital role in our survival within a constantly changing environment, ensuring that acquired knowledge is applied cautiously when needed. However, dysfunctions in learning mechanisms can lead to undesirable behaviours (Dunsmoor & Paz, 2015; Dymond, Dunsmoor, Vervliet, Roche, & Hermans, 2015). Since naturally occurring stimuli may present themselves across various different encounters, the ability to generalise learning across diverse stimuli and situations becomes indispensable. Equally crucial is the capacity to discern between different stimuli and different events, thereby mitigating overgeneralisation and

preventing manifestations of inappropriate behavioural responses. This delicate equilibrium between generalisation and specificity is vital for any organisms engaged in learning. Understanding how humans and other species achieve this balance has been a central focus for research for many years (Hull, 1943). This balance is particularly critical in the context of fear learning. Overgeneralisation of fear can manifest across various mental health disorders, including specific phobias, obsessive-compulsive disorders, generalised anxiety and post-traumatic stress disorder (DiFazio et al., 2022; Dunsmoor & Paz, 2015). Within these conditions, individuals often exhibit defensive responses that extend beyond their initial fear triggers, resulting in a diverse array of inappropriate reactions (Dunsmoor & Paz, 2015; Hsu et al., 2015). For instance, a fear of public speaking may escalate to encompass all social interaction (social anxiety disorder), whilst exposure to certain sounds can precipitate anxiety, impacting one's ability to engage in conversations or attend any form of social gathering (Dunsmoor & Paz, 2015; Dymond et al., 2015). Thus, understanding the intricate interplay between generalisation and specificity in fear learning is paramount for developing effective interventions and treatment approaches tailored to the nuanced mechanisms underlying fear dysregulation in mental health disorders. This thesis will therefore delve into the potential cellular mechanisms that govern this delicate balance and explore how different neuromodulator systems may control fear learning.

B. The neurocircuitry of fear and reward

Understanding the neurocircuitry of fear and reward involves examining the intricate processes through which the brain encodes, integrates, and expresses responses to different stimuli. Since Pavlov's early work, it has been well established that a neutral stimulus can acquire affective properties through repeated pairing with a biologically significant event, leading to a conditioned response (Pavlov, 1927). This highlights how specific neural circuits orchestrate both physiological and behavioural responses. The formation of fear memories involves complex neural mechanisms that extend beyond immediate defensive responses to aversive stimuli. This is evidenced by the temporal dynamics of fear expression, where the greatest level of freezing is observed when animals are tested 24-hours post conditioning rather than immediately after training (Bolles & Fanselow, 1980). Additionally, freezing behaviours are more pronounced when rodents are placed in the same chamber where they were initially conditioned compared to a different context (Bolles & Fanselow, 1980). These observations indicate that fear memory formation occurs in specific neural circuits that encode and store associations between neutral stimuli and aversive events, rather than being a direct response to the aversive stimulus itself.

i. The amygdala in fear learning

Overwhelming evidence from anatomical, functional and lesion studies in rodents and humans has established the amygdala as a critical structure in fear learning and memory (Cheng, Knight, Smith, Stein, & Helmstetter, 2003;

J. LeDoux, 2003). Firstly, early work from several laboratories has provided a clear depiction of the neuroanatomy of conditioned fear (Davis, 1992; Fanselow, 1994; J. LeDoux, 2003), highlighting how the transmission of information about the CS and the US to the amygdala, and subsequent control of fear reactions, is mediated through output projections to behavioural and autonomic systems (Beyeler et al., 2016; Janak & Tye, 2015). Secondly, the involvement of the amygdala in fear conditioning has also been established by a series of lesion and electrophysiology experiments (J. LeDoux, 2003). Pre-training neurotoxic lesions of the amygdala attenuates the acquisition of both CS induced and contextual fear conditioning (Cousens & Otto, 1998; Stephen Maren, 1999). Additionally, lesions of the amygdala post-training completely abolish the expression of a conditional fear response (Cousens & Otto, 1998; Stephen Maren, 1999). These fear memory deficits persist even when lesions are made one month after training, demonstrating the amygdala's role in long-term storage of fear memories (S. Maren & Fanselow, 1996). Finally, and perhaps most importantly fear conditioning in humans also relies on the amygdala. Deficits in the perception of emotional meaning of different faces, especially of faces that depict fearful states, occurs in people with damage to their amygdala (Adolphs, Tranel, Damasio, & Damasio, 1995). Damage to the amygdala also impairs people’s auditory cues (Scott et al., 1997). Consistent with this, fear conditioning increases amygdala activity, measured using functional magnetic resonance imaging, and as the person is exposed to the CS and US pairing the CS increasingly activates the amygdala (Cheng et al., 2003). Together this evidence strongly indicates the central role of the

amygdala in fear conditioning, and importantly, that the amygdala's role in fear learning is conserved across species, including both rodents and humans.

ii. Anatomical structure and information flow in the amygdala

The amygdala comprises approximately 13 distinct regions (Fig 1.1) (Duvarci & Pare, 2014; J. LeDoux, 2003; Sah, Faber, Lopez De Armentia, & Power, 2003), with recent single-cell RNA sequencing revealing 130 distinct neuronal cell types (Hochgerner et al., 2023). In general, the lateral amygdala (LA) functions as the primary entry point for sensory inputs into the amygdala (Duvarci & Pare, 2014; J. LeDoux, 2003). It receives direct sensory inputs from the thalamic pathways (J. E. LeDoux, Farb, & Ruggiero, 1990) and cortical pathways (Quirk, Armony, & LeDoux, 1997). Sensory information is then transferred to the basolateral amygdala (BLA) (Y. Sun, Gooch, & Sah, 2020), which projects to other amygdala nuclei and various brain regions to coordinate behaviour (Beyeler et al., 2016). The central medial amygdala (CeM) in particular, serves as the principal source of amygdala projections to brainstem structures that mediate fear responses (Duvarci & Pare, 2014; J. LeDoux, 2003). However, not all sensory inputs results in fear activation. This selective response is due, in part, to the flexible gating of information transfer from the LA to the CeM, via the BLA, which varies depending on the specific pattern of environmental cues confronting the organism (Paré, Royer, Smith, & Lang, 2003). This delicate maintenance of specific learning within the amygdala structures may be facilitated by the GABAergic inhibitions of the BLA by the intercalated neurons (ITC) that surround the amygdala complex

(Fig 1.1). This complex information processing within the amygdala structures suggests a finely tuned equilibrium conducive to specific learning.

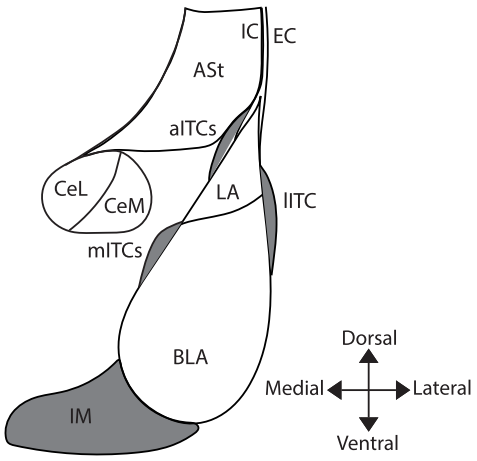

Figure 1.1. Amygdala subnuclei and structure. Cartoon depicting coronal drawing of amygdala on right-hemisphere of the brain. Grey shaded area represent intercalated cell groups surrounding the amygdala. apITCs – apical intercalated cells ASt – amygdalo-striatal transition zone, BLA – basolateral amygdala nucleus, CeL – central lateral amygdala nucleus, CeM – central medial amygdala nucleus, EC – external capsule, IC – internal capsule, lITCs – lateral intercalated cells, mITCs – medial intercalated cells

iii. Auditory information circuits mediating fear learning

Given that the LA integrates and associates the neutral auditory information with the aversive information during learning (Blair, Sotres-Bayon, Moita, & Ledoux, 2005), it becomes crucial to identify the circuits transmitting these signals and the nature of the information from these pathways. Multiple brain regions contribute to this process, with conditioned sensory information such as auditory tones arriving via sensory thalamic nuclei and cortical pathways (Janak & Tye, 2015; Romanski, Clugnet, Bordi, & LeDoux, 1993), while unconditioned aversive and noxious information can reach the LA through various routes including the posterior thalamus, periaqueductal gray and parabrachial nucleus (Basbaum & Fields, 1984; Jean ‐ Franiçois Bernard,

Dallel, Raboisson, Villanueva, & Bars, 1995; Lanuza, Moncho-Bogani, & Ledoux, 2008)

Two major sources of auditory information that participate in fear learning are the auditory thalamus and the auditory cortex (Romanski & LeDoux, 1992). Anatomical tracing studies has found that auditory thalamic regions, including the medial geniculate nuclei (MGN) and posterior intralaminar nuclei (PiL) provide strong inputs to the amygdala (Fig 1.2) (Doron & Ledoux, 1999; Linke, Braune, & Schwegler, 2000; Woodson et al., 2000) and damage to the LA interferes with fear conditioning to an auditory CS (J. LeDoux, 2003).

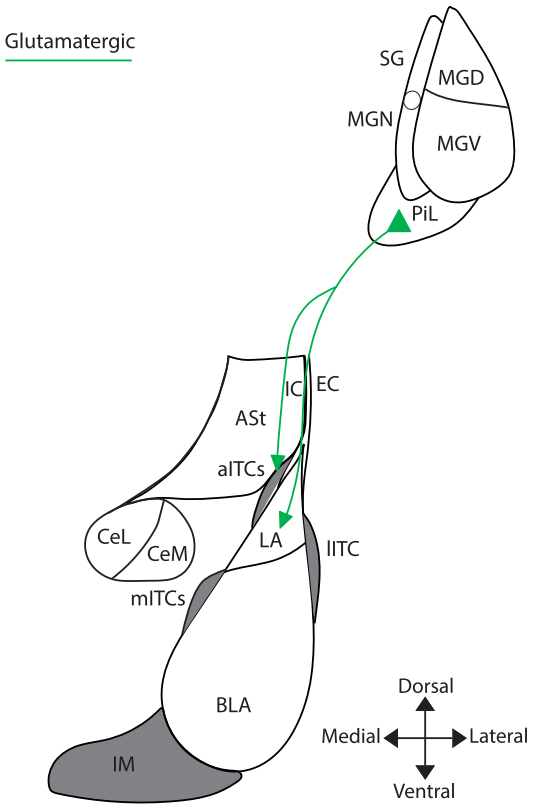

Figure 1.2. The subnuclei of the auditory thalamus send projections to the amygdalo-striatal transition zone, apical intercalated cells and LA. Cartoon depicting glutamatergic projections from the auditory thalamus to the amygdala**.** apITCs – apical intercalated cells ASt – amygdalo-striatal transition zone, BLA – basolateral amygdala nucleus, CeL – central lateral amygdala nucleus, CeM – central medial amygdala nucleus, EC – external capsule, IC –

internal capsule, lITCs – lateral intercalated cells, MGD – medial geniculate body dorsal, , MGN: medial geniculate nuclei, MGV – medial geniculate body ventral, mITCs – medial intercalated cells, SG – suprageniculate nucleus, PiL – posterior intralaminar thalamic nuclei

Additionally, evidence supporting the importance of the MGN in fear conditioning is provided by studies showing that lesions of auditory thalamic nuclei after learning impairs fear expression (Romanski & LeDoux, 1992). However, the auditory thalamic regions are not the only source of auditory information that is relayed to the amygdala. Strong projections also exist from the auditory cortex to the LA (Kim & Cho, 2017; Romanski & LeDoux, 1992), with optogenetic inhibition of auditory cortex terminals in the LA reducing conditioned fear responses (Kim & Cho, 2017). Although auditory information may enter the LA from both the auditory cortex and the MGN there are several lines of evidence that indicate the MGN-amygdala pathway is more important for fear learning. Firstly, single unit recordings of neurons in the LA, MGN and auditory cortex found that cells in the LA and MGN responds more rapidly to auditory stimulation than cells in the auditory cortex (Quirk et al., 1997), suggesting that the MGN and LA pathways receive direct auditory information for the initial processing of fear learning. Secondly, fear conditioning also increases the proportion of neurons that respond to the tone (Quirk et al., 1997), however, this only occurs in the LA and MGN (Quirk et al., 1997). Increases in tone responding neurons in the auditory cortex only occurs for later responding cells (20-100ms after tone onset) (Quirk et al., 1997). This therefore suggests that the cortical pathways learn more slowly over the conditioning trials than the thalamic pathways, indicating that fear memory formation likely occurs in the LA through MGN pathways. Finally, positron-emission tomography (PET) imaging in human studies during a Pavlovian

conditioning paradigm found that activity in the amygdala correlates with activity in the MGN and not the auditory cortex (Morris et al., 1996). Collectively, these findings establish the MGN-LA pathway as the primary sensory route through which auditory threat information is rapidly processed and encoded, highlighting the critical role of this direct MGN-amygdala circuit in transforming sensory inputs into fear memories.

iv. Aversive information circuits mediating fear learning

Multiple brain regions transmit aversive unconditioned stimulus information to the LA. Lesion studies have revealed pathways for shock information processing, as lesions of the insular cortex nuclei block fear acquisition (Shi & Davis, 1999). Electrophysiological recordings have identified nociceptive specific neurons in the parabrachial nucleus of the brainstem that project to the amygdala (J. F. Bernard & Besson, 1990). Anatomical tracing confirms these connections, showing topographically organised projections from nociceptive regions to specific amygdala subdivisions (J. F. Bernard, Alden, & Besson, 1993). These thalamic, cortical, and brainstem pathways collectively ensure robust transmission of aversive information to the amygdala during fear learning. Importantly, emerging evidence suggests the auditory thalamus may serve as an additional route for unconditioned stimulus information (Weinberger, 2011), providing a unique circuit where both conditioned and unconditioned signals potentially converge before reaching the LA.

While the auditory thalamus is traditionally viewed as a relay for auditory information (Romanski et al., 1993), converging anatomical, physiological, and

functional evidence suggests it also transmits unconditioned somatosensory stimulus information to the LA.

Anatomical tract tracing studies in cats and rats have identified the MGN as a target of spinal cord pathways (Calford & Aitkin, 1983; J. E. Ledoux, Ruggiero, Forest, Stornetta, & Reis, 1987; Massopust, Hauge, Ferneding, Doubek, & Taylor, 1985; Rouiller & de Ribaupierre, 1985). Specifically, the PiL and the MGN receiving a moderate to high level of terminal expression originating from spinal cord nuclei (J. E. Ledoux et al., 1987; Rouiller & de Ribaupierre, 1985).

Single unit recordings provide physiological evidence, demonstrating that, transcutaneous electrical stimulation of the contralateral hind paw strongly activates neurons in the PiL and MGN (Bordi & LeDoux, 1994). A subset of these neurons responds to both auditory and electrical stimulation (Bordi & LeDoux, 1994) indicating that the MGN and PiL may be the first point of convergence of the CS and US. More intriguingly, neurons responding only to electrical stimuli show drastically increased firing rates when presented with combined tone and electrical stimulation (Bordi & LeDoux, 1994) suggesting integrative processing may occur at this level before reaching the LA.

This somatosensory information received by the MGN is relayed to the amygdala. Cells in the MGN and PiL regions that are activated antidromically by amygdala stimulation were identified, with the LA division being most effective at producing these responses (Bordi & LeDoux, 1994). Furthermore, lesions of MGN and PiL reduces C-Fos expression in the amygdala when

rodents were given a footshock, indicating that footshock information received in the LA is being partly transmitted from these regions (Lanuza et al., 2008). Collectively, these findings establish the MGN as a significant relay station that receives unconditioned stimulus information from the spinal cord and transmits it to the LA during fear learning, potentially serving as an integration site for both conditioned and unconditioned stimuli.

v. Synaptic plasticity results from delivery of convergent information to the LA

Long-term potentiation (LTP), initially studied in the hippocampus (Bliss & Lomo, 1973) has been extensively characterised in amygdala pathways as a cellular mechanism underlying fear learning. The molecular cascade involves glutamate binding to AMPA receptors, depolarising the cell and relieving the magnesium block on NMDA receptors (Lüscher & Malenka, 2012). This allows calcium influx through NMDA receptors, triggering intracellular events that lead to gene induction and protein synthesis, stabilising long-term synaptic modifications (Dudai, 1989; Huang & Kandel, 1998).

The LA serves as the primary site for CS-US integration during fear conditioning. Firstly, single-unit recording from the LA cells demonstrate that some neurons response to both the neutral CS and aversive US information (Romanski et al., 1993), with many neurons showing enhanced CS-elicited responses after conditioning (Quirk et al., 1997). More recent work has identified a significant population of LA neurons with increased responsiveness after CS-US pairing (J. A. Taylor et al., 2021), directly

demonstrating plasticity during fear learning. Secondly, LTP is readily induced in the MGN-amygdala pathway following fear conditioning, with multiple studies demonstrating increased neuronal responses to the CS post-training (Clugnet & LeDoux, 1990; Kim & Cho, 2017; Quirk et al., 1997; Rogan, Stäubli, & LeDoux, 1997). This plasticity occurs in both the LA and MGN (J. A. Taylor et al., 2021) suggesting that the thalamic pathways could be contributing to LA plasticity (Weinberger, 2011).

The plasticity of MGN-LA during fear conditioning predominantly involved AMPA receptor trafficking at postsynaptic sites. While NMDA-dependent forms of LTP do exist at this synapse (Li, Phillips, & LeDoux, 1995), fear conditioning particularly engages AMPA receptors insertion. This is evidenced by studies showing that disruption of AMPA receptor insertion attenuated fear learning (Rumpel, LeDoux, Zador, & Malinow, 2005). Additionally, electrophysiological recordings after fear learning reveal increased AMPA/NMDA ratios, indicating larger AMPA-mediated responses and thus indicating additional AMPA receptors at LA synapses (Kim & Cho, 2017). This AMPA-mediated plasticity represents a critical mechanism for encoding fear memories in the MGN-LA pathway.

Plasticity in the amygdala can be regulated through various mechanisms that control the excitability of LA neurons. LTP can be experimentally induced by stimulating the MGN itself (Clugnet & LeDoux, 1990), or the internal capsule which carrying auditory information to the amygdala (Bissière, Humeau, &

Lüthi, 2003). GABAergic inhibition regulates amygdala LTP, with reduced inhibitory transmission facilitating plasticity (Bissière et al., 2003). These regulatory mechanisms underscore the importance of investigating how neuromodulator systems influence synaptic plasticity during fear learning.

While the LA serves as the primary integration site for CS-US associations during fear learning, recent evidence suggests a complementary role for the CeA, where neurons responsive to footshock contribute to LA plasticity through retrograde signalling (Yu et al., 2017). Nevertheless, the extensive body of research demonstrating convergent sensory inputs (Romanski et al., 1993), associative plasticity (Quirk et al., 1997), and AMPAR-mediated LTP in the LA (Rogan et al., 1997), firmly establishes the LA as the critical locus for fear memory formation, with the CeA primarily functioning to translate these memories into appropriate defensive behaviours.

C. The amygdalo-striatal transition zone

The amygdalo-striatal transition zone (ASt), a discrete anatomical region situated between the lateral amygdala and ventral striatum (Fig 1.3), is emerging as a critical integration hub for diverse neuromodulator signals (Riley et al., 2024). However, its exact function in encoding valence and directing behaviour remains unknown. The ASt is often grouped with the tail of the striatum in anatomical and functional studies due to their close proximity, but the functional significance of this anatomical relationship is still unclear. Given the anatomical and functional similarities between the ASt and tail of striatum

(Valverde, Fournié-Zaluski, Roques, & Maldonado, 1996; Y. Wang et al., 2023), they will be considered as a single functional unit throughout this thesis.

i. Connectivity with fear circuits

The ASt is rapidly activated by aversive stimuli, has the neural circuitry necessary for processing sensory information and may be a site where dopamine modulates learned associations. Electrophysiological studies demonstrate that ASt neurons fire action potentials in response to multiple sensory modalities, including auditory, visual, and somatosensory stimuli, with particularly strong responses to aversive stimuli like footshock (Romanski et al., 1993; Uwano, Nishijo, Ono, & Tamura, 1995). These ASt neuronal responses occur rapidly, similar to those in the LA, but faster than responses in the BLA and CeA (Uwano et al., 1995). This rapid sensory processing in the ASt results from its anatomical connections, including dense projections from the MGN (Fig 1.3) (J. E. LeDoux et al., 1990). The similar rapid response timing in both the ASt and LA indicates that sensory information reaches these regions early in the processing pathway and is involved in the initial processing of fear learning.

This information processing may be modulated by dopamine as the ASt receives substantial dopaminergic innervation from midbrain regions, including the substantia nigra (SNr) and ventral tegmental area (VTA) (Fig 1.3) (Jean-Francois Poulin et al., 2018). Functional evidence for active dopaminergic signalling in the ASt comes from studies showing electrical stimulation of the ASt induces local dopamine released measured by fast-scan cyclic voltammetry (Riley et al., 2024) and human PET imaging studies that

demonstrate dopamine release in the ASt during sensorimotor and cognitive tasks (Lappin et al., 2008). This convergence of rapid sensory processing capabilities and dopaminergic modulation suggests that the ASt may function as an integrative hub where dopamine could modulate the sensory inputs and influence associative learning processes. However, the precise dynamics of dopamine signalling during fear-related behaviours and its potential role in modulating sensory associations in the ASt remain to be characterised.

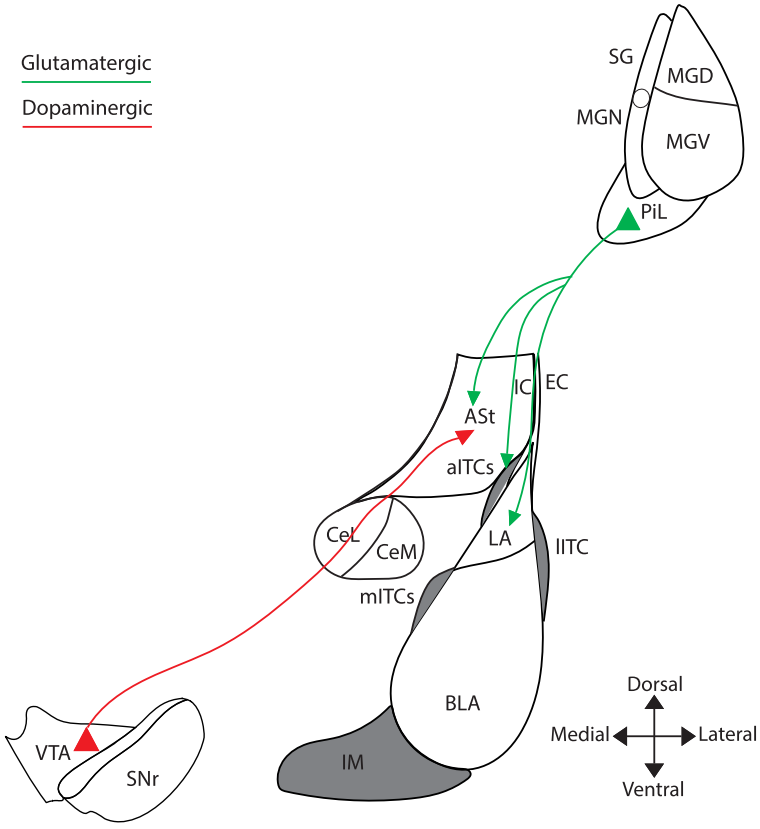

Figure 1.3. Ventral tegmental area and MGN project to the amygdalo-striatal transition zone. Cartoon depicting glutamatergic projections from the PiL subnuclei of the auditory thalamus to the ASt and dopaminergic projections from the VTA to the ASt. apITCs – apical intercalated cells ASt – amygdalo-striatal transition zone, BLA – basolateral amygdala nucleus, CeL – central lateral amygdala nucleus, CeM – central medial amygdala nucleus, EC – external capsule, IC – internal capsule, lITCs – lateral intercalated cells, MGD – medial geniculate body dorsal, , MGN: medial geniculate nuclei, MGV – medial geniculate body ventral, mITCs – medial intercalated cells, SG – suprageniculate nucleus, SNr – substantia nigra, PiL – posterior intralaminar thalamic nuclei, VTA – ventral tegmental area

ii. Neuronal population of the ASt

The ASt exhibits a rich neuropeptide profile characterised by high expression of neuromodulator peptides. In situ hybridisation and immunohistochemistry studies reveal dense expression of opioid peptides mRNA and protein in the ASt (Y. Wang et al., 2023; Jingyi Zhang & McDonald, 2016). This peptide expression pattern mirrors that found in the dorsal striatum (Gagnon et al., 2017), suggesting similar neuronal populations exist in both regions. Indeed, cellular characterisation studies confirm that the ASt contains neuronal populations similar to those in the striatum (Gagnon et al., 2017; Zhou, Wilson, & Dani, 2002), consisting predominantly of GABAergic medium spiny neurons (MSN), with sparse cholinergic interneurons (Y. Wang et al., 2023). Following striatal organisation patterns, enkephalin expression in the ASt is restricted to D2-expressing MSNs (Y. Wang et al., 2023) and dynorphin expression is restricted to D1-expresing MSNs (Y. Wang et al., 2023). This organisation creates a neurochemical environment in the ASt that parallels striatal regions but is anatomically positioned at the boundary between the amygdala and striatum, potentially allowing peptidergic modulation to influence both fear learning and reward related processing.

iii. The role of ASt in fear learning

The ASt contributes to fear learning and expression through distinct neuronal populations that differentially regulate defensive behaviours. Recent *in vivo* calcium imaging showed that D2 MSNs in the ASt respond to both footshock and tone presentations (Kintscher, Kochubey, & Schneggenburger, 2023). Furthermore, optogenetic silencing of these D2 neurons using Adora2a^{cre} mice

increases conditioned freezing behaviour. Given the dense dopaminergic innervation of the ASt (Jean-Francois Poulin et al., 2018), these changes in D2 MSN activity may result from dopamine receptor activation. The ASt's position as both a recipient of sensory information and a source of various peptides suggests it may serve as an important regulatory node for adjusting fear learning.

D. Dopaminergic modulation of fear learning

While neural circuits underlying fear conditioning are well characterised, the role of specific neurotransmitter systems in regulating these circuits remains less well understood. Dopamine, critical for motivation, motor function and cognition (Nieoullon & Coquerel, 2003), is particularly well-positioned to modulate fear learning.

i. Dopaminergic input in amygdala circuits

The amygdala is a major target of mesolimbic dopamine projections from the VTA and SNr (Asan, 1998), innervating both excitatory and inhibitory neurons (Muller, Mascagni, & McDonald, 2009; Pinard, Muller, Mascagni, & McDonald, 2008). The functional significance of these dopaminergic inputs is demonstrated by multiple lines of evidence, including pharmacological studies showing that D2 receptor antagonism in either the VTA or amygdala reduces freezing in contextual fear conditioning (de Souza Caetano, de Oliveira, & Brandão, 2013), and optogenetic studies demonstrating that inhibition of VTA terminals in the amygdala diminishes conditioned freezing responses (Tang,

Kochubey, Kintscher, & Schneggenburger, 2020). Experiments using high-performance liquid chromatography (HPLC) assays detect increased dopamine levels in both VTA and amygdala during fear conditioning (de Oliveira et al., 2011), providing direct evidence of dopamine release during emotional learning. This anatomical and functional evidence establishes dopaminergic projections from midbrain regions as a key modulatory system that can regulate amygdala dependent fear learning. However, this functional importance of VTA in fear learning presents an interesting anatomical paradox as VTA neurons predominantly target the BLA and CeA (Fig 1.4) (Jean-Francois Poulin et al., 2018).

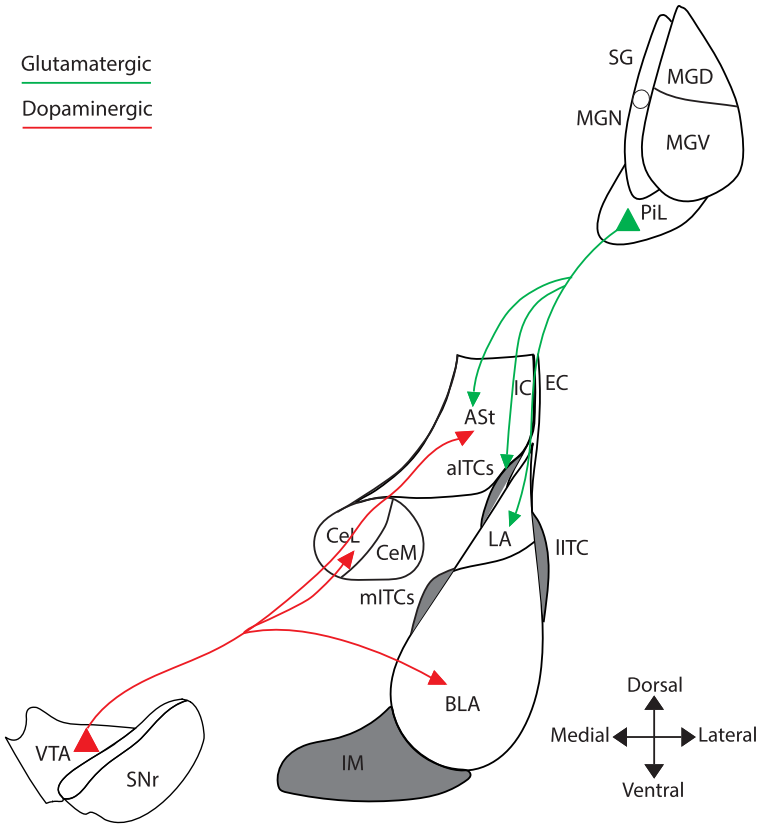

Figure 1.4. Dopaminergic afferents from the VTA targets the BLA and CeA but not the LA. Cartoon depicting dopaminergic projections from the VTA to the BLA and CeA. apITCs – apical intercalated cells ASt – amygdalo-striatal transition zone, BLA – basolateral amygdala nucleus, CeL – central lateral amygdala nucleus, CeM – central medial amygdala nucleus, EC – external capsule, IC – internal capsule, lITCs – lateral intercalated cells, MGD – medial

geniculate body dorsal, , MGN: medial geniculate nuclei, MGV – medial geniculate body ventral, mITCs – medial intercalated cells, SG – suprageniculate nucleus, SNr – substantia nigra, PiL – posterior intralaminar thalamic nuclei, VTA – ventral tegmental area

This anatomical organisation appears mismatched with the known circuits of fear learning, as fear learning and dopamine mediated plasticity at MGN-amygdala are thought to occur primarily in LA (Bissière et al., 2003; Quirk et al., 1997), rather than the BLA where VTA projections are densest (Jean-Francois Poulin et al., 2018). This anatomical paradox suggests that other neurotransmitter systems may play important roles alongside dopamine in coordinating fear learning across amygdala subregions where dopaminergic innervation is sparse.

ii. The role of dopamine in fear learning

Dopamine plays a critical role in fear learning through receptor-specific mechanisms that have been extensively characterized in pharmacological studies. While dopamine producing neurons are primarily localised to specific midbrain regions (Brandão & Coimbra, 2019), dopamine receptors are widely distributed throughout the central nervous system, with abundant D1- and D2-receptor mRNA expression in the amygdala (A. Mansour et al., 1990). This widespread receptor distribution enables dopamine to exert powerful effects on fear processing, as demonstrated by systemic pharmacological. Administration of tyrosine, a catecholamine precursor, enhances conditioned freezing (Morrow, Elsworth, & Roth, 1996), while amphetamines and other indirect dopamine agonists potentiate fear startle responses and attenuate extinction (Borowski & Kokkinidis, 1998). More specific receptor-targeted studies further clarify dopamine's role by revealing the distinct contributions of receptor subtypes. D1 receptor activation strongly promotes fear learning and

expression, as demonstrated by both antagonist and agonist studies. D1 receptor antagonism with the selective antagonist SCH 23390 impairs fear conditioning acquisition (Inoue, Izumi, Maki, Muraki, & Koyama, 2000) and reduces fear-potentiated startle (Greba & Kokkinidis, 2000), indicating D1 signalling is necessary for fear learning. Conversely, D1 receptor activation with the selective agonist SKF 38393 enhances fear learning and potentiates acoustic startle in fear-extinguished rats (Borowski & Kokkinidis, 1998), showing that increased D1 activation is sufficient to amplify fear responses. D2 receptor effects on fear learning are more complex to interpret. D2 receptor antagonists increase freezing behaviour (Blackburn & Phillips, 1990), while D2 agonists attenuate second-order fear conditioning (Nader & LeDoux, 1999). This opposing effects to D1 modulation of fear learning likely reflect the dual actions of D2 receptors as both postsynaptic receptors and presynaptic autoreceptors that regulate dopamine release (C. P. Ford, 2014), making their net effects on fear circuits difficult to predict without considering the specific neural context. Nevertheless, the consistent findings across these pharmacological studies establish dopamine as a key modulator that predominantly enhances fear learning

iii. Dopamine modulation of synaptic plasticity

One mechanism through which dopamine could modulate fear learning is by regulating synaptic plasticity within amygdala circuits. Dopamine receptor signalling in the amygdala involves distinct molecular pathways, with D1-like (D1 and D5) and D2-like (D2, D3, D4) receptors coupled to opposing G-protein cascades. D1-like receptors activate cAMP synthesis through G_s while D2-like

receptors inhibit cAMP through G_i (Lee, Lee, & Kim, 2016). This molecular distinction underlies their opposing effects on neuronal activity, with D1-like activation enhancing and D2-like activation inhibiting neural responses. Both receptor families are distributed throughout amygdala nuclei, with D1 showing the highest expression in ITCs and D2 more broadly distributed throughout (Maltais, Côté, Drolet, & Falardeau, 2000). At the synaptic level, dopamine facilitates LTP at thalamo-amygdala synapses through a disinhibitory mechanism involving suppression of feedforward GABAergic transmission (Bissière et al., 2003). This disinhibition creates conditions permissive for plasticity induction, providing a cellular mechanism for dopamine's enhancement of fear learning.

iv. Reward prediction error

Dopamine's role in fear learning can be effectively understood through the lens of prediction error signalling, a framework originally developed in reward learning research (Schultz, 2016), but with significant implications for understanding aversive learning mechanisms. The reward prediction error hypothesis provides valuable insights into how dopamine might function during fear conditioning, potentially explaining the precise timing and adaptive significance of dopamine release during threat learning situations (Schultz, 2016). This model proposes that dopamine neurons encode the discrepancy between expected and actual outcomes, serving as a teaching signal that guides behaviour (Schultz, 1998, 2016). In reward learning, electrophysiological recordings from dopamine neurons in the VTA and SNr demonstrate clear prediction error encoding. Initially, these neurons fire action

potentials upon receiving an unexpected reward, such as palatable food (Schultz, Apicella, & Ljungberg, 1993). However, after learning, these neurons no longer respond to the reward itself but instead fire at the time of the predictive cue (Schultz et al., 1993). If an expected reward is omitted, dopamine neurons show a depression in their firing rate below baseline at the time the reward was expected, signalling a negative prediction error, which updates the behavioural to accommodate (Schultz et al., 1993). Similar dopamine dynamics have been observed during fear conditioning. Initially, dopamine neurons respond to the aversive US such as a footshock. As learning progresses, dopamine release shifts from the US to the predictive auditory CS (Bayer & Glimcher, 2005; Keiflin & Janak, 2015). This temporal shift in dopamine signalling coincides with the animal learning to predict the aversive event, as evidenced by the emergence of defensive behaviours in response to the CS. By encoding prediction errors, dopamine helps update the predictive value of environmental stimuli, facilitating the formation and modification of associative memories that allow organisms to anticipate and adaptively respond to both rewards and threats in their environment Importantly, while this prediction error framework was first established for dopamine, emerging evidence suggests it may be a general computational principle that extends to other neuromodulator systems, including opioids (Gavan P. McNally & Cole, 2006)

E. Opioid modulation of fear learning

While the influence of the dopaminergic systems has been extensively studied in fear learning, the endogenous opioid system is emerging as a critical yet often overlooked modulator of fear acquisition and expression. Endogenous opioids appear to regulate fear learning through at least two distinct mechanisms.

Firstly, opioids mediate conditioned hypoalgesia, a phenomenon where pain sensitivity is reduced when an animal is exposed to fear associated aversive stimuli. When an animal encounters a CS previously paired with an aversive event, endogenous opioids are released in pain-processing circuits, diminishing the perception of painful stimuli (Miguez, Laborda, & Miller, 2014). Early pharmacological studies demonstrated the essential role of opioid transmission in this process, as opioid receptor antagonism blocks the development of this conditioned pain suppression (Helmstetter & Fanselow, 1987). This adaptive mechanism allows animals to respond effectively to threats even when injured, potentially enhancing survival.

Secondly, opioids directly influence the fundamental mechanisms of fear learning itself. Systematic manipulation studies reveal that opioid receptor activation attenuates fear acquisition (Westbrook, Greeley, Nabke, & Swinbourne, 1991), while antagonism enhances it (Westbrook et al., 1991). Importantly, these effects derive from central rather than peripheral opioid signalling (Fanselow, Calcagnetti, & Helmstetter, 1988), suggesting direct

actions on neuronal circuits involved in fear memory formation rather than simply altering peripheral pain sensation. This facilitation of fear learning is also observed in second-order fear conditioning, where a new neutral stimulus (CS2) acquires fear properties after being paired with the previously conditioned stimulus (CS1). For example, after a tone (CS1) is paired with a shock (US), the tone can then function as the signal for the US when paired with a light (CS2), even though the light was never directly paired with shock (Michalscheck, Leidl, Westbrook, & Holmes, 2021). Studies show that opioid antagonists block this second-order conditioning process even in the absence of a noxious stimulus like shock (Michalscheck et al., 2021), indicating that endogenous opioids are necessary for fear learning beyond just processing painful stimuli

Together, these findings establish endogenous opioid signalling as an essential regulatory mechanism in fear learning, potentially serving to calibrate fear responses and prevent maladaptive over-learning of threat associations.

i. Endogenous opioids the amygdala

The endogenous opioid system, comprising opioid receptors and their peptide ligands, is widely distributed throughout the central nervous system and modulates numerous complex physiological and pathophysiological processes including pain perception, fear responses, attachment formation, drug addiction and decision-making (Le Merrer, Becker, Befort, & Kieffer, 2009; Gavan P. McNally, 2009). The opioid peptides arise from post-translational modifications of distinct precursor proteins, preproopiomelanocortin, preproenkephalin, preprodynorphin, with each

precursor generating multiple active peptides (Le Merrer et al., 2009; Gavan P. McNally, 2009). The major opioid peptides, including β-endorphin, Met-enkephalin, Leu-enkephalin, and dynorphin, bind with to at least three major receptor subtypes: μ- (MOR), δ- (DOR), κ- (KOR) (Williams, Christie, & Manzoni, 2001). These peptides show preferential receptor binding, with enkephalins activating both DOR and MOR, β-endorphin strongly preferring MOR, and dynorphin predominantly activating KOR. All three major opioid receptor subtypes (MOR, DOR, and KOR) are G-protein coupled receptors (GPCRs) coupled to $G_{i/o}$-G-proteins, whose activation all produce similar cellular effects (Williams et al., 2001). Opioid receptor activation inhibits neural signalling, including suppression of synaptic transmission and reduction of cellular excitability (Faber & Sah, 2004; Winters et al., 2017). These effects are mediated through G_i- and G_o-protein interactions with intracellular effectors, including inhibition of adenylyl cyclase and voltage-activated calcium channels (Williams et al., 2001), activation of a G-protein-activated inwardly rectifying potassium conductance (GIRK) (Vaughan, Ingram, Connor, & Christie, 1997), and inhibition of neurotransmitter release (Williams et al., 2001). This widespread inhibitory action on neural signalling positions the opioid system as a powerful modulator of synaptic plasticity and circuit dynamics across brain regions involved in emotional learning and memory

The anatomical distribution of opioid receptors and their endogenous ligands closely aligns with key nodes of fear learning circuitry. BLA neurons show a distinctive pattern of opioid receptor expression, with high levels of DOR and moderate MOR immunoreactivity (Jacobsen et al., 2006; Poulin et al., 2006),

while ITC and ASt neurons exhibit robust MOR expression (Jean-François Poulin, Chevalier, Laforest, & Drolet, 2006). The distribution of endogenous opioid peptides complements this receptor organisation, with the enkephalin precursor protein (ppENK) showing strong expression in the CeA and moderate levels in the BLA (Jean-François Poulin et al., 2006). Notably, high enkephalin expression is found in the ASt and ITC, a major target of MGN projections (J. E. LeDoux et al., 1990; Jean-François Poulin et al., 2006) suggesting opioidergic modulation may be particularly important at this thalamo-amygdala interface in fear processing.

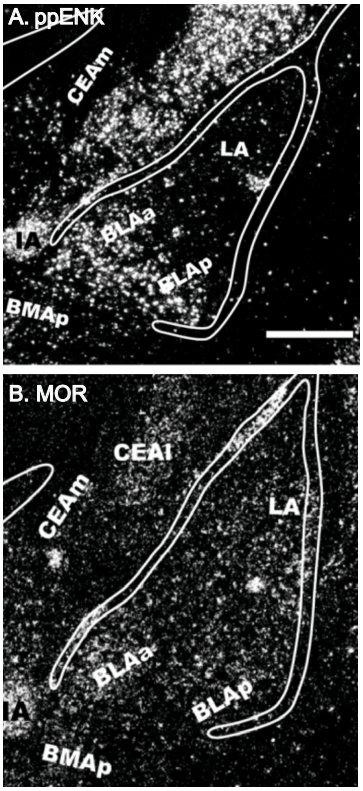

Figure 1.5. Endogenous opioid expression in the caudal amygdala. In situ hybridisation for (A) preproenkephalin mRNA (ppENK) and (B) MOR mRNA. Figure adapted from Poulin et al. (2006)

Functional studies have demonstrated active opioid signalling in fear-related circuits. Electrophysiological studies provide direct evidence for endogenous opioid signalling in the amygdala. Moderate electrical stimulation of the main island intercalated cells (IM) readily released endogenous opioids which acted at multiple sites (Winters et al., 2017). Once released the endogenous opioid activates MOR to hyperpolarise IM neurons and inhibit GABA release and activates DOR to inhibit glutamate release from BLA neurons (Winters et al., 2017). Given the high expression of enkephalin in both the apical ITC (aITC) clusters and ASt, similar opioidergic modulation may occur in these fear-related circuit nodes.

Endogenous opioids are released during behaviourally relevant conditions that may influence fear learning. Aversive experiences such as stress, which share neural mechanisms with fear conditioning, trigger measurable opioid release in the amygdala (DiFazio et al., 2022). PET radioligand binding studies reveal changes in opioid receptor occupancy consistent with endogenous opioid release in the amygdala that correlates with individual differences in stress responsivity (Love, Stohler, & Zubieta, 2009). The functional significance of this stress-induced opioid release is demonstrated by studies showing that opioid receptor blockade with naltrexone prevents stress induced analgesia in rodent forced swim tests (Le Roy et al., 2011). Collectively, these studies demonstrate that endogenous opioids are released in the amygdala during aversive experiences, providing direct evidence that opioid signalling is engaged during conditions relevant to fear learning.

Importantly, an individual's emotional state appears to influence endogenous opioid release patterns, suggesting that fear learning may be modulated by state-dependent opioid signalling. Patients with major depressive disorder show altered patterns of opioid receptor occupancy during social rejection tasks, indicating differences in endogenous opioid release compared to healthy controls where nucleus accumbens and amygdala opioid release correlates with social motivation (Hsu et al., 2015). Similarly, chronic pain conditions and substance use alter opioid receptor availability, with PET imaging revealing changes in opioid receptor radioligand binding in neuropathic pain models in rodents (Thompson et al., 2018) and alcohol consumption alters MOR occupancy in the amygdala, orbital frontal cortex and nucleus accumbens (NAc), with more pronounced effects in heavy drinkers (Mitchell et al., 2012). This evidence for state-dependent opioid signalling suggests that an individual's emotional and physiological condition may influence fear learning through altered patterns of endogenous opioid release.

The converging evidence from electrophysiological, neuroimaging, and behavioural studies establishes that endogenous opioids are positioned within fear circuits, actively released during aversive experiences, and capable of modulating both excitatory and inhibitory neurotransmission. This anatomical and functional organization may enable opioid signalling to fine tune fear learning processes according to environmental demands and physiological states.

ii. Regulation of opioid signalling by peptidases

The signalling capacity of endogenous opioids is tightly regulated by specific peptidases that degrade the opioid peptides into inactive fragments and therefore, controls their extracellular concentrations. Three distinct peptidases hydrolyse endogenous opioids (Fig 1.6). A neutral endopeptidase (NEP), a dipeptidyl carboxypeptidase I (also known as angiotensin converting enzyme (ACE)) and an aminopeptidase N (APN) (Hiranuma et al., 1998). These peptidases are highly expressed in regions where sensory information converges, including the MGN and amygdala (Waksman, Hamel, Delay-Goyet, & Roques, 1986), precisely matching the distribution of opioid receptors and endogenous enkephalin (Jean-François Poulin et al., 2006). Both ACE and NEP cleave the Gly3-Ph4 bond on the enkephalin molecule, whilst APN cleaves the Try1-Gly2 bond (Fig 3.1) (Marvizon, Wang, Lao, & Song, 2003)

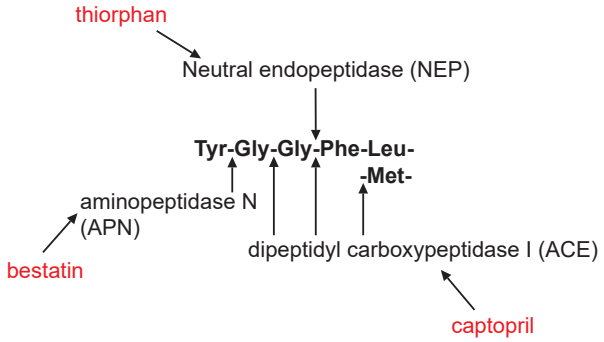

Figure 1.6. Degradation of enkephalin by peptidases. Met-enkephalin is hydrolysed by various peptidases. The schematic shows the cleavage site (arrows) of met-enkephalin by their respective peptidases (APN, NEP, ACE) and their corresponding inhibitors in red (bestatin, thiorphan, and captopril). Figure adapted from Marvizón *et al* (2003).

Peptidase inhibitors reveal the crucial role of these enzymes in regulating endogenous opioid signalling, as demonstrated by studies showing that

blocking peptidase activity uncovers opioid-mediated effects on synaptic transmission in the IM, that are not detectable under normal conditions (Winters et al., 2017). This suggests that ongoing peptidase activity normally limits the physiological impact of released endogenous opioids. Peptidase inhibitors like bestatin (APN inhibitor), thiorphan (NEP inhibitor), and captopril (ACE inhibitor) (Fig 1.6) can substantially enhance and prolong opioid signalling by preventing the rapid degradation of opioid peptides after their release (G. C. Gregoriou, Patel, Winters, & Bagley, 2020; Marvizon et al., 2003; Winters et al., 2017). Importantly, peptidase regulation extends beyond enkephalins to include other neuropeptides relevant to emotional processing, such as substance P, nociceptin, and neurotensin (Hooper, Kenny, & Turner, 1985; Marvizon et al., 2003). This regulated degradation system provides a sophisticated control mechanism for dynamically adjusting opioid signalling efficacy in neural circuits.

iii. Opioids as a learning signal

While opioid signalling has traditionally been associated with conditioned analgesia during fear learning (Bolles & Fanselow, 1980), mounting evidence suggests a more fundamental role in fear learning beyond pain modulation. The classic view proposes that opioid receptor antagonists facilitate fear acquisition by preventing the activation of descending analgesic pathways that would normally reduce nociceptive processing of aversive stimuli like footshock (Fanselow, 1998). However, opioid modulation extends to higher-order learning processes. Systemic administration of the opioid receptor antagonist naltrexone before training enhances fear acquisition as measured

by increased freezing responses to CS presentations, suggesting endogenous opioids normally constrain fear learning. This facilitation of fear learning is also observed in second-order fear conditioning where no direct painful US is experienced and instead the learnt CS is paired with a new CS (Michalscheck et al., 2021). Opioid signalling also regulates fear extinction learning, with opioid receptor antagonist naloxone impairing the reduction of fear responses during extinction training. (G. P. McNally & Westbrook, 2003). This is significant as extinction learning generally occurs in the absence of US presentation. Rather than simply reducing US detection through analgesia, opioid signalling appears to modulate how aversive experiences are encoded, suggesting a role in regulating associative learning processes. The observation that systemic administration of opioid receptor antagonists enhances both first- and second-order fear conditioning suggests that endogenous opioids may serve as a dedicated fear inhibition signal, actively constraining fear learning across different conditioning protocols. Importantly, these behavioural studies primarily used naloxone or naltrexone, which are non-selective antagonists but have higher affinity for MOR than other opioid receptors subtypes (Williams et al., 2001), suggesting that endogenous opioids acting at MOR may be particularly important for limiting fear learning. This fear-inhibiting role is supported by the anatomical and functional overlap between opioid and dopamine systems. In the ASt, medium spiny neurons expressing D2 receptors also express enkephalin (Y. Wang et al., 2023), while VTA neurons projecting to the amygdala show hyperpolarisation in response to met-enkephalin, indicating suggesting there may be functional MOR or DOR opioid receptors on dopaminergic terminals (Christopher P. Ford, Mark, &

Williams, 2006). These overlapping expression patterns suggest potential bidirectional interactions between opioid and dopamine signalling, where opioids might inhibit dopamine release or vice versa, providing a mechanism for fine-tuning fear learning signals. Together, these findings suggest that endogenous opioid signalling may serve as a specific learning signal that regulates fear acquisition and expression, operating distinct from its role in pain modulation.

F. Studying neuropeptide release

Understanding peptide modulation in fear circuits has been severely constrained by methodological limitations that prevent accurate measurements of peptide release in behaviourally relevant contexts. Conventional approaches for detecting peptide release suffer from significant compromises between temporal and spatial resolution as well as peptide specificity (F. Sun et al., 2018). Microdialysis, capable of directly sampling extracellular peptide operates at temporal resolution too slow to capture neuropeptide dynamics critical for understanding function during brief behavioural events like presentation of CS or fear responses (Chefer, Thompson, Zapata, & Shippenberg, 2009). This limitation makes its almost impossible to correlate peptide release with specific components of fear learning, such as the acquisition of CS-US association (F. Sun et al., 2018). Electrochemical approaches like fast-scan cyclic voltammetry offer superior temporal resolution but have been largely limited to monitoring monoamine neurotransmitters (Bull, Bakhtiar, & Sheehan, 1991; Kile et al., 2012), thus it

is largely unable to be used for peptides, such as opioids. Indirect measurements, such as examining changes in synaptic transmission due to endogenous peptide actions (Winters et al., 2017), can detect functional consequences of endogenous peptide release but cannot distinguish between different peptides. Additionally, these methods depend heavily on having a sufficiently sensitive effectors detect the released peptides. If the cellular response being measured has low sensitivity to opioid modulation, peptide release may occur without producing detectable changes in synaptic transmission, potentially underestimating the actual extent of endogenous opioid activity. Human neuroimaging approaches using PET with radioligand displacement have revealed valuable information about peptide release during emotional states (Love et al., 2009), but their resolution is far too coarse for circuit-level analysis. Together, these technical constraints have created a significant knowledge gap regarding the precise dynamics of peptide signalling during emotional learning, particularly how peptide release may be coordinated with other neuromodulator systems like dopamine to regulate synaptic plasticity and behaviour.

ii. GPCR sensors for detecting neuropeptides

Recent advances in genetically encoded fluorescent sensors have created new opportunities for studying peptide release dynamics in fear circuits with unprecedented spatiotemporal resolution. The development of dopamine sensors such as GrabDA has enabled more direct visualisation of dopamine binding events in behaving animals, with this sensor incorporating a human D2 receptor domain with a strategically inserted circularly permuted GFP

(cpGFP) that translates dopamine binding into fluorescence changes (F. Sun et al., 2018). Similar design principles have been applied to create sensors for neuropeptides, including opioids (Dong et al., 2024; Rappleye et al., 2022), offering new tools for investigating peptide modulation of fear circuits.

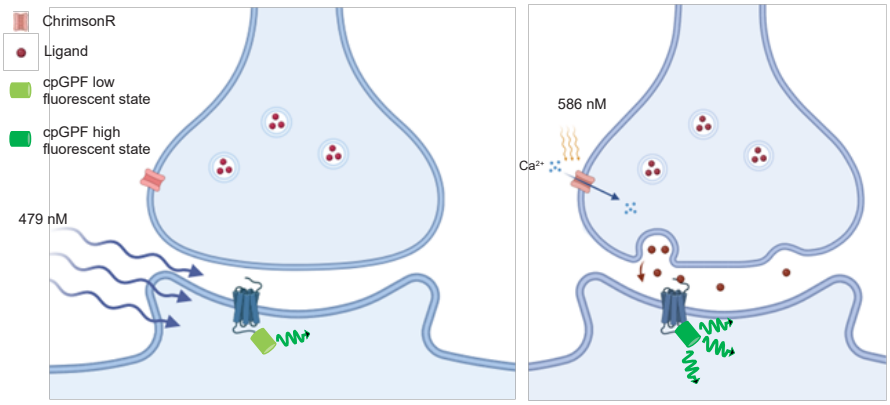

Figure 1.7 Schematic of a fluorescent protein-based biosensor. Resting state, circularised GFP exhibits baseline fluorescence when excited by blue light. Upon ligand binding, a conformational change in the protein structure leads to enhanced fluorescent output Ligand release can be controlled using red light-activated optogenetics. Figure made with Biorender

While these sensors can provide estimates of extracellular peptide concentration and potentially neurotransmitter release (Fig 1.8 B) (F. Sun et al., 2018), they are most powerful when combined with complementary techniques that can reveal the functional consequences of neuromodulator release, such as electrophysiology. Traditional electrophysiological approaches could detect the downstream effects of peptides on neural activity (Winters et al., 2017) but couldn't determine the precise release dynamics or concentrations involved (Fig 1.8 A).

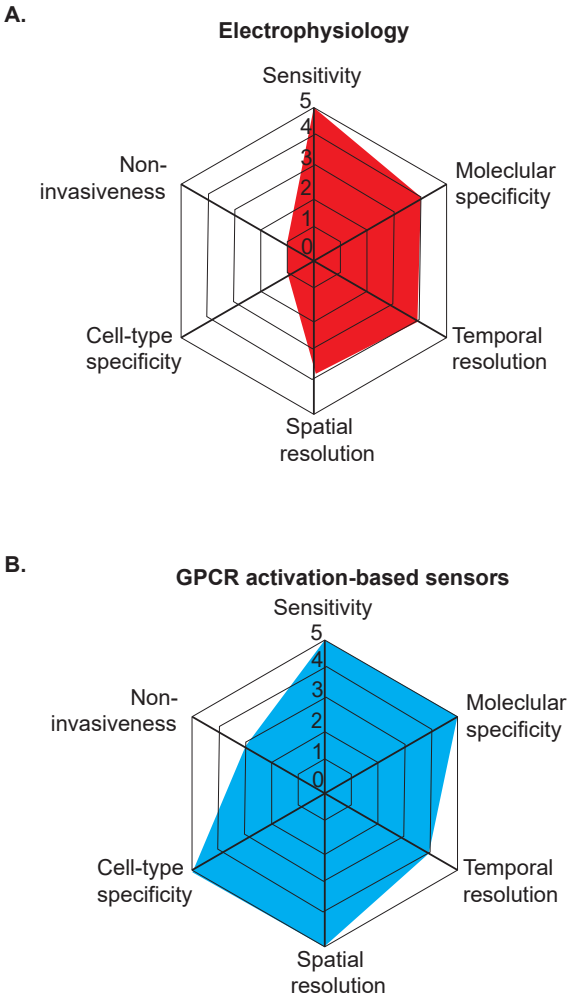

Figure 1.8. Overview of electrophysiology and GPCR activation-based sensor for detecting peptide transmission. (A) Radar graph summarizing the properties of electrophysiology, including sensitivity, molecular specificity, temporal resolution, spatial resolution, cell-type specificity and non-invasiveness, with each property ranging from 0 to 5. (B) Same as A but for GPCR activation-based sensor methods. Figure adapted from Qian *et al* (2023)

The combination of optical sensors with electrophysiological recordings now makes it possible to directly correlate release events with their functional effects on circuit activity, providing more complete insights into neuromodulator signalling. Additionally, given the sensor's distinct excitation wavelengths (F. Sun et al., 2018), combination with optogenetic is also possible, enabling simultaneous optogenetic stimulation of specific pathways

while monitoring neurotransmitter release through fluorescent sensors without interference. The combination of optical sensors with electrophysiological, optogenetic, and behavioural approaches thus creates a powerful methodology for dissecting the circuit mechanisms through which specific inputs engage neuromodulator systems during fear learning

G. Hypothesis and Aims

The acquisition and expression of fear and reward learning relies, in part, on synaptic plasticity of the auditory thalamic afferents carrying the conditioned auditory information to the lateral amygdala. Dopamine signalling in the amygdala is thought to gate LTP induction, thereby driving fear learning. However, it is often overlooked that midbrain dopaminergic neurons project more robustly into the basal amygdala and the ASt, than the LA. In particular, the ASt also receives significant thalamic and dopaminergic input and is rich in the endogenous opioid enkephalin. This strongly suggests that auditory thalamic activity during fear and reward learning induces the release of endogenous opioids, yet the impact of these opioids on fear learning within the amygdala remains underexplored. Additionally, the striatal-like nature of the ASt, which contains both D1 and D2 MSNs, positions it as a critical intersection where opioids and dopamine are likely to interact. Manipulating opioid or dopamine signalling could disrupt fear and reward learning processes. Therefore, I hypothesise that: ***Endogenous opioids released by auditory thalamus activity will reduce sensory input from the auditory thalamus and diminish dopamine signalling in the ASt, thereby reducing fear***

learning. Consequently, dysregulation of this opioid modulation could lead to maladaptive fear learning outcomes

The specific aims of the thesis are:

1. **To characterise MGN inputs to the amygdala and determine whether MGN activation triggers endogenous opioid release in the amygdala**
2. **To investigate the functional properties of VTA-ASt projections and determine whether opioids inhibit this dopaminergic input**
3. **To determine whether opioids modulate synaptic plasticity at MGN-amygdala synapses**

Chapter 2
Materials and Methods

A. Animals

Male Sprague-Dawley rats (4-12 weeks olds) and Male Long-Evans (10-12 weeks old) acquired from the Animal Resources Centre (Ozgene ARC, Australia). Animals were housed in groups of up to 6, maintained on a 12/12-hour light-dark cycle and provided with food and water *ad libitum*. All experiments were undertaken as per a protocol approved by the University of Sydney Ethics Committee (1637/2019) and The University of New South Wales, Sydney.

B. AAV and tracer expression

All AAV's or tracers were injected *in vivo* into specific brain regions. Details of AAVs are listed below (Table 2.1)

Viral strain	**Source**	**Identifier**
AAV8-Syn-ChR2(H134R)-GFP	Addgene	58880-AAV8
AAV5-Syn-ChrimsonR-tdT	Addgene	59171-AAV5
AAV9-hSyn-δlight	UNC Vector Core	N/A
AAV9-hSyn-GRAB-DA2h	Addgene	140554-AAV9
AAV5-EF1α-UMASS2A	Bruchas Lab*	N/A
AAV9-PENK-KO-sgRNA1	CMRI**	N/A
AAV9-Control non-targeting-sgRNA	CMRI**	N/A

FluoSpheres (Red/Orange) Microspheres	Thermofisher	F8794

Table 2.1 List of viral and tracer reagents. *UMASS were kindly given to us by Bruchas Lab (Rappleye et al., 2022). **Viral plasmids were made by Neely Lab (Dr Cesar Moreno) and packaged into AAVs at Children Medical Research institute (CMRI, Western Sydney Local Health District, AU)

C. Stereotaxic injections

Rats aged 4-6 weeks old, were deeply anaesthetised with 5% isoflurane, afterwards rats were maintained in deep anaesthesia with 1.5-3% isoflurane mixed with oxygen (1 L/min). Rats would then have their heads shaved and be placed on the stereotaxic apparatus (model 942, Kopf instruments, USA). Incisor bars were used to achieve a flat skull position. Following, rats would then receive a subcutaneous injection of carprofen (5 mg/kg, Cenvet, Australia) and a subcutaneous injection of bupivacaine above the skulls (5%, Cenvet, Australia). A single incision was made down the centre of the head the expose the skull. Holes were drilled above the brain regions designated for injection. Co-ordinates relative to bregma (in mm) for injections listed below (Table 2.2)

Brain region	Anteroposterior	Mediolateral	Dorsoventral
Lateral Amygdala	-2.5	±5.2	-7.4
Basolateral Amygdala	-2	±4.5	-8.6
Amygdalo-striatal transition zone	-2.4	±4.6	-7.4
Medial Geniculate Nucleus	-5.4	±3.1	-6.2

Ventral Tegmental Area	-5.3	±0.8	-8.2
Nucleus Accumbens	+1.8	±1.8	-7.9
Central Amygdala	-2.0	±4.1	-8.5

Table 2.2 List of stereotaxic injection coordinates. Table showing anteroposterior, mediolateral and dorsoventral coordinates relative to bregma (in mm)

Injections were performed with glass pipettes (Drummond Scientific, USA) pulled using a PC-10 micropipette puller (Narishige, Japan). Glass pipettes were first backfilled with mineral oil before loading viral solutions. Upon completion of the injection, the pipette would be left in place for 5 minutes before rapidly retracting it. Following withdrawal of the pipette, the skull openings were sealed with bone wax (Coherent Scientific, Australia) and the incision closed with silk sutures. Rats were then removed from the stereotaxic apparatus and given an intraperitoneal injection of cephazolin (100mg/ml, Hospira, Australia) and 1ml of normal saline. Rats were left to recover for 7 days post-surgery.

D. Brain slice preparation

Rats were deeply anaesthetised with isoflurane within a vacuum sealed chamber. Rats were then decapacitated and the brain was rapidly removed and submerged in ice-cold cutting aCSF (artificial spinal cord fluid) solution containing (in mM) 125 NaCl, 25 $NaHCO_3$, 11 D-glucose, 2.5 KCL, 1.25 NaH_2PO_4, 2.5 $MgCl_2$, 0.5 $CaCl_2$ and continuously saturated with carbogen (95% O_2, 5% CO_2). Osmolarity of the aCSF was 295 mOsm/L and the solution

was kept at a pH of 7.3. Coronal brain slices containing the amygdala were cut a thickness of 280μM using a Leica VT1200 S vibratome (Leica Biosystems, Germany). Brain slices were then transferred to a bath containing cutting solution and incubated at 34°C for an hour before electrophysiology recording to promote neuron recovery and equilibrate to room temperature. In some cases, the brain slices would first be transferred to NMDG recovery solution for 10 minutes before being placed in the cutting aCSF. NMDG recovery solution contained (in mM) 93 NMDG chloride, 2.5 KCl, 1.2 NaH2PO4, 30 NaHCO3, 20 HEPES, 25 D-Glucose, 5 sodium ascorbate, 2 thiourea, 3 sodium pyruvate, 10 MgCl2, 0.5 CaCl2, pH 7.3, 300-310 mOsm/L maintained at 34°C.

E. Electrophysiology

For electrophysiological recordings, brain slices were transferred to a recording chamber and continuously superfused with recording aCSF containing (in mM) 125 NaCl, 2.5 KCL, 1.25 NaH_2PO4, 1 $MgCl_2$, 2 $CaCl_2$, 25 $NaHCO_3$ and 11 glucose, brain slices were saturated with carbogen and heated to 32-35°C using an inline heater (Warner instruments, USA) and the temperature was monitored using a thermistor. Brain slices were visualised using an Olympus BX51WI upright microscope (Olympus, Japan) with a x10/0.3-numerical-aperture (NA) water-immersion objective, or a x40/0.8 NA water-immersion objective and Dodt gradient differential interference contrast optics (Thorlabs, USA). Neurons of interest were identified by their location and morphology. Whole-cell patch clamp recordings were made using patch

pipettes (2-5MΩ) pulled on a P-1000 micropipette puller (Sutter Instruments, USA) and filled with caesium chloride internal solution containing (in mM) 140 CsCl, 5 HEPES, 10 EGTA, 2 $CaCl_2$, 2 Mg_2ATP, 0.3 NaGTP, 3 QX-314.CL and 0.05% biocytin or potassium gluconate internal solution containing (in mM) 135 potassium gluconate, 8 NaCl, 2 Mg_2ATP, 0.3 NaGTP, 11 EGTA, 10 HEPES and 0.05% biocytin. Both internal solutions were pH 7.3 and 280-285 mOsm/L. The liquid junction potential of -4mV and -13.2mV respectively was not corrected during recordings. In all experiments, series resistance (<20 MΩ) was continuously monitored and experiments in which series resistance change by >20% were excluded from analysis. To record evoked excitatory post synaptic currents (eEPSC) bipolar electrodes were placed in the internal capsule to stimulate thalamic terminals projecting to the LA. Neurons in the LA were then at -70mV using a patch-clamp amplifier (Multiclamp 700B, Axon Instruments, USA). To isolate glutamatergic currents, recordings were made in the presence of the $GABA_A$ antagonists picrotoxin and SR95531.

F. Electrophysiology acquisition and analysis

Electrophysiological signals were amplified, low pass filtered (5 kHz), digitised and acquired (sampled at 10 kHz) using a Multiclamp 700B amplifier and recorded, stored and analysed with Axograph Acquisition software v18.0.0 (Molecular Devices, USA). For paired pulse recordings, synaptic currents were evoked every 15 seconds via paired stimulating pulses (1-100 V, 100 µs, 50 ms interpulse interval). The paired-pulse ratio (PPR) was calculated as 2^{nd} pulse amplitude/ 1^{st} pulse amplitude. For endogenous opioid release

experiments, a moderate stimulus protocol was used (1-100 V, 5 stimuli at 150 Hz, followed by single test pulse 200 ms later). Peak amplitude was used as the measure of synaptic currents. Peak amplitude was quantified as the mean peak amplitude of 8 consecutive stimulated synaptic currents after the responses had reached a plateau. To determine drug effects, the peak amplitude of the currents generated from the first pulse of the paired stimuli, or the test pulse of the moderate stimuli was used. In experiments examining kinetics properties of the synaptic currents, rise time from 10-90% of the peak and synaptic decay were measured. For synaptic decay kinetics, a double exponential consisting of a fast and slow component was fitted to the normalised currents. The weighted time constant (τ_w) was then calculated using the following equation:

$$\tau_w = \left(\frac{A_{fast} \times \tau_{slow}}{A_{fast} \times A_{slow}}\right) + \left(\frac{A_{slow} \times \tau_{slow}}{A_{fast} \times A_{slow}}\right)$$

Where A = decay amplitude

And τ = time constant

The AMPA/NMDA ratio was examined in some experiments by quantifying the relative contribution of postsynaptic AMPA and NMDA receptors. For AMPA receptors, the peak amplitude of the postsynaptic current at -70 mV was measured and for NMDA receptors, the average amplitude of the current 300 ms post stimulation at +40 mV was measured. To determine whether synapses were monosynaptic, the synaptic jitter, defined as the variability of latency to 1% peak onsets was measured. Synaptic jitter of < 0.7 ms indicated

a monosynaptic connection. Synaptic jitter of a response was calculated as the standard deviation of the peak onsets.

All statistical analysis was performed using GraphPad Prism (GraphPad, USA). All results are expressed as the mean ± SEM between slices unless stated otherwise. Statistical tests used are stated in text and considered significant if $p < 0.05$.

G. Fluorescent slice imaging

Brain slices were taken using the same methods stated above, 4-6 weeks after rats were injected with either AAV9-hSyn-δlight or AAV9-hSyn-GRAB-DA2h. After recovery slices were placed in an imaging chamber and recording aCSF perfused at a flow rate of 2mL/min. An upright Olympus BX51WI was equipped with an ANDOR iXon life 888 EMCCD camera (Oxford instruments, UK) controlled using Micro-Manager 2.0 (NIH). Slices were imaged using a x10/0.3-numerical-aperture (NA) water-immersion objective, or a x40/0.8 NA water-immersion objective. Fluorophores were excited using a CoolLED illumination system. Specifically, green fluorescence was excited by the 400-500 nM LED wavelength which was filtered through an excitation filter with a centre wavelength of 485 (475-495 nM, Semrock, USA). Red fluorescence was excited by the 500-750 nM LED wavelength which was filtered through an excitation filter with a centre wavelength of 586 nM (510-538 nM, Semrock, USA). Green fluorescence was collected using a 510-540 nM filter and red fluorescence was collected using a 611-645 nM filter (Semrock, USA). The dual-band excitation filters allowed for simultaneous excitation and emission

for both green and red fluorescence (Brightline Pinkel filter set, Semrock, USA) Full frame (512x512 pixels) was captured at a rate of 4 Hz. For electrical stimulations, a bipolar electrode was positioned in either the AST or the LA. For optical stimulations, the x40 objective was placed above the area of interest. Imaging and stimulation were synchronised using an Arduino board with custom-written software. During imaging, drugs were applied via bath application at a flow rate of 2 mL/min. Images were analysed using FIJI (NIH) (Schindelin et al., 2012). The change in fluorescence was measured by hand circling regions of interests (ROIs) of an image in FIJI. The ROIs measured mean gray value over each captured frame. Measurements were then imported into Excel and the $\Delta F/F_0$ was calculated using the equation below.

$$\Delta F/F_0(\%) = \frac{(F_i - F_{baseline})}{F_{baseline}} \times 100$$

Where F_i is the ROIs mean fluorescence for each frame

And $F_{baseline}$ is the average fluorescence for 20 frames before stimulation or 2 minutes prior to drug application

Spatial/temporal analysis was performed on the recorded videos using custom-written software.

Area under the curve (AUC) measurement were calculated using GraphPad Prism's integrated analysis function. In brief, fluorescent images were corrected or photobleaching using ImageJ's bleach correction plugin. AUC values were computed using the trapezoidal rule from stimulus onset until the end the recordings.

The custom-written code for ImageJ macro and Arduino control used in this thesis has been provided by Professor Yulong Li (Peking University) and is available at https://github.com/OTsensor/elec_stim_arduino (Qian, Wang, Wang, et al., 2023)

H. Optogenetics

For optogenetic experiments, animals were injected with viruses containing the blue-light sensitive rhodopsin ChR2 or red-shifted ChrimsonR. ChR2 was excited by the 400-500 nM LED wavelength which was filtered through an excitation filter with a centre wavelength of 485 (475-495 nM, Semrock, USA). ChrimsonR was excited by the 500-750 nM LED wavelength which was filtered through an excitation filter with a centre wavelength of 586 nM (510-538 nM, Semrock, USA). For electrophysiology experiments using optogenetics a single pulse or paired pulse stimulus of a 1 ms pulse width was delivered and optical excitatory post synaptic currents (oEPSC) were recorded. For fluorescent imaging involving optogenetics, the channel rhodopsin's were stimulated using 100, 250 or 500 stimuli at 50 Hz and a 10 ms pulse width. Post-hoc immunohistochemistry was performed on all injections site and animals with off-target injections were excluded.

I. Drugs

All drugs were made into a stock solution (1-10mM) before diluting to a working concentration in aCSF immediately before superfusion onto brain slices. The stock solutions for all drugs except thiorphan were, made in Milli-Q water.

Thiorphan was dissolved in DMSO to achieve a 0.01% working concentration of DMSO. Drugs and reagents were obtained from the following sources: CNQX, DAMGO, CTAP, U69593, norBNI, Deltorphin II, ICI 174,864 and D-AP5 were from Tocris (Bristol, UK). Picrotoxin, thiorphan, captopril, bestatin, and methionine-enkephalin were from Sigma (Missouri, USA). Dopamine was obtained from Cayman Chemicals (Michigan, USA). Eticlopride was obtained from HelloBio (Bristol, UK). All drugs were stored according to manufacture recommendations.

J. Immunohistochemistry

Slices were prepared for immunohistochemistry from perfused animals and following electrophysiology experiments for post-hoc staining. For the perfusion, animals were deeply anaesthetised with isoflurane and a lethal dose of lethabarb was injected intraperitoneal (0.2ml/kg). Following the complete abolishment of reflexes, animals were perfused through the ascending aorta with a flush solution containing 3,000 units per mL heparin in a 0.5% NaNO2/0.9% saline solution, subsequently followed by 4% paraformaldehyde (PFA) solution in a 0.1M phosphate buffered saline (PBS, pH 7.4). Brains were then carefully extracted and fixed overnight in 4% PFA at 4°C. Following overnight fixation, brains were thoroughly washed three times with PBS and embedded in optimal cutting temperature compound (OCT) and frozen at -80°C. Prior to sectioning brains were equilibrated at -20°C for at least an hour. Coronal sections 40 µM thick were cryosectioned using a cryostat (cryostat FSE). Slices where then transferred into cryoprotectant solution comprised of 40% PBS, 30% glycerol and 30% ethylene glycol and stored at -30°C until required for immunohistochemistry.

For immunohistochemistry, slices were first blocked in 10% normal goat serum, 0.5% bovine serum albumin, 0.3% Triton X-100 in PBS for one hour at room temperature. Slices were then washed (3 X 10 min wash) before incubated with relevant primary antibodies. For GFP, slices were incubated overnight at 4°C with rabbit anti-GFP (1:1000, Invitrogen, A6455) diluted in 5% normal goat serum, 0.3% Triton X-100 in PBS. For met-enkephalin and TH slices were incubated for 2 days in either rabbit anti-Met-enkephalin (1:1000 Immunostar, AB572250) or sheep anti-tyrosine hydroxylase (1:1000, Millipore, AB1542) diluted in 5% normal goat serum, 0.3% Triton X-100 in PBS. Slices were then washed (3 x 10 min wash) before incubation at room temperature for two hours in corresponding secondary antibodies. For GFP and Met-enkephalin donkey anti-Rabbit Alexa Flour 488 (1:500, Thermofisher, AB2535792) or donkey anti-rabbit Alexa Flour 568 (1:500, Abcam, AB175692) for TH, donkey anti-Sheep Alexa Flour 568 (1:500, Abcam, AB175712) diluted in 5% normal goat serum, 0.3% Triton X-100 in PBS. The nuclear stain DAPI (1:1000, Thermofisher) was added at the final 30 minutes of this incubation period. Slices were then washed (3 x 10 min) in PBS and mounted onto using Prolong Gold Antifade (Life Technologies). Slices were imaged on either a Nikon C2 confocal microscope or Lecia Thunder wide-field microscope.

For electrophysiology experiments, coronal slices (280 μM) were fixed overnight in 4% PFA at 4°C. These slices were subsequently washed three times with PBS and stored in cryoprotectant solution at -30°C until immunohistochemical processing. Before staining, the cryoprotectant was

removed from slices through six PBS washes. Slices were then incubated for 1 hour at room temperature in blocking solution containing 10%

K. Pavlovian behaviour paradigm

All behavioural experiments were carried out by collaborators at The University of New South Wales, Sydney.

Conditioned suppression was used as the measure of fear in all experiment (J. O. Yau, C. Chaichim, J. M. Power, & G. P. McNally, 2021). The rats first received magazine training (Day 1) with fixed ratio 1 (FR1) reinforcement in addition to free pellets every 300 seconds. Magazine training terminated after 60 minutes or when the rats reached 100 lever presses. Training progressed on day 2 with FR1. On day 3, level pressing was maintained on a variable interval (VI) 30 second schedule. On day 4 and until the end of the experiment, rats were maintained on a VI 60 second schedule. All session terminated at 60 minutes unless noted otherwise. On days 9-10 rates were pre-exposed to the conditioned stimuli with four presentations of each 60 second CS per sessions, with intertrial intervals between 400 and 720 seconds. To prepare for fibre photometry rats were tethered to dummy patch cables on days 7-9.

Rats then underwent fear conditioning on days 11-14. Each day, the rat was connected to patch cables delivering at least 10 mW of 625 nm light before starting the session. Fear conditioning consisted of four pairing per session of

a 30 second auditory stimulus (85 dB, 18 kHz) that co-terminated with a 0.5 second, 0.5 mA footshock. The intertrial intervals ranged from 500 to 900 seconds. On Day 15, rats were tested for fear responses with four presentations of the CS alone (no shock).

L. Fibre Photometry

All behavioural experiments were carried out by collaborators at The University of New South Wales, Sydney (J. O.-Y. Yau, C. Chaichim, J. M. Power, & G. P. McNally, 2021)

Fibre photometry recording was made during each CS-US pairing using fibre photometry systems from Doric lenses and Tucker Davis Technologies (RZ50, Synapse). Two excitation wavelengths, 495 nm (sensor signal) and 405 nm (isosbestic control signal) from Doric LEDs controlled by dual channel programmable LED drivers, were channelled into 0.39 NA, 400 mm core multimode prebleached patch cables via a Doric Dual Fluorescence Mini Cube (FMC2, Doric Lenses). Light intensity at the patch tip was maintained at 10-30 mW across sessions to prevent photo-bleaching. The sensor and isosbestic fluorescent signals were relayed through patch cables, amplified and measured by Doric Fluorescence Detectors. Signals were digitized at 1kHz and recorded and analysed using Synapse software. The 405 nm isosbestic signal was used to control for movement artifacts and photobleaching.

M. Statistical analysis

Statistical analyses were conducted without predetermined sample size calculations. Data were assumed to follow normal distributions. Equal variance was also assumed throughout and was not formally tested. All results are presented as mean ± SEM, with two-sided statistical testing performed. Statistical significance was evaluated using appropriate parametric and non-parametric approaches depending on data characteristics. Parametric analyses included paired and unpaired Student's tests, repeated measured ANOVA and one-way ANOVA with Tukey's post hoc corrections where multiple comparisons were necessary. Non-parametric tests include Mann-Whitney U tests with Fisher's post hoc adjustment, where appropriate. Statistical analysis was performed using Graphpad Prism (version 8.0)

Chapter 3

Auditory thalamic activation triggers endogenous opioid release in the amygdala

A. Introduction

Endogenous opioids play a complex role in fear learning that extends beyond their traditional association with pain inhibition (Gavan P. McNally, 2009). While initially thought to primarily influence fear acquisition through analgesic effects (Bolles & Fanselow, 1980), more recent evidence have revealed their direct involvement in fear learning (Gavan P. McNally, 2009). The best evidence for this comes from studies showing that systemic administration of the opioid receptor antagonist naloxone enhances both first- and second-order fear conditioning, with the latter occurring in the absence of direct painful stimuli (Michalscheck et al., 2021). These findings indicate endogenous opioids actively inhibit fear learning through mechanisms independent of pain processing. This suggests that endogenous opioids are released during this learning and then act on the LA related circuits to modify plasticity and thus learning.

The behavioural effects of naloxone on fear learning (Michalscheck et al., 2021) suggests that endogenous opioids must be expressed within fear learning circuits to modulate this learning. Within the amygdala, endogenous opioids peptides show distinct patterns of expression across various subregions that are involved in fear learning (Jean-François Poulin et al., 2006). The endogenous opioid, enkephalin is prominently expressed in the aITCs surrounding the LA and in the CeA. Enkephalin expression is also found at a low but detectable level within the LA itself (Jean-François Poulin et al.,

2006). This distributed expression suggests multiple potential sources of endogenous opioids that could influence fear learning.

The neighbouring ASt is another potential source as it contains a particularly significant population of enkephalinergic neurons. Recent single-cell RNA sequencing reveals that the ASt contains distinct populations of D1 and D2 expressing MSNs (Y. Wang et al., 2023), mirroring the striatal MSN populations (Gagnon et al., 2017). In the striatum, these MSN population are precisely organised, with D1 expressing MSN (about 45% of neurons) producing dynorphin and substance P (Gagnon et al., 2017), while D2 expressing MSN (about 45% of neurons) producing enkephalin (Gagnon et al., 2017), with the remaining neurons being primarily cholinergic interneurons (Gagnon et al., 2017). This molecular pattern appears to be conserved in the ASt as evidenced by mRNA data showing similar D1 and D2 MSN co-expressing with dynorphin and enkephalin respectively (Y. Wang et al., 2023). The presence of enkephalin expressing neurons (Y. Wang et al., 2023), combined with dense MGN innervation of the ASt (J. E. LeDoux et al., 1990), suggests that sensory input could drive significant endogenous opioid release, providing a key source of endogenous opioids during fear learning.

The distribution of opioid receptors within the fear circuits suggests multiple potential sites where released enkephalin could modulate fear learning. Moderate levels of MOR and high levels of the DOR are expressed within the BLA (Jean-François Poulin et al., 2006). Additionally strong expression of MORs in the MGN have been found in radioligand and in-situ hybridisation

studies which suggests that MGN neurons express MOR (Alfred Mansour et al., 1994; Sharif & Hughes, 1989). This anatomical arrangement suggests that enkephalin released during fear learning could act to inhibit MOR containing MGN inputs projecting to the amygdala, thus acting as a fear inhibiting neurotransmitter.

The role of the MGN-LA circuit is well characterised in fear conditioning (J. LeDoux, 2003), however, how endogenous opioids modulate information processing at these synapses remains poorly understood. Previous studies have identified several mechanisms through which opioids influence fear circuits. Firstly, MOR opioids activate voltage-dependent potassium channels in putative LA pyramidal neurons, which reduces their excitation by synaptic inputs (Faber & Sah, 2004). Secondly, opioids can regulate local inhibitory networks, with MOR activation decreasing GABAergic transmission in local inhibitory circuits, including reducing inhibition in the BLA (Gabrielle C. Gregoriou, Kissiwaa, Patel, & Bagley, 2019; Winters et al., 2017). These two sites of action provide a potential mechanism for how endogenous opioids might alter synaptic plasticity at the MGN-LA synapse. While these effects on postsynaptic excitability and inhibitory control are established, the question of whether opioids directly modulate sensory information delivery via MGN-LA inputs have not been addressed. Thus, understanding the cellular mechanisms by which endogenous opioids may regulate MGN-LA transmission is essential for determining their role in LA dependent learning.

Peptidases exert powerful control over opioid signalling through degradation mechanisms that limit the duration of peptides action (Marvizon et al., 2003). Three key peptidases, APN, NEP and ACE are widely distributed throughout the brain and cleave enkephalins at specific peptide bonds, rapidly terminating their signalling (Hui, Wang, & Lajtha, 1983; Schwartz, 1983; Waksman et al., 1986). Importantly, these peptidases show substrate specificity. Whilst met-enkephalin is rapidly degraded by all three peptidases, β-endorphin is resistant to APN hydrolysis (Hui et al., 1983). This regulation is evident in studies using the specific peptidase inhibitors, thiorphan (NEP inhibitor), captopril (ACE inhibitor) and bestatin (APN inhibitor), which significantly enhance met-enkephalin induced receptor activation but have minimal effect on β-endorphin (Marvizon et al., 2003). In the amygdala specifically, recent studies in the IM show that inhibition of glutamate release by enkephalin increases when all three peptidase inhibitors are present (G. C. Gregoriou et al., 2020). However, inhibition of neprilysin alone produces similar enhancement, indicating it is the predominant peptidase regulating enkephalin signalling in this region (G. C. Gregoriou et al., 2020). This tight peptidase control over enkephalin signalling suggests that the duration and spread of opioid action in fear circuits is precisely controlled. This could have important implication for how these peptides may modulate neural activity or potentially influence synaptic plasticity mechanisms, with the balance between release and degradation shaping the acquisition and expression of fear. In addition, peptidase inhibitors can be used as experimental tools to enhance endogenous opioid concentrations and thus allow detection of low levels of peptide release and

additionally, the sensitivity of endogenous opioids to peptidases may help establish which endogenous opioid is being detected.

Understanding how endogenous opioids may inhibit fear learning requires precise measurement of when and where peptide release occurs during the learning process. However, studying neuropeptide signalling has historically been challenging due to technical limitations. While microdialysis has been the standard for measuring extracellular concentrations (Chefer et al., 2009; Qian, Wang, Xia, & Li, 2023), its sampling rate is slow, typically 10 minutes (Chefer et al., 2009; Qian, Wang, Xia, et al., 2023) and therefore, cannot capture the rapid dynamics of neuropeptide signalling during complex behaviours (Fig 3.1 A) (Al-Hasani et al., 2018). Fast-scan cyclic voltammetry offers better temporal resolution (within 10 ms of stimulus) (Qian, Wang, Xia, et al., 2023; Robinson, Hermans, Seipel, & Wightman, 2008) and better sensitivity with measurements of concentration down to 1 nM possible (Robinson et al., 2008), but it is not well established to study neuropeptide concentrations (Fig 3.1 B) (Inutsuka, Ino, & Onaka, 2021). Alternative approaches using indirect measurements, such as monitoring opioid effects on presynaptic glutamate release (Winters et al., 2017), can precisely detect endogenous opioid release, but cannot distinguish between different peptides and how far these opioids spread (Fig 3.1 C).

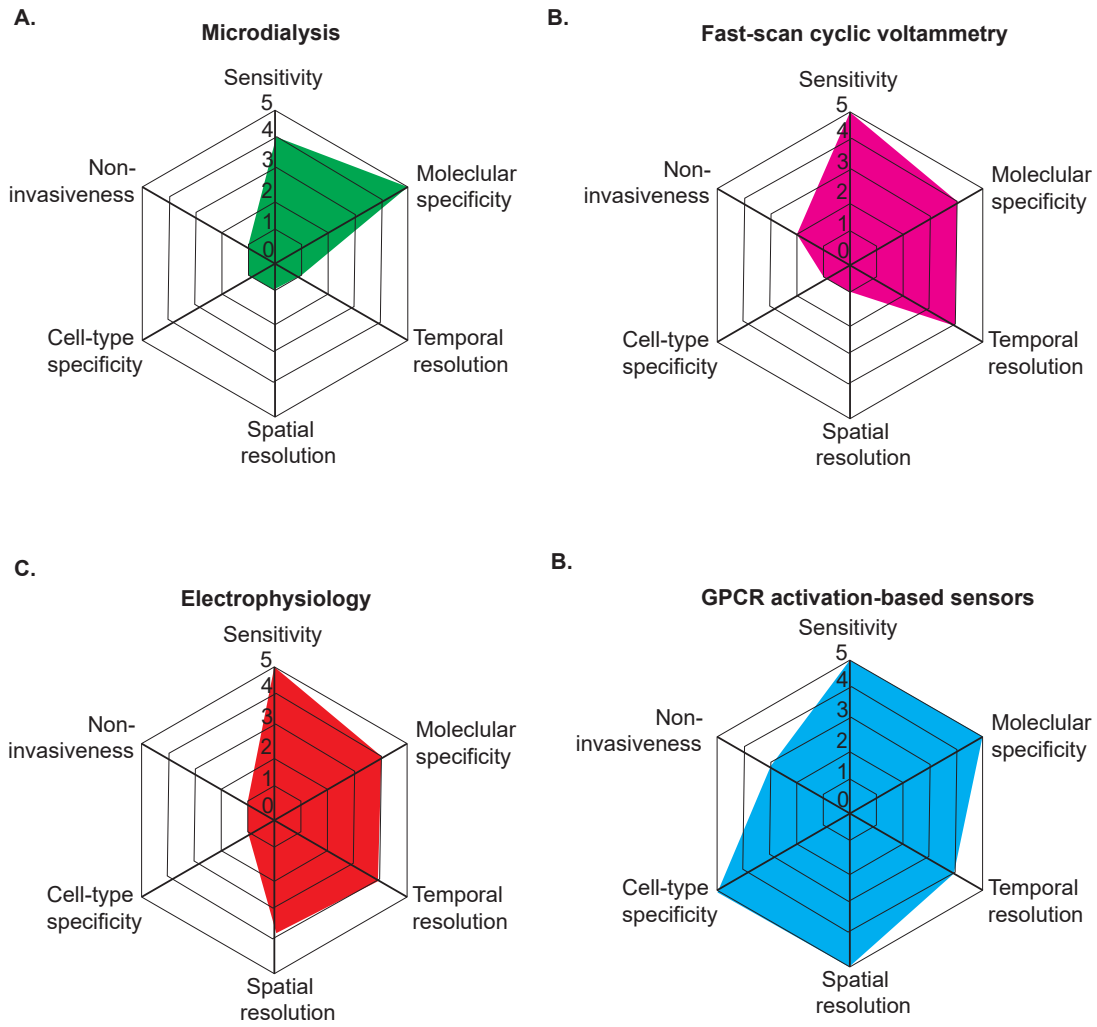

Figure 3.1. Overview of common methods for detecting peptide transmission. (A-B) Radar graphs summarising each methods properties including, sensitivity, molecular specificity, temporal resolution, spatial resolution, cell-type specificity, and non-invasiveness with each property ranging from 0 to 5. Figure adapted from Qian *et al* (2023)

These technical limitations have particularly hindered understanding of how endogenous opioids modulate neural circuits during rapid events like fear learning, where precise timing of multiple neuromodulators release may be crucial for associative plasticity. Recent development of genetically encoded GPCR-activation based sensors has enabled more direct visualisation of opioid receptor activation with high temporal resolution.

There are two genetically encoded opioid receptor-based sensors, with one a mutant DOR and one a mutant MOR. Both of these sensors have a cpGFP insertion between the 3rd intracellular loop and 6th transmembrane domain (Dong et al., 2024; Rappleye et al., 2022). Insertion of the cpGFP eliminates the receptor's β-arrestin and G-protein signalling capabilities but when agonists bind to these receptors, the resulting conformational change increases fluorescence emitted by the receptor (Dong et al., 2024; Rappleye et al., 2022). These fluorescent changes enable real-time visualisation of opioid receptor activation and thus inference of the extracellular opioid concentration.

The mutation of the native receptors into GPCR-sensors can change their pharmacological profile. The DOR based sensor, δ-light, maintains the pharmacological selectivity of the native receptor (Dong et al., 2024). The sensor detects met-enkephalin binding with high sensitivity (EC50 ~ 6.5 nM) (Dong et al., 2024) closely matching the affinity of met-enkephalin for the native DOR (pIC50 ~ 7.4 nM) (Hui et al., 1983). Similar to the native DOR, met-enkephalin exhibits higher potency at activating the sensor compared to dynorphin A and β-endorphin, and agonist responses are blocked by the DOR selective antagonist ICI 174,864 and the non-selective antagonist naloxone (Dong et al., 2024). In contrast, the pharmacology of the MOR based sensor, UMASS, differs from native MOR. Whilst it has good, albeit lower, sensitivity to met-enkephalin (KD = 99 nM), it has low sensitivity to the other endogenous MOR agonist β-endorphin (Rappleye et al., 2022). Similarly to the native MOR, UMASS has low sensitivity to dynorphin A and agonist actions are blocked by

naloxone (Rappleye et al., 2022). Therefore, both δ-light and UMASS can sensitively detect enkephalin in a highly selective manner over the other endogenous opioids.

A significant difference between the sensors is their subcellular localisation. Whilst δ-light is primarily localised to the soma of the neuron, as the sensor contains a proximal restriction and clustering tag at its C-terminus (Dong et al., 2024), UMASS has membrane trafficking and endoplasmic reticulum export sequences (Rappleye et al., 2022). This results in a broader distribution of UMASS throughout the plasma membrane, including on the dendritic branches (Rappleye et al., 2022). The differences in sensor location may therefore sample opioid concentrations at different sites on the cell.

These opioid sensors enable more direct detection of the extracellular endogenous opioid concentration in behaving animals. To do this both sensors can be packaged into adeno-associated viruses (AAVs) and expressed in specific brain regions to monitor opioid signalling *in vivo*. In the NAc, these sensors reveal precise patterns of opioid concentration change, where time-locked changes in fluorescence were detected during reward-seeking behaviours and specifically blocked by opioid antagonists indicating opioid receptor activation (Dong et al., 2024). While these sensors have primarily been validated with reward-related behaviours, their ability to detect real-time opioid dynamic makes them particularly valuable for investigating rapid neural events during fear learning, where precise timing of neuromodulator release

may be crucial for associative plasticity and learning. Moreover, the differential sensitivity of these sensors to the various opioid peptides (Dong et al., 2024; Rappleye et al., 2022), combined with distinct peptidase regulation of these peptides (Hui et al., 1983), provides a powerful strategy for distinguishing which endogenous opioid is released during behaviours. These technological advances provide powerful new tools for investigating how endogenous opioids modulate neural circuits during aversive learning.

Given the strong enkephalin expression in the ASt and dense MGN innervation patterns, combined with the localised distribution of the endogenous opioid system, it was hypothesised that: *increased MGN activity drives endogenous opioid release in the ASt*, *which would act through MOR to inhibit glutamate release from the MGN-LA pathway, thereby reducing fear learning.* This study represents a critical step in understanding how neurotransmitter modulation shapes fear learning mechanisms

The specific aims of Chapter 3 are:

1. To characterise the anatomical and functional properties of the MGN projection to the LA and the ASt
2. To determine whether MGN activation triggers endogenous opioid release in the amygdala
3. To examine dynamics of endogenous opioid signalling during fear learning

B. Results

3.1 The anatomical and functional properties of the MGN projection to the LA and the AST

This section addresses aim 3.1: To characterise the anatomical and functional properties of the MGN projection to the LA and the ASt.

To address aim 3.1, I will determine the nature, strength and opioid sensitivity of the AST synaptic input to the LA and the ASt.

3.1.1 The auditory thalamus projects to both ASt and LA

The MGN provides a major source of auditory and other information to the amygdala (J. E. LeDoux et al., 1990), with its projections to the lateral amygdala being crucial for auditory fear learning (Quirk et al., 1997). Specific MGN projections to only fear responsive neurons in the ASt have also been identified (Kim & Cho, 2017). However, whether MGN inputs are differentially distributed to distinct output pathways within the LA remain unknown and while anatomical tracing studies have shown projections to the ASt (J. E. LeDoux et al., 1990), the functional connectivity to the general ASt population has not been characterised. Therefore, in these experiments I aimed to examine how MGN inputs are organised within the amygdala and ASt circuits. I first wanted to confirm these established pathways form the MGN-LA as well as provide additional anatomical detail for MGN-ASt projections.

To compare the connectivity of the MGN to the LA and ASt, a virus expressing an anterograde green-fluorescent protein and an excitatory opsin (AAV8-Syn-

ChR2(H134R)-GFP) was microinjected into the MGN (Fig 3.2 A). In particular, I targeted the PiL as this subregion provides the densest projections to the LA (J. E. LeDoux et al., 1990). After a minimum of 6 weeks, post-hoc immunohistochemistry was performed to stain for GFP, this allows for visualisation of MGN terminal fields in the amygdala. A total of 16 rats successfully expressed the opsin in the medial geniculate nucleus (Fig 3.2 B). Intense GFP fluorescence was detected in the medial geniculate nucleus, with GFP^+ cell bodies located within the PiL (Fig 3.2 C). Consistent with previous tract-tracing experiments (J. E. LeDoux et al., 1990), the projection from the PiL resulted in moderate terminal expression in the LA (Fig 3.2 D). Notably, examination of the ASt revealed much denser GFP expression (Fig 3.2 D). The high density of MGN terminals in the ASt suggests this region may receive strong auditory input, potentially enabling more robust responses to auditory stimuli. These anatomical tracing experiments confirm that there are moderate levels of MGN terminals in the LA and much higher levels in the ASt, showing a pattern consistent with previous studies of the MGN projection in the LA (J. E. LeDoux et al., 1990; Leppla et al., 2023; J. A. Taylor et al., 2021) and indicating a more general projection pattern rather than to specific fear-responsive neurons in the ASt (Kim & Cho, 2017)

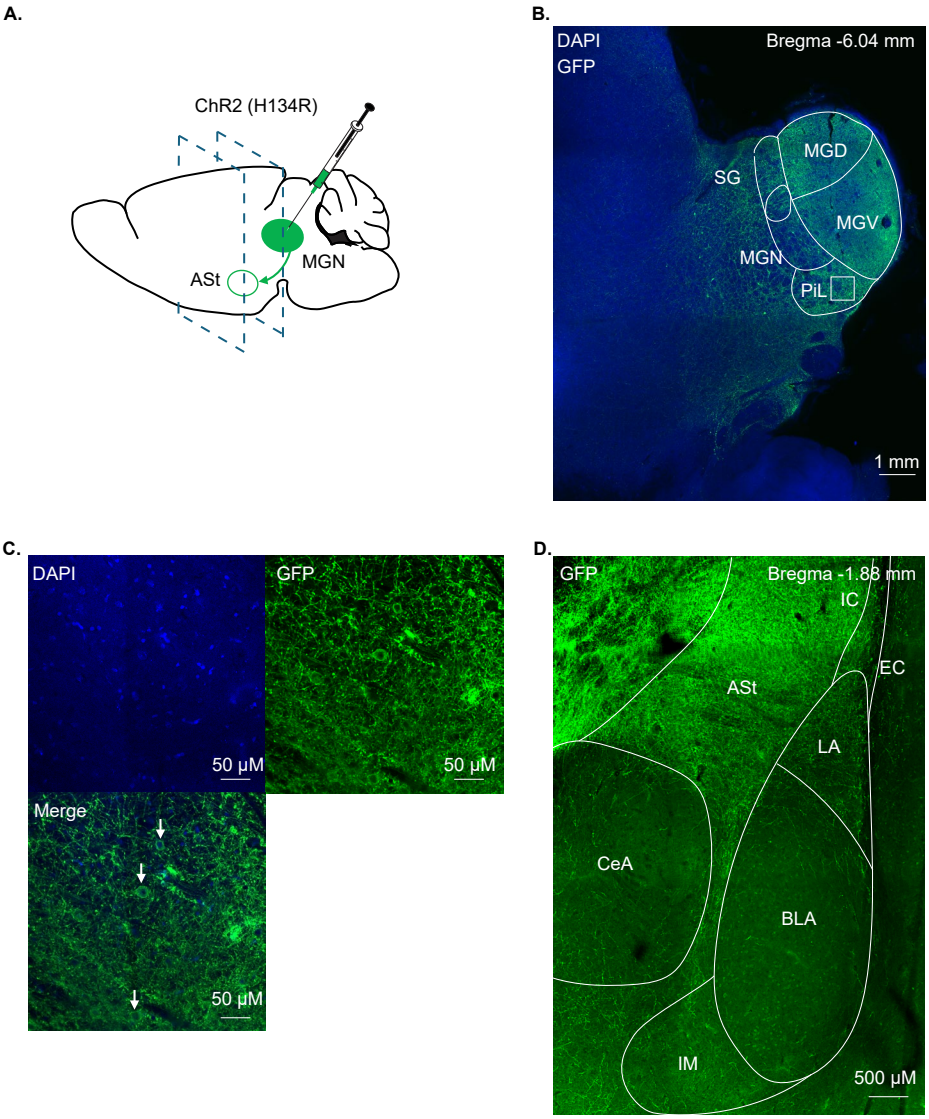

Figure 3.2. Projections from the MGN target the ASt and LA. (A) Sagittal schematic diagram indicating AAV8-Syn-ChR2(H134R)-GFP injections into the MGN (B) Low magnification confocal image of DAPI (blue) and GFP (green) expression in the MGN. Expression was seen in all subregions of the medial geniculate nucleus and GFP$^+$ positive cell bodies were found localised in the PiL. (C) High magnification image of white box in B showing colocalisation of DAPI (blue) and ChR2-GFP (green). White arrows indicate GFP$^+$ cells (D) Low magnification confocal image showing Chr2-GFP (green) expression in the amygdala. High levels of GFP expression seen in the ASt and moderate levels in the LA. Bregma coordinates indicated on the bottom let of images. ASt – amygdalo-striatal transition zone, BLA – basolateral amygdala, CeA – central amygdala, EC – external capsule, IC – internal capsule, IM – main island intercalated cells, LA – lateral amygdala, MGD – dorsal medial geniculate body, MGN – medial geniculate nucleus, MGV – ventral medial geniculate body, PiL – posterior intralaminar complex, SG – supra geniculate nucleus.

3.1.2 Auditory thalamus engages both fear and reward circuits

The MGN provides input to both the LA and the ASt (Fig 3.2). (Ressler & Maren, 2019). Given the importance of the MGN-LA synapse in fear learning (J. LeDoux, 2003), understanding its projection patterns to reward and aversive circuits may reveal how sensory inputs are distributed to these functionally distinct pathways. Previous studies have characterised MGN connections to randomly selected LA neurons (Kwon et al., 2014), but whether MGN inputs specifically target output neurons projecting to different downstream regions remains unknown.

To identity LA neurons that project to these downstream targets, red-orange retrograde tracing beads (FluoSpheres) were microinjected into the CeA or NAc (Fig 3.3 A). After a minimum of 3 days, coronal brain slices containing the amygdala and NAc were taken for imaging. Post-hoc imaging of bead expression revealed successful targeting of the NAc injection site, with fluorescent beads confined to NAc core subregions (Fig 3.3 B). Similarly, examination of the CeA injection sites revealed localisation of fluorescence beads with the targeted region (Fig 3.3 C).

Within the amygdala, there was a high density of bead positive neurons in both the LA and the BLA (Fig 3.3 D and E). Whilst the BLA is considered the main output region of the amygdala (Beyeler et al., 2016), these findings demonstrate that the LA itself maintains direct projections to regions involved in distinct behavioural responses.

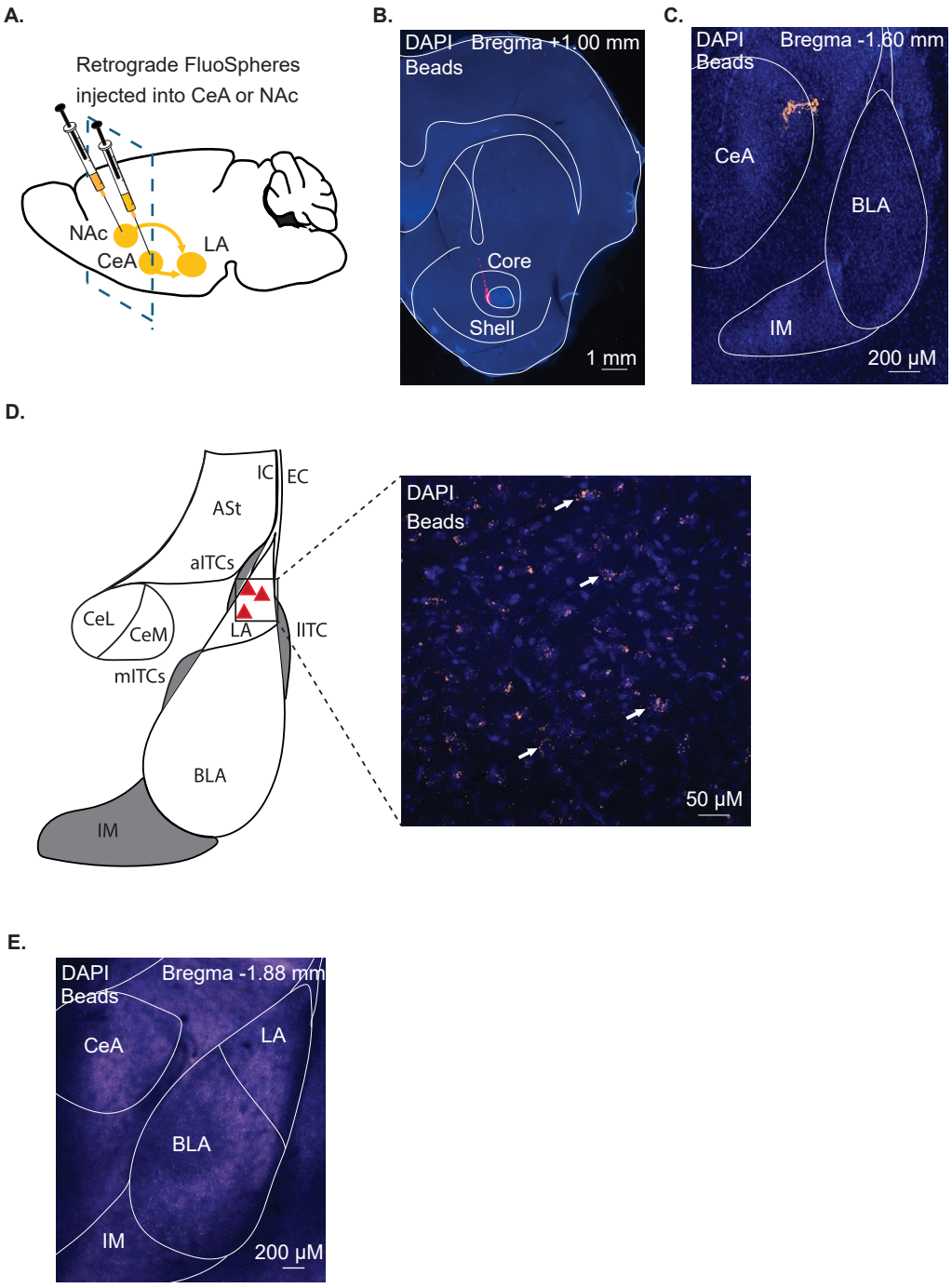

Figure 3.3. LA putative principal neurons projects to both the CeA and the NAc core. (A) Sagittal schematic diagram indicating retrogradely tracing beads (FluoSpheres (red-orange 565/580) injection into either the NAc or CeA (B) Low magnification confocal image of DAPI (blue) and bead (red) injection in the NAc. Beads were found localised within the NAc core. (C) Low magnification confocal image of DAPI (blue) and bead (red) injection in the amygdala. Beads were seen confined within the CeA (D) Schematic of amygdala showing location of projection neurons within the LA and a high magnification image of DAPI (Blue) and beads (red) in the lateral amygdala. White arrows indicate bead positive neurons (E) Low magnification confocal image of DAPI (blue) and bead (red) expression in the amygdala resulting from a NAc injection. Bregma coordinated for

indicated on bottom left of images. Similar levels of beads were found in the LA and BLA. BLA – basolateral amygdala, CeA – central amygdala, IM – main island intercalated cells.

Having identified LA neurons that project to the CeA and NAc (Fig 3.3), the next aim was to determine whether MGN inputs differentially innervate these distinct projection populations. To do this a virus expressing the excitatory opsin CHR2 (AAV8-Syn-ChR2(H134R)-GFP) was microinjected into the MGN concurrently with a microinjection of the retrograde tracing beads into either the CeA or NAc (Fig 3.4 A). At least 6 weeks later whole-cell patch clamp recordings were conducted in acute brain slices containing bead positive LA neurons. This approach enables selective activation of MGN inputs onto identified LA projection neurons. The membrane potential of bead positive neurons was voltage-clamped at -70 mV to prevent activation of voltage-gated conductance's and to isolate AMPA receptor mediated currents. To isolate direct MGN inputs and in order to eliminate any contamination from local inhibitory circuits, recordings were performed in the presence of the $GABA_A$ receptor antagonist picrotoxin (100 μM).

Paired pulse blue light (475-495 nM) stimulation of MGN terminals in the LA resulted in optically evoked excitatory post-synaptic currents (oEPSCs) in bead-containing principal neurons (Fig 3.4 B). These responses were significantly inhibited by the AMPA/kainate receptor antagonist CNQX (10 μM), indicating they were mediated by glutamate (Baseline: 64.39 ± 9.55 pA; CNQX: 15.59 ± 3.39 pA, P = 0.01, n = 4, paired Student's t-test baseline versus CNQX, Fig 3.4 B and C). Synaptic jitter, measured as the standard deviation

of response latencies from stimulus onset, was used to help determine whether the connection direct. A jitter of < 0.7 ms is indicative of direct monosynaptic connections (Doyle & Andresen, 2001). A single cell, with a jitter of 1.57 ms, was excluded from further analysis. For the remaining cells the jitter was 0.24 ± 0.1 ms (n = 25). This suggests that a very large proportion of LA neurons receiving MGN input are receiving monosynaptic connections.

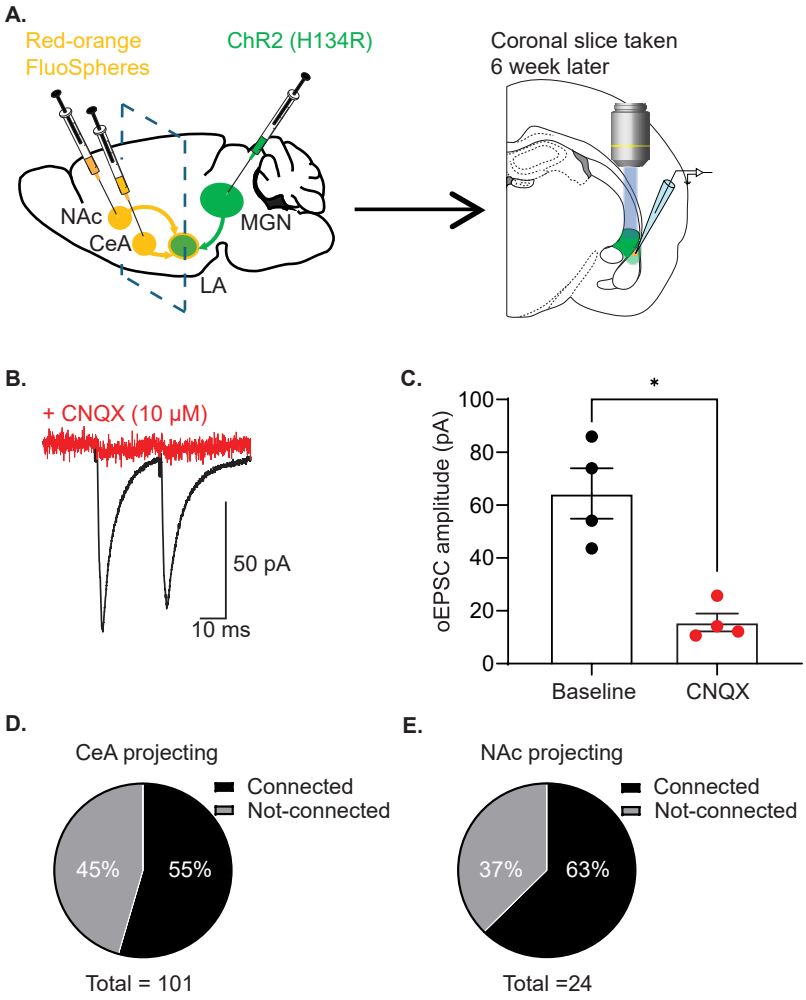

Figure 3.4. The MGN forms synaptic connections with LA projection neurons. (A) Sagittal schematic diagram indicating AAV8-Syn-ChR2(H134R)-GFP into the MGN concurrently with retrogradely tracing beads (FluoSpheres (red-orange 565/580)) into either the CeA or NAc. Coronal schematic diagram of the amygdala indicating recording location. Bead positive neurons in the lateral amygdala were chosen. (B) Representative trace from a bead positive LA neuron showing baseline amplitude of oEPSC and inhibition by CNQX (10 µM). (C) Graph showing inhibition of oEPSC amplitude by CNQX. Each point on the graph represents a single neuron. Bars on graph represent the mean ± SEM.

* P < 0.05 paired Student's t-test baseline versus CNQX (D) Pie chart chowing percentage of connected versus not connected neurons in the CeA (E) Pie chart chowing percentage of connected versus not connected neurons in the NAc

In total, oEPSCs were detected in 55% of CeA-projecting and 63% of NAc-projecting neurons (Fig 3.4 D and E). The oEPSCs in the CeA-projecting neurons had an average amplitude of 94.99 ± 11.48 pA (n = 25), while NAc-projecting neurons showed an average amplitude of 98.72 ± 16.82 pA (n = 15, mean ± SEM). There were no significant differences in the MGN innervation patterns to either projection populations (CeA-projecting: 55/101 connected, NAc-projecting: 15/24 connected Fisher's exact test, P = 0.71, Fig 3.4 D and E). Additionally, the amplitude of oEPSCs in both CeA and NAc-projecting neurons was comparable to previously reported MGN-evoked response in unlabelled LA principal neurons (> 100 pA) (Kim & Cho, 2017; Kwon et al., 2014; Lucas, Jegarl, Morishita, & Clem, 2016). These recordings demonstrate that the MGN is functionally connect to both CeA and NAc-projecting LA neurons, with equivalent connectivity rates and similar responses amplitude between these populations. This distribution of MGN inputs to LA neurons indicates that MGN inputs are not selectively distributed based on their downstream projections.

3.1.3 Auditory thalamic inputs show rostral-caudal organisation in the LA

Previous anatomical studies have demonstrated that MGN projections to the LA follow a rostral-caudal gradient, with denser MGN innervation of caudal amygdala regions (J. E. LeDoux et al., 1990). To determine whether this anatomical organisation is reflected in functional connectivity, I compared the

GFP expressing terminal intensity and the rate of oEPSC connections in rostral amygdala slices (Fig 3.5 A, anterior-posterior Bregma coordinate of < -1.60 mm) (J. E. LeDoux et al., 1990)and caudal amygdala slices (Fig 3.5 B, anterior-posterior Bregma coordinate of > -1.60 mm) (J. E. LeDoux et al., 1990).

Post-hoc analysis revealed GFP intensity is higher in caudal than rostral amygdala sections (Fig 3.5 A and B). Examination of the functional connectivity data from these slices showed that a higher proportion of MGN-connected LA neurons were found in caudal amygdala slices (Rostral: 26.7% responders; Caudal: 75.4% responders, P = 0.003, Fisher's exact test, Fig 3.5 C). This rostral-caudal difference was observed in both CeA and NAc-projecting populations. Together, these data demonstrate that the MGN has stronger synaptic inputs to the caudal amygdala and suggest that auditory processing in the amygdala may be organised along the rostral-caudal axis.

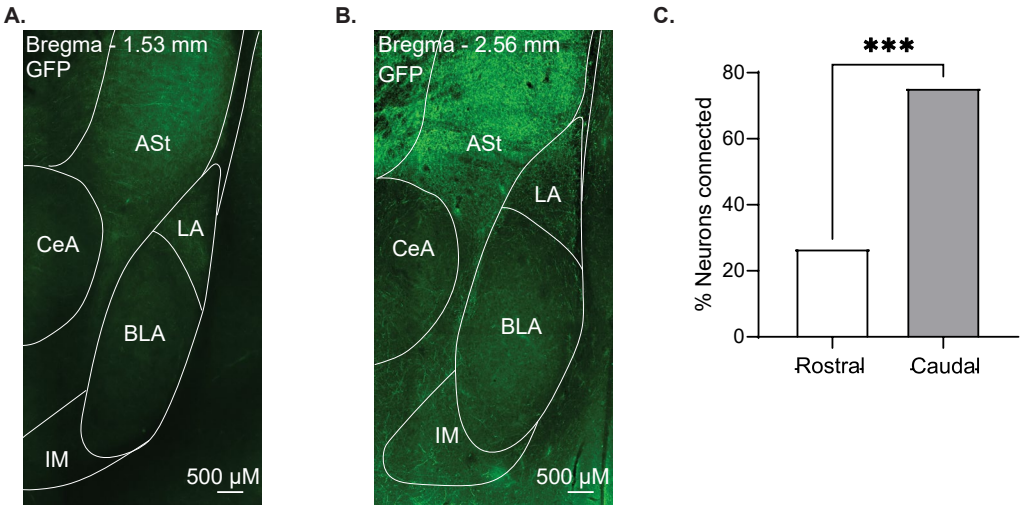

Figure 3.5. MGN synaptic inputs preferentially target the caudal amygdala. (A). Low magnification confocal image of GFP (green) in rostral amygdala (Bregma -1.53 mm).

Relatively sparse GFP-expression is seen in the ASt and LA. (B) Low magnification confocal image of GFP (green) in caudal amygdala (Bregma – 2.56 mm). Compared to rostral amygdala the ASt and LA showed strong GFP-expression. (C) Graph showing higher percentage of cells responsive to optical stimulation of MGN terminals in caudal (bregma -2.56 mm) than in rostral (bregma -1.53 mm) amygdala slices. *** P < 0.005, Fisher's exact test. ASt – amygdalo-striatal transition zone, BLA – basolateral amygdala, CeA – central amygdala, IM – main island intercalated cells, LA – lateral amygdala. Bars on graph represent % neuron connected

3.1.4 Opioids inhibit auditory MGN terminals in the LA through MOR activation

It is possible that endogenous opioids could inhibit fear learning by modulating the MGN to LA synapse, however the opioid sensitivity of this synapse is unknown. Given that there is evidence for expression of MOR in MGN neurons, based on radioligand and mRNA studies (Alfred Mansour et al., 1994; Sharif & Hughes, 1989), I next investigated whether MOR and DOR opioids could modulate glutamate release from the MGN terminals in the LA. To specifically isolate and investigate opioid receptor expression at the MGN-LA pathway, the excitatory opsin ChR2 (AAV8-Syn-ChR2(H134R)-GFP) was microinjected into the MGN as per the experiment above. Whole-cell patch clamp recordings from LA putative pyramidal neurons, visually identified by their morphology, were performed at -70 mV (Fig 3.6 A) in the presence of the $GABA_A$ receptor antagonist picrotoxin (100 μM).

To determine whether MOR activation inhibits glutamate release from MGN terminals I bath applied selective opioid receptor agonists and antagonists and determined whether they alter the oEPSC amplitude or altered the paired pulse ratio. Application of the selective MOR agonist DAMGO (1uM) significantly inhibited oEPSCs in all recorded neurons (45.24 ± 6.66%

inhibition from baseline; baseline: 93.32 ± 12.62 pA; DAMGO: 46.72 ± 9.04 pA; P = 0.02, n = 8, paired Students t-test, Fig 3.6 B and C) with a concurrent significant increase in paired-pulse ratio (PPR) (baseline: 0.69 ± 0.05 PPR; DAMGO: 0.91 ± 0.07 PPR, P = 0.02, n = 8, paired Students t-test, Fig 3.6 D). This inhibition was completely reversed by CTAP (Fig 3.6 E, 8.09 ± 3.72% inhibition of oEPSC; DAMGO: 46.72 ± 9.04 pA; CTAP: 85.54 ± 17.77 pA, P = 0.003, n = 8 paired Students t-test). These results demonstrate that MOR activation reduces glutamate release from MGN terminals through a presynaptic mechanism, as evidence by the decreased amplitude and increased paired-pulse ratio.

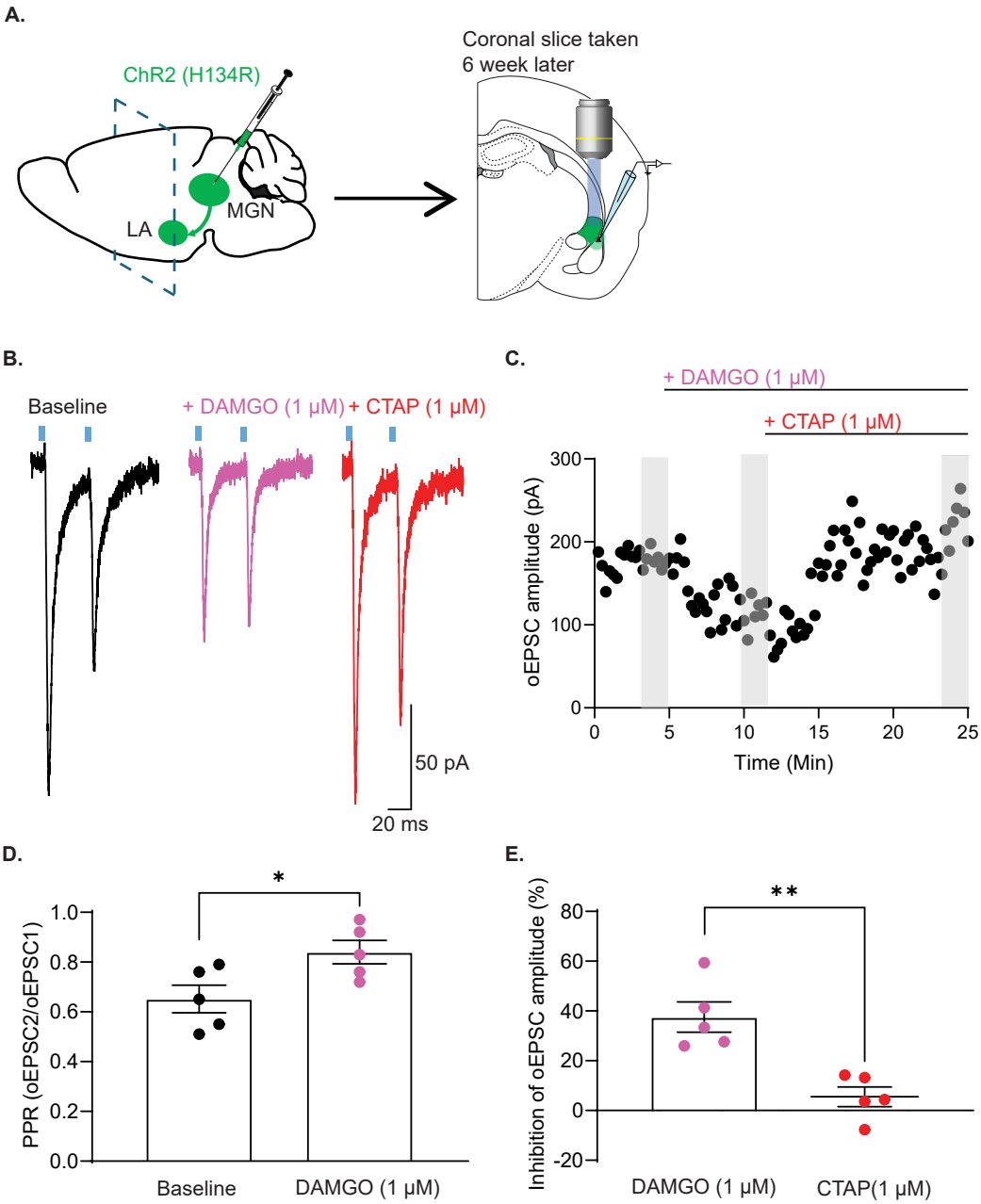

Figure 3.6. Activation of presynaptic MOR on MGN terminals inhibit glutamate release in LA (A) Sagittal schematic diagram indicating AAV8-Syn-ChR2(H134R)-GFP injection into the MGN. Coronal schematic diagram indicating recording location in the LA. (B-C) representative traces and time plot from a putative LA projection neuron showing baseline amplitude of oEPSC at MGN-LA synapse and inhibition of amplitude following application for DAMGO (1 μM) and then reversal by CTAP (1 μM). Blue bars on trace represent optical stimulation points. Grey bars on time plot illustrate where baseline and drug effects were measured. (D) Graph of PPR in baseline and DAMGO. * $P < 0.05$, ** $P < 0.01$ paired student's t-test. (E) Graph showing percentage inhibition of oEPSC amplitude (from baseline) by for DAMGO (1 μM) and then reversal by CTAP (1 μM). Bars on graph represent mean ± SEM

In contrast, when the DOR-selective agonist and then antagonist were applied in the presence of CTAP, no change in the oEPSC amplitude was observed (Deltorphin II: 2.98 ± 1.75% inhibition from baseline, P = 0.13, n = 4, paired Students t-test, ICI 174,886: - 0.03 ± 2.53% inhibition from baseline, P = 0.79, n = 3, paired Student's t-test, Fig 3.7 A and B, data expressed as mean ± SD). Together this data indicates that glutamate release at MGN-LA synapses is inhibited by activation of MOR but not DOR. This may be a potential mechanism through which endogenous opioids could limit fear learning by inhibiting the MGN activation of LA neurons that is important for fear learning.

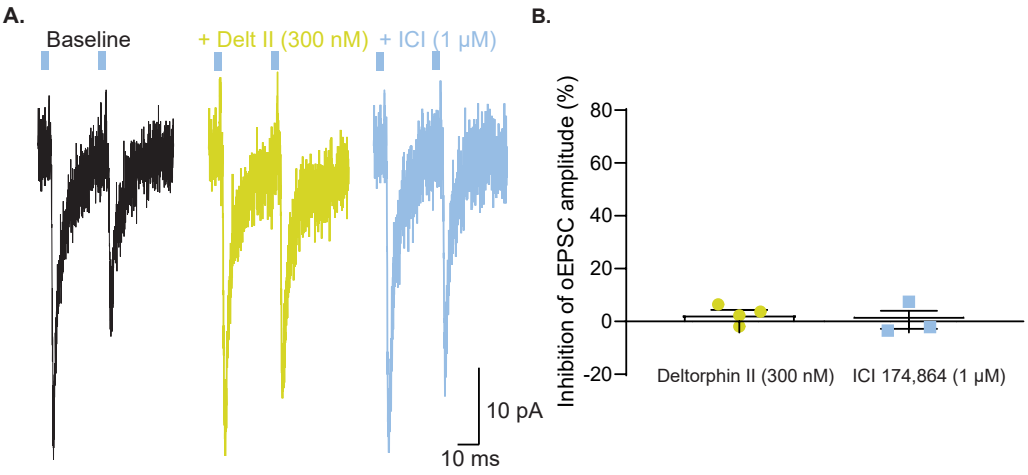

Figure 3.7. Presynaptic MGN terminals are not DOR sensitive. (A) Representative traces and from a putative LA projection neuron showing baseline amplitude of oEPSC after CTAP at MGN-LA synapse and no effects on amplitude following application for Deltorphin II (300 nM) and ICI 137,864 (1 μM). Blue bars on trace represent optical stimulation points. (B) Graph showing percentage inhibition of oEPSC amplitude (from baseline) with no effects Deltorphin II (300 nM) and ICI 137,864 (1 μM). Bars on graph represent mean ± SD.

3.1.5 Projections from the MGN strongly target the ASt

Previous anatomical data showed dense MGN terminal expression in the ASt (Fig 3.2), but whether these terminals form functional synapses onto ASt neurons remained to be determined. As the ASt is predominantly comprised

of MSNs (Y. Wang et al., 2023), I next investigated whether MGN inputs form function connections to putative MSNs in the ASt.

To investigate the connectivity of MGN inputs to the ASt, a virus expressing the red-shifted excitatory opsin ChrimsonR (AAV5-Syn-ChrimsonR-tdT) was microinjected into the MGN (Fig 3.8 A). ChrimsonR was selected for these experiment because it has faster kinetics than ChR2 while maintaining similar channel conductance properties (Lin, 2011), which would be advantageous for subsequent experiments requiring rapid stimulation protocols and to allow imaging of green sensor responses After a minimum of 6 weeks, I observed high expression of ChrimsonR-tdT in the ASt and lower expression in the LA (Fig 3.8 B), consistent with the previous experiment using ChR2-GFP (Fig 3.2). I then performed whole-cell patch clamp recordings from visually identified putative MSNs, selected based on their characteristic small soma size and low membrane capacitance < 15 pF (Rangel-Barajas, Boehm, & Logrip, 2021). These morphological and electrophysiological properties distinguish the recorded neurons from the sparse cholinergic interneurons present in the ASt (Lim, Kang, & McGehee, 2014). Recordings were made from these putative MSNs in the presence of the $GABA_A$ antagonist picrotoxin (100 μM) and their membrane potential was voltage-clamped at -70 mV. A single pulse of orange light (576-596 nM) stimulation of the MGN terminals in the ASt resulted in oEPSCs in all recorded neurons (n = 18). Synaptic jitter analysis revealed a mean latency to onset of 0.34 ± 0.05 ms (Fig 3.8 D, n = 18) suggesting a consistent and direct monosynaptic connection from the MGN to ASt putative MSNs. No neurons were excluded from this study due to high jitter. Overall,

the average oEPSC recorded from putative MSN was 171.95 ± 33.35 pA (n = 18). Notably, using the same stimulation strength the amplitude of the MGN-ASt oEPSCs was significantly larger compared to amplitude of oEPSC from MGN-LA projection neurons seen in the previous experiment (ASt medium spiny neurons: 171.95 ± 33.35 pA, n = 18; LA projection neurons: 64.39 ± 9.55 pA, n = 4, P = 0.006, unpaired Student's t-test, ASt versus LA). These data demonstrate ubiquitous monosynaptic MGN input to putative MSNs in the ASt, with a larger response amplitude compared to LA neurons. However, the different opsins used between experiments (ChrimsonR versus ChR2) should be considered when interpreting these amplitude differences.

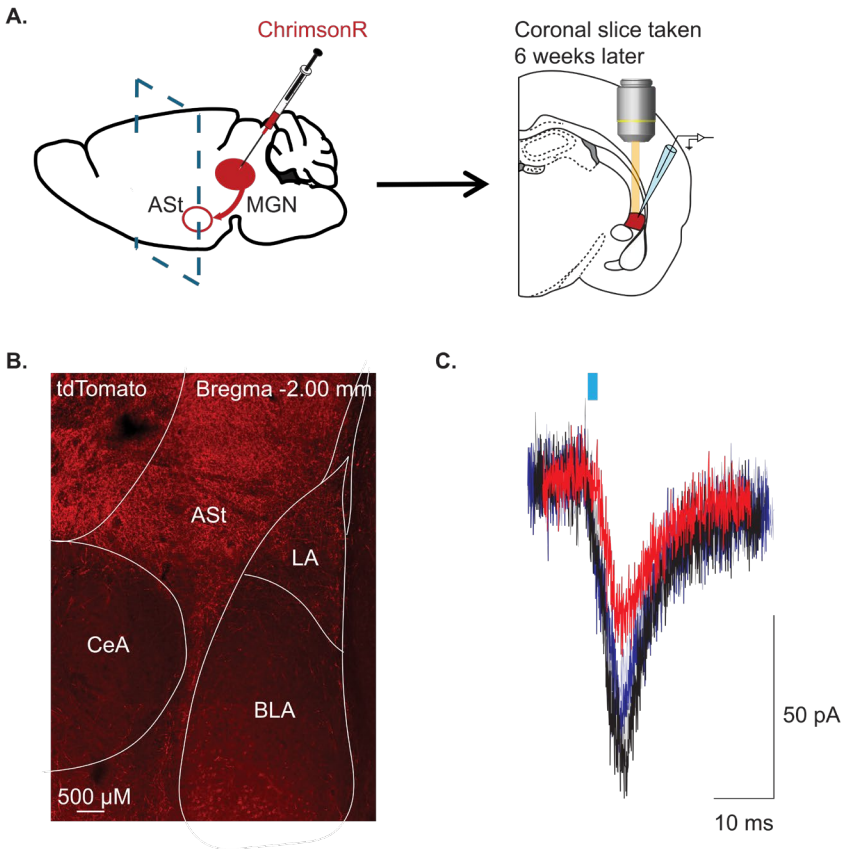

Figure 3.8. MGN forms strong monosynaptic connections to putative ASt MSNs. (A) Sagittal schematic diagram indicating injection of AAV5-Syn-ChrimsonR-tdT into the medial geniculate nucleus. Coronal schematic diagram of the amygdala showing recordings location in the ASt (B) Low magnification confocal image of the ChrimsonR-

tdTomato expression. Strong expression was seen in the ASt and low expression in the LA similar to previous ChR2-GFP expression. (C) Example trace from amygdalo-striatal transition zone neuron demonstrating a monosynaptic connection with jitter < 0.7 ms. Red, blue and black traces represent traces from different episodes of the same neuron. Blue bar indicates optical stimulation point.

Application of the AMPA/kainate antagonist CNQX (10 μM) resulted in substantial attenuation of the oEPSC, but residual current persisted (79.8 ± 2.7% inhibition from control; baseline: 116.66 ± 31.51 pA; CNQX; 22.25 ± 5.18 pA, P = 0.018, n = 5, paired Student's t-test baseline versus CNQX, Fig 3.9 A and B). It has been suggested that some LA synaptic inputs have NMDA receptor-mediated synaptic responses under basal resting membrane conditions (Li et al., 1995). Therefore, to examine similar properties in the ASt, the NMDA receptor antagonist AP5 (100 μM) was applied following CNQX administration, with recordings maintained at -70 mV holding potential. In preliminary experiments the application of AP5 following CNQX further inhibited the oEPSC (87.9 ± 1.6% inhibition from control; CNQX: 22.25 ± 5.18 pA; APV: 7.34 ± 5.6 pA, P = 0.03, n = 3, unpaired Student's t-test, Fig 3.9 A and B, data represented as mean amplitude ± SD due to small sample size). Although this thesis did not directly test whether MGN-LA contained NMDA activation at resting membrane potentials, the similar residual current after CNQX application suggest that this may also be the case (Fig 3.4). (Li et al., 1995; Radley et al., 2007)This preliminary data indicates that there may be a contribution from NMDA receptors at the MGN-AST synapse and whether this also occurs at the MGN-LA synapse awaits testing.

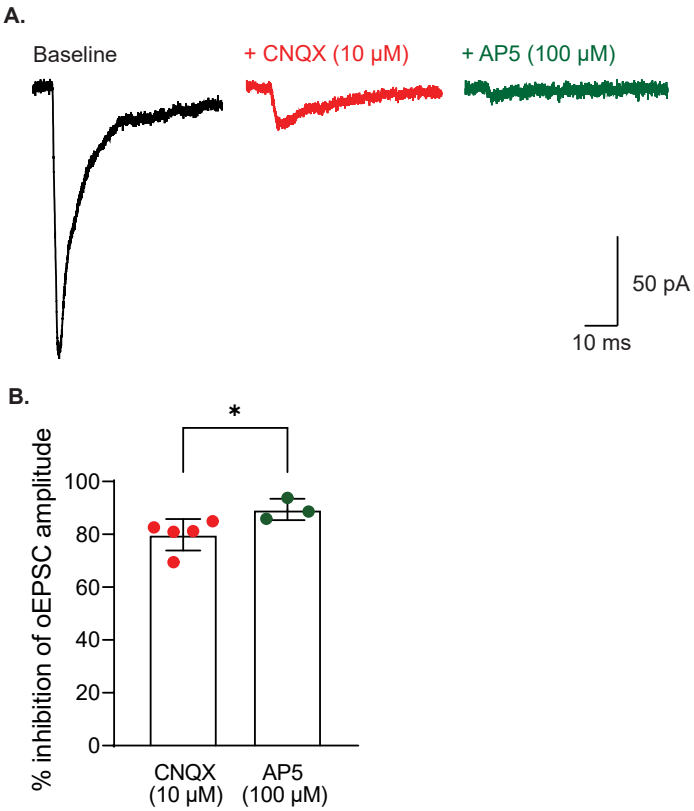

Figure 3.9. Glutamate release from the MGN to putative AST MSNs activate both AMPA and NMDA receptors. (A) Representative traces of a putative MSN in the ASt showing inhibition of baseline by CNQX (10 µM) and further inhibition by AP5 (100 µM). (B) Graph showing percentage inhibition of oEPSC amplitude (from baseline) by CNQX (10 µM) and AP5 (100 µM). Each individual point represents a single neuron. Bars represent mean ± SD. * $P < 0.05$, paired Student's t-test.

Taken together these data indicate that the MGN provides substantial monosynaptic glutamatergic innervation to both the LA and ASt (Fig 3.10). The MGN-ASt pathways shows higher connectivity rates (100% AST vs ~55% LA) and larger response amplitudes (171.95 ± 33.35 pA vs 64.39 ± 9.55 pA) compared to MGN-LA connections. Within the LA, MGN inputs follow a rostral-caudal gradient of anatomical and functional organisation, indicating compartmentalised auditory processing along this axis. Additionally, activation of MOR inhibits release from MGN terminals in the LA, suggesting a possible site of opioid modulation of fear learning. In the ASt, MGN provides

widespread monosynaptic input to all putative MSNs (Fig 3.10), with synaptic responses mediated by both NMDA and non-NMDA receptors. The strong innervation of the ASt suggests that this pathway may represent a significant route for auditory, and other, information processing in the amygdala during fear learning

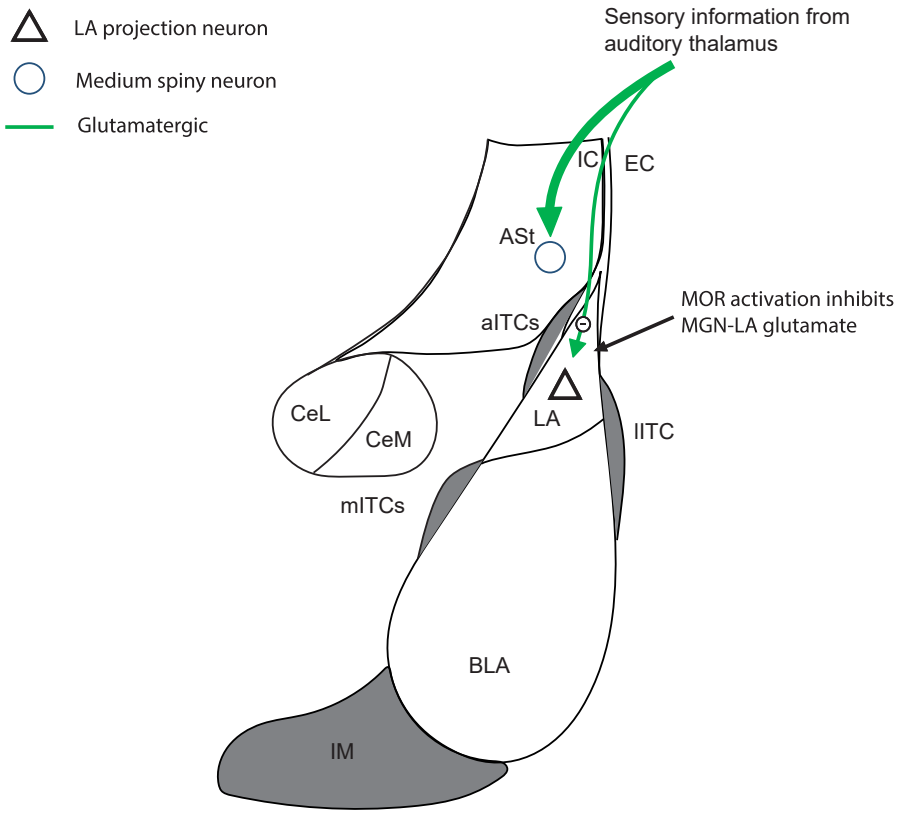

Figure 3.10. MGN connectivity to the amygdala. Cartoon amygdala diagram showing the inputs of the MGN. Lateral amygdala neurons receive moderate input. Neurons of the amygdalo-striatal transition zone receive strong MGN input indicted by bolder arrow resulting in stronger activation of putative medium spiny neurons. MOR activation on MGN-LA terminals inhibits glutamate release onto LA putative pyramidal neurons. ASt – amygdalo-striatal transition zone, BLA – basolateral amygdala nucleus, CeL – central lateral amygdala nucleus, CeM – central medial amygdala nucleus, EC – external capsule, IC – internal capsule, lITCs – lateral intercalated cells, mITCs – medial intercalated cells

3.2 Activation of the MGN triggers endogenous opioid release in the amygdala

This section addresses aim 3.2: To determine whether MGN activation triggers endogenous opioid release in the amygdala

To address aim 3.2, I will investigate whether stimulation of MGN terminals in the amygdala produces endogenous opioid release and characterise the endogenous peptide using both electrophysiological recording and optical biosensors

3.2.1 The ASt expresses enkephalin

Given the dense MGN inputs to the ASt and previous evidence that there is enkephalin expression in the ASt (Jean-Francois Poulin et al., 2018; C. Wang, Kang-Park, Wilson, & Moore, 2002), I wanted to determine whether there is enkephalin immunoreactivity in the ASt of the caudal amygdala. To do this I perfused rats and performed immunohistochemistry for enkephalin immunoreactivity on caudal amygdala slices. The CeA displayed high levels of met-enkephalin-like immunoreactivity (Fig 3.11), consistent with previous studies describing dense enkephalin expression in this region (Jingyi Zhang & McDonald, 2016). Notably, the ASt exhibited similarly robust met-enkephalin immunoreactivity (Fig 3.11). In contrast, the LA showed minimal, but detectable met-enkephalin expression (Fig 3.11), as has been observed previously (Winters et al., 2017). This confirmation of high enkephalin immunoreactivity in the caudal ASt, combined with the new findings of dense functional MGN innervation (Fig 3.8 and Fig 3.9), positions this region as a

potential site for MGN triggered endogenous opioid release that could act in the LA.

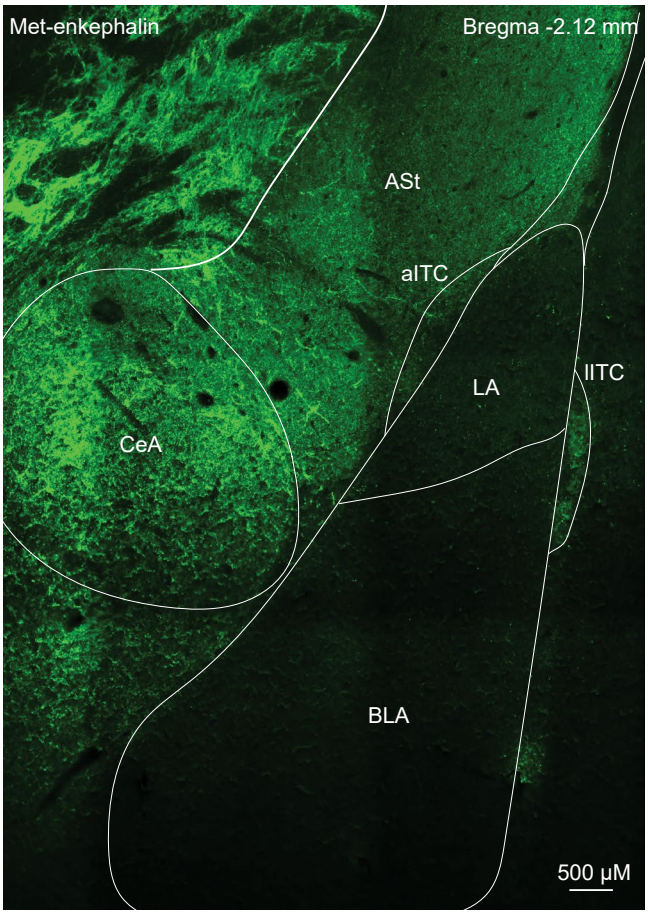

Figure 3.11. The ASt shows high levels of met-enkephalin like immunoreactivity. Low magnification confocal image of met-enkephalin immunoreactivity in the amygdala. The amygdalo-striatal transition zone and central amygdala nucleus show strong levels of met-enkephalin immunoreactivity. Sparse expression is seen in the lateral amygdala. aITC – apical intercalated cells, ASt – amygdalo-striatal transition zone, BLA – basolateral amygdala, CeA- central amygdala, lITC – lateral amygdala.

3.2.2 MGN activity drives endogenous opioid release in the AST

Given that I have confirmed high enkephalin immunoreactivity in the caudal ASt (Fig 3.11) and that the MGN makes a strong glutamatergic synaptic input to ASt neurons (Fig 3.8), I next investigated whether MGN activity could trigger endogenous opioid release. To do this I used two experimental approaches: electrophysiology (section 3.2.2) and opioid sensor imaging (section 3.2.3).

MGN activity drives endogenous opioid release and modulation of synapses in the AST

Detecting endogenous peptide signalling in brain tissue is challenging, in part, due to rapid enzymatic degradation by peptidases (Marvizon et al., 2003). Previous work has demonstrated that peptidase inhibitors can unmask otherwise undetectable peptide mediated effects (Winters et al., 2017). Therefore, I applied a cocktail of peptidase inhibitors, consisting of thiorphan (10 μM), bestatin (10 μM) and Captopril (1 μM), during recordings, to potentially increase the endogenous opioid inhibition of glutamate release from MGN terminals. Subsequent application of opioid receptor antagonists is used to reveal any endogenous opioid inhibition of the MGN-ASt synapse. This approach provides a way to detect endogenous opioid release or signalling that might otherwise be masked by rapid peptide breakdown.

To investigate whether MGN activity triggers opioid release in the ASt, I optically controlled the activity of MGN terminals in the ASt using the same viral approach as in Figure 3.2. Six weeks after AAV5-Syn-ChrimsonR-tdT microinjection (Fig 3.12 A) I made whole-cell patch-clamp recordings from

putative ASt MSNs in acute brain slices (Fig 3.12 A). I voltage clamped the neuron to -70 mV and a single orange light stimulation was used to stimulate oEPSCs (Fig 3.12 B). Application of the cocktail of peptidase inhibitors did not alter the oEPSCs amplitude (4.29 ± 5.68% inhibition from baseline; baseline: 385.89 ± 81.13 pA; PI: 367.23 ± 72.10 pA, P = 0.51, n = 6, paired Student's t-test baseline versus cocktail of peptidase inhibitors, Fig 3.12 C-E). To reveal endogenous opioid actions, I bath applied the opioid receptor antagonist naloxone (10 μM). Naloxone did not alter the oEPSC amplitude (4.55 ± 3.97% increase from PI; PI 281.69 ± 69.01 pA; naloxone: 289.61 ± 64.84 pA, P = 0.3, n = 7, paired Student's t-test PI versus naloxone, Fig 3.12 C-E). Unlike in the Im, where low-intensity stimulation was sufficient to trigger opioid release (Winters et al., 2017), single stimulation of MGN terminals was insufficient in producing endogenous opioid actions in the AST. Given that my earlier findings indicate MGN terminals express functional MORs capable of inhibiting glutamate release (Fig 3.8), the lack of effect of both peptidase inhibitors and naloxone suggests that while these synapses can respond to opioids (Fig 3.8), single stimulation may be insufficient to trigger endogenous opioid release from AST enkephalinergic neurons.

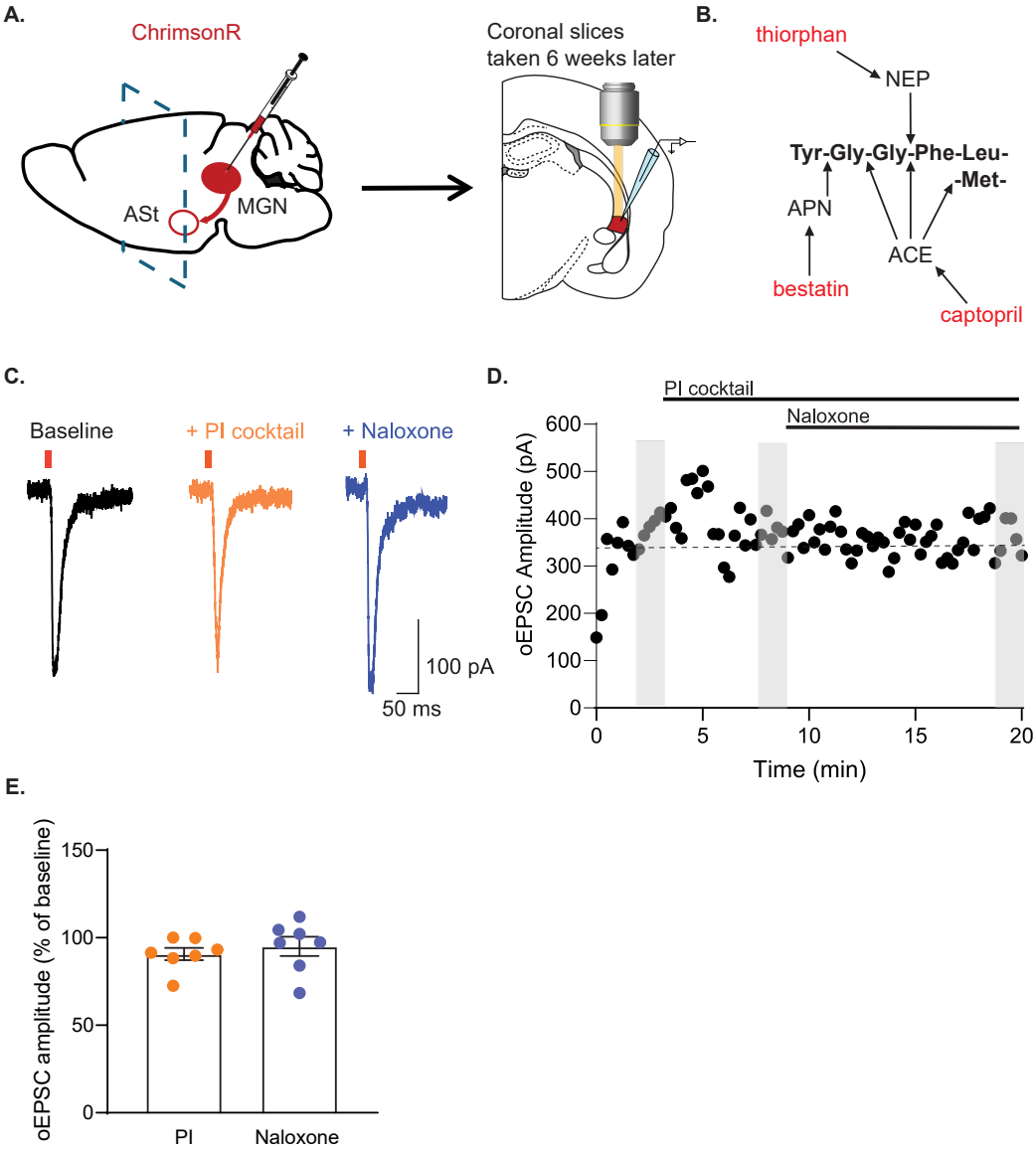

Figure 3.12. Single stimulations of MGN do not induce endogenous opioid release in the AST. (A) Sagittal schematic indicating AAV5-Syn-ChrimsonR-tdT injections into the medial geniculate nucleus. Cartoon schematic of the amygdala showing recordings location. (B) Schematic showing degradation of enkephalin by various peptidases and their corresponding peptidase inhibitors. Figure adapted from Marvizón *et al* (2003). (C-D) Representative traces and time plot from an ASt neuron showing no effects on oEPSC amplitude when applying the cocktail of peptidase inhibitors (PI cocktail: thiorphan 10 μM, bestatin 10 μM, captopril 1 μM) and naloxone (10 μM). Orange bar indicates optical stimulation point. Grey bars on time plot illustrates where baseline and drug measurement were taken (D) Graph showing percentage of baseline of oEPSC amplitude during peptidase inhibition and naloxone (10 μM). Each point represents a single neuron. Bars on graph represents the mean ± SEM.

Since single stimulation was insufficient to trigger opioid release in the ASt, I therefore tested whether a moderate stimulation protocol could reveal endogenous opioid signalling. This stimulation protocol consists of an initial 5 stimulation at 150 Hz to strongly depolarise ASt neurons and possibly trigger endogenous opioid release, followed 200 ms later with a 'test' pulse to probe whether the endogenous opioid is inhibiting glutamate release (Fig 3.13 A). This stimulation protocol could be achieved using the faster ChrimsonR opsin (Lin, 2011). Unless otherwise noted, opioid effects were analysed on the test oEPSC. This protocol was selected based on previous demonstrations of its efficacy in driving endogenous opioid release and subsequent presynaptic inhibition of glutamate release (Winters et al., 2017).

Using the same experimental approach, whole-cell recordings were obtained from putative ASt MSNs while delivering moderate optical stimulation to ChrimsonR expressing MGN terminals. Application of peptidase inhibitors did not alter baseline oEPSC amplitudes (-4.29 ± 5.6 % increase from baseline; baseline 385.16 ± 81.13 pA; PI 367.23 ± 72.10 pA; P = 0.51, n = 6, paired Student's t-test baseline versus PI, Fig 3.13 C-E). Subsequent naloxone application produced a significant increase in oEPSC amplitude that exceeded baseline levels across all neurons (28.5 ± 10.7% increase from PI; PI: 367.23 ± 72.10 pA; naloxone: 410.63 ± 92.69 pA, P = 0.04, n = 6, paired Student's t-test PI versus naloxone, Fig 3.13 C-E). This naloxone induced increase was observed both on the test pulse and on the first pulse of the moderate stimulus delivered 15 seconds later (Fig 3.13 A). Using this electrophysiological approach this data indicates that the moderate stimulation of the MGN inputs

triggers endogenous opioid release in the ASt that acts back on MGN terminals to reduce glutamate release. (Winters et al., 2017)

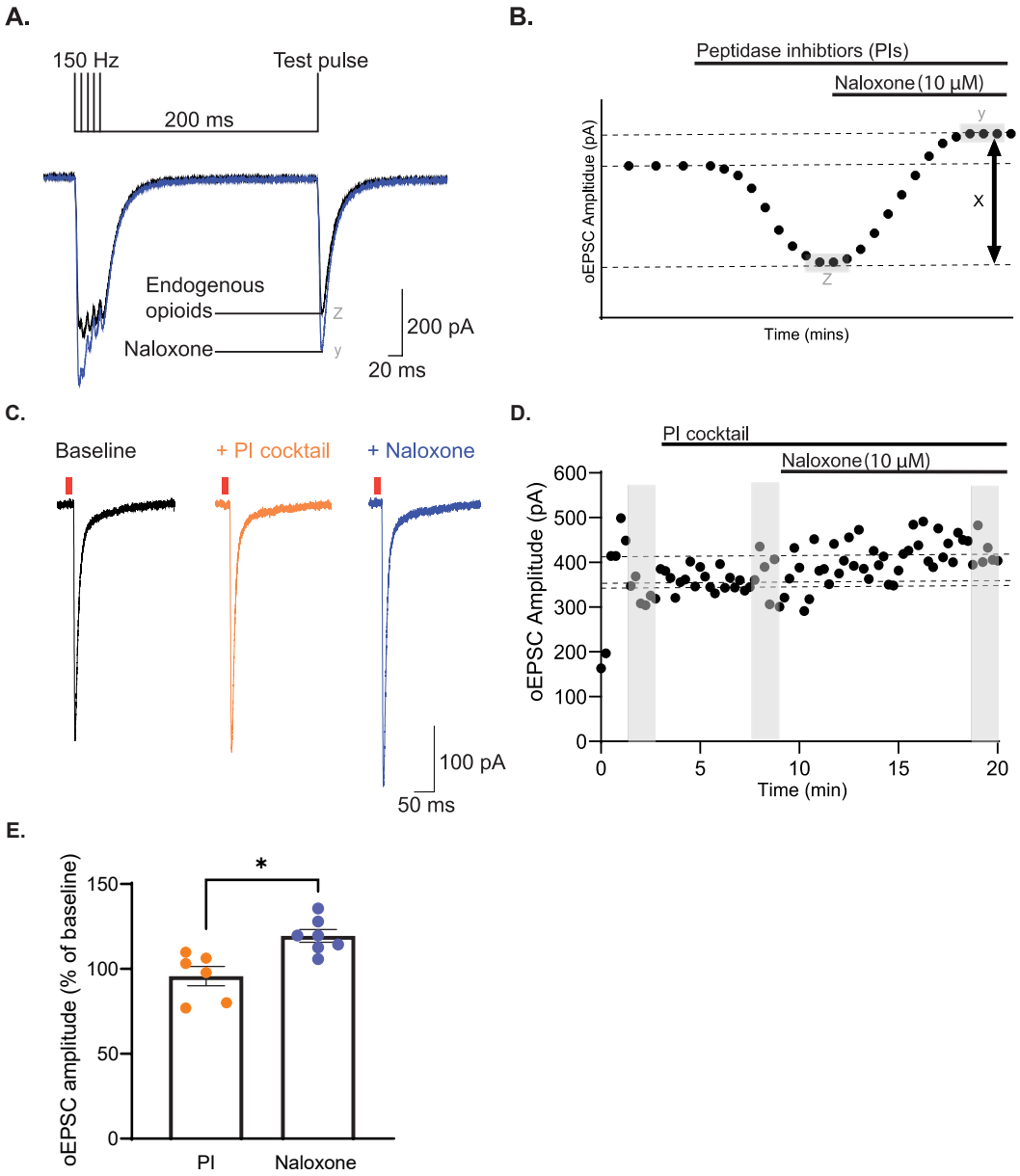

Figure 3.13. Moderate stimulation of MGN terminals induces endogenous opioid release in the ASt. (A) Moderate stimulation protocol for endogenous opioid release. The moderate stimulus pulse train consists of a 5-stimuli train followed by a single test pulse 200 ms. Example traces from an amygdalostriatal transition zone neuron below show oEPSCs evoked by the stimulation paradigm. The moderate stimulus causes currents to peak every stimulation (B Experimental design. Naloxone induced increase was calculated as : x = ((y – z) / z) * 100. (C-D) Representative traces and time plot from an ASt neuron showing no effects on oEPSC amplitude when applying the cocktail of peptidase inhibitors (PI cocktail: thiorphan 10 µM, bestatin 10 µM, captopril 1 µM) and increase oEPSC after applying naloxone (10 µM). Orange bar indicates optical stimulation point. Grey bars on time plot illustrates where baseline and drug measurement were taken (E) Graph showing percentage of baseline of oEPSC amplitude during peptidase

inhibition and naloxone blockade. Each point represents a single neuron. Bars on graph represents the mean ± SEM. * P < 0.05 paired Student's t-test

3.2.3 MGN activity drives endogenous opioid release and activation of GPCR sensors in the ASt and LA

While the previous experiments demonstrated activity-dependent opioid signalling through effects on glutamate release (Fig 3.12 and Fig 3.13), using the two opioid sensors will allow more direct visualization of opioid binding from MGN driven endogenous opioid release.

3.2.3.1 Characterisation of δ-light pharmacology in the AST and LA

The virally packaged δ-light sensor was microinjected into the amygdala to achieve targeted expression (Fig 3.14 A). After a minimum of 4 weeks, brain slices were taking for live-fluorescence imaging. Strong expression of δ-light was seen throughout the injection site but predominantly localised to neuronal cell bodies, this is likely due to the proximal clustering tag of the δ-light sensor (Fig 3.14 B). Initial validation experiments assessed sensor function in acute slice preparations. To do this I bath applied a maximal concentration of met-enkephalin (10 μM, Winters et al., 2017) which produced a robust fluorescence increase that was reversed by naloxone (Fig 3.14 B and C, 10 μM).

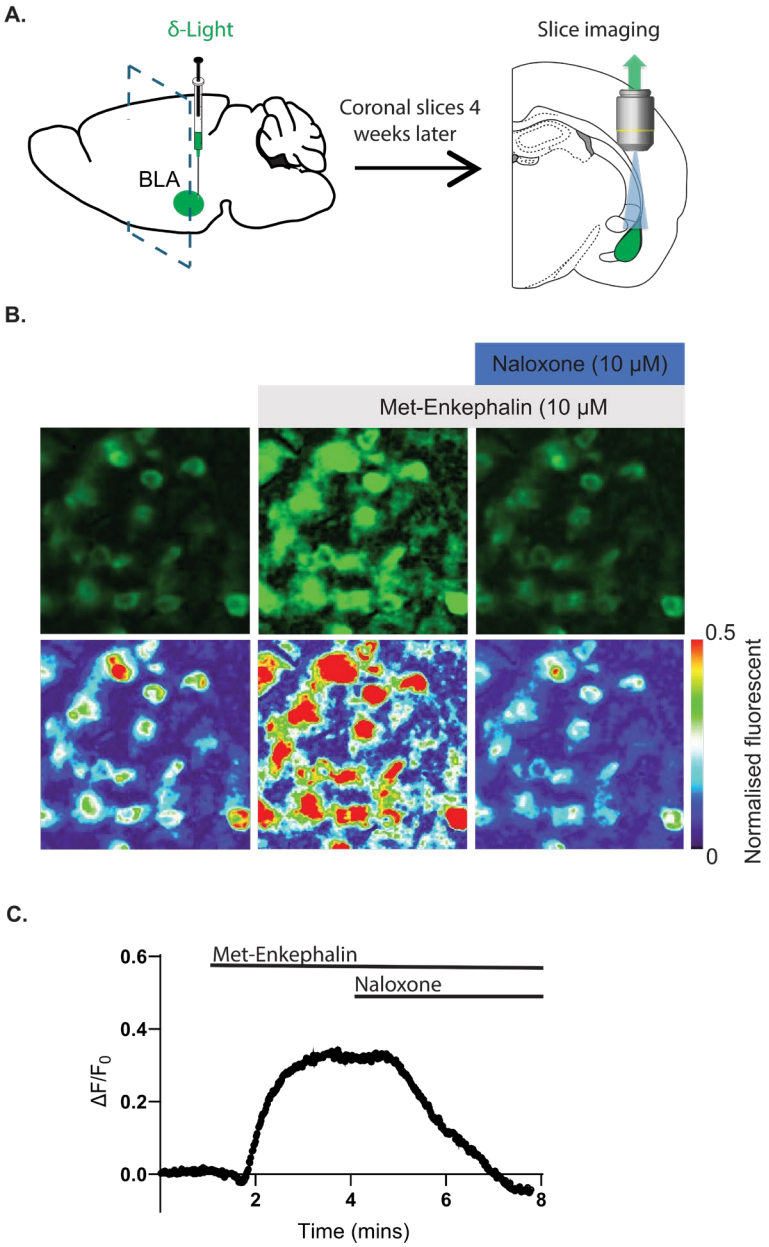

Figure 3.14. δ-light detects exogenous met-enkephalin binding. (A) Sagittal schematic indicating AAV9-hSyn-δlight injection into the basolateral amygdala . Cartoon schematic of the amygdala indicating recording location (B) Example recording images and pseudo coloured heat maps of δ-light fluorescence in the BLA showing increased fluorescent during application of exogenous met-enkephalin (10 μM) and antagonism in naloxone (10 μM). Images represented average fluorescent taken as 8 frames before drug application (C) Example time plot showing $\Delta F/F_0$ showing increases during met-enkephalin application and reversal with naloxone.

To investigate δ-light selectivity for detecting enkephalin, concentration-response curves were established by applying increasing concentrations of the opioid peptides met-enkephalin, dynorphin A-17, and β-endorphin. Met-enkephalin produced concentration-dependent increases in fluorescence intensity, with maximal responses observed at 10 μM and an estimated EC_{50} value of 705 nM (Fig 3.15 A and C). This EC50 value represents an approximately 100-fold shift compared to the EC50 generated from cell culture preparations (Dong et al., 2024). This higher EC50 may be due to the reduced drug access to receptors in brain slices than to isolated cells in culture. Despite the lower EC50 generated form these experiments, met-enkephalin effects were still seen at low concentrations (100 nM, Fig 3.15 A and C), suggesting the sensor expression in whole animals can still detect physiologically relevant changes in enkephalin levels (Winters et al., 2017). In contrast, dynorphin showed no response across all concentrations tested, while β-endorphin produced only minimal increases in fluorescence at 1 μM (Fig 3.15 B and C). (Williams et al., 2001). Therefore, the pharmacology I observed in amygdala slices is consistent with the properties of this sensor expressed in cell lines (Dong et al., 2024). The sensitivity of this sensor to enkephalin but not to β-endorphin or dynorphin suggests that it is most likely to detect release of endogenous enkephalin in brain slices or *in vivo*.

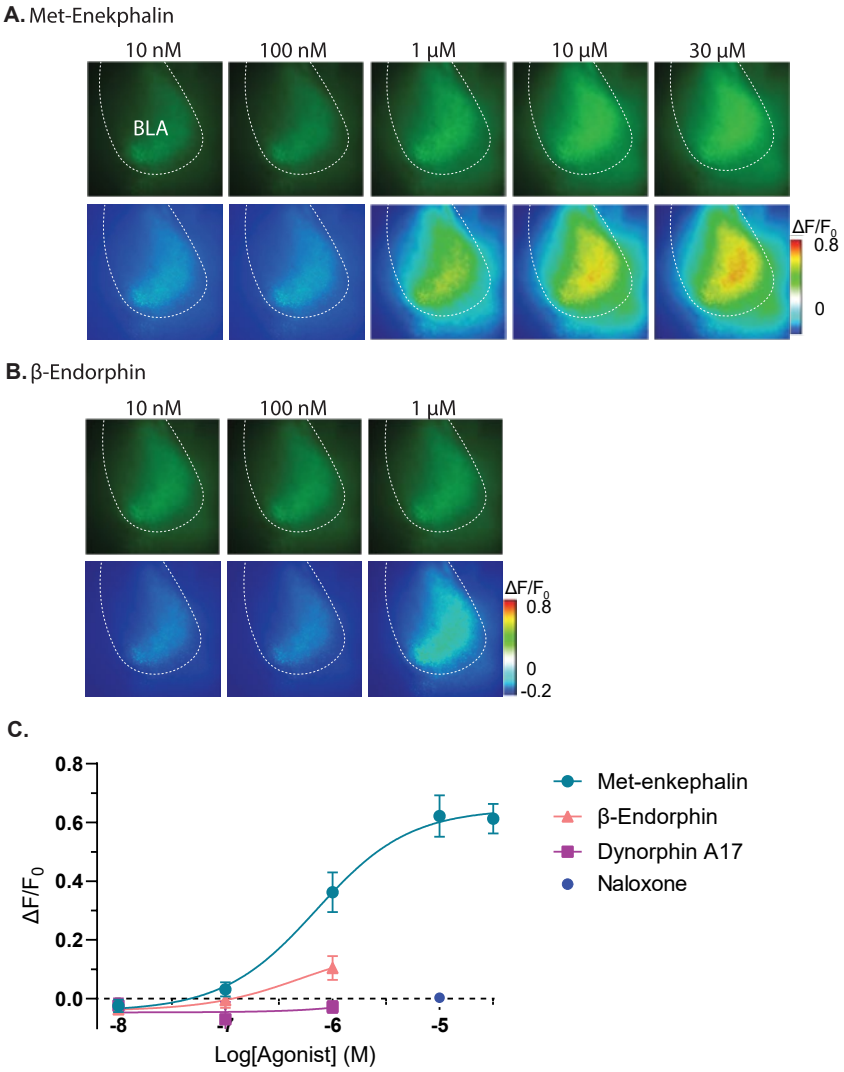

Figure 3.15. Met-enkephalin concentration dependently increases δ-light fluorescence. (A) Example images and pseudo coloured heat maps of δ-light fluorescence taken during the application of each different concentration of met-enkephalin. As the met-enkephalin concentration increases, fluorescence is observed to increase as well. (B) Example images and heat maps of δ-light fluorescence taken during the application of each difference concentration of β-endorphin. Fluorescence changes are only seen at 1 µM concentrations. (C) Concentration response curve of different peptide induced changes in fluorescence ($\Delta F/F_0$). Each point represents mean ± SEM. Non-linear regression was fitted without constraints. BLA – basolateral amygdala

3.2.3.2 Endogenous opioid release measured using δ-light

To determine whether endogenous opioids activate the opioid sensors in the amygdala I used two stimulation approaches. Firstly, I electrically stimulated locally in the ASt to depolarise ASt neurons and secondly, I optically activated MGN terminals.

Local electrical stimulation triggers endogenous opioid release

To determine whether local electrical stimulation in the AST could trigger endogenous opioid release experiments were performed in acute brain slices expressing the δ-light sensor (Fig 3.16 A) with a stimulating electrode placed in the ASt. *In vivo* characterisation studies using δ-light have shown that 100 stimulations at 50 Hz was sufficient in driving opioid induced fluorescent changes (Dong et al., 2024), this therefore provided a starting point for electrical stimulation in slice preparations.

The electrical stimulation triggered robust, time-locked increases in fluorescent intensity (Fig 3.16 B). Application of the cocktail of peptidase inhibitors to protect the peptide from degradation, did not enhance the peak fluorescent signal (Fig 3.16 B and C) but did lengthen the response as reflected in the significant increases in the area under the curve (AUC) (Baseline: 0.14 ± 0.04 AUC, n = 4; PI; 0.38 ± 0.10 AUC, P = 0.042, n = 3, paired Student's t-test baseline versus PI, Fig 3.16 B and D, data presented as mean ± SD). Addition of the opioid receptor antagonist naloxone (10 μM) significantly inhibited the stimulation-induced fluorescence signal (Baseline: 1.78 ± 0.21% peak $\Delta F/F_0$; Naloxone -0.03 ± 0.08% peak $\Delta F/F_0$, P = 0.048, n

= 4, Fig 3.16 B-C), indicating that the observed changes in fluorescence specifically reflected δ-light activation.

By quantifying the $\Delta F/F_0$ at various distances from the stimulation centre and across time points after onset of stimulation, a relative spread of peptide activity can be generated (spatial-temporal analysis). Spatial-temporal analysis revealed that peptidase inhibitors not only prolonged the signal but also increased the spread of the signal from the initial stimulation site (Fig 3.16 E and F). These results provide direct visualisation of endogenous opioid levels in the ASt and demonstrate that reducing peptidase activity prolongs the signal and increases its spread form the stimulation site.

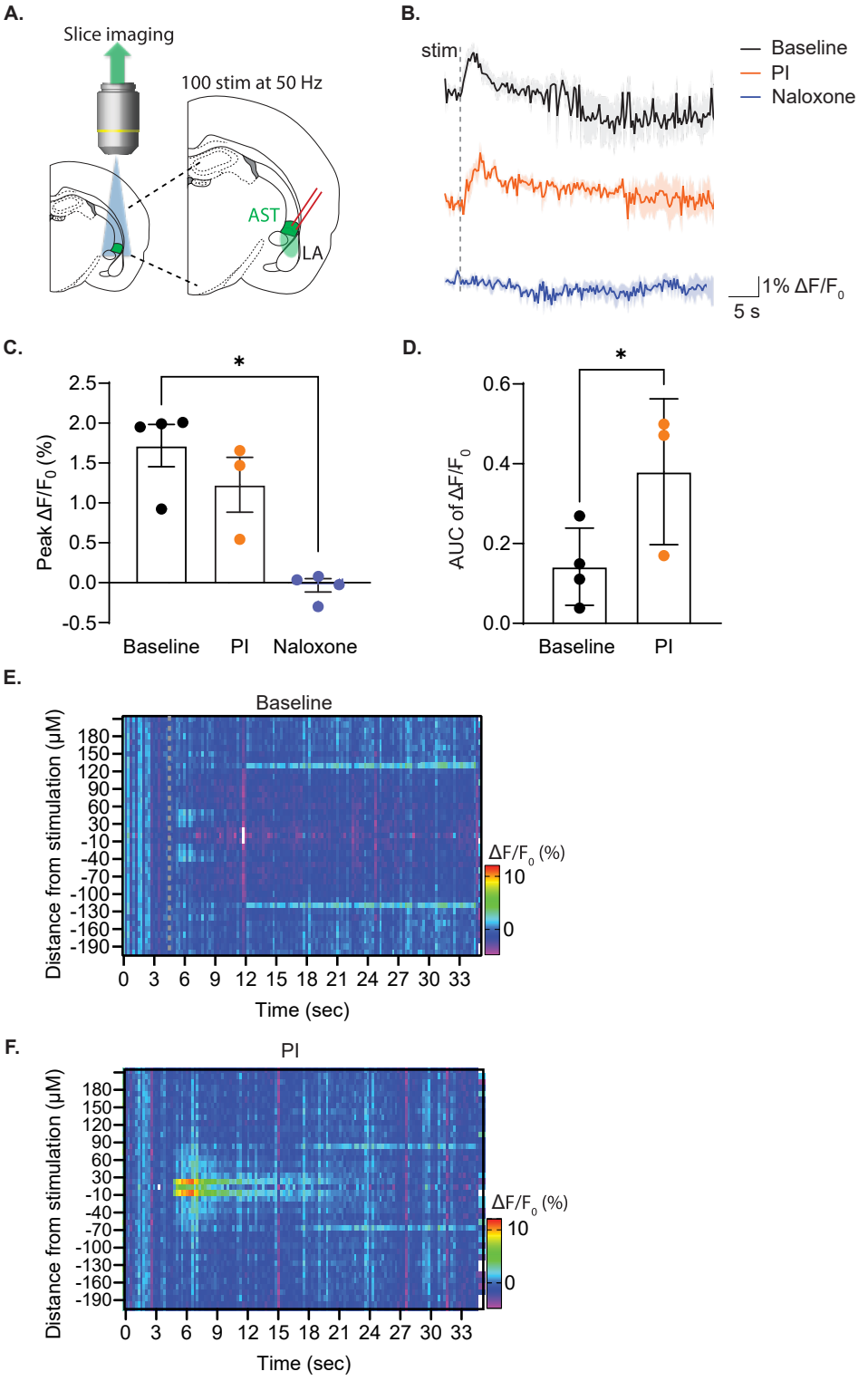

Figure 3.16. Electrical stimulation of the AST induced endogenous opioid release as measured by δ-light fluorescent changes (A) Coronal schematic showing locating of δ-light imaging and stimulating electrode placement in the ASt (B) Traces showing percentage $\Delta F/F_0$ of δ-light fluorescence measured in the amygdalo-striatal transition zone during baseline, peptidase inhibitor application (PI :thiorphan 10 μM, bestatin 10 μM, captopril 1 μM) and naloxone (10 μM). Each traces shows mean ± SEM (C) Graph showing peak $\Delta F/F_0$ taken as 8 frames post stimulation. The peptidase inhibitors do not

affect peak fluorescence. Naloxone completely abolishes the response. Each individual point represents a single slice. Bar graph shows mean ± SEM. (D) Graph showing peptidase inhibitors increase the area under the curve (AUC) calculated form $\Delta F/F_0$ traces. Bar graph shows mean ± SEM. (E-F) Example pseudo coloured heat maps of fluorescence responses from a single ASt recording during (E) baseline and (F) peptidase inhibitors application Each heat map shows the percent $\Delta F/F_0$ at various distances measured from the centre of the stimulation point across time. *P < 0.05, paired and unpaired Student's t-test

The significant spread of opioid signalling during ASt stimulation, particularly under conditions of reduced peptide degradation, suggests that opioids could potentially influence activity in the neighbouring LA. Given this spread and the existence of ASt-LA projections (C. Wang et al., 2002) this raised the question of whether direct stimulation of the LA could also trigger endogenous opioid release.

To investigate this possibility, experiments were performed in acute brain slices expressing the δ-light sensor, with the stimulating electrode now placed in the LA (Fig 3.17 A). Electrical stimulation triggered time-locked increases in fluorescence intensity (Fig 3.17 B). Application of the cocktail of peptidase inhibitors did not enhance peak fluorescent signals but significantly enhanced the fluorescent signal, as measured by an increase in the area under the curve (AUC) (Baseline: 0.15 ± 0.03 AUC; PI; 0.29 ± 0.08 AUC, P = 0.02, n = 5, paired Student's t-test baseline versus PI, Fig 3.17 E). The opioid receptor antagonist naloxone (10 μM) significantly inhibited the stimulation-induced fluorescence signal, the LA (Baseline: 1.01 ± 0.34% peak $\Delta F/F_0$; Naloxone -0.20 ± 0.41% peak $\Delta F/F_0$ P = 0.02, n = 5, Fig 3.17 B and C), again indicating the specificity of the sensor response to opioid receptor activation. These findings are similar to the effects seen in the ASt (Fig 3.16). Additionally, spatial/temporal analysis

revealed a larger spread of the signal when peptidase activity was inhibited compared to baseline activity, indicating binding events further away from the stimulation point (Fig 3.17 E and F). These results demonstrate that electrical stimulation in the LA can also trigger endogenous opioids release, suggesting either the low enkephalin expression in the LA is sufficient to cause effects or that ASt enkephalinergic neurons sends direct projections into the LA.

Met-enkephalin is rapidly degraded by peptidases, whereas β-endorphin is resistant to breakdown (Hui et al., 1983; Marvizon et al., 2003). The enhancement of stimulation-induced fluorescent signals by peptidase inhibitors in both the ASt and LA suggests enkephalin may be the primary opioid peptide being released. Together with the sensor's greater sensitivity to met-enkephalin and the well-documented dense enkephalin expression in these regions (Dong et al., 2024; Y. Wang et al., 2023), these findings provide initial evidence that the observed fluorescent signals likely reflect endogenous enkephalin release in both the ASt and LA

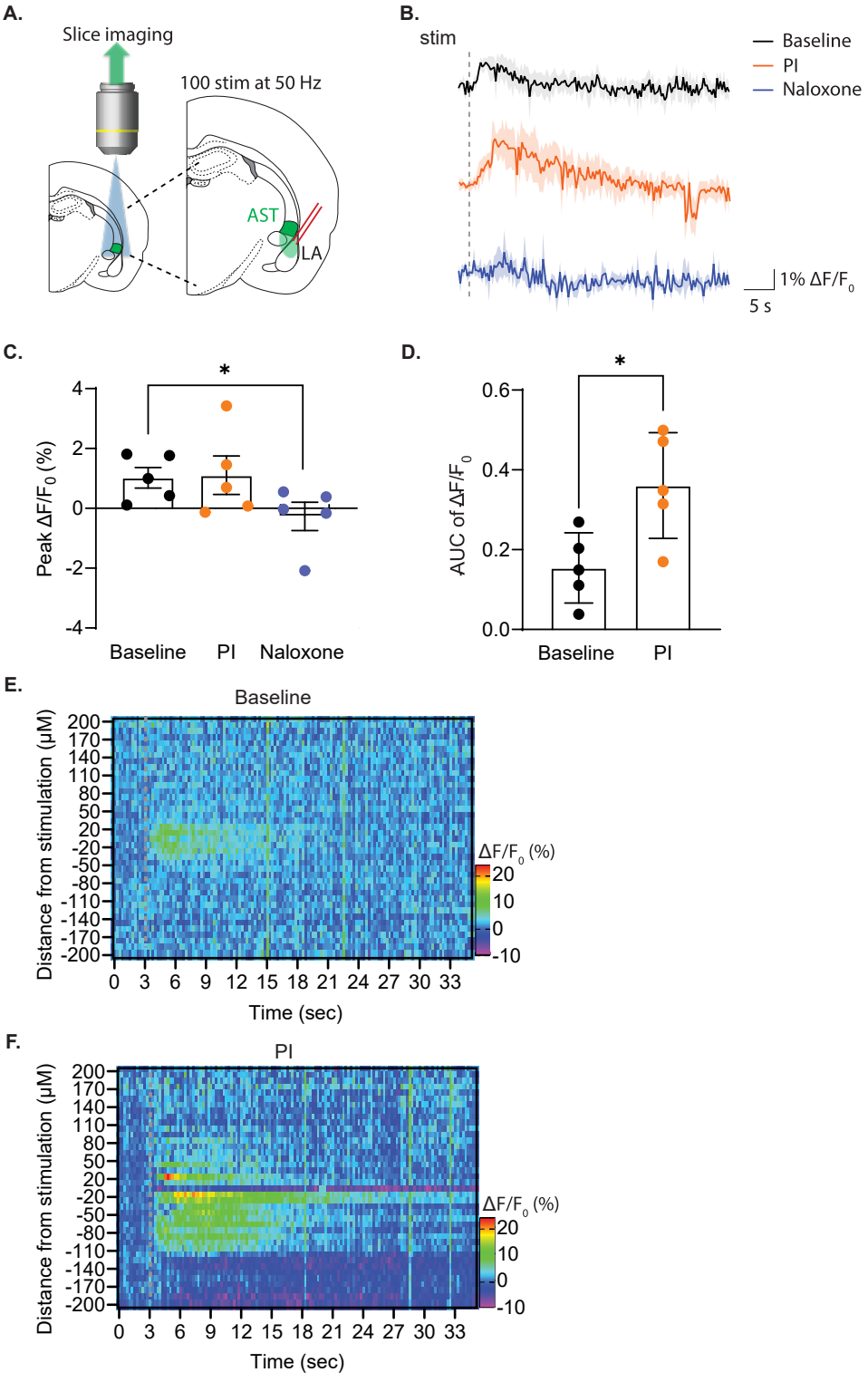

Figure 3.17. Electrical stimulation of the LA induces endogenous opioid release as measured by δ-light fluorescence (A) Coronal schematic showing locating of δ-light imaging and stimulating electrode placement in the LA (B) Traces showing percentage $\Delta F/F_0$ of δ-light fluorescence measured in the LA during baseline, peptidase inhibitor application (PI :thiorphan 10 μM, bestatin 10 μM, captopril 1 μM) and naloxone (10 μM). Each traces shows mean ± SEM (C) Graph showing peak $\Delta F/F_0$ taken as 8 frames post stimulation. The peptidase inhibitors do not affect peak fluorescence. Naloxone completely abolishes the response. Each individual point represents a single slice. Bar

graph shows mean ± SEM. (D) Graph showing peptidase inhibitors increase the area under the curve (AUC) calculated form $\Delta F/F_0$ traces. Bar graph shows mean ± SEM. (E-F) Example pseudo coloured heat maps of fluorescence responses from a single LA recording during (E) baseline and (F) peptidase inhibitors application. Each heat map shows the percent $\Delta F/F_0$ at various distances measured from the centre of the stimulation point across time. *P < 0.05, paired and unpaired Student's t-test

MGN activity triggers endogenous opioid release

The robust MGN innervation of the ASt, that activates all putative MSNs (Fig 3.8), suggested that activation of this pathway could trigger opioid release. To achieve pathway specificity, virus expressing ChrimsonR (AAV5-Syn-ChrimsonR-tdT) was microinjected into the MGN while the virus expressing δ-light sensor was microinjected into the ASt (Fig 3.18 A). This dual approach enabled selective terminal control using red-shifted wavelengths without interference with the sensor signalling, which is excited at blue wavelengths. Blue-light stimulations were also kept at intensity between 1-3% to avoid activation of ChrimsonR (Klapoetke et al., 2014).

Optical stimulation of the MGN terminals in the ASt using orange light triggered time locked robust changes in δ-light fluorescence (Fig 3.18 B). Application of the cocktail of peptidase inhibitors did not enhance the peak fluorescence (Fig 3.18 B and C) but did significantly increase the area under the curve (AUC) (Baseline: 24.24 ± 6.27 AUC, n = 11; PI: 145.5 ± 17.6, n = 6, P = 0.0032, paired Student's t-test baseline versus PI, Fig 3.18 B and D). Application of naloxone significantly inhibited the fluorescence signal in the ASt, indicating these signals are likely due to δ-light activation from increased extracellular opioid concentration (Baseline: 3.74 ± 0.78% peak $\Delta F/F_0$, n = 9; Naloxone: -0.11 ± 0.62% peak $\Delta F/F_0$, n = 8, P = 0.007, paired Student's t-test baseline versus PI, Fig 3.18 B and C). Notably, optical stimulation produced larger fluorescent

changes compared to electrical stimulation of the same region (Electrical: 1.78 ± 0.21% peak $\Delta F/F_0$, n = 4; Optical: 3.74 ± 0.71% peak $\Delta F/F_0$, n = 10, P = 0.02, unpaired Student's t-test electrical versus optical, Fig 3.16 B-C).

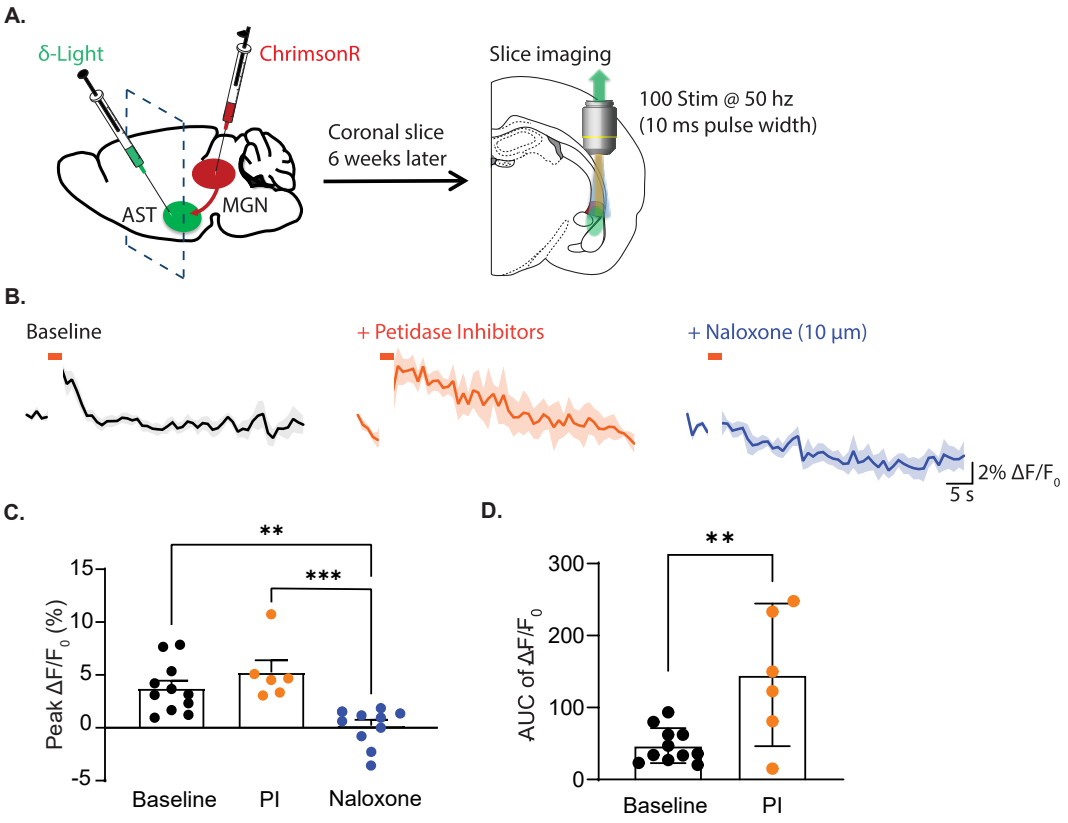

Figure 3.18. Optical stimulation of MGN terminals in AST induced opioid receptor activity in the ASt (A) Sagittal schematic indicating AAV5-Syn-ChrimsonR-tdT injection into the medial geniculate nucleus and AAV9-hSyn-δlight injection into the amygdalo-striatal transition zone. Coronal schematic diagram of the amygdala indicating dual channel imaging approach and recording location (B) Traces showing percentage $\Delta F/F_0$ of δ-light fluorescence measured in the amygdalo-striatal transition zone during baseline, peptidase inhibitor application (PI :thiorphan 10 µM, bestatin 10 µM, captopril 1 µM) and naloxone (10 µM). Each traces shows mean ± SEM. Orange bar indicates optical stimulation point. (C) Graph showing peak $\Delta F/F_0$ taken as 8 frames post stimulation. The peptidase inhibitors do not affect peak fluorescence. Naloxone completely abolishes the response. Each individual point represents a single slice. Bar graph shows mean ± SEM. (D) Graph showing peptidase inhibitors increase the area under the curve (AUC) calculated form $\Delta F/F_0$ traces. Bar graph shows mean ± SEM. *P < 0.05, **P < 0.01, *** P < 0.005,

Given previous observations that peptidase inhibitors enhanced the spread of opioid signalling from the ASt, and the known anatomical connections between

these regions (C. Wang et al., 2002), this provided an opportunity to examine how MGN-evoked opioid release in the ASt might influence the LA.

During optical stimulation of MGN terminals, δ-light sensor responses were simultaneously monitored in the LA. These recordings reveal a detectable time-locked increase in fluorescent induced by MGN terminal stimulation (Fig 3.19 A). Application of the cocktail of peptidase inhibitors did not enhance the peak fluorescence signal (Fig 3.19 A and B) but significantly increased the area under the curve (Baseline: 31.42 ± 3.4 AUC, n = 7; PI: 65 ± 18,9, n = 6, P = 0.04, paired Student's t-test baseline versus PI, Fig 3.19 C). Naloxone significantly inhibited these responses (Baseline: 2.09 ± 0.28% peak $\Delta F/F_0$, n = 7; Naloxone: -0.35 ± 0.51% peak $\Delta F/F_0$, n = 6, P = 0.011, paired Student's t-test baseline versus PI, Fig 3.19 A and B). Notably, the change in fluorescence measured in the LA was smaller than fluorescence changes measured in the ASt (LA: baseline: 2.09 ± 0.28% peak $\Delta F/F_0$, n = 7; ASt: 3.74 ± 0.78% peak $\Delta F/F_0$, n = 9, P = 0.028, unpaired Student's t-test, ASt versus LA). This reduced response in the LA could result from enkephalin diffusing form its source in the ASt to the LA, with peptide degradation occurring during this diffusion process. These results demonstrate that opioid signals can be detected in the LA following MGN terminal stimulation in the ASt. Together, these findings reveal that activation of MGN terminals in the ASt can trigger opioid release that extends beyond the ASt to influence the LA, a key site for fear learning (J. LeDoux, 2003).

The ability to detect these signals using the δ-light sensor and the specific enhancement of the signal from peptidase inhibition extends the earlier electrophysiological evidence for MGN-evoked enkephalin release in the ASt. However, whilst this data suggests the ASt as the source of the increase in extracellular enkephalin concentration the aITCs may also contribute to the endogenous opioid release as these neurons express high levels of enkephalin (Y. Wang et al., 2023), and are densely innervated by MGN inputs (Asede et al., 2021). Future experiment will therefore investigate the involvement of aITCs in endogenous opioid release induced by MGN inputs.

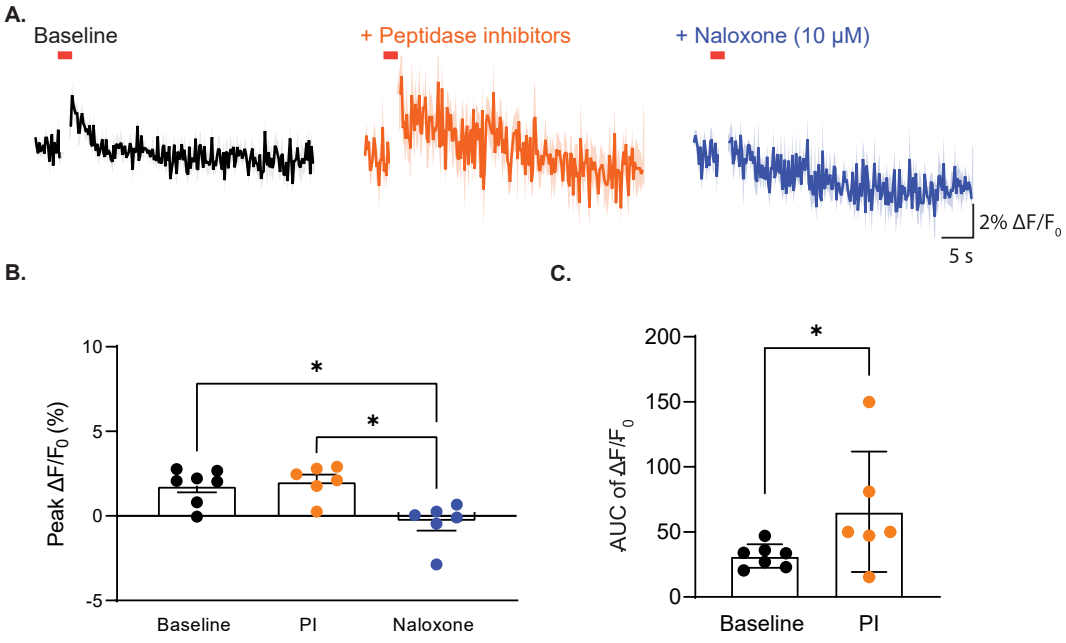

Figure 3.19. Optical stimulation of MGN terminals in AST induced opioid receptor activity in the LA (A) Traces showing percentage $\Delta F/F_0$ of δ-light fluorescence measured in the lateral amygdala during baseline, peptidase inhibitor application (PI :thiorphan 10 μM, bestatin 10 μM, captopril 1 μM) and naloxone (10 μM). Each traces shows mean ± SEM. Orange bar indicates optical stimulation point. (B) Graph showing peak $\Delta F/F_0$ taken as 8 frames post stimulation. The peptidase inhibitors do not affect peak fluorescence. Naloxone prevents the response. Each individual point represents a single slice. Bar graph shows mean ± SEM. (C) Graph showing peptidase inhibitors increase the area under the curve (AUC) calculated form $\Delta F/F_0$ traces. Bar graph shows mean ± SEM. *P < 0.05, paired and unpaired Student's t-test

3.2.3.3 MGN activity induced physiologically relevant levels of endogenous opioid release

My previous characterisation of the δ-light sensor established a concentration-response relationship for met-enkephalin in slice preparations (Fig 3.15). This relationship provided an opportunity to estimate the concentration of endogenously released opioids in the amygdala brain slices. By comparing the magnitude of stimulation-induced fluorescent changes ($\Delta F/F_0$) to the concentration-response curve generated from figure 3.15, the peak concentration of endogenously released opioids was estimated to be approximately 90 nM in both the ASt and LA (Fig 3.20). While this concentration might appear relatively low, as a result of the high affinity of opioid receptors for enkephalin and 100 nM enkephalin inhibits synaptic transmission in the amygdala by ~20% (Winters et al., 2017). This suggests that the observed levels of endogenous opioid release I measured using the sensor likely reach physiologically relevant concentrations. Together, these findings demonstrate that activation of MGN terminals in the amygdala triggers endogenous opioid release at concentrations capable of modulating synaptic transmission in these circuits.

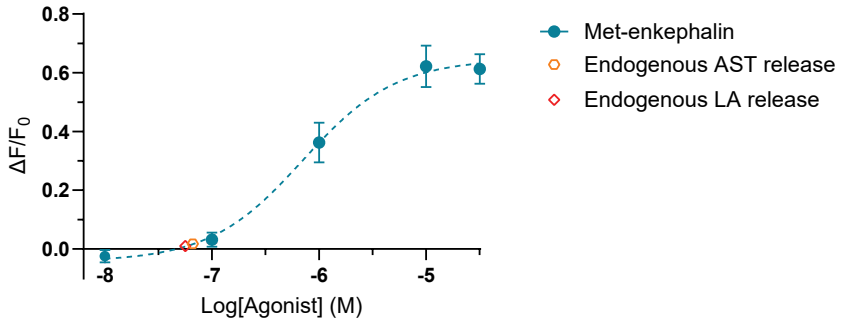

Figure 3.20. Plotting $\Delta F/F_0$ values from MGN induced changes reveal low concentrations of endogenous enkephalin release. Concentration response curve of met-enkephalin responses generated from figure 3.12 shown in dotted lines. Optical stimulation of the medial geniculate nucleus produced $\Delta F/F_0$ values of ~0.03 and ~0.02 in the ASt and LA respectively.

3.2.3.4 Endogenous opioid release measured using the UMASS opioid sensor.

Characterisation of UMASS pharmacology in the AST and LA

The opioid sensor δ-light used in the earlier experiments has a proximal restriction and clustering tag restricting its expression to cell soma (Dong et al., 2024). Given that most synapses form on dendritic spines rather than the cell soma (Ludwig, Apps, Menzies, Patel, & Rice, 2016; Nelson Spruston, 2008), I also utilised an unrestricted μ-opioid receptor based sensor, UMASS (Rappleye et al., 2022) that may detect endogenous opioids in different cellular domains.

Experiments were therefore repeated using the UMASS sensor to investigate how this difference in localisation may alter the responses. The virally packaged UMASS sensor (AAV5-EF1α-UMASS2A) was microinjected into the amygdala to achieve targeted expression (Fig 3.21 A). Notably, expression of the sensor within the amygdala was strong but lacked any definition of cell bodies (Fig 3.21 B) compared to the defined cell soma expression seen with δ-light (Fig 3.15).

A concentration-response curve was generated using increasing met-enkephalin concentrations and the effect of 1 μM concentrations of β-endorphin and dynorphin was determined. Met-enkephalin activated the sensor in a concentration dependent manor, achieving maximal fluorescence at 30 μM (Fig 3.21 C). In contrast, dynorphin A and β-endorphin at 1 μM concentrations did not increase fluorescence (Fig 3.21 C). Met-enkephalin had

an estimated EC50 of 17.8 μM, approximately 25-fold less potent than at δ-light and a smaller maximal response (Fig 3.19 B). The apparent EC50 generated from this study is approximately 100-fold lower than values obtained from initial cell culture studies but the selectivity for endogenous agonists is entirely consistent with the properties of this sensor expressed in cell lines (Rappleye et al., 2022). Therefore, like the δ-light sensor, UMASS may be able to reliably detect changes in extracellular met-enkephalin concentrations.

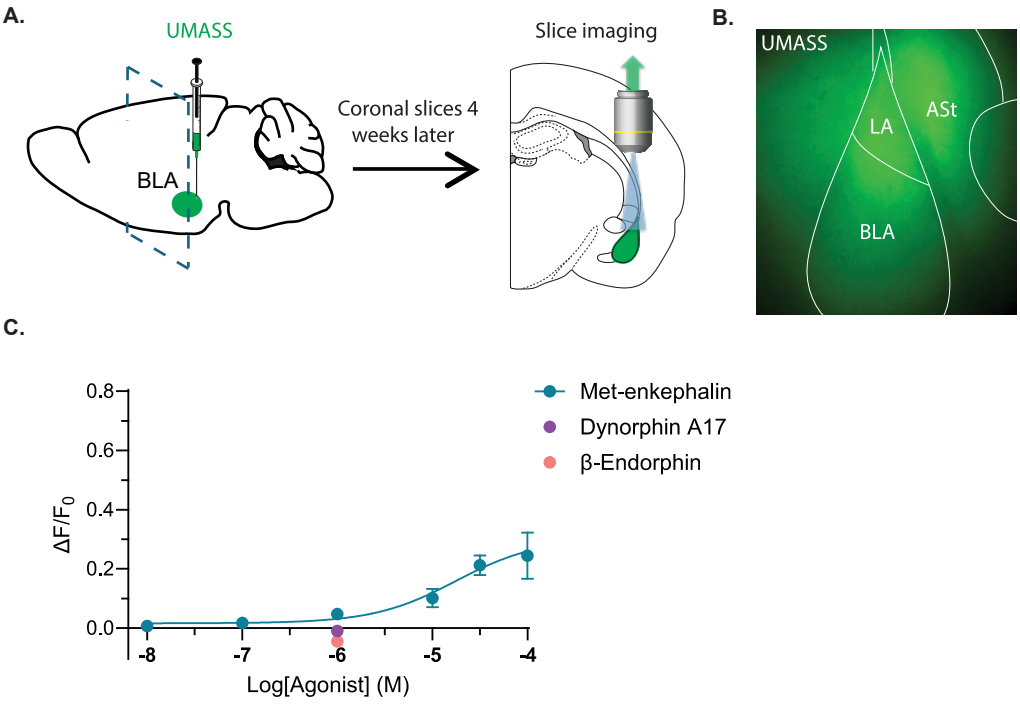

Figure 3.21. Met-enkephalin concentration dependently increases UMASS fluorescence. (A) Sagittal schematic diagram showing AAV5-EF1α-UMASS2A injection into the amygdala. Coronal schematic image of the amygdala showing recording location. (B) Example image of UMASS sensor expression during baseline. Compared to δ-light there is a lack of defined cell bodies. (C) Concentration response curve of different peptide induced changes in fluorescence ($\Delta F/F_0$). Each point represents mean ± SEM. Non-linear regression was fitted without constraints.

UMASS provides reliable detection of endogenously released opioids

Having established that UMASS can reliably detect changes in extracellular met-enkephalin concentrations in slice preparations, despite its reduced sensitivity compared to δ-light, the sensor was next used to examine endogenous opioid release in the ASt.

Electrical stimulation of the ASt produced time-locked increases in UMASS fluorescence (Fig 3.22 B and C). These fluorescent changes were significantly enhanced by peptidase inhibitors seen by increases in the area under the curve (Baseline: 0.18 ± 0.03 AUC; PI: 0.35 ± 0.05 AUC, P = 0.03, paired Student's t-test baseline versus PI, Fig 3.22 C) and significantly inhibited by naloxone (Baseline: 4.81 ± 0.82% peak $\Delta F/F_0$; n = 6, Naloxone: -0.91 ± 1.02% peak $\Delta F/F_0$; n = 7; P = 0.002; one-way ANOVA; Baseline vs Naloxone; Fig 3.22 C). Despite differences in sensitivity to exogenous enkephalin, the relative fluorescent increase of UMASS and δ-light in response to endogenous opioids were similar (UMASS: 3.93 ± 0.97% peak $\Delta F/F_0$; n = 7; δ-light: 3.74 ± 0.71% peak $\Delta F/F_0$, n = 11, P = 0.88, unpaired Student's t-test UMASS versus δ-light Fig 3.22 E). This may reflect that that UMASS's unrestricted expression across the neuron potentially places it at sites closer to endogenous opioid release sites (Ludwig et al., 2016).

Given the previous findings that endogenous opioid activity spreads from the initial point of stimulation, recordings were performed in the LA during ASt

stimulations. Stimulation of the ASt caused increases in fluorescence in the LA (2.71 ± 0.88% peak $\Delta F/F_0$; n = 7; Fig 3.22 D). Application of peptide of the cocktail of peptidase inhibitors did not increase peak fluorescence but prolonged the signal as measured by an increase in the area under the curve. Naloxone significantly inhibited stimulation induced increases in fluorescence (Baseline: 3.92 ± 1.05% peak $\Delta F/F_0$; Naloxone: -0.81 ± 0.81% peak $\Delta F/F_0$; n = 7; P = 0.001; one-way ANOVA; Baseline vs Naloxone; Fig 3.22 D). Since UMASS expression is present on dendrites, these LA signals might better reflect opioid activity form ASt release. Overall, these results validate the use of an unrestricted sensor in detecting endogenous opioid signal and complement our earlier observations with δ-light.

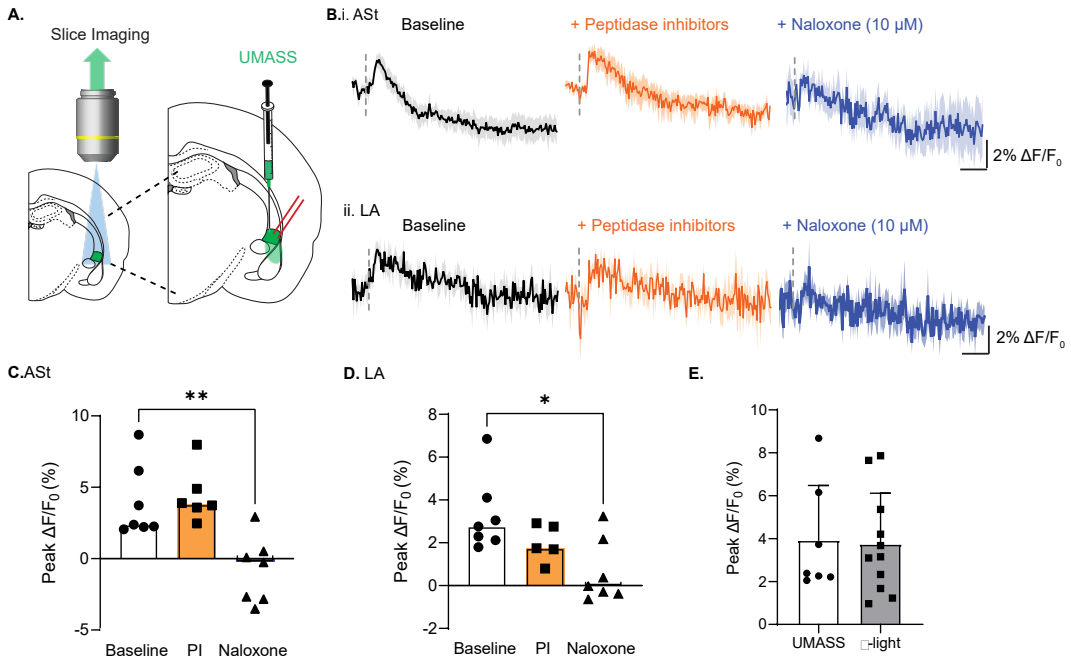

Figure 3.22. Electrical stimulation of the ASt induced endogenous opioid released in the ASt and LA as measured by UMASS fluorescent changes (A) Coronal schematic diagram of the amygdala showing recording location and stimulating electrode placed in the amygdalo-striatal transition zone. (B) Traces showing percentage $\Delta F/F_0$ of δ-light fluorescence measured in the (i) AST and (ii) LA during baseline, peptidase inhibitor application (PI :thiorphan 10 μM, bestatin 10 μM, captopril 1 μM) and naloxone (10 μM). Each traces shows mean ± SEM. Grey dotted line indicates stimulation point. Graphs showing peak $\Delta F/F_0$ taken as 8 frames post stimulation in the (C) ASt and (D) LA.

Each individual point represents a single slice. (C) Graph showing no differences in peak $\Delta F/F_0$ taken as 8 frames post stimulation measured using either UMASS or δ-light. Bar graph shows mean ± SEM. * P < 0.05, ** P < 0.001, One way ANOVA with Tukey's post hoc multiple comparisons tests.

3.2.3.5 CRISPR mediated viral knockdown of enkephalin

The previous experiments strongly suggest enkephalin as the primary endogenous opioid being released, based on both sensors' high selectivity for met-enkephalin and the enhancement of signals by peptidase inhibitors. To further test the possibility of enkephalin being the primary opioid we experimentally reduced expression of enkephalin and then determined whether this reduced opioid sensor responses in the AST.

To do this, our lab adapted a CRISPR based approach originally developed for mice (Castro et al., 2021). The CRISPR system works by introducing small deletions or insertions into the proenkephalin (PENK) gene, disrupting the production of preproenkephalin and thus lowering enkephalin synthesis (Castro et al., 2021). Their work demonstrated successful viral enkephalin knockdown by 30-50% in the NAc. To apply this system in rats we generated a target sequence for rat pre-proenkephalin and packaged into a viral vector. To test the modified CRISPR virus, unilateral microinjections of different volumes of AAV9-PENK-KO-sgRNA1 were made into the ASt (Fig 3.23 A). After 4 weeks, animals were perfused, and brain sections (40 µM thickness) were collected across the rostral-caudal extent of the ASt, from -1.20 to -2.56 mm relative to bregma. Serial sections were processed for met-enkephalin immunohistochemistry and fluorescence intensity was measured in the ASt of matched regions of viral injected and non-injected hemispheres. Fluorescent measurement of the ASt in the non-injected hemisphere show high expression

of met-enkephalin across all slices taken (Fig 3.23 B), indicating enkephalin expression across the ASt. The virally injected hemispheres had notably lower expression of enkephalin in the ASt (Fig 3.23 B). Enkephalin expression was quantified by setting the fluorescence intensity of the non-injected hemisphere as 100% and calculating the relative reduction in the CRISPR virus injected hemisphere. Analysis revealed that animals with a 500 nL viral injection had reduced enkephalin immunoreactivity by approximately 50% in the infected hemisphere compared to controls sides (47.21 ± 4.66 % inhibition of fluorescence, n = 9, Fig 3.24 C). Lower injection volumes (250 and 100 nL) resulted in reduced levels of knockdown (250 nL: 3.00 ± 2.96 % inhibition of fluorescence, n = 4; 100 nL: 11.61 ± 5.67% inhibition of fluorescence n = 5, Fig 3.23 C), suggesting that larger volumes were necessary for optimal viral spread and gene editing. These results demonstrate that the modified CRISPR construct can effectively reduce enkephalin expression in the rat ASt, with the larger injection volumes necessary to produce knockdown comparable to levels reported in mice (Castro et al., 2021)

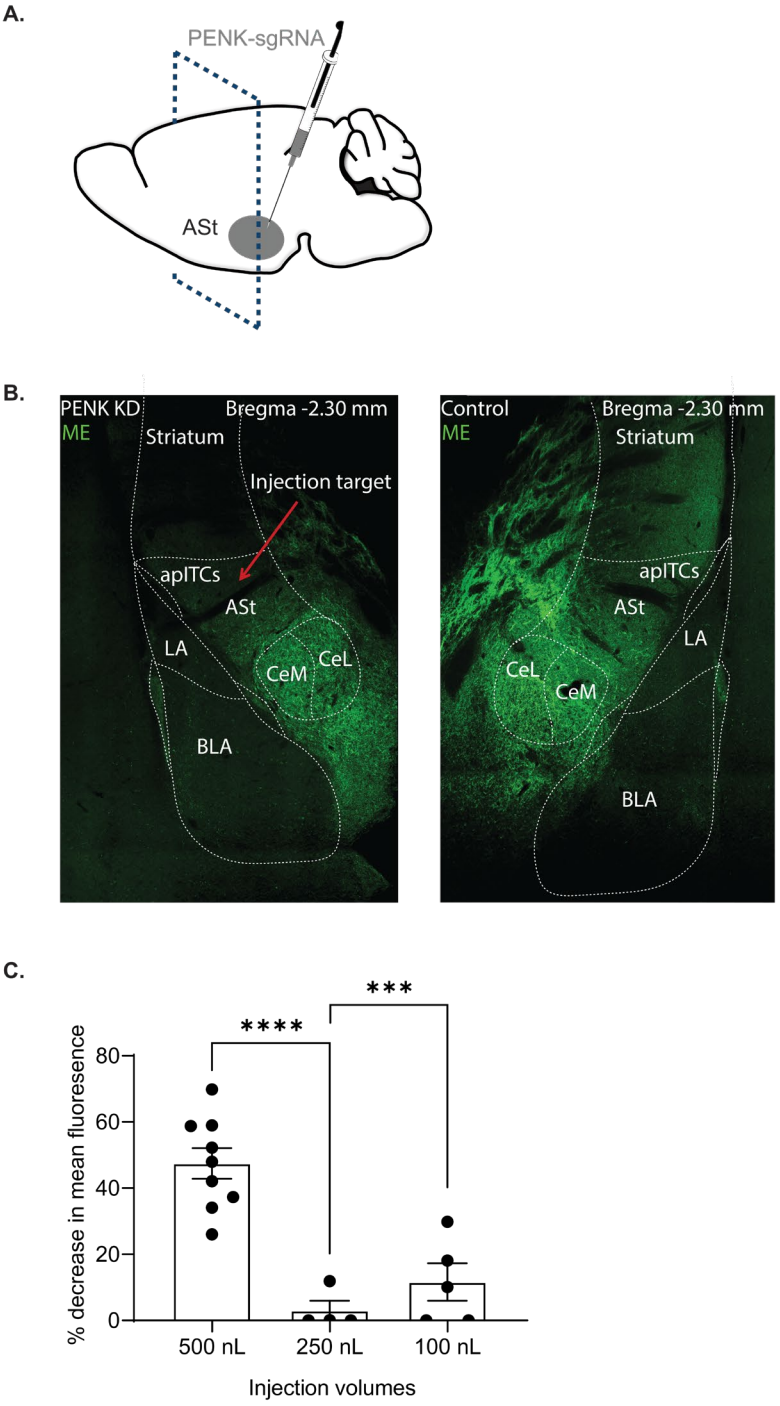

Figure 3.23. PENK sg-RNA viral knockdown decreases enkephalin like immunoreactivity in the ASt. (A) Sagittal schematic diagram indicating AAV9-PENK-KO-sgRNA1 injection into the amygdalo-striatal transition zone (B) Low magnification confocal images of met-enkephalin immunoreactivity in the amygdala of the knockdown and control slices. The knockdown produced less met-enkephalin expression in the ASt which extends into the striatum in some cases. Red arrow indicates injection site. (C) Graph showing percentage inhibition of fluorescence in the virally injected hemisphere compared to control. Each individual points represent a single slice taken at different rostral-caudal coordinated across the amygdala. Bars on graph represent mean ± SEM. *** $P < 0.005$, **** $P < 0.0001$, unpaired Student's t-test

To assess the functional effectiveness of the enkephalin knockdown virus, the previously validated opioid sensor δ-light was employed. The δ-light sensor and the PENK knockdown virus were bilaterally co-injected into the ASt (Fig 3.24 A). After a period of 4 weeks, coronal brain slices were prepared for live imaging.

In the ASt, I observed a variety of responses. In control slices and in some knockdown slices electrical stimulation produced time-locked fluorescent increases, which were blocked by naloxone (Fig 3.24 B). Given this variability in the response in knockdown tissue there was no significant difference in the fluorescence change in the ASt between knockdown and control (Control: 1.60 ± 0.20% $\Delta F/F_0$; PENK knockdown: 1.23 ± 0.80% $\Delta F/F_0$, n = 5, P = 0.67, unpaired Student's t-test Control versus PENK knockdown, Fig 3.24 D). Whereas electrical stimulation of the LA produced no detectable changes in fluorescent signal in knockdown animals (Fig 3.24 C) with a significant reduction in stimulation induced fluorescent changed (Control: 1.50 ± 0.56% $\Delta F/F_0$, n = 6; PENK knockdown: 0.06 ± 0.001% $\Delta F/F_0$, n = 5, P = 0.045, unpaired Student's t-test Control versus PENK knockdown Fig 3.24 C).

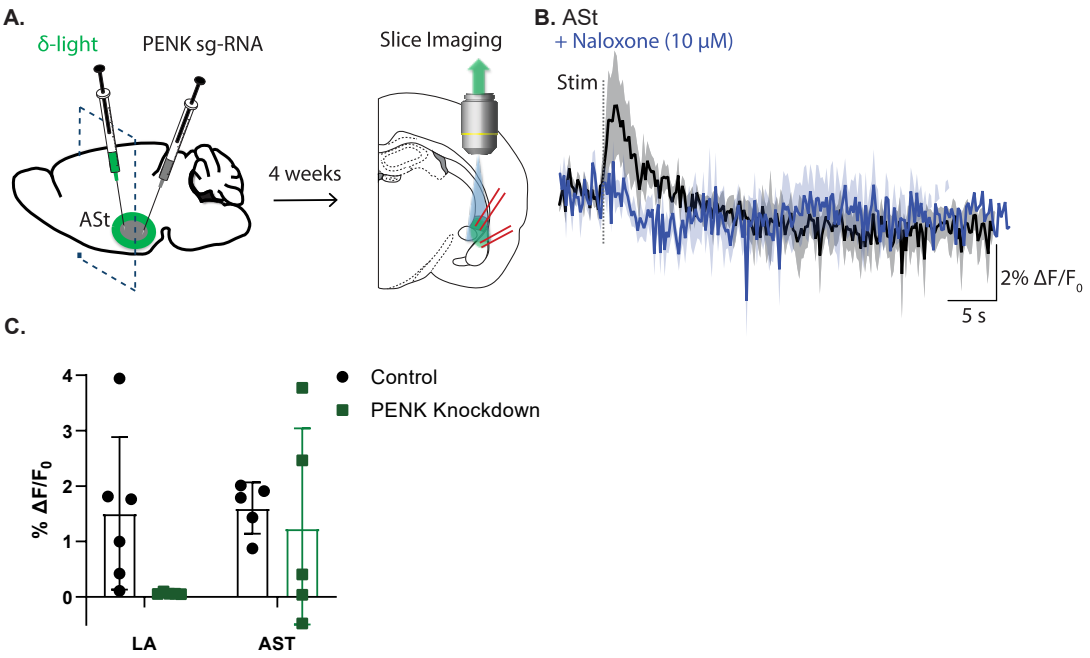

Figure 3.24. PENK sg-RNA knockdown reduces δ-light signals in the LA but not the ASt. (A) Sagittal schematic indicating AAV9-hSyn-δlight and AAV9-PENK-KO-sgRNA1injection into the ASt. Coronal schematic diagram indicating placements of stimulating electrodes in the lateral amygdala or the amygdalo-striatal transition zone. (B) Traces showing percentage $\Delta F/F_0$ of δ-light fluorescence measured in the ASt during baseline naloxone (10 μM). Each traces shows mean ± SEM. Grey dotted line indicates stimulation point. (C) Graph showing reduced percentage $\Delta F/F_0$ in the lateral amygdala in PENK knockdown. Reponses in the ASt showed a mixed results from the knockdown with 3 out of 5 neurons producing detectable responses. Each individual point represents a single neuro. Bar graph represents mean ± SEM

Post-hoc analysis of met-enkephalin immunoreactivity revealed that the slices showing detectable δ-light signals (FIG 3.25 D) had minimal PENK knockdown (Fig 3.25 B). When I plotted the fluorescence changes ($\Delta F/F_0$) against the levels of enkephalin knockdown there was a strong correlation (Fig 3.25 E). Specifically, greater knockdown corresponded to lower opioid signals (R^2 = 0.95, Fig 3.25 E). These results indicate that reducing enkephalin expression using the CRISPR virus decreases stimulation induced opioid signals, providing further evidence that enkephalin is the primary source of the opioid signals observed throughout the chapter.

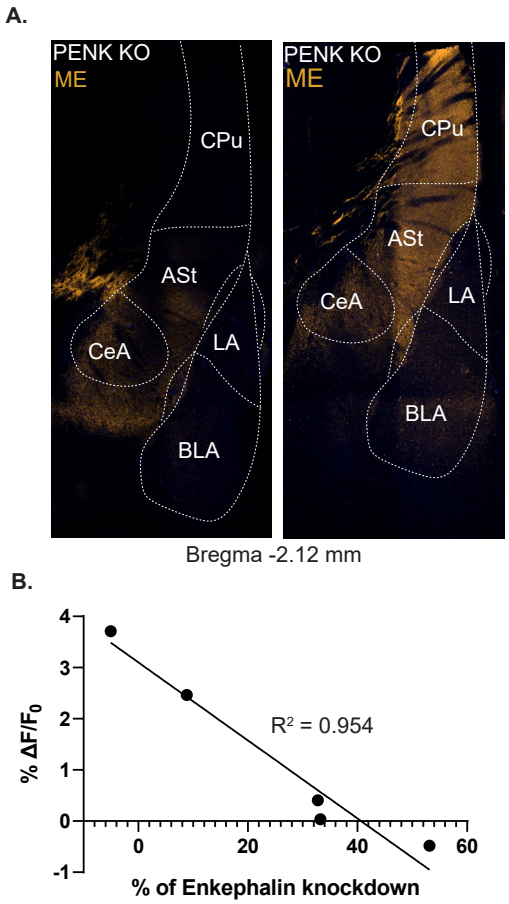

Figure 3.25. PENK sg-RNA knockdown reduces δ-light signals in a knockdown dependent manner (A) Low magnification confocal images of met-enkephalin immunoreactivity in the amygdala after viral knockdown. The virus produced variable knockdowns in the same animal with low levels of met-enkephalin expression and intact met-enkephalin expression (B) Correlation analysis between % of enkephalin knockdown and % $\Delta F/F_{0.}$ R^2 = 0.95

Taken together, these data demonstrate using two experimental approaches that MGN activation triggers endogenous enkephalin release in the amygdala. Firstly, electrophysiological recordings revealed that moderate stimulation of MGN terminals produced naloxone-sensitive inhibition of glutamate release. Secondly, direct visualisation using opioid sensors confirmed that both electrical stimulation of the ASt and optical stimulation of MGN terminals

triggers opioid receptor activation indicating increased extracellular endogenous opioid concentration, which is estimated to be ~90 nM. Several pieces of data indicate the endogenous opioid is enkephalin. Firstly, the optical signals were enhanced by peptidase inhibitors, there was dense enkephalin immunoreactivity in the ASt and reducing enkephalin expression reduced the opioid sensor response. As the sensor responses spread beyond the immediate stimulation site, particularly when protected from degradation, these findings establish a pathway where MGN activation drives ASt neurons to release enkephalin, which can modulate synaptic transmission at various sites within amygdala fear circuits including presynaptic inhibition of MGN-LA glutamate release.

3.3. Opioid dynamics in the BLA during fear learning

This section addresses aim 3.3: To examine dynamics of endogenous opioid signalling during fear learning

To address aim 3.3, I will determine whether fear conditioning increases endogenous opioid sensor activation *in vivo.* These experiments were performed by our collaborators at The University of New South Wales, Sydney.

My experiments thus far have demonstrated that endogenous opioids are released from MGN activation in the ASt and LA in amygdala slices. Endogenous opioids play a key role in fear learning, with systemic opioid receptor blockage enhancing both first- and second order fear conditioning (Michalscheck et al., 2021). Therefore, I next investigated whether the endogenous opioids release observed *in vitro* occurs in the BLA during fear learning in a behaving animal using fibre photometry.

The δ-light opioid sensor was injected into the BLA. Following recovery, animals were trained to lever press for reward (Fig 3.26 A). After successful lever press training, animals then underwent auditory fear conditioning with 3 CS-US pairings. Fear learning was quantified by CS+ induced lever press suppression quantified using a suppression ratio (see Methods B for detail). Post-conditioning CS presentation significantly reduced lever pressing, confirming acquisition of a fear response (Pre-exposure (PE): 0.523 ± 0.02

suppression ratio; n = 11, Training session 3: 0.051 ± 0.03 suppression ratio; n = 11; $p < 0.0001$; unpaired Student's t-test; Fig 3.26 B).

Initial CS presentations failed to generate opioid transients while the US induced a robust time-locked fluorescent increase (Fig 3.26 B). With repeated presentations, CS-induced opioid signalling increased as US-induced signals decreased (CS1 AUC: 3.296 ± 0.76; n = 11, US1 AUC: 9.071 ± 0.58; n = 11, $p < 0.0001$, two-way ANOVA; CS1 vs US1; Fig 3.26 D and E). These results reveal a dynamic pattern of opioid release in the BLA during fear learning. Initially, opioids are released in response to the aversive US, which likely activates multiple neuronal pathways including the MGN (Bordi & LeDoux, 1994). As training progresses, this opioid release shifts to also occur during the CS presentation, suggesting that auditory cues alone become capable of triggering opioid release. This pattern indicates that while initial opioid release is driven by footshock related activation, the auditory CS eventually gains the ability to drive endogenous opioid release. This response to auditory stimulation aligns with the *in vitro* findings showing that direct MGN activation can trigger opioid release.

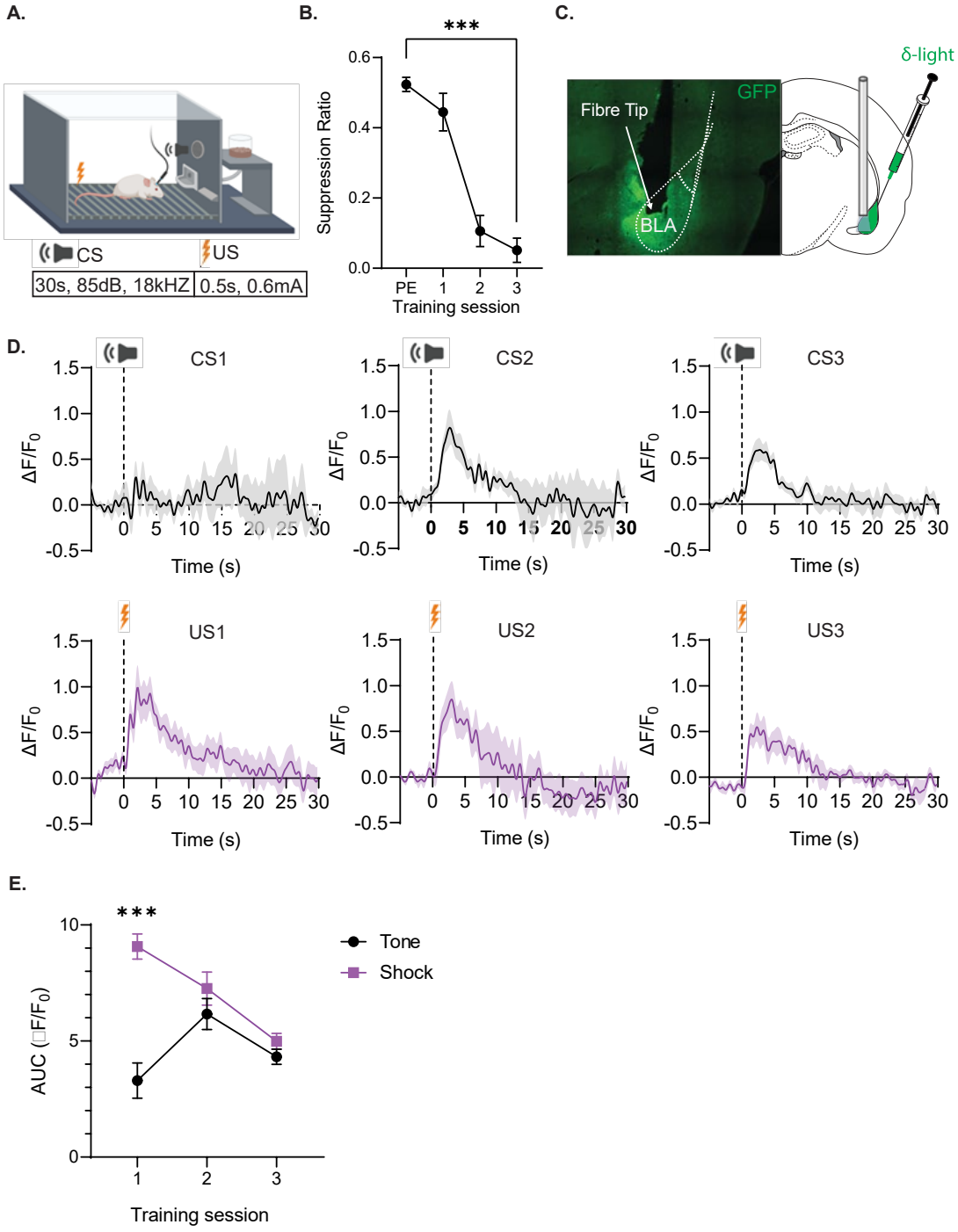

Figure 3.26. BLA opioid release exhibits prediction error-like dynamics during fear conditioning. (A) Cartoon diagram of a skinner box for the fear learning protocol. Rats that previously learnt to level press for reward undergo fear training consisting of multiple pairings a tone with a shock (B) Graph showing decreases in suppression ratio across training days (C) Cartoon schematic of the amygdala, AAV9-hSyn-δlight and fibre placement in the basolateral amygdala Low magnification confocal images showing fibre tip location and δ-light expression in the same region (D) Traces showing $\Delta F/F_0$ of δ-light fluorescence measured BLA during each tone and shock pairing. As learning progressed the tone induced changes in fluorescence increases whereas the shock induced responses decreases (E) Graph showing area under the curve of $\Delta F/F_0$ for each tone and shock pairing. Each point represent mean ± SEM, n = 11. *** $P < 0.001$ unpaired Student's t-test

C. Discussion

The experiments in this chapter used anatomical tracing, electrophysiology, optical sensors and behavioural training to characterise how MGN inputs are organised within amygdala circuits and their ability to trigger endogenous opioid release. Using viral approaches to label and control MGN terminals, I found that projections from the MGN target both LA and ASt, with particularly dense ASt innervation (Fig 3.27). Whole-cell recordings revealed that MGN activation could trigger endogenous opioid release, which was more directly visualised using newly developed opioid sensors. MGN terminals in the LA are inhibited by activation of MOR providing a site where endogenous opioids could act to reduce fear learning (Fig 3.27). Finally, fibre photometry during fear conditioning demonstrated that endogenous opioids are released and that these opioid signals show dynamic patterns, shifting from US to CS presentations as animals learn the association. The MGN-LA pathway serves as a critical circuit for auditory fear learning (J. LeDoux, 2003). Although the MGN is a division of the auditory thalamus, at the beginning of fear learning these neurons are actually more strongly activated by foot shock than the tone, with tone responses increasing as fear learning progresses (J. A. Taylor et al., 2021). Therefore, the MGN-amygdala synaptic pathway may activate amygdala neurons in response to both the footshock and the tone across fear learning. I found that this information from the MGN is delivered to both LA and ASt neurons but that there were likely differences between the strength of the connection.

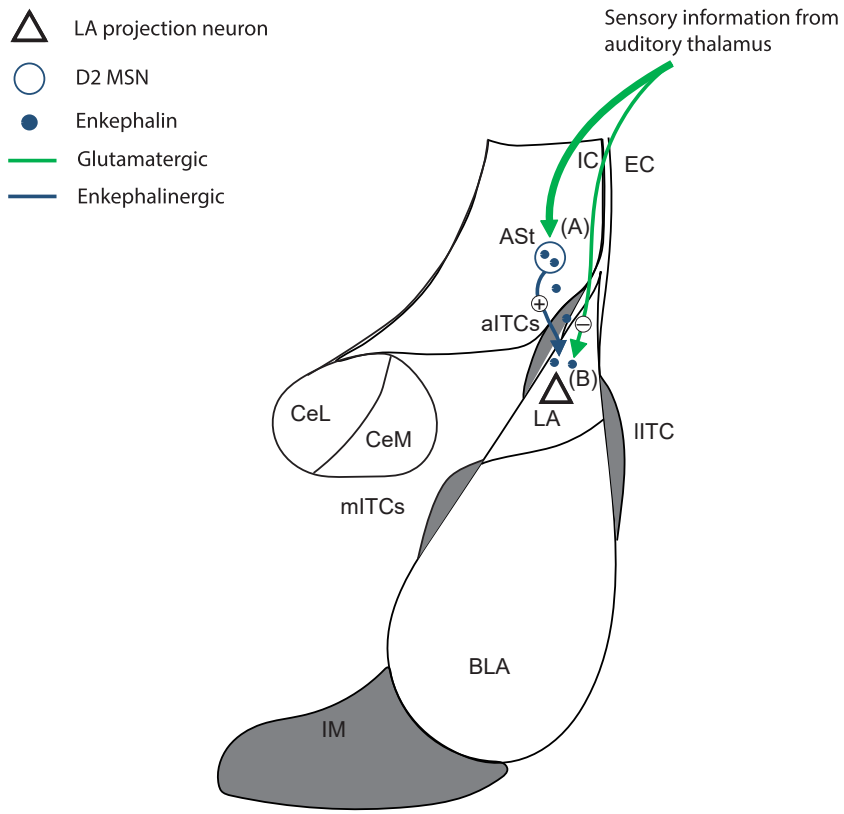

Figure 3.27. Endogenous opioid released from ASt inhibits the MGN-LA input (A) During fear learning, sensory stimuli activate auditory thalamic projections to the ASt. This activation triggers enkephalin release from D2-expressing medium spiny neurons in the ASt, which release enkephalin both locally and into the LA (B) The released enkephalin acts on auditory thalamic terminals, inhibiting glutamate release.

Previous studies established that the MGN projects to the LA, forming a critical pathway for fear learning (J. E. LeDoux et al., 1990). While general connectivity between MGN and LA neurons has been examined (Kwon et al., 2014), the distribution of these inputs to specific LA output pathway remained unknown. Anatomical tracing in this study revealed MGN terminal fields in the LA, with GFP^+ fibres showing a rostral-caudal gradient of innervation density. This gradient was reflected in functional connectivity, where electrophysiological recordings found a higher proportion of MGN-responsive neurons in caudal compared to rostral regions. Overall, approximately 50% of

LA projection neurons received functional MGN input, lower than he previously reported connectivity rate of around 84% to putative pyramidal neurons (Kwon et al., 2014). The lower connectivity rate in these experiments likely reflects the specific focus on labelled projection neurons targeting the CeA or NAc, rather than sampling from the general LA population (Kwon et al., 2014) and potential variations in the extent of opsin expression in the MGN and LA between studies. Importantly, this study provides the first direct examination of how MGN inputs are distributed to specific LA output pathways, revealing similar connectivity rates between CeA and NAc-projecting populations. This balanced distribution of sensory information to both fear and reward-related output pathways suggests that MGN provides equivalent sensory drive to circuits mediating different behavioural responses, allowing downstream regions rather than sensory inputs to determine the ultimate behavioural outcome

At MGN-LA synapses, met-enkephalin produced robust suppression of glutamate release through activation of MOR. The presynaptic locus of this effect was indicated by an increase in paired-pulse ratio during, and the MOR specificity was demonstrated through selective agonist (DAMGO) and antagonist (CTAP) effects. These findings align with anatomical studies showing dense MOR expression in the MGN, revealed through both autoradiography and in situ hybridisation (Alfred Mansour et al., 1994; Sharif & Hughes, 1989), with minimal KOR or DOR expression, explaining why met-enkephalin effects occur primarily through MOR activation (Alfred Mansour et al., 1994). This suppression of MGN input to the LA may represent a direct

cellular mechanism for opioid mediated reduction of fear learning. During fear conditioning, auditory information from the MGN drives LA neurons to encode fear (Quirk et al., 1997). By reducing glutamate release at these synapses, enkephalin would attenuate sensory signals reaching he LA, potentially explaining how opioid release reduces fear learning. However, it is worth noting that this hypothesis remains to be tested in our future experiments and opioid inhibition of MGN-LA transmission could be one of several mechanisms by which endogenous opioids regulate fear learning.

Previous anatomical studies identified projections from the MGN to the ASt (J. E. LeDoux et al., 1990), but whether these projections form functional synapses remained unclear. This study provides the first direct functional characterisation of the general MGN-ASt connectivity using a combination of viral tracing and electrophysiology. Anatomical tracing experiments revealed dense MGN terminal fields in the ASt, extending previous findings by demonstrating widespread terminal expression in this region (J. E. LeDoux et al., 1990; C. Wang et al., 2002). Whole-cell recordings confirmed this anatomical observation, revealing functional MGN connections to all recorded putative MSNs in the ASt. While previous work identified MGN connections to only specific fear-responsive ASt neurons (Kim & Cho, 2017), these findings demonstrate ubiquitous MGN connectivity across the general MSN ASt population. While the electrophysiological and morphological properties of recorded neurons were consistent with MSNs (Rangel-Barajas et al., 2021), a potential limitation is the lack of molecular confirmation of cell identity. However, given that MSNs comprise approximately 95% of neurons in striatal

regions (Lim et al., 2014), it is highly likely that the recorded population predominantly consisted of MSN's. Therefore, these findings establish the MGN-ASt pathway as a robust glutamatergic circuit that could directly drive putative ASt MSN activity, potentially in response to footshock or auditory stimulation during fear learning.

Several lines of evidence support the interpretation that MGN provides stronger synaptic input to the ASt compared to LA. First, the denser terminal expression in ASt was consistent across different viral constructs (both ChR2-GFP and ChrimsonR), suggesting this is a biological rather than technical difference. While different opsins were used for recordings (ChR2 for LA, ChrimsonR for ASt), both have similar channel conductance properties (Lin, 2011; Lin, Lin, Steinbach, & Tsien, 2009) likely making response amplitude comparisons valid. Furthermore, this stronger ASt innervation pattern has been observed in previous anatomical studies (J. E. LeDoux et al., 1990; C. Wang et al., 2002), providing additional validation of this organisational principle.

The synaptic responses of MGN to putative ASt MSNs showed consistent monosynaptic properties with fast kinetics indicating direct MGN drive of these neurons. The discovery of direct glutamatergic MGN projections to the ASt expands our understanding of auditory processing in extended amygdala regions, particularly given the presence of NMDA-mediated synaptic transmission at resting membrane potentials in the ASt. MGN-LA spines show

uniquely high expression of NMDA receptor subunits compared to other rodent forebrain regions (Radley et al., 2007) and similar expression might exist at MGN-ASt synapses, explaining the effects seen. However, technical limitations in voltage-clamp control, may also arise. One such issue could be inadequate space clamping, where the voltage control from the recording fails to uniformly clamp distant dendritic regions (N. Spruston, Jaffe, Williams, & Johnston, 1993). Consequently, whilst the soma might be held at -70 mV, dendritic compartment could remain at more depolarised potentials where NMDA receptors are still active (Lüscher & Malenka, 2012; Radley et al., 2007), resulting in the observed currents. Nevertheless, given the strong functional connectivity observed between MGN and ASt neurons, this pathway is well-positioned to drive activity in ASt neurons in response to auditory stimulation.

The robust MGN inputs to the ASt could also impact inhibitory signalling within the amygdala as ASt MSNs are GABAergic (Y. Wang et al., 2023). However, whilst GABAergic transmission from ASt neurons likely occurs following MGN activation, it is important to note that the AST-LA connections are relatively sparse (C. Wang et al., 2002), potentially limiting direct GABAergic inhibition of LA neurons. Additionally, more compelling evidence for the role of neuropeptide modulating fear learning can be discerned from optogenetic manipulation studies. Specifically, optogenetic inhibition of D1 MSNs in the ASt reduces fear learning, whereas inhibition of D2 MSNs increases fear learning (Kintscher et al., 2023). Inhibiting D1 MSNs would decrease GABA release, theoretically disinhibiting target regions and thus enhancing fear

learning. Additionally, given that both populations of MSNs are GABAergic (Y. Wang et al., 2023), their inhibition should produce similar behavioural effects if GABA were the primary mediator of these circuits. Instead, the effects of D2 MSN inhibition, which increases fear learning, is consistent with increased the fear learning seen after reducing opioid actions in vivo (Michalscheck et al., 2021). Therefore, while GABA release from ASt neurons likely occurs, it is likely the neuropeptide release from these MSNs driven by strong MGN input that may be playing a more significant role in regulating fear learning.

The finding that MGN activation drives all recorded ASt neurons suggests widespread activation of the diverse peptide populations in this region (Y. Wang et al., 2023). Two complimentary approached were used to demonstrate that MGN activation triggers endogenous opioid release, electrophysiology and opioid sensors. Firstly, electrophysiological recordings indicated that a moderate stimulation of MGN terminals produced naloxone sensitive inhibition of glutamate release from MGN terminals. While this approach revealed functional consequence of opioid signalling, its main limitation was relying on indirect measurement through changes in synaptic transmission. This indirect approach cannot distinguish which specific opioid peptides are being released, as multiple endogenous opioids can produce similar effects on the same receptor. Furthermore, this method provides limited information about the spread and temporal dynamics of opioids signalling, making it difficult to fully characterise the pattern of release.

The second approach using opioid sensors provides more direct visualisation of opioid receptor activation. The development of GPCR-based sensors provides critical technical advances for studying extracellular endogenous opioid levels. While these sensors were previously characterised in cell culture (Dong et al., 2024; Rappleye et al., 2022), this study presents validation and application of these sensors in amygdala brain slices preparations. In brain slices, I observed that the sensors maintained their expected subcellular distribution patterns previously described (Dong et al., 2024; Rappleye et al., 2022), with δ-light predominantly seen in the cell soma and UMASS showing broader distribution throughout the neuronal membrane. Initial pharmacological characterisation of the two opioid sensors using exogenous opioid agonists and antagonists found the expected specificity, with both sensors showing concentration dependent responses to met-enkephalin consistent with the characterisation in cell lines and the native opioid receptor on which they were based. The increased EC50 in both sensors for met-enkephalin represents an expected increase from cell culture preparations (Dong et al., 2024; Rappleye et al., 2022). I confirmed their selectivity in brain slices, observing no response to dynorphin and minimal response to β-endorphin only at 1 μM for δ-light only. The adaption of these sensors to amygdala slice preparation established them as a reliable tool for detecting circuit-specific endogenous enkephalin release in fear related circuits. \

Despite differences in their molecular properties, as evidenced by the increase EC50 and lower maximal responses, both sensors detected comparable relative fluorescent changes following ASt stimulation. This similarity in signal

amplitude, despite UMASS's lower affinity, suggests the broader distribution effectively compensates for reduced sensitivity by capturing release events at physiologically relevant synaptic sites. The reliability of these measurements was further validated through peptidase inhibition experiments, where both sensors showed consistent enhancement of signal magnitude and spatial spread, indicating robust detection of physiological opioid release.

The sensors revealed that both electrical stimulation of the ASt and optical stimulation of the MGN terminal in the ASt induced a naloxone sensitive activation of opioid receptors, suggesting that activation of ASt neurons increase the extracellular concentration of endogenous opioids. Given the rapid rise in fluorescence immediately following stimulation, this signal likely reflects direct opioid peptide release. This concentration was estimated to be approximately 90 nM, which in a previous study produced a ~20% inhibition of synaptic transmission in the amygdala (Winters et al., 2017). Interestingly, there were differences in the stimulation parameters required to detect opioid release between electrophysiological and optical approaches. Electrophysiological detection required fewer stimuli (5 stimulation at 150 Hz) compared to the large 100 stimulation at 100 Hz stimuli needed for optical detection. While my data suggests that the endogenous opioid concentration was ~90 nM, this may not represent the true concentration occurring during physiological release, as the sensor-based measurement depends on several factors. For sensors to report changes, the opioids must bind to the mutant receptor, therefore factors such as sensor location relative to release sites, density of sensor expression as well as the sensors pharmacology can affect

detection sensitivity. This limitation necessitated the use of a larger stimulation protocol to generate sufficient extracellular concentration of endogenous opioids for reliable optical detection. Despite these methodological differences in stimulation protocols, both approaches presented complementary evidence that MGN activation triggers opioid release from ASt neurons and given the existence of functional MORs could act retrogradely to inhibit MGN-LA synaptic transmission.

Given that the ASt contains neurons expressing enkephalin, dynorphin and substance P (Y. Wang et al., 2023), it is possible that MGN stimulation triggers release of multiple neuropeptides. While alternative opioid signals cannot be definitively excluded, as for example dynorphin A could be broken down into enkephalin fragments (Dixon & Traynor, 1990). Several lines of evidence suggest enkephalin may be the primary opioid mediating these effects. Firstly, pharmacological profiling of the sensors revealed strong specificity for met-enkephalin in slice preparations, which produced concentration-dependent increases in fluorescence, while dynorphin showed no response and β-endorphin produced only minimal changes specifically at 1 μM. This pharmacological profile matches native δ-opioid receptors, where met-enkephalin demonstrates higher potency compared to other opioid peptides (Williams et al., 2001). Secondly, the peptidase inhibition experiments align with this possibility. Enhancement of the opioid signal by peptidase inhibitors is consistent with enkephalin's known degradation profile, as met-enkephalin is rapidly degraded by peptidases while β-endorphin shows resistance to APN hydrolysis (Hui et al., 1983; Marvizon et al., 2003). Thirdly, anatomical data

from these experiments reveals dense enkephalin expression in the ASt consistent with mRNA studies (Y. Wang et al., 2023), identifying potential cellular sources for these signals. Finally, additional support comes from PENK knockdown experiments, where reduction of the enkephalin precursor attenuated the opioid signals. This convergence of pharmacological, anatomical, and genetic evidence strongly suggests enkephalin as the primary opioid.

This study provides several lines of evidence supporting the ASt as the primary source of endogenous enkephalin. Firstly, targeted PENK knockdown specifically in the ASt significantly reduced fluorescent changes in the ASt and the LA, demonstrating a direct causal relationship. Secondly, the high density of MGN terminal in the ASt combined with the functional connectivity to all recorded neurons creates robust activation that could drive enkephalin release from the ASt. Thirdly, enkephalin immunohistochemistry revealed dense expression in the ASt region, consistent with mRNA studies (Y. Wang et al., 2023). Nevertheless, the aITCs may provide an alternative source. These cells express high levels of enkephalin (Y. Wang et al., 2023), are densely innervated by MGN inputs (Asede et al., 2021), and undergo fear learning-induced plasticity unlike MGN-ASt synapses (Asede et al., 2021). Additionally, optogenetic activation of aITC suppresses MGN-LA glutamatergic transmission, suggesting a feedforward inhibitory role (Asede et al., 2021). Unlike the D2-expressing MSN in the ASt that predominantly express enkephalin (Y. Wang et al., 2023), enkephalinergic neurons in the aITC are D1 expressing (Y. Wang et al., 2023). Further investigation using selective

dopamine receptor pharmacology would therefore help delineate the relative contributions of ASt and aITC to MGN-induced enkephalin release.

The spread of the endogenous opioid signals and measurements of opioid receptor activation in the LA is particularly significant, as the LA represents a key site for fear learning (J. LeDoux, 2003). Several potential mechanisms arise from this work that may contribute to endogenous opioids acting in the LA inhibit fear learning. First, as demonstrated in this study, opioids could act as a retrograde inhibitor of MGN terminals. MGN activation triggers enkephalin release which then acts back on presynaptic MORs on MGN terminals to inhibit glutamate release from MGN terminals, potentially dampening the sensory drive that triggers fear learning. Second, endogenous opioids could directly inhibit LA principal neurons themselves (Faber & Sah, 2004). Additionally, given that fear learning increases dopamine levels in the amygdala (de Oliveira et al., 2011), endogenously released opioids could interact with dopamine signalling. However, while these multiple sites of opioid action provide a potential mechanism for fear inhibition, their relative contribution in effecting behavioural responses remain to be tested in our future experiments.

The experiments with peptidase inhibitors reveal a fundamental mechanism controlling opioid signalling in these circuits. Application of peptidase inhibitors produced robust enhancement of both the magnitude and spread of opioid signals, demonstrating tight peptidase control over opioid transmission. This regulation takes on particular significance given that adenylyl cyclase

signalling directly modulates peptidase activity (G. C. Gregoriou, Patel, Pyne, Winters, & Bagley, 2023). The broader implications of this adenylyl cyclase-peptidase coupling are particularly relevant given that multiple behaviourally significant states increase adenylyl cyclase/PKA signalling, including fear learning in the BLA (Goosens, Holt, & Maren, 2000; Schafe & LeDoux, 2000; Weeber et al., 2000), and exposure to alcohol or cocaine (Nestler, 2004). Given the robust enhancement of opioid signals observed with peptidase inhibition in the current experiments, these activity-dependent changes in peptidase function likely represent a key mechanism for regulating opioid transmission.

Finally, these experiments provide direct evidence of endogenous opioid release in the amygdala during fear learning, a process that may potentially occur alongside dopamine release in these circuits (de Oliveira et al., 2011). The presence of both neurotransmitter systems during fear learning suggests potential interactions. Pharmacological studies demonstrate that opioid receptor blockade using naloxone enhances first-order fear conditioning in humans (Eippert, Bingel, Schoell, Yacubian, & Büchel, 2008) and both first and second-order fear conditioning in rodents (Michalscheck et al., 2021). The involvement of opioids in second-order conditioning, where learning occurs in the absence of a noxious stimulation, indicates a direct role of opioids in the learning processes rather than enhancing analgesic effects. This is particularly significant as it suggests opioid signalling serves as a learning signal independent of pain processing. This is further evidenced by the temporal dynamics of opioid release found in the study, which closely parallel

dopaminergic prediction error signals (Schultz, 1998), with initial US presentations generating robust responses that gradually shift to CS presentations through learning. These findings establish endogenous opioids as key a modulator of associative learning processes in fear circuits and suggest a broader role for opioid signalling in emotional learning beyond their classical involvement in pain modulation.

This study reveals new insights into the organisation and signalling mechanisms of MGN circuits in the amygdala. The anatomical and functional experiments demonstrate dense MGN innervation of both LA and ASt regions, with particularly extensive connectivity to ASt neurons. These findings suggest broader roles for MGN beyond classical auditory processing, as the complete connectivity to ASt neurons positions this pathway to potentially influence multiple peptide systems. The experiments further characterised opioid release in these circuits using novel biosensors, with multiple lines of evidence suggesting enkephalin as a key signal. The sensitivity of these opioid signals to peptidase inhibition reveals an important regulatory mechanism, particularly given that various behavioural states can alter peptidase activity through changes in adenylyl cyclase signalling. While several potential sites of opioid actions were identified, their relative contribution to fear learning remain to be determined. Future studies using selective manipulation of enkephalin populations could also delineate the source of endogenous enkephalin. Together, these data expand our understanding of how sensory inputs may engage peptidergic modulation in amygdala circuits, while also validating new technical approaches for studying rapid neuropeptide dynamics

Chapter 4
Opioid modulation of dopamine signalling in the amygdala

A. Introduction

The reliable association of information about sensory stimuli from the environment and specific aversive or appetitive outcomes fundamentally shapes adaptive behaviours. This associative learning process can be modulated by multiple neuromodulator systems, with both opioids (Gavan P. McNally, 2009) and dopamine (Nader & LeDoux, 1999) playing important roles in fear learning. Endogenous opioids likely limit fear learning (Gavan P. McNally, 2009), whilst dopamine promotes fear acquisition and expression (Nader & LeDoux, 1999). However, whether these two neuromodulator systems interact with each other remains unknown. It is possible that these systems could interact in the ASt, as this region is strongly innervated by dopaminergic neurons from the VTA (Jean-Francois Poulin et al., 2018) and as seen in chapter 3, endogenous opioids are readily released in the ASt following auditory thalamic activation. This chapter therefore investigates the dopaminergic projection from the VTA to the ASt and how these signals may be modulated by local opioid signalling during fear learning

The VTA contains a heterogeneous population of neurons with distinct neurotransmitter profiles. This region comprises mostly of dopaminergic neurons (~60%) (S. R. Taylor et al., 2014) with approximately half of these co-expressing the glutamatergic transmission marker vesicular glutamate transporter 2 (VGluT2). (Nair-Roberts et al., 2008). Beyond these dopaminergic neurons, the VTA also contains purely GABAergic (~35%) and purely glutamatergic neurons (~2-5%) (S. R. Taylor et al., 2014). Of particular

relevance to fear learning circuits, these diverse VTA neurons project to various amygdala subdivisions with a specific pattern of innervation. The ASt and CeA receive strong VTA projections, while the BLA shows moderate innervation, and the LA receives relatively sparse inputs (Jean-Francois Poulin et al., 2018). Many of these VTA neurons that project to amygdala regions co-express markers for both dopamine and glutamate (Jean-Francois Poulin et al., 2018), suggesting co-release of both neurotransmitter at their terminals. This co-release capability creates a system where both fast acting glutamatergic and slower dopaminergic signals could potentially influence fear learning through ASt and amygdala pathways.

While traditionally studied for its involvement of reward behaviours through dopamine release (J. Cai & Tong, 2022), the VTA has emerged as an important region for processing aversive stimuli (J. Cai & Tong, 2022). Recent studies have demonstrated that specific VTA neuronal populations, particularly glutamatergic neurons are activated by and required for innate defensive responses (Barbano et al., 2020). Furthermore, optogenetic activation of VTA glutamatergic projections to the lateral habenula can directly induce aversive behaviours (Root, Mejias-Aponte, Qi, & Morales, 2014), demonstrating that VTA circuits can also actively participate in aversive processing. Given the ASt's role in processing aversive information and orchestrating fear behaviours (Kintscher et al., 2023; Mills et al., 2022), understanding the functional organisation of VTA-ASt projection, particularly, is crucial for understanding how these circuits contribute to fear learning and behaviour (J. Cai & Tong, 2022).

Multiple lines of pharmacological evidence demonstrate that dopamine acts as a critical facilitator of fear learning through its actions in the amygdala. Firstly, the activity of D1 receptors in the amygdala promotes fear learning, as antagonising D1 receptors in the amygdala prevents fear conditioning acquisition (Guarraci, Frohardt, & Kapp, 1999; Inoue et al., 2000), while activating D1 receptors with SKF 38393 enhances fear learning and restores fear responses in previously extinguished animals (Borowski & Kokkinidis, 1998). D2 receptor activation also modulates fear learning, with D2 agonists attenuating second-order fear conditioning (Nader & LeDoux, 1999) and D2 antagonist increasing freezing behaviour (Blackburn & Phillips, 1990). Together, these pharmacological findings establish dopamine as an essential facilitator of fear learning in the amygdala, acting through distinct receptor mediated mechanisms to enable fear memory formation.

The opposing effects of dopamine and endogenous opioids on fear learning suggests potential interactions between these neuromodulator systems. One possibility is that opioids might inhibit dopamine release in amygdala circuits thereby reducing fear learning. Evidence from other brain regions demonstrates that opioids can regulate dopamine release through multiple mechanisms. In the nucleus accumbens KOR are expressed on VTA terminals and their activation inhibits dopamine release (Britt & McGehee, 2008). In contrast, while activation of MOR also inhibits dopamine release this inhibition is indirect, relies on inhibition of cholinergic interneurons and only occurs under some conditions (Britt & McGehee, 2008). Specifically, activation of MORs on cholinergic interneurons suppresses acetylcholine release, which decreases

nicotinic receptor activation on dopamine terminals (Britt & McGehee, 2008). Importantly, VTA neurons projecting to the amygdala show different opioid sensitivity compared to those projecting to the striatum (Christopher P. Ford et al., 2006). VTA neurons projecting to the BLA show greater sensitivity to MOR agonists compared to KOR agonists, while the opposite pattern is observed in striatal projection (Britt & McGehee, 2008; C. P. Ford, 2014) Whether similar mechanisms operate in amygdala circuits, particularly in regions receiving dense VTA input like the ASt is unknown. Given that extensive evidence supports opioids as fear-inhibitory signals (Gavan P. McNally, 2009; G. P. McNally & Westbrook, 2003; Michalscheck et al., 2021), opioid inhibition of dopamine release in the amygdala could represent a key mechanism for this fear suppression.

Direct measurement of dopamine signalling presents significant technical challenges and has limited our understanding of potential neuromodulator interactions. While dopamine receptors couple to GIRK channels (Lledo, Homburger, Bockaert, & Vincent, 1992), allowing potential measurements through whole-cell patch camp recordings, this approach has typically required GIRK overexpression to achieve reliable robust signals (Y. Cai & Ford, 2018). Alternative methods have been able to detect dopamine release in the amygdala, such as fast-cyclic voltammetry during central amygdala electrical stimulation (Bull et al., 1991), but these measurements lack instantaneous temporal resolution and sensitivity to detect low levels of dopamine concentrations (Kile et al., 2012). Similarly, while HPLC assays have demonstrated increased dopamine levels in the amygdala during fear learning

(de Souza Caetano et al., 2013), these measurements also lack temporal resolution (F. Sun et al., 2018). The development of the D2 receptor-based fluorescent sensor GrabDA (F. Sun et al., 2018), similar to the opioid sensors used in chapter 3, offers a new approach to directly visualise dopamine binding events with near instantaneous temporal resolution. These GRAB sensors incorporate a conformationally sensitive fluorescent protein (cpGPF) into the receptor structure (F. Sun et al., 2018), allowing for real time optical readout of neurotransmitter binding. The GrabDA2h sensor specifically provides excellent sensitivity (EC50 ~ 7 nM), fast kinetics, and high specificity for dopamine over other catecholamines, enabling detection of both tonic and phasic dopamine release in vivo (F. Sun et al., 2018).

Data from chapter 3 suggests that auditory thalamic stimulation readily triggers release of endogenous enkephalins from the ASt. Given the strong VTA input to the ASt (Jean-Francois Poulin et al., 2018), this places the ASt as a potential key site for interaction between dopaminergic and opioid systems. It was hypothesised that: *VTA inputs release dopamine in the amygdalo-striatal transition zone, and that this dopamine release is inhibited by locally released endogenous opioids*

The specific aims are:

1. To examine the anatomical and functional nature of VTA projections to the ASt
2. To determine if VTA projections release dopamine in the amygdalo-striatal transition zone

3. To determine whether opioids regulate dopamine signalling in the amygdala

B. Results

4.1 The anatomical and functional properties of VTA projections to the ASt

This section addresses aim 4.1: To characterise the anatomical and functional nature of VTA projections to the ASt.

To address aim 3.1, I will investigate the nature and strength of VTA synaptic input to the ASt using immunohistochemistry and electrophysiology

4.1.1 Ventral tegmental area projects strongly to the amygdalo-striatal transition zone

The ventral tegmental area (VTA) sends projections to the amygdala and the adjacent ASt, with these connections anatomically mapped through detailed tracing studies (Jean-Francois Poulin et al., 2018). (Jean-Francois Poulin et al., 2018). In this first experiment I aimed to build a more detailed picture of the VTA inputs to the ASt.

To investigate VTA inputs to the ASt, an anterograde, red-shifted fluorescent viral opsin ChrimsonR (AAV5-Syn-ChrimsonR-tdT) was microinjected into the VTA (Fig 4.1 A). After a minimum of 6 weeks, coronal brain slices containing the amygdala were taken and slices where mounted to visualise VTA terminal fields in the amygdala. The opsin was successfully expressed in the VTA of 5 animals. Viral expression resulted in intense tdTomato fluorescence within the

VTA, with minimal spread to the adjacent SNr (Fig 4.1 B). Examination of terminal fields in the amygdala revealed dense tdTomato expressing fibers in both the CeA and ASt (Fig 4.1 C) and low expression in the LA (Fig 4.1 C). (Jean-Francois Poulin et al., 2018). The dense terminal expression is consistent with previously reported anatomical studies (Jean-Francois Poulin et al., 2018).

This experiment demonstrated that the VTA provides robust inputs to both the CeA and ASt and that our viral injections successfully targeted the appropriate region of the VTA.

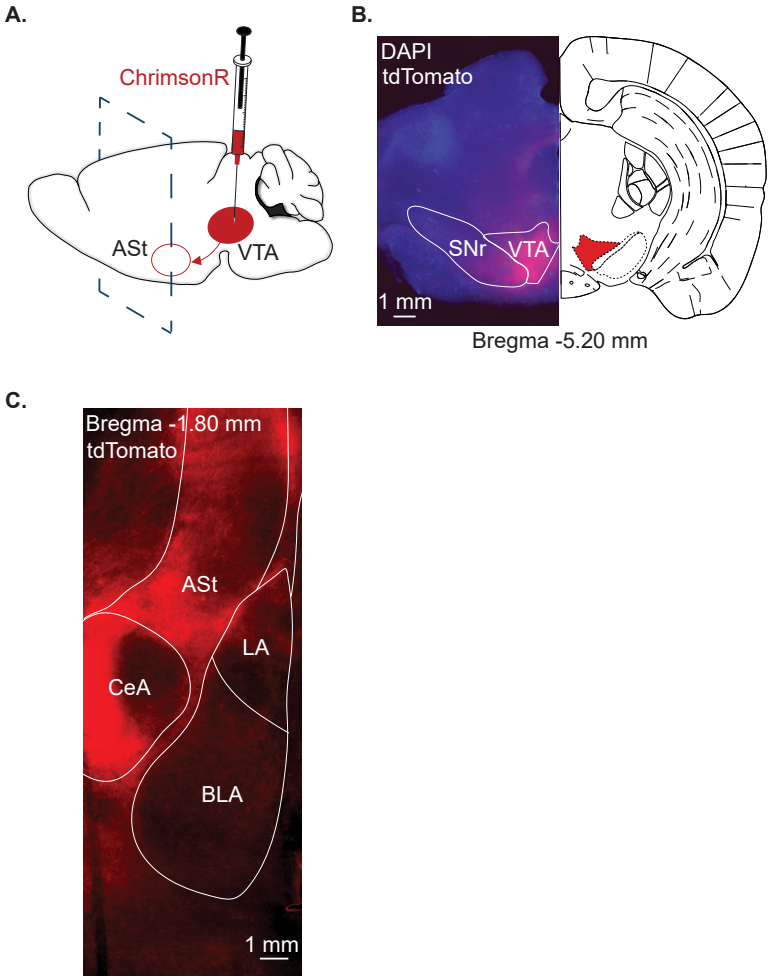

Figure 4.1. VTA projections target the ASt and CeA. (A) Sagittal schematic indicating AAV5-Syn-ChrimsonR-tdT injection into the VTA. (B) Low magnification wide-field image showing DAPI (blue) and ChrimsonR-tdT (red) expression in the VTA. ChrimsonR-tdT expression was confined to the VTA. The imaged slice corresponded to a Bregma coordinate of -5.20 mm (C) Low magnification wide-field image showing ChrimsonR-tdT (red) expression in the amygdala. High level of ChrimsonR-tdT is seen in the CeA and ASt. ASt – amygdalo-striatal transition zone, BLA – basolateral amygdala, CeA – central amygdala, LA – lateral amygdala, SNr – substantia nigra, VTA – ventral tegmental area

4.1.2 VTA forms sparse functional excitatory connectivity with ASt neurons

Anatomical data has revealed that VTA neurons expressing the vesicular glutamate transporter (Vglut2) make strong projections to the CeA, BLA and the ASt (Jean-Francois Poulin et al., 2018). However, when these terminals are stimulated optogenetically the synaptic responses in CeA and BLA neurons were sparse and small, with ~30% neurons connected and an average amplitude of approximately 8 pA (Mingote et al., 2015). The functional properties of the VTA-ASt synaptic connections have not been examined.

To examine functional properties of VTA-ASt connections, whole-cell patch clamp recordings were performed in ASt neurons while optogenetically stimulating VTA terminals using the excitatory opsin ChrimsonR. The membrane potential of neurons was held at -70 mV and recording were done in the presence of the $GABA_A$ receptor antagonist picrotoxin (100 μM). Putative MSNs were selected based on visualised small cell morphology and membrane capacitance values under 15 pF, similar to recordings from ASt neurons in chapter 3.

Paired pulse orange light stimulation of the VTA terminals evoked responses in only in 2 out of 15 AST neurons recorded. One of the neurons had an

average amplitude of 16pA (neuron 1), whilst the other neuron (neuron 2) displayed variable amplitude ranging from 10-200 pA (Fig 4.2 B). Analysis of synaptic jitter, measured as the standard deviation of response latencies from stimulus onset, revealed that the jitter for neuron 1 displayed monosynaptic properties (jitter = 0.65 ms, Fig 4.2 B), whilst neuron 2 showed higher jitter values indicative of polysynaptic transmission (jitter = 1.45 ms, Fig 4.2 B) and was not considered a direct VTA-AST synaptic connection. The synaptic response in neuron 1 displayed fast kinetics with an average rise time of 0.4 ms and a weighted decay constant of 11.43 ms which is consistent with AMPA receptor-mediated currents (Angulo, Rossier, & Audinat, 1999). This suggests that connections between the VTA and neuron 1 is likely glutamatergic in nature. Therefore, the direct connection rate was 1/15 neurons. Overall, the low connectivity rate and small likely AMPA-mediated, currents align with the sparse connectivity patterns previously observed in both VTA-BLA and VTA-CeA (Mingote et al., 2015). This experiment therefore demonstrates that despite anatomical evidence of VGlut2 expressing VTA projections to the ASt, functional excitatory connections to MSNs are very sparse.

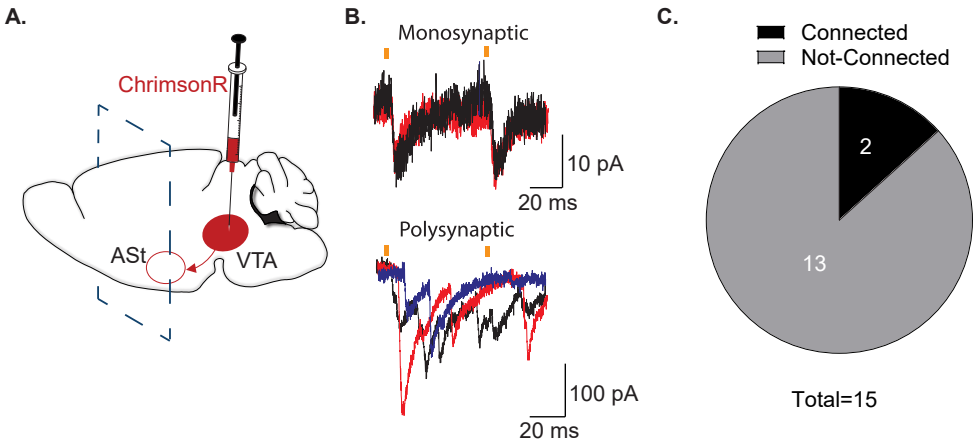

Figure 4.2. Functional connections from the VTA to ASt are sparse. (A) Sagittal schematic diagram indicating AAV5-Syn-ChrimsonR-tdT injection into the VTA. (B) Example traces showing oEPSC from putative ASt MSNs indicating a directly connected cell (top) and an indirectly connected cell (bottom). Black, red and blue traces indicate different episodes from the same recording. Orange bars indicate optical stimulation points. (C) Pie chart showing number of connected versus non-connected cells. A total of 2 cells shown in (B) were connected out of 15 neurons recorded.

4.2 Dopamine release from VTA projections in the ASt

This section addresses aim 3.2: To determine if VTA projections release dopamine in the ASt

To address aim 3.2, I will use immunohistochemistry to identify dopaminergic terminal expression in the ASt and then investigate whether stimulation of VTA terminals in the ASt produces dopamine release using optical biosensors

4.2.1 The ASt strongly expresses tyrosine hydroxylase

Given the low frequency of glutamatergic connectivity observed in the VTA-ASt projections, it is possible that dopamine may be the predominant neurotransmitter in this pathway. This possibility is supported by evidence that VTA neurons contain high levels of cells co-expressing both the enzyme required for dopamine production, tyrosine hydroxylase (TH), and Vglut2 (Jean-Francois Poulin et al., 2018), suggesting these terminals likely contain dopaminergic machinery. I therefore investigated whether TH is expressed in the ASt.

To examine the presence of dopaminergic input in the amygdala, post-hoc immunohistochemistry staining for TH was performed on slices used in the previous experiments. The staining revealed dense TH immunoreactivity in the CeA and low expression in the basolateral amygdala (BLA) (Fig 4.3) matching the expression profile of VTA terminal projections seen previously (Fig 4.1). Notably high levels of TH expression were also seen in the ASt (Fig 4.3). This

expression profile matches the pattern of VTA terminal projections observed in the previous experiment (Fig 4.1). The dense TH immunoreactivity observed in the ASt provides anatomical evidence for significant dopaminergic input to this region. However, TH staining alone cannot definitively identity the source of these terminals as TH is expressed in dopaminergic neuron from the substantia nigra (Jean-Francois Poulin et al., 2018), as well in noradrenergic neurons (Pickel, Joh, & Reis, 1975) Nevertheless, this experiment demonstrates substantial dopaminergic machinery in the ASt, suggesting that dopamine may be released in the VTA-ASt pathway. Specific co-labelling experiments would be necessary to confirm the precise origin of these terminals

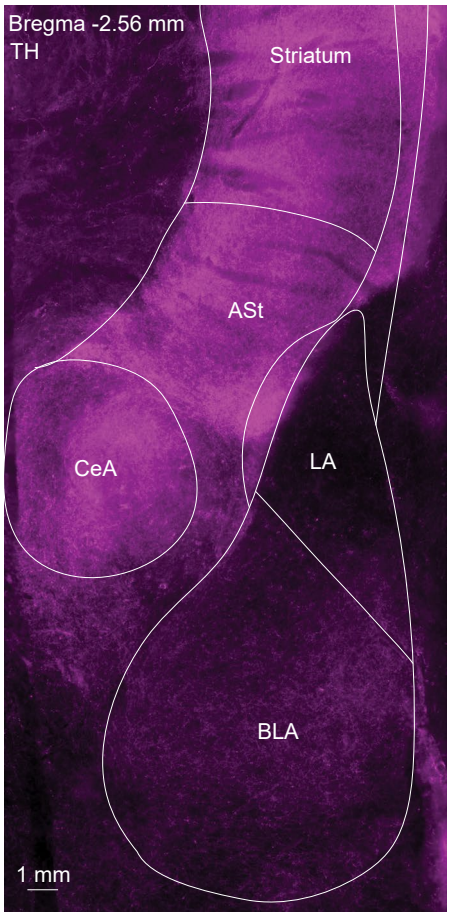

Figure 4.3. Amygdalo-striatal transition zone expression high levels of the dopamine synthesis rate-limiting enzyme tyrosine hydroxylase. Low magnification wide-field image of tyrosine hydroxylase immuno-reactivity in the amygdala. Low to moderate levels of expression seen in the BLA, whilst high levels of expression are seen in the CeA, ASt and striatum. ASt – amygdalo-striatal transition zone, BLA – basolateral amygdala, CeA – central amygdala, LA – lateral amygdala.

4.2.2 Characterisation of GrabDA in the amygdala

The strong VTA innervation of the ASt combined with strong expression of TH in the same region suggests that VTA terminals could be releasing dopamine. I therefore wanted to investigate whether this was the case using the fluorescent dopamine sensor GrabDA.

To validate the functionality of GrabDA in the amygdala slices as a measure of dopamine release, the GrabDA (AAV9-hSyn-GRAB-DA2h) was microinjected into the amygdala (Fig 4.4 A) and wide-field fluorescent recordings were performed during bath application of dopamine and selective antagonists. For these experiments a maximal concentration of 30 μM of dopamine was chosen for these experiments based on the sensor's properties and the known actions of dopamine within the amygdala (Gabrielle C. Gregoriou et al., 2019; F. Sun et al., 2018). For these experiments the selective D2-receptor antagonist eticlopride was chosen as it selectively blocks GrabDA in cell culture (Egan, Herrick-Davis, & Teitler, 1998)(Sun et al., 2018).

At least 4 weeks after the viral injection, coronal brain slices containing the ASt were taken for live imaging. Notably, GrabDA expression was seen throughout the injection target. This expression was strong but diffuse with sparse expression in cell soma (Fig 4.4 B). Bath application of dopamine (30 μM) produced robust increases in GrabDA fluorescence (4.4 B and C), indicating successful detection of dopamine binding events. The specificity of the signal was indicated through application of the D2-selective antagonist eticlopride (Fig 4.4 B and C), which reversed the dopamine-induced increase in fluorescence. This demonstration mirrors the previous validation of an opioid sensor and shows that wide-field slice recording can effectively measure dopamine activation of GrabDA in amygdala brain slices. Additionally, the lack of cell body expression is consistent with the sensor not containing restriction motifs (F. Sun et al., 2018), similar to the UMASS opioid sensor used in

chapter 3. Consequently, this approach allows for the measurement of endogenous dopamine release, providing a validated approach for subsequent investigations of VTA-mediated dopamine release.

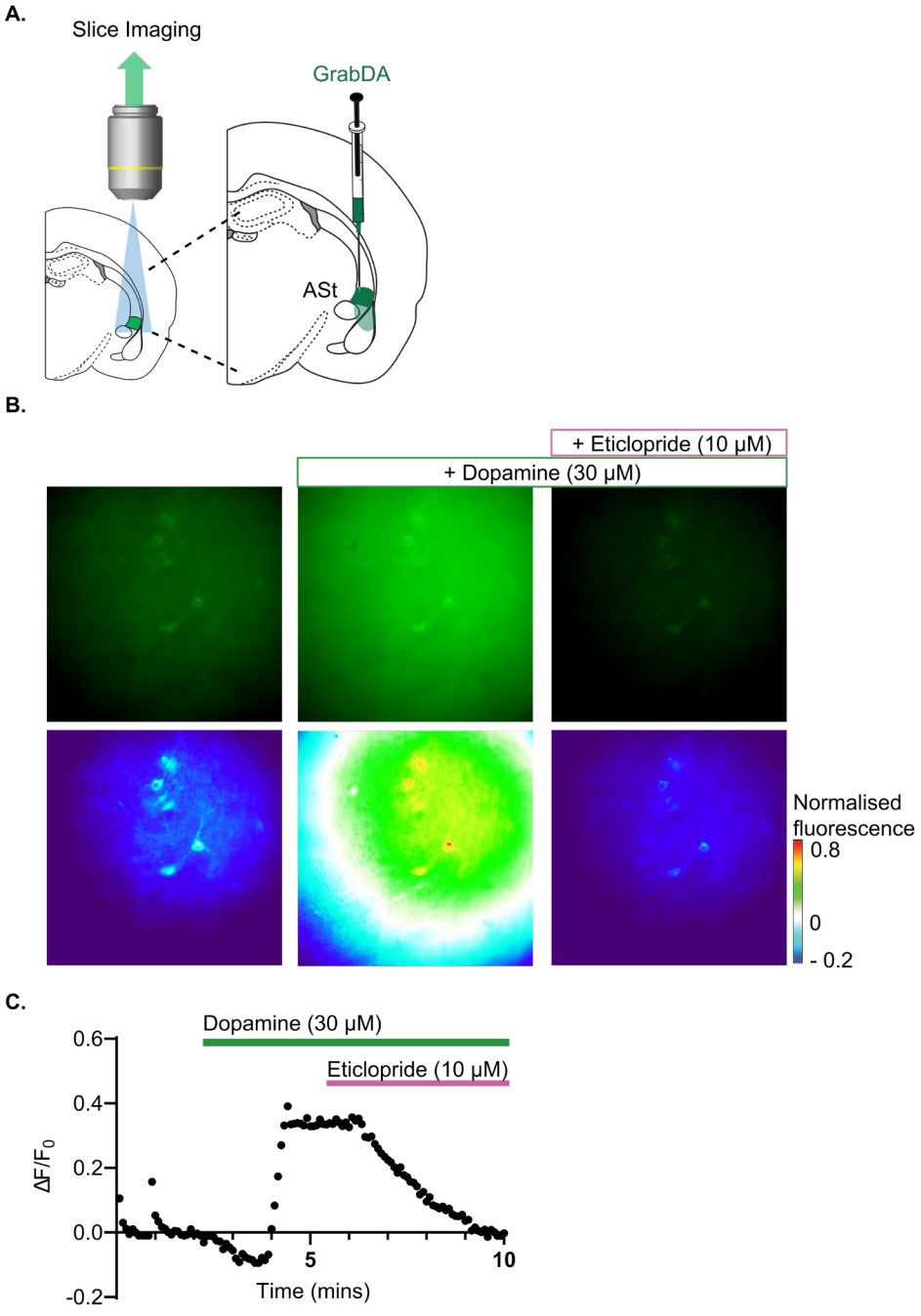

Figure 4.4. GrabDA detects exogenous dopamine binding. (A) Coronal cartoon schematic diagram of the amygdala indicating recording location and injection of AAV9-hSyn-GRAB-DA2h into the amygdalo-striatal transition zone (B) Example recording images and pseudo coloured heat maps of GrabDA fluorescence in the ASt showing

increased fluorescent after application of exogenous dopamine (30 μM) and reversal after eticlopride (10 μM). (C) Example time plot showing $\Delta F/F_0$ showing increases during dopamine application and reversal with eticlopride\

4.2.3 VTA activity triggers dopamine release in the ASt and LA

Having validated GrabDA's ability to detect dopamine in my slice preparation, the next step was to examine endogenous dopamine release form VTA terminals in the ASt. Data from chapter 3 utilised a stimulation protocol consisting of 100 stimulations at 50 Hz, which induced reliable endogenous opioid mediated fluorescent changes. This provided a starting point for stimulation parameters for dopaminergic release.

To investigate VTA-mediated dopamine release in the ASt, the red-shifted excitatory opsin ChrimsonR (AAV5-Syn-ChrimsonR-tdn) was microinjected into the VTA whilst GrabDA was microinjected into the ASt (Fig 4.5 A). Similar to experiments in chapter 3 this dual-expression strategy enables selective activation of VTA terminals while monitoring dopamine release through fluorescent changes.

Optical stimulation of VTA terminals resulted in time locked, rapid increases in GrabDA fluorescence within the ASt (Fig 4.5 B) that likely corresponds to stimulated dopamine release. Initially, the 100 stimulations caused relatively small fluorescence changes (1.09 ± 0.18% $\Delta F/F_0$, n = 5, Fig 4.6 B). To enhance the dopamine release, 250 stimuli were then tested. However, this did not produce a significantly larger event when compared to the 100 stimuli

(1.49 ± 0.82% $\Delta F/F_0$, n = 3, P = 0.46, unpaired Student's t-test 100 stimulations versus 250 stimuli, Fig 4.5 B-C). Therefore, to further increase the stimulation strength and elicit a more robust response, 500 stimuli were applied. Using 500 stimulations resulted in significantly larger GrabDA responses (3.24 ± 0.61% $\Delta F/F_0$, n = 9, P = 0.049, unpaired Student's t-test, 100 stimuli versus 500 stimuli, Fig 4.5 B-C), allowing for clearer detection of the fluorescent transients. Thus, 500 stimuli were chosen as the optimal stimulation for the following experiments.

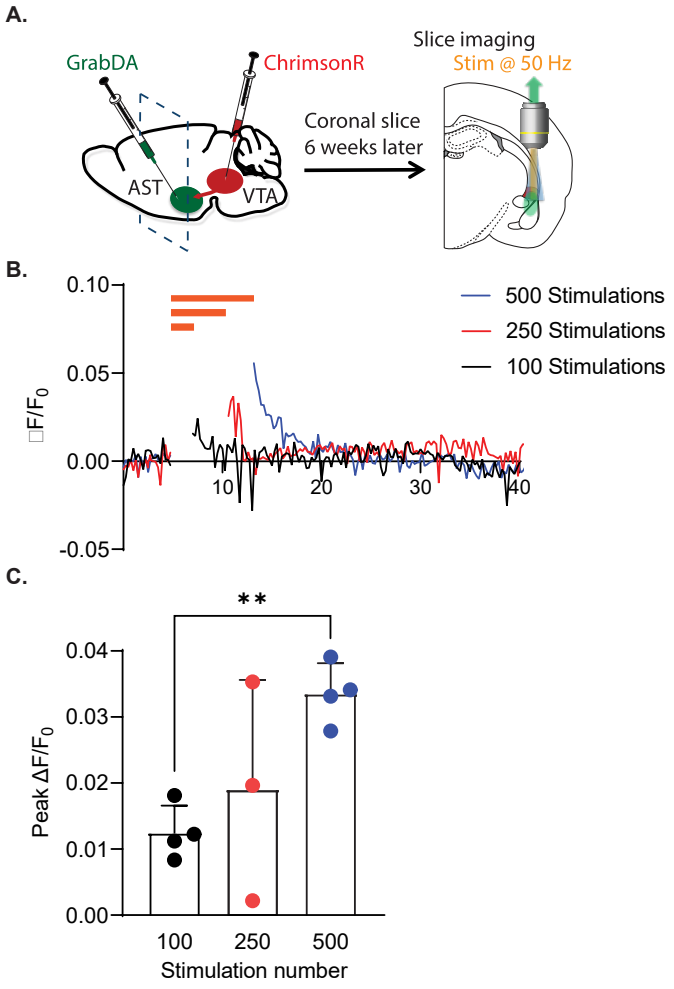

Figure 4.5. VTA terminals release dopamine in a stimulation dependent manner. (A) Sagittal schematic diagram indicating AAV5-Syn-ChrimsonR-tdT into the VTA and AAV9-hSyn-GRAB-DA2h into the ASt. Coronal cartoon diagram of the amygdala indicating recording location (B). Example traces showing larger peak $\Delta F/F_0$ recorded in the ASt by different optical stimulation numbers. Orange bar indicates stimulation point. (B) Graph

showing peak $\Delta F/F_0$ measured as the first 8 frames after stimulation during different stimulation numbers. Each individual point represents a single slice recording. Bar graph indicated mean ± SD. ** P < 0.01 unpaired Student's t-test

I also examined whether VTA terminal stimulation increased GrabDA fluorescence in the LA. Stimulation-induced transients were detected in the LA on the same slices (4.19 ± 1.35% $\Delta F/F_0$, n = 4, Fig 4.6 C and D). To confirm that these transients were due to an agonist activating GrabDA I applied the D2 antagonist eticlopride. Eticlopride significantly inhibited the stimulation induced GrabDA transients in the ASt (Baseline: 3.24 ± 0.61% $\Delta F/F_0$; Eticlopride: 0.81 ± 0.28% $\Delta F/F_0$, n = 9, p = 0.0007, paired Student's t-test baseline versus eticlopride. Fig 4.6 A-B) and the LA (Baseline: 4.19 ± 1.35% $\Delta F/F_0$; Eticlopride -0.19 ± 0.43% $\Delta F/F_0$, n = 4, p = 0.04, paired Student's t-test baseline versus eticlopride, Fig 4.6 C and D). The GrabDA transients in the LA, indicate either the diffusion of dopamine from the ASt to the LA, similar to the behaviours of enkephalins, or direct dopamine release from sparse VTA projections to the LA.

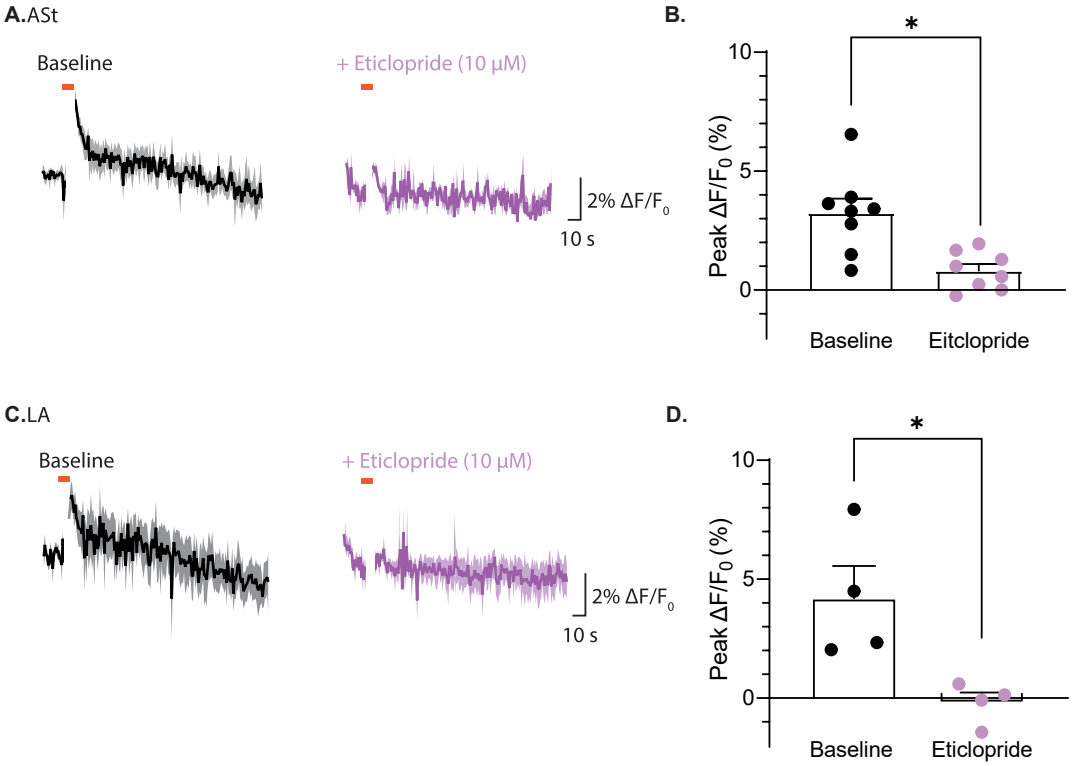

Figure 4.6. Dopamine induced fluorescence changes are seen in the ASt and LA (A) Example traces showing % $\Delta F/F_0$ measured in the ASt during baseline and no response during eticlopride. Each trace represent mean ± SEM (B) Graph showing peak % $\Delta F/F_0$ in the ASt measured as the first 8 frames after stimulation during baseline and eticlopride application Each individual point represents a single slice recording. Bar graph indicated mean ± SEM. (C-D) Same and A and B respectively but for the LA. * $P < 0.05$ paired Student's t-test.

While anatomical studies suggest that VTA terminals may contain a mix of neurotransmitters (Jean-Francois Poulin et al., 2018), these findings demonstrate that dopamine acts as the primary neurotransmitter released from VTA terminals in the ASt. Furthermore, the effects of this dopamine release extend to the LA, highlighting the broader impact of VTA dopaminergic signalling.

4.3 Regulation of dopamine signalling by opioids in the amygdala

This section addresses aim 4.3: To determine whether opioids regulate dopamine signalling in the amygdala.

To address aim 4.3, I will investigate whether exogenous and endogenous opioids modulate dopamine release from VTA terminals in the ASt and LA using optical biosensors

4.3.1 Dopamine release from VTA terminals in the AST is inhibited by enkephalin

Given the opioid sensitivity of dopamine release in the NAc (Britt & McGehee, 2008) and the opioid sensitivity of some VTA neurons projecting to the amygdala (Christopher P. Ford et al., 2006), the next experiment(Christopher P. Ford et al., 2006; Jean-Francois Poulin et al., 2018; Y. Wang et al., 2023) investigated whether dopamine release in the ASt could be influenced by opioid receptor activation.

To examine opioid-mediated effects on dopamine release, GrabDA and the excitatory opsin ChrimsonR were utilised (Fig 4.7 A) following the same experimental protocol as in figure 4.5. Optical stimulation generated consistent time-locked fluorescence changes in the ASt, which were significantly inhibited by the application of the D2 antagonist eticlopride, indicating dopamine release (Baseline: 3.24 ± 0.61% $\Delta F/F_0$; Eticlopride: 0.81 ± 0.28% $\Delta F/F_0$, n = 8, P = 0.018, One-way ANOVA, Tukey's post-hoc multiple comparison baseline

versus eticlopride, Fig 4.7 B and C). Met-enkephalin significantly reduced the optically induced fluorescence change (Baseline: 3.24 ± 0.61% $\Delta F/F_0$; Met-enkephalin: 0.75 ± 0.35% $\Delta F/F_0$, n = 8, P = 0.016, One-way ANOVA, Tukey's post-hoc multiple comparison baseline versus met-enkephalin, Fig 4.7 B-C). This reduction was fully reversed by the subsequent application of CTAP, a MOR-selective antagonist (Met-enkephalin: 0.75 ± 0.35% $\Delta F/F_0$; CTAP: 3.36 ± 0.60% $\Delta F/F_0$, n = 8, P = 0.011, One-way ANOVA, Tukey's post-hoc multiple comparison met-enkephalin versus CTAP, Fig 4.7 B and C).

The application of KOR agonists and antagonists produced no effect on GrabDA signal in the ASt (Baseline: 3.24 ± 0.61% $\Delta F/F_0$, n = 8; U69: 2.11 ± 0.53% $\Delta F/F_0$, n = 5, P = 0.55, One-way ANOVA, Tukey's post-hoc multiple comparison baseline versus U69, Fig 4.7 B and C).

These results demonstrate that dopamine release from VTA terminals in the ASt is selectively inhibited by MOR but not KOR or DOR activation. This selective inhibition by met-enkephalin reveals a possible mechanism through which endogenous opioids could regulate dopaminergic signalling and in turn fear learning in the ASt. The lack of effects of KOR drugs aligns with previous pharmacology data obtained from BLA projecting VTA neurons (Christopher P. Ford et al., 2006). This suggests that VTA projections to the ASt likely originate from a neuronal population similar to those projecting to the BLA.

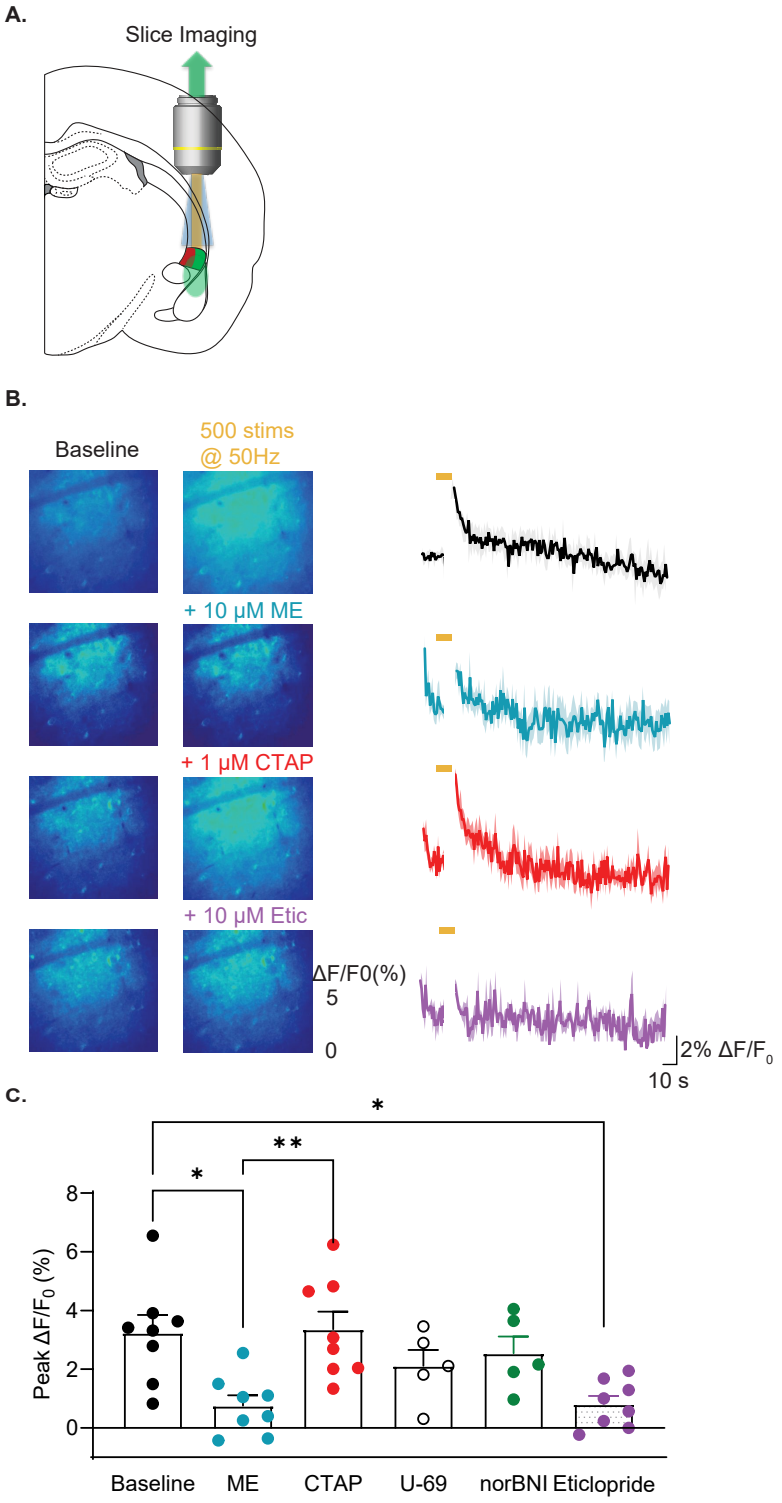

Figure 4.7. VTA terminals in the ASt release dopamine. (A) Coronal schematic diagram of recording location in the ASt. (B) Example pseudo coloured heat-map images and traces showing fluorescence changes recorded in the ASt after optical stimulation protocol and inhibition of optically induced fluorescence change by met-enkephalin (10 µM). Application of CTAP (10 µM) reversed the inhibition and eticlopride (10 µM) prevented it. Each trace represent mean ± SEM (C) Graph showing peak % $\Delta F/F_0$ measured as the first 8 frames after stimulation during each drug application. The

KOR agonist (U69 3 μM), and antagonist (norBNI 10 nM) did not have an effect on the peak % $\Delta F/F_0$. Each individual point indicates a single slice recording. Bar graph represents mean ± SEM. * P < 0.05, ** P < 0.01, One-way ANOVA with Tukey's post-hoc multiple comparison.

4.3.2 Dopamine release from VTA terminals in the LA is inhibited by enkephalin

The LA is a critical site for fear learning and associative plasticity (J. LeDoux, 2003). Data from the previous experiment detected dopamine signalling in the LA following VTA terminal stimulation (Fig 4.6). This raises the important question of whether opioids might also modulate dopamine signalling in this key learning region, potentially providing a mechanism for opioid regulation of fear learning. Using the same experimental setup as above (Fig 4.7), the effects of met-enkephalin and the MOR antagonist CTAP on optically evoked dopamine release from VTA terminals were examined in the LA.

Optically evoked GrabDA responses in the LA also showed a significant reduction during met-enkephalin application (Baseline: 3.36 ± 1.34% $\Delta F/F_0$; Met-enkephalin: 0.34 ± 0.35% $\Delta F/F_0$, n = 5, p = 0.034, One-way ANOVA, Tukey's post-hoc multiple comparison baseline versus met-enkephalin, Fig 4.8 A and B). This effect was fully reversed by CTAP (Met-enkephalin: 0.34 ± 0.35% $\Delta F/F_0$; CTAP: 5.88 ± 1.43% $\Delta F/F_0$, n = 5, p = 0.04, One-way ANOVA, Tukey's post-hoc multiple comparison met-enkephalin versus CTAP, Fig 4.8 A and B), demonstrating that VTA-released dopamine influences LA neurons and can be modulated by met-enkephalin. This finding is particularly significant given the LA's established role in fear learning (J. LeDoux, 2003)

While VTA projections to the BLA express MOR, unlike those projecting to the striatum (Christopher P. Ford et al., 2006). This MOR expression profile and the data from this study suggest that VTA dopamine release in both the ASt and the LA may be inhibited through direct activation of MOR on VTA terminals. Notably, this regulation appears distinct from striatal circuits, where MOR effects on dopamine release are indirect and works through cholinergic interneuron suppression (Britt & McGehee, 2008)

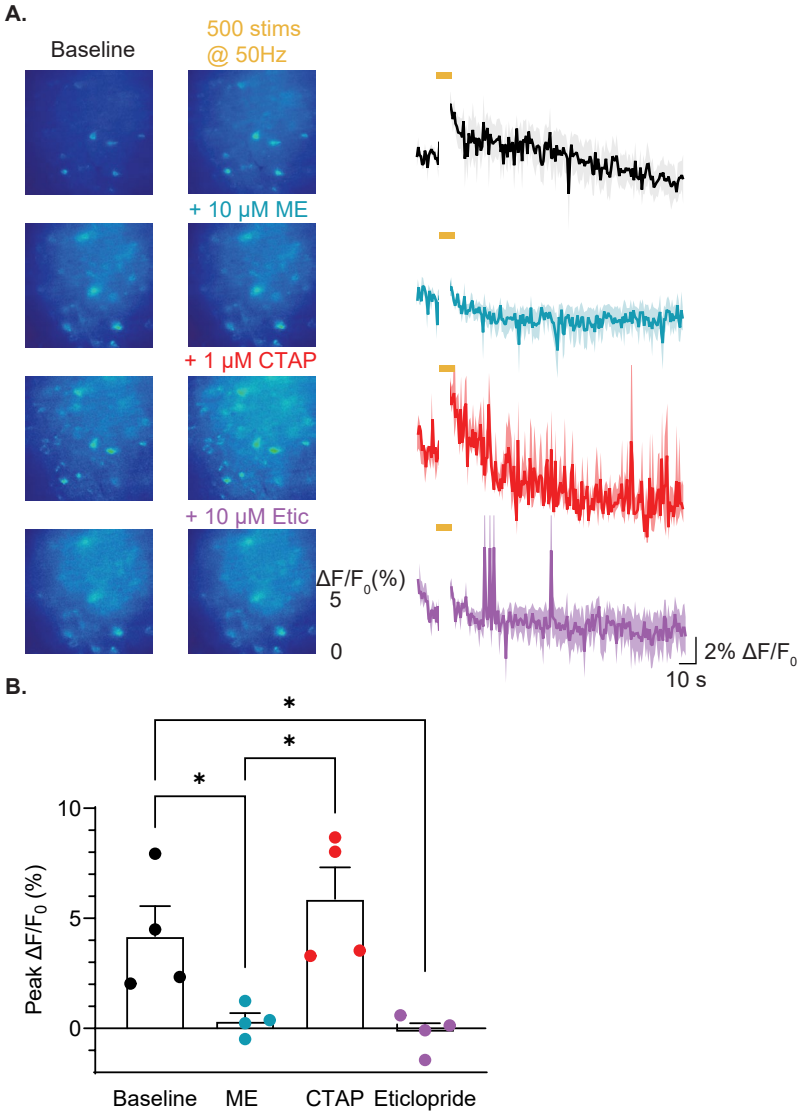

Figure 4.8. Optical stimulation of VTA terminals induce dopamine signals in the LA. (A) Example pseudo coloured heat-map images and traces showing fluorescence changes recorded in the LA after optical stimulation protocol and inhibition of optically

induced fluorescence change by met-enkephalin (10 μM). Application of CTAP (10 μM) reversed the inhibition and eticlopride (10 μM) blocked it. Each trace represent mean ± SEM (C) Graph showing peak % $\Delta F/F_0$ measured as the first 8 frames after stimulation during each drug application. Each individual point indicates a single slice recording. Bar graph represents mean ± SEM. * $P < 0.05$, One-way ANOVA with Tukey's post-hoc multiple comparison.

4.3.3 Endogenous opioids released from ASt activation inhibits VTA dopamine release

Previous data from chapter 3 suggests that auditory thalamus activity triggers endogenous enkephalin release in the amygdala. The source of this endogenous enkephalin release likely originates from the ASt or nearby areas such as the apITC. This raised the question of whether this endogenously released enkephalin could modulate VTA dopaminergic signalling in the ASt. Therefore, a preliminary experiment was conducted to test this.

To investigate whether this endogenous enkephalin modulates dopamine signalling, stimulating electrodes were placed in the ASt while GrabDA signals were recorded in the same region using the same stimulation protocol as the previous experiment (Fig 4.9). In initial experiments, recordings were conducted in the presence of the cocktail of peptidase inhibitors (thiorphan 10μM, bestatin 10 μM and captopril μM), these peptidase inhibitors were previously used to prevent peptides degradation and to optimise detection of endogenous opioid effects (chapter 3).

Optical stimulation of VTA terminals produced a time-locked increase in fluorescence (Fig 4.8 A). When a moderate electrical stimulation (Fig 3.13) of the ASt was applied simultaneously with optical stimulation of VTA terminals,

I observed inhibition of the fluorescent signal (Baseline: 3.81 ± 2.79% $\Delta F/F_0$; Moderate stimulation: 0.64 ± 2.14% $\Delta F/F_0$, P = 0.045, n = 3, paired Student's t-test, data expressed as mean ± SD, Fig 4.9 B and C). This reduction was reversed by applying the MOR-selective antagonist CTAP during moderate stimulations (Moderate stimulation: 0.64 ± 2.14% $\Delta F/F_0$; CTAP: 3.18 ± 4.8% $\Delta F/F_0$; P = 0.048, n = 3, paired Student's t-test, data expressed as mean ± SD, Fig 4.9 B-C). Application of eticlopride prevented optically induced fluorescent changes, indicating this signalled likely result from GrabDA activity (Fif 4.9 B and C).

These preliminary findings suggest that endogenously released enkephalin can effectively modulate VTA dopamine signalling in the ASt, as demonstrated by the suppression of dopamine release during electrical stimulation and its reversal by CTAP. While further experiments are needed to fully characterise this interaction, these initial results point to a potential circuit mechanism linking auditory thalamus driven enkephalin release to dopamine modulation.

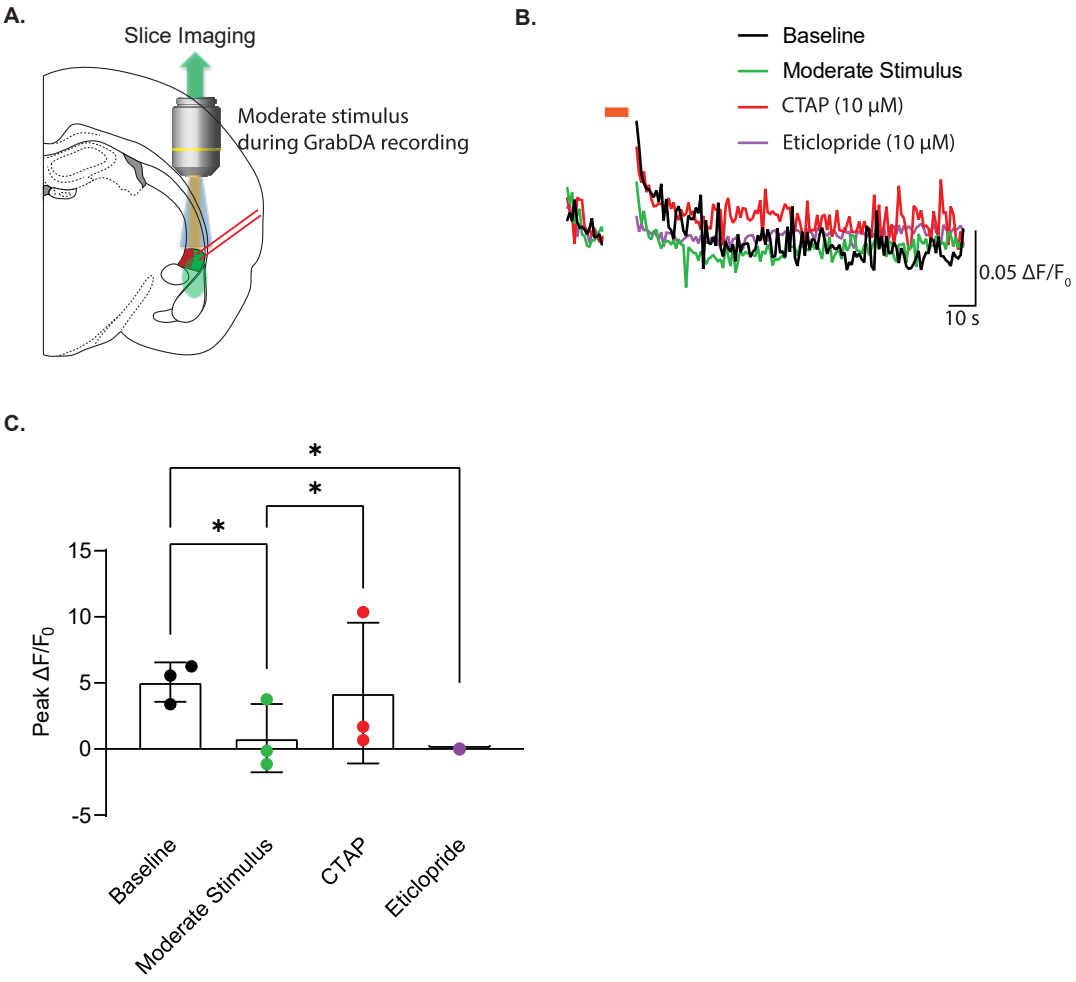

Figure 4.9. Endogenously released enkephalin inhibits VTA dopamine release. (A) Coronal cartoon schematic showing recording location and stimulating electrode placement in the ASt. (B) Example traces showing peak $\Delta F/F_0$ inhibiting when ASt is moderately stimulated during VTA optical stimulation. Application of CTAP (10 μM) reversed the inhibition and eticlopride (10 μM) completely blocked it. Graph showing peak % $\Delta F/F_0$ measured as the first 8 frames after stimulation during each condition application. Each individual point indicates a single slice recording. Bar graph represents mean ± SD. * $P < 0.05$, paired Student's t-test.

C. Discussion

The experiments in this chapter demonstrate three key findings regarding VTA projections to the ASt. First, despite clear anatomical projections, VTA terminals form sparse functional glutamatergic connections onto ASt neurons, with only 1 out of 15 cells directly connected. Second, optical stimulation of VTA terminals produces robust dopamine release in the ASt and LA detected using the GrabDA sensor. Third, this dopamine release is inhibited by MOR activity, with both exogenous and potentially endogenous enkephalin reducing dopamine release through a CTAP sensitive mechanism.

The characterisation of VTA-ASt projections reveals an unexpectedly sparse glutamatergic connectivity pattern despite clear anatomical projections (Poulin et al., 2018). While physiological recordings identified functional glutamatergic connections in only 1 out of 15 ASt neurons, this limited connectivity could stem from circuit organisation, or the non-specific viral approach employed. The VTA comprises a heterogeneous population (S. R. Taylor et al., 2014), suggesting that non-selective viral expression could have labelled both glutamatergic and non-glutamatergic populations. Although the majority of VTA dopaminergic neurons projecting to the amygdala co-express VGluT2 (Jean-Francois Poulin et al., 2018), distinct populations of VGluT2-only and GABAergic neurons exist, with GABAergic projections specifically targeting the central amygdala and striatal regions (S. R. Taylor et al., 2014). Additionally, the sparse glutamatergic connectivity parallels findings in VTA-BLA and VTA-CeA projections (Mingote et al., 2015), suggesting a conserved

organisational principle that may enable precise control over specific neuronal ensembles rather than broad excitatory transmission throughout the structure. The current findings may also indicate a predominant role for dopaminergic transmission in this circuit, consistent with the well-established dopaminergic projections from VTA to striatal regions (Jean-Francois Poulin et al., 2018). Together, these findings suggest that while VTA projections to the AST may provide sparse glutamatergic inputs, this excitatory transmission may not be the primary mode of VTA-ASt communication.

Analysis of synaptic properties revealed two distinct connection types, one monosynaptic connection exhibiting fast kinetics consistent likely with direct AMPA receptor-mediated transmission, and one polysynaptic connection with slower kinetics suggesting involvement of intermediate neurons. The polysynaptic response, observed in the presence of $GABA_A$ receptor blockade, points to several possible circuit mechanisms. While local GABAergic interneurons are unlikely to mediate this response due to picrotoxin blockade, the ASt contains cholinergic interneurons which are also present in low numbers (Y. Wang et al., 2023), could serve as intermediaries. Similar to striatal circuits, where midbrain projections can drive robust bursts in cholinergic interneurons despite their low numbers (Y. Cai & Ford, 2018), VTA activation might engage cholinergic transmission that are signalling through nicotinic receptors (Britt & McGehee, 2008; Zhou et al., 2002), thus contributing to the slow currents observed. However, without specific manipulations of these potential intermediate circuits, the exact mechanisms underlying the polysynaptic response remains to be determined.

The implementation of GrabDA sensors revealed robust dopaminergic transmission in the VTA-ASt circuit. Several lines of evidence support the proposal that the observed fluorescent changes reflect dopamine release. First, the GrabDA sensor was validated in slice preparation, showing robust increases in fluorescence to bath-applied dopamine that were blocked by the D2-seelctive antagonist eticlopride. Whilst this sensor can also detect norepinephrine (F. Sun et al., 2018), it has an 80-fold lower affinity for norepinephrine compared to dopamine (F. Sun et al., 2018). Combined with specific optical stimulation of VTA terminals (Jean-Francois Poulin et al., 2018) and not broad electrical stimulation, this strongly suggests that the detected signals represent dopamine release.

The requirement for a strong 500 stimulation protocol compared to the lower 100 pulses sufficient for detecting opioid release suggest there may be differences between the release dynamics of monoamines and neuropeptides, or experimental factors may contribute to this difference. One possible difference between the dopamine and opioid release is that there is complex regulation of dopamine transmission that likely contributes, particularly through D2 autoreceptors (C. P. Ford, 2014). These inhibitory autoreceptors, located on both VTA soma-dendritic regions and axon terminals, create feedback mechanisms controlling dopamine release. At terminals, released dopamine acts back through G_i/G_o-coupled D2 receptors to inhibit the probability of vesicular dopamine release (C. P. Ford, 2014). Additionally, D2 autoreceptor activation increases dopamine uptake by enhancing DAT surface expression (C. P. Ford, 2014). The necessity for increased stimulation might

reflect these regulatory mechanisms, as stronger stimulation would be required to overcome autoreceptor-mediated inhibition and reduced fluorescent signals due to enhanced dopamine clearance or reduced vesicular release. An additional reason that higher stimulation is required could be due to differences in density of dopamine and opioid release sites and their proximity to the sensors. In fact, the spatial distribution of dopaminergic containing terminals might be sparser than opioid release sites as only ~50% of ASt projecting VTA neurons contain evidence of dopamine in their terminals (Jean-Francois Poulin et al., 2018). An alternative explanation is that the difference is due to the experimental approach. GrabDA sensors have lower sensitivity to its native ligand compared to the δ-light sensor (Dong et al., 2024; F. Sun et al., 2018) and therefore higher levels of extracellular dopamine may need to be induced for reliable detection. There may also be additional factors, yet to be recognised, about dopamine release or these sensors function that contribute to the different stimulation required for responses.

Given the high TH expression and VTA synaptic inputs in the ASt, that I confirmed in these experiments, I expected dopamine release in the AST. Surprisingly, despite sparse dopaminergic innervation of the LA (Jean-Francois Poulin et al., 2018), robust dopamine signals were also detected in this region when VTA terminals were stimulated. This observation presented two possible interpretations, either dopamine undergoes volume transmission from the more densely innervated AST compared to LA, or there are direct VTA projections to the LA that are functionally significant despite their limited number. The latter explanation seems more likely for several reason. First,

dopamine signals in the LA were comparable in magnitude to those observed in the ASt, which would be unusual if they resulted solely from diffusion, as dopamine itself is heavily recycled through reuptake mechanisms (Y. Cai & Ford, 2018), additionally, while dopaminergic terminals from the VTA to LA are fewer in number compared to the ASt (Jean-Francois Poulin et al., 2018), they are still present and their positioning could enable significant modulation of LA neuronal activity. These findings, combined with the sparse glutamatergic connectivity observed, suggest that dopamine serves as the primary neurotransmitter in VTA-ASt projections. The capacity of dopamine to signal in the LA highlights the potential importance of even sparse dopaminergic projection in regulating fear learning circuits.

The investigation of opioid modulation of VTA dopamine release in the ASt reveals important insights into the regulation of this circuit. Previous studies have shown that VTA neurons projecting to different targets exhibit distinct properties. BLA-projecting neurons show greater sensitivity to met-enkephalin compared to KOR agonists whereas striatum projection neurons show greater sensitivity to the KOR selective agonist U69 compared to met-enkephalin (Christopher P. Ford et al., 2006). This target specific opioid sensitivity can be used as a fingerprint for identifying the origin of VTA inputs. The present study demonstrates that met-enkephalin significantly reduces stimulation-evoked dopamine release in the ASt through MOR activation, with this effect reversed by CTAP. This pharmacological profile mirrors VTA projections to the BLA but differs from striatal circuits where KOR modulates neuronal activity (Christopher P. Ford et al., 2006), providing strong evidence that VTA inputs

to the ASt originate from the same neuronal population as those projecting to the BLA. This organisation is particularly interesting as while the ASt shares several striatal-like properties (Y. Wang et al., 2023), its VTA inputs are functionally more similar to amygdala circuits than classical striatal pathways. However, future experiments will be required to test whether MOR agonists directly or indirectly reduce dopamine release from VTA terminals in the AST.

Enkephalin modulation of VTA dopamine release has important implications for dopamine dependent amygdala learning. Preliminary findings from this study showed that electrical stimulation of the ASt triggered enkephalin release which then reduced dopamine transients through a CTAP-sensitive mechanisms. Given that opioids have been implicated as being a fear inhibiting neuromodulator (Michalscheck et al., 2021), the ability of enkephalin to inhibit dopamine release may represent one mechanism underlying this effect, as dopamine signalling is associated with fear generation (Bissière et al., 2003; Tang et al., 2020). Notably, dopamine release measured in the LA showed similar modulation by met-enkephalin, with robust inhibition. This consistent regulation in both ASt and LA suggests a common mechanism for opioid-dopamine interaction and further provides evidence that ASt projection in VTA neurons share more similarity to the BLA projection population (Y. Cai & Ford, 2018). Given the critical role of LA in fear learning (J. LeDoux, 2003), this modulation could represent a key mechanism through which opioids regulate the fear learning process. To directly test this in future experiments I will inject a retrograde CRE AAV into the AST/LA and then inject a CRE dependent MOR CRISPR virus into the VTA. This will specifically delete MOR

on VTA neurons that project to the AST/LA and allow me to test whether this knockdown enhances fear learning.

The interaction between opioid and dopamine systems could extend beyond fear-related behaviours. The ASt receives diverse inputs, including both conditioned auditory and unconditioned somatosensory information via the auditory thalamus (Weinberger, 2011) and its neurons respond to rewarding stimuli (Mills et al., 2022). Therefore, multiple behavioural events could trigger enkephalin release and subsequent modulation of dopamine signalling. For example, stress directly induces endogenous opioid release in the amygdala, as demonstrated by PET imaging studies showing changes in opioid receptor occupancy during sustained pain challenges, particularly in high-impulsivity individuals (Love et al., 2009). Mood disorders also alter this endogenous opioid system, with major depressive disorder patients showing disrupted patterns of opioid release during social rejection tasks, contrasting with healthy controls where amygdala opioid release correlates with social motivation (Hsu et al., 2015). Together, these findings suggests that the opioid modulation of dopamine release observed in the current study could represent a mechanism through which various emotional and motivational states could influence amygdala circuit function. By inhibiting dopaminergic transmission, endogenous opioids released during different behavioural context might regulate emotional responses and adaptive behaviours across multiple domains.

Overall, the current chapter revealed multiple aspects of VTA-ASt circuit organisation. The sparse glutamatergic connectivity, involving both direct and indirect connections, suggests precise rather than broad excitatory control. VTA terminals produce robust dopamine release in both the ASt and LA, indicating that dopamine likely serves as the primary neurotransmitter in these pathways. The demonstration that met-enkephalin can inhibit dopamine release through MOR suggests a mechanism by which various behavioural states that trigger opioid release could modulate dopaminergic transmission in the amygdala. Together these findings expand our understanding of how endogenous opioid can coordinate information flow within amygdala circuits through regulation of dopamine signalling.

Chapter 5
Opioid modulation of synaptic plasticity in the amygdala

A. Introduction

The amygdala serves as a critical hub for emotional learning and memory, where synaptic plasticity mechanisms such as LTP underlie the formation of fear memories (Clugnet & LeDoux, 1990; Rich, Huang, & Torregrossa, 2019). Neuromodulators play crucial roles in gating this plasticity, with dopamine emerging as a key facilitator of LTP induction through its actions on local circuits (Bissière et al., 2003). While dopamine's roles in enabling synaptic plasticity is increasingly well understood, the potential modulatory effects of other neurotransmitter systems, particularly endogenous opioids, remain unknown. Studies have revealed sophisticated interactions between dopamine receptor subtypes and their differential effects on distinct neuronal populations within the amygdala (Bissière et al., 2003; Lorétan, Bissière, & Lüthi, 2004), providing important mechanistic insights into how dopamine permits LTP. Understanding how opioid receptor activation might interact with or counter these dopaminergic mechanisms represents a critical gap in our knowledge of amygdala plasticity regulation.

The MGN to LA pathway represents a critical circuit for auditory fear conditioning, serving as the primary route through which both the CS and US can reach the amygdala to initiate defensive responses (J. LeDoux, 2003; Weinberger, 2011). This MGN-LA projection undergoes robust synaptic facilitation during fear learning, making it a key pathway for emotional memory formation (J. LeDoux, 2003). At the cellular level, this plasticity manifests as LTP, characterised by enhanced synaptic efficacy (Quirk et al., 1997).

Specifically at this pathway, this LTP likely results from increased AMPA insertion to the post-synaptic membrane (Kim & Cho, 2017; Quirk et al., 1997; Rogan et al., 1997). Consistent with this single unit recording reveal that LA neurons respond more strongly to auditory cues after fear conditioning (Quirk et al., 1997). The relationship between MGN-LA plasticity and fear learning has been further established through molecular manipulation targeting AMPA receptor tracking (Rumpel et al., 2005). In this study, Rumpel and colleagues (2005) demonstrated that viral-mediated expression of constructs that prevent AMPA receptor delivery to synapses specifically impairs both the acquisition and retention of fear memories (Rumpel et al., 2005). Additionally, approximately 30% of LA neurons undergo AMPA receptor-dependent plasticity during fear learning and blocking this plasticity in as few as 10% of LA neurons was sufficient to disrupt fear memory formation (Rumpel et al., 2005), establishing AMPA receptor trafficking as an essential mechanism for MGN-LA plasticity and fear learning. Furthermore, additional evidence comes from studies showing that fear conditioning increases the AMPA/NMDA receptor ratio at MGN-LA synapses (Kim & Cho, 2017; McKernan & Shinnick-Gallagher, 1997) and that optogenetic manipulation of this pathway can bidirectionally control fear memories (Nabavi et al., 2014). Collectively, this convergent evidence establishes the MGN-LA pathway as the principal circuit through which auditory information is encoded, with synaptic plasticity serving as the cellular mechanisms for fear memory formation and storage. Notably, most prior investigations of MGN-LA plasticity have employed electrical stimulation of the internal capsule, which carry MGN inputs to the LA (J. E. LeDoux et al., 1990), leaving open the questions about pathway specificity.

This chapter therefore will utilise electrical stimulation and optogenetic techniques to selectively stimulate MGN terminals in the LA to examine plasticity mechanisms in this critical pathway.

LTP induction typically employs protocols that require coordinated activity of both presynaptic and postsynaptic neurons (Huang & Kandel, 1998; Lisman & Spruston, 2005). Standard approaches include high-frequency stimulation, which releases sufficient neurotransmitter to depolarise the postsynaptic neuron and pairing this protocol with additional postsynaptic depolarisation of the neurons in the form either spiking the postsynaptic neuron or voltage clamping at positive membrane potentials (Papatheodoropoulos & Kouvaros, 2016). In the MGN-LA pathway studies have generally used this approach when studying LTP, reflecting the Hebbian principle of synaptic plasticity (Huang & Kandel, 1998; Marc G. Weisskopf, Bauer, & LeDoux, 1999). Critically, in slice preparations, robust LTP induction in this pathway typically requires pharmacological blockade of GABAergic transmission (Grover & Yan, 1999), highlighting the powerful inhibitory control over plasticity in this circuit. Without $GABA_A$ receptor antagonists, most stimulation protocols fail to induce LTP (Bissière et al., 2003), underscoring the importance of either experimental disinhibition or endogenous neuromodulator systems that can regulate inhibitory tone. Interestingly, studies have demonstrated that MGN neurons can respond to both auditory (CS) and somatosensory (US) stimuli (Bordi & LeDoux, 1994) and strong activation of MGN inputs alone can trigger calcium influx sufficient for synaptic plasticity in the amygdala (Marc G. Weisskopf et al., 1999). This convergence of both the CS and US information at the

presynaptic level suggests that strong MGN input alone might drive synaptic strengthening in LA neurons. Therefore, this chapter focuses on examining how neuromodulation systems regulate this presynaptic-driven form of plasticity in the MGN-LA pathway.

The amygdala contains a diverse interneuron population that can regulate information flow through the circuit (Jai S. Polepalli, Gooch, & Sah, 2020) and may provide the powerful inhibition that limits plasticity in the LA. Optogenetic recordings reveal that MGN axons establish substantial connection with interneurons, with approximal 60% of MGN inputs forming synapses onto GABAergic cells (Lucas et al., 2016; Woodson et al., 2000). Additionally, whole-cell recordings reveal that interneurons receive a larger glutamatergic drive from the MGN compared to LA principal neurons (Lucas et al., 2016), positioning feedforward inhibition as the dominant initial response to auditory input. While research has predominantly focused on plasticity onto principal neurons, the robust connectivity and enhanced glutamatergic drive suggests that interneuron plasticity may represent an alternative pathway through which auditory information and subsequent fear learning are regulated.

Neuromodulator systems can effectively regulate synaptic plasticity in the amygdala, with dopamine emerging as a key permissive signal for LTP induction in the MGN-LA pathway (Bissière et al., 2003). Data from chapter 4 indicated that the ventral tegmental area (VTA) releases dopamine into the LA. Additionally, in-situ hybridisation studies reveal expression of both D1 and

D2 receptor subtypes throughout the amygdala (Maltais et al., 2000), indicating released dopamine can exert its effects in amygdala circuits. Indeed, compelling evidence suggests that dopamine facilitates LTP (Bissière et al., 2003). Several key observations suggests that D2 receptor activation in the amygdala supresses feedforward inhibition though a presynaptic mechanism, which allows the induction of LTP (Bissière et al., 2003). Firstly, application of the D2 agonist quinpirole significantly reduced the amplitude of inhibitory postsynaptic currents (IPSC) evoked by electrical stimulation of internal capsule (Bissière et al., 2003). Secondly, quinpirole decreased miniature inhibitory post synaptic current (IPSC) amplitudes in LA principal neurons and these effects persisted despite blockade of postsynaptic G-protein signalling, indicating a presynaptic origin of effects (Bissière et al., 2003). Most critically, application of dopamine enabled LTP induction whilst GABAergic transmission was intact (Bissière et al., 2003). These findings provide strong evidence for a disinhibitory model where dopamine, acting through D2 receptors, suppresses GABAergic transmission to permit sufficient postsynaptic depolarisation for LTD induction (Bissière et al., 2003). Under normal conditions, internal capsule stimulation evokes powerful feedforward inhibition that prevents LTP, but dopamine's suppression of this inhibition allows the necessary excitatory drive for plasticity. While this GABAergic mechanism is well-supported (Bissière et al., 2003; Lorétan et al., 2004), dopamine’s complex actions on amygdala circuits suggests additional mechanisms may be present. D1 receptor activation increases membrane excitability in amygdala pyramidal neurons (Kröner, Rosenkranz, Grace, & Barrionuevo, 2005), potentially enhancing postsynaptic responsiveness. This complexity therefore raises important

questions about how other neuromodulator systems might interact with or counteract this dopaminergic mechanism.

Endogenous opioids could also be powerful modulators of MGN-LA plasticity in the amygdala. Endogenous opioids can promote or limit LTP in other brain regions, such as the hippocampus. With DOR (Bramham, Milgram, & Srebro, 1991) or MOR (Bramham & Sarvey, 1996) activation promoting LTP and KOR activation limiting LTP (Terman, Wagner, & Chavkin, 1994; M. G. Weisskopf, Zalutsky, & Nicoll, 1993) in the hippocampus. Endogenous opioids are well placed to modulate LTP in the amygdala as opioid receptors are differentially expressed in the amygdala (Jean-François Poulin et al., 2006) and endogenous opioid peptides, including enkephalin, are highly expressed in amygdala subdivisions (Jean-François Poulin et al., 2006; Jingyi Zhang & McDonald, 2016). Additionally, data from chapter 3 suggests that MGN terminal stimulation triggers enkephalin release in the LA. (Bramham et al., 1991; Bramham & Sarvey, 1996; Lüscher & Malenka, 2012; Terman et al., 1994; M. G. Weisskopf et al., 1993)Once released there are multiple possible sites where the endogenous opioids could act. This includes, the MOR mediated suppression of glutamate release from MGN terminals (Chapter 3) and the inhibition of the excitability of LA principal neurons (Rogan et al., 1997) (Faber & Sah, 2004). This combination of presynaptic inhibition of glutamate release and postsynaptic suppression of excitability would provide a likely mechanism for opioids suppression of MGN-LA LTP, consistent with the role of opioids being fear inhibitory (Gavan P. McNally, 2009). However, opioids also inhibit GABA release from the GABAergic intercalated neurons that

project to the BLA (Gabrielle C. Gregoriou et al., 2019; G. C. Gregoriou et al., 2023) and this action may facilitate MGN-LA LTP. Therefore, based on opioid system expression, opioid release and opioid actions, it is possible that endogenous opioids could limit or enhance MGN-LA LTP.

The complex interplay between dopaminergic and opioidergic systems in the amygdala presents multiple potential mechanisms for regulating synaptic plasticity and fear learning. While dopamine's role in enabling LTP through modulation of local inhibitory circuits is well established (Bissière et al., 2003), opioids may oppose this plasticity through both dopamine-dependent and independent mechanisms. These include inhibition of dopamine release (as seen in chapter 4), suppression of glutamate release from MGN terminals (as seen in chapter 3), or direct modulation of pyramidal neuron excitability (Faber & Sah, 2004). Understanding how these mechanisms interact to regulate synaptic plasticity is crucial for understanding emotional learning and memory formation. Therefore, this chapter tests the hypothesis that: *Opioids signalling through MOR will supress the formation of LTP from the medial geniculate nucleus to lateral amygdala pathway*

The specific aims are

1. To establish synaptic plasticity of the MGN to LA pathway using optogenetics
2. To determine if the MGN to LA interneuron pathway undergoes synaptic plasticity
3. To determine if opioids modulate synaptic plasticity at the MGN to LA pathway

4. To determine if endogenous opioids modulate synaptic plasticity of the MGN to LA pathway

B. Results

5.1 Synaptic plasticity of the MGN to LA pathway

This section addresses aim 5.1: To establish synaptic plasticity of the MGN to LA pathway using optogenetics

To address aim 5.1, I will investigate whether a range of optogenetic stimulation protocols of MGN terminals in the LA can induce long-term potentiation

5.1.1 High-frequency optical stimulation of MGN terminals did not induce LTP in lateral amygdala neurons

While previous studies have demonstrated LTP at this synapse using electrical stimulation (Bissière et al., 2003), pathway specific LTP using optogenetic stimulation of MGN inputs has not been previously reported. Therefore, I first investigated whether selective activation of MGN terminals could induce LTP at MGN-LA synapses. Building on the functional connectivity of MGN-LA pyramidal neurons established in chapter 3, this experiment focused on pathway-specific plasticity.

To address this question, the excitatory virally expressed opsin ChR2 (AAV8-Syn-ChR2(H134R)-GFP) was microinjected into the MGN (Fig 5.1 A). After a minimum of 6 weeks coronal brain slices containing the amygdala were prepared for electrophysiology. Whole-cell patch clamp recording was obtained from putative LA pyramidal neurons voltage clamped at -70 mV.

Pyramidal neurons were identified based on their characteristic triangular soma and measured capacitance of > 25 pF (Beyeler & Dabrowska, 2020). To record changes due to synaptic plasticity, a baseline level of oEPSC was taken for 5 minutes, I then applied a high-frequency stimulation protocol (100 light pulses at 100 Hz repeated 3 times, Fig 5.1 B). The resulting oESPCs were then monitored for 20 minutes post-stimulation to assess LTP induction. The high-frequency stimulation (HFS) protocol of 100 stimulations at 100 Hz was chosen based on its ability to produce LTP in hippocampal slices that matches the magnitude and time course of LTP generated during *in vivo* spatial memory tasks (Papatheodoropoulos & Kouvaros, 2016). Recordings were performed in the presence of the $GABA_A$ antagonist picrotoxin (100 μM), as GABA acting at $GABA_A$ receptors limits postsynaptic depolarisation during LTP induction (Grover & Yan, 1999).

Despite these conditions, high-frequency optical stimulation of MGN terminals did not induce LTP in lateral amygdala neurons, as oEPSC amplitude remained stable at baseline levels following HFS (-13.91 ± 2.148 % Increase from baseline; baseline: 80.13 ± 38.82 pA, post-HFS: 70.905 ± 35.73 pA, P = 0.061, n = 4, paired Student's t-test baseline versus post-HFS, Fig 5.1 A and D). These results indicate that high-frequency optical stimulation of MGN terminals is insufficient to induce LTP at MGN synapses onto LA pyramidal neurons

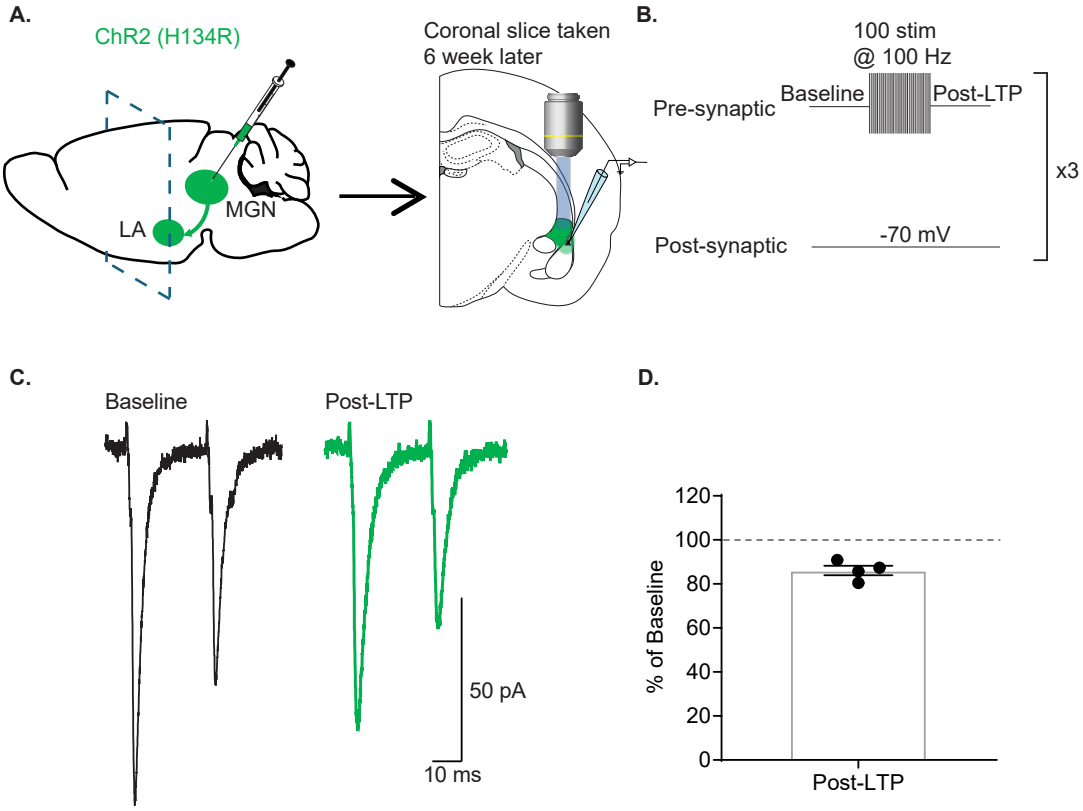

Figure 5.1. High-frequency optical stimulation fails to induce long-term potentiation at the MGN-LA synapse. (A) Sagittal schematic diagram indicating AAV8-Syn-ChR2(H134R)-GFP injection into the MGN. (B) Optical stimulation protocol. Presynaptic terminals received 100 light pulses at 100 Hz while the postsynaptic neuron was voltage-clamped at -70 mV repeated 3 times. (C) Representative oEPSC traces of putative LA pyramidal neuron during baseline period and following high-frequency optical stimulation. (D) Graph showing oEPSC amplitude normalised to baseline (%) after high-frequency stimulation. Each individual point on graph represents a single neuron. Bar on graph represents mean ± SEM

5.1.2 High frequency optogenetic stimulation combined with depolarisation did not induce LTP at the MGN-LA synapse

I next investigated whether providing optimal conditions for postsynaptic depolarisation would facilitate LTP induction at this synapse. To address this question, I modified the experimental protocol to combine the high-frequency stimulation with direct postsynaptic depolarisation (Fig 5.2 A), an approach that reliably induces LTP in other brain regions (Lisman & Spruston, 2005) and in the LA using electrical stimulation of auditory thalamic inputs (Bissière et al., 2003).

Whole-cell recording was obtained from LA pyramidal neurons as described above, but during the high-frequency stimulation protocol, I voltage-clamped the postsynaptic neuron at 0 mV instead of -70 mV. This manipulation was designed to provide maximal depolarisation coincident with presynaptic activation.

Despite providing both strong synaptic stimulation and postsynaptic depolarisation, this protocol also failed to induce LTP, as oEPSC amplitude remained at baseline levels following stimulation (-11.92 ± 3.68% increase from baseline; baseline 122.89 ± 49.12 pA; post-HFS; 106.89 ± 41.38 pA, P = 0.19, n = 3, paired Student's t-test baseline versus post-HFS, Fig 5.2 B and C). These results indicate that even under conditions designed to maximise postsynaptic depolarisation during presynaptic activation, high-frequency optical stimulation of MGN terminal fails to induce LTP at the MGN-LA synapse.

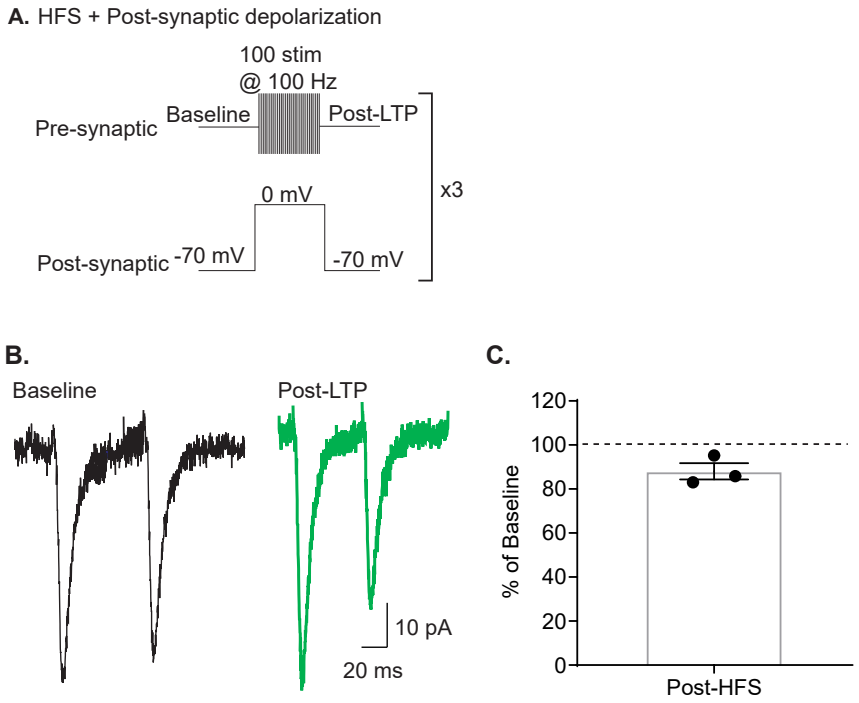

Figure 5.2. HFS optical stimulation combined with post synaptic depolarisation fails to induce long-term potentiation at the MGN-LA synapse. (A) Optical stimulation protocol. Presynaptic terminals received 100 light pulses at 100 Hz while the postsynaptic neuron was voltage clamped at 0 mV repeated 3 times. (B) Representative oEPSC traces of putative LA pyramidal neuron during baseline period and following high-frequency optical stimulation. (D) Graph showing oEPSC amplitude normalised to baseline (%) after high-frequency stimulation. Each individual point on graph represents a single neuron. Bar on graph represents mean ± SEM.

5.1.3 Spike timing dependent plasticity did not induce LTP at the MGN-LA synapse

I next examined whether a more physiologically relevant stimulation protocol could induce LTP at this synapse. To address this question, I implemented a spike timing-dependent plasticity (STDP) protocol designed to mimic the temporal coordination of neuronal activity that occurs during associative learning (Fig 5.3 A) (Bi & Poo, 1998; Lisman & Spruston, 2005; Shouval, Wang, & Wittenberg, 2010).

Whole cell patch clamp recordings were obtained from LA pyramidal neurons while optically stimulating MGN terminals. The STDP protocol consisted of 10 optical stimuli delivered at 30 Hz, with each stimulus followed 5 ms alter by postsynaptic current injections sufficient to trigger action potentials, this was repeated 15 times every 10 seconds (Fig 5.3 A). During the STDP protocol the neurons were held in current clamp without any current injections, whilst oEPSC were recorded with neurons voltage clamped at -70 mV.

However, despite matching the temporal requirements for associative plasticity, this protocol also failed to induce LTP in MGN-LA synapses, as oEPSC amplitude remained at baseline levels (-8.43 ± 5.81% increase from baseline; baseline: 106.12 ± 24.63 pA; post-LTP: 95.32 ± 21.12 pA, P = 0.16, n= 5, paired Student's t-test baseline versus post-LTP, Fig 5.3 B and C). These results indicate that even with a stimulation protocol that closely mimics the physiological conditioned associated with associative learning, MGN-LA synapses do not exhibit activity-dependent potentiation under these experimental conditions

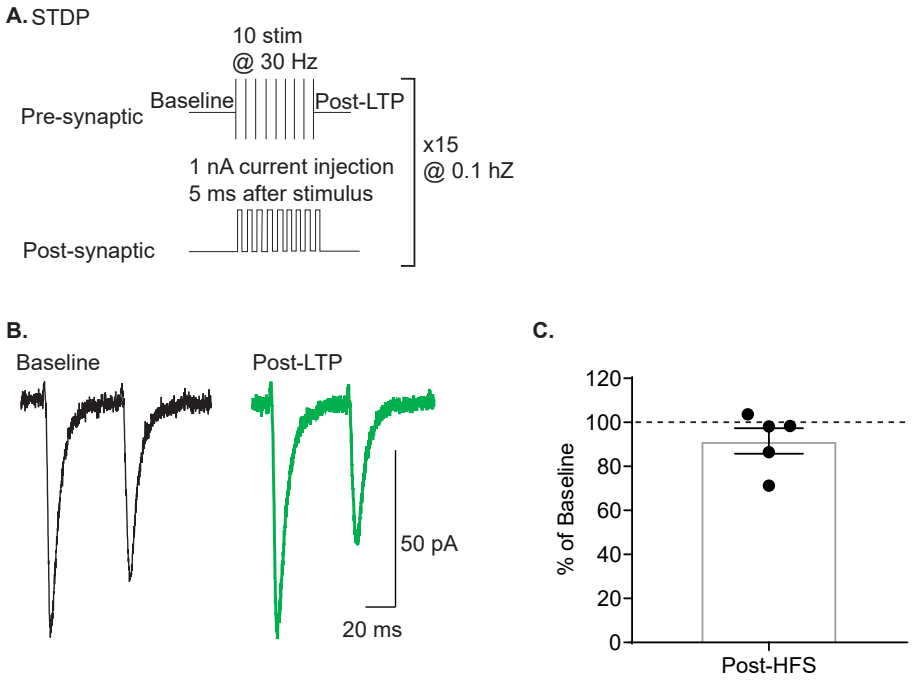

Figure 5.3. Spike time dependent plasticity protocols fail to induce long-term potentiation at the MGN-LA synapse. (A) Optical stimulation protocol. Presynaptic terminals received 10 light pulses at 30 Hz followed 5 ms after by a 1 nA current injection in the post-synaptic neuron, this was presented 15 times once every 10 seconds (0.1 Hz). (B) Representative oEPSC traces of putative LA pyramidal neuron during baseline period and following high-frequency optical stimulation. (D) Graph showing oEPSC amplitude normalised to baseline (%) after high-frequency stimulation. Each individual point on graph represents a single neuron. Bar on graph represents mean ± SEM

Together, these data indicate that optical stimulation of MGN terminals is insufficient to induce LTP in LA neurons under multiple induction protocols. Neither high-frequency stimulation alone, HFS paired with postsynaptic depolarisation, nor STDP protocols produced changes in synaptic strength at MGN-LA synapses, as measured by oEPSC amplitude. The consistent failure to induce LTP across multiple established protocols suggests that optogenetic stimulation may not fully replicate the physiological activation of MGN terminals required for synaptic plasticity, possibly due to limitations in ChR2 kinetics or its ability to trigger sufficient neurotransmitter release.

5.2 Synaptic plasticity of the internal capsule to LA synapse

This section addresses aim 5.2: To determine if the MGN to LA interneuron pathway undergoes synaptic plasticity

To address this aim, I will determine the nature of internal capsule inputs onto both putative pyramidal and interneurons and examine whether stimulation of the internal capsule can exhibit synaptic plastic.

5.2.1 Electrical stimulation of the internal capsule evokes strong responses in both putative LA pyramidal neurons and interneurons

Given the limitations observed with direct optogenetic stimulation of MGN terminals, subsequent experiments investigated whether electrical stimulation of the internal capsule, which carries MGN afferents and other input pathways to the lateral amygdala, could successfully induce LTP, as has been observed previously, (J. E. Ledoux et al., 1987). Firstly, I aimed to characterise synaptic responses evoked by electrical stimulation of the internal capsule onto putative LA pyramidal neurons.

To investigate the characteristics of electrical stimulation of the internal capsule, electrical stimulators were placed in the internal capsule and whole cell patch clamp electrophysiology was performed on putative LA pyramidal neurons (Fig 5.4 A). All recording were conducted in the presence of the $GABA_A$ antagonist picrotoxin (100 μM). Paired pulse electrical stimulation resulted in an evoked excitatory post-synaptic current (eEPSC) in all recorded neurons. Synaptic jitter, measured as the standard deviation of response

latencies from stimulus onset, was used to indicate monosynaptic connection (Doyle & Andresen, 2001). The average synaptic jitter was 0.12 ± 0.05 ms (n = 7). No neurons were excluded from this experiment for having a synaptic jitter > 0.7 ms. Application of the AMPA/kainate receptor antagonist significantly attenuated the eEPSC (91.5 ± 2.56% inhibition from baseline; baseline: 221.25 ± 120.57 pA; CNQX: 12.9 ± 7.29 pA, n = 7, P = 0.045, paired Student's t-test baseline versus CNQX, Fig 5.4 B and C). These results establish that electrical stimulation of the internal capsule reliably activates direct glutamatergic inputs to LA pyramidal neurons.

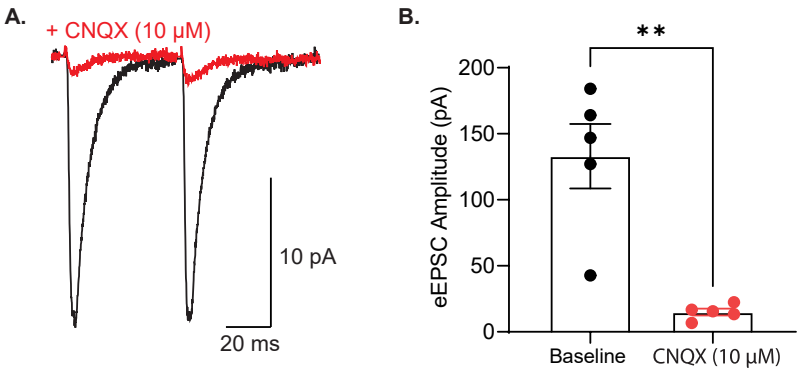

Figure 5.4. Internal capsule stimulation produces glutamatergic responses in putative LA pyramidal neurons. (A) Cartoon schematic of coronal amygdala indicating stimulating electrode placement in the internal capsule and recording of putative LA pyramidal neurons. (B) Representative trace of a recording in the LA showing eEPSC during baseline and CNQX (10 µM) application. (B) Graph showing eEPSC amplitude (pA) baseline and CNQX (10 µM) application. Each individual point on graph represents a single neuron. Bars on graph represents mean ± SEM. *P < 0.05 paired Student's t-test

I next investigated whether electrical stimulation of the internal capsule also activates synaptic inputs onto interneurons in the lateral amygdala. While LTP studies have predominantly focused on pyramidal neurons (Bissière et al., 2003), interneurons play crucial roles in regulating information flow within the amygdala circuits (Gabrielle C. Gregoriou et al., 2019). To characterise

internal capsule inputs onto LA interneurons, whole cell patch clamp electrophysiology was performed on visually identified LA interneurons while. The interneuron was identified based on their distinct morphological characteristics, including small soma as well as having a capacitance of less than 15 pF (Gabrielle C. Gregoriou et al., 2019). Recordings were conducted in the presence of the $GABA_A$ receptor antagonist picrotoxin (100 μM).

Electrical stimulation resulted in eEPSC in all putative LA interneurons (Fig 5.5 A-B). No cells were excluded due to synaptic jitter (0.11 ± 0.06 ms, n = 5). Application of the AMPA/kainate receptor antagonist significantly attenuated the eEPSC (85 ± 4.69% inhibition from baseline; baseline: 133.02 ± 24.45 pA; CNQX: 14.97 ± 2.54 pA, n = 5, P = 0.004, paired Student's t-test baseline versus CNQX, Fig 5.5 A and B). Notably, unlike previous reports showing that parvalbumin positive interneurons in the lateral amygdala receives stronger glutamatergic drive than pyramids (Lucas et al., 2016) the results from this study indicate there is no difference between putative LA pyramidal neurons and interneuron in receiving glutamatergic drive from internal capsule stimulation (Pyramidal neuron: 221 ± 120.57 pA, n = 7; Interneuron: 133.02 ± 24.45 pA, n = 5, P = 0.28, unpaired Student's t-test pyramidal neuron versus interneuron). These results demonstrate that the MGN input and other input pathways conveyed through the internal capsule provides direct glutamatergic excitation to both putative principal neurons and interneurons within the LA.

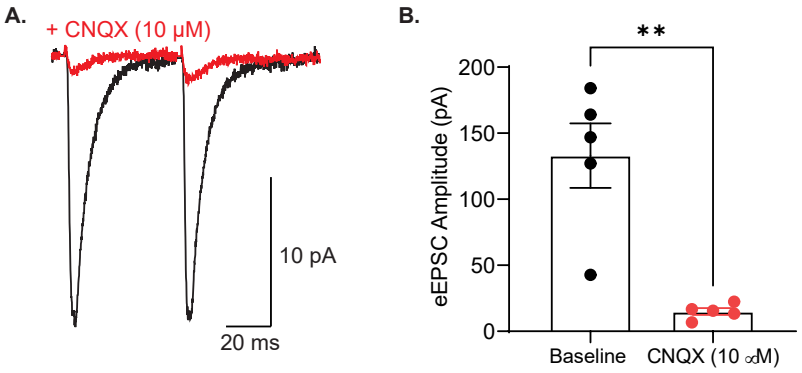

Figure 5.5. Internal capsule stimulation produces glutamatergic responses in putative LA interneurons. (A) Representative trace of a recording in the LA showing eEPSC during baseline and CNQX (10 μM) application. (B) Graph showing eEPSC amplitude (pA) baseline and CNQX (10 μM) application. Each individual point on graph represents a single neuron. Bars on graph represents mean ± SEM. **P < 0.01 paired Student's t-test

5.2.2 High-frequency stimulation of the internal capsule induces LTP onto putative pyramidal neurons

While previous studies demonstrated that pairing internal capsule stimulation with postsynaptic action potentials via depolarising current injection induces LTP (Bissière et al., 2003), high-frequency stimulation alone can often provide sufficient postsynaptic depolarisation (Papatheodoropoulos & Kouvaros, 2016). The MGN processes both auditory and somatosensory information (Weinberger, 2011), suggesting that the strong presynaptic activation alone might trigger plasticity. Therefore, this experiment examined whether high-frequency stimulation of the internal capsule alone could induce LTP, in contrast to previous studies that paired stimulation with postsynaptic depolarisation (Bissière et al., 2003)

To examine internal capsule-induced plasticity, an electrical stimulator was positioned in the internal capsule while recordings were obtained from LA

pyramidal neurons. LTP induction was attempted using the same high-frequency stimulation previously used in Figure 5.1, while maintaining neurons at their resting membrane potential in current-clamp mode. Electrical postsynaptic currents (eEPSCs) were monitored at a holding potential of -70 mV in voltage-clamp configuration before and after LTP induction (Fig 5.6 A).

When GABAergic transmission remained intact, this stimulation protocol failed to induce LTP, as evidenced by unchanged eEPSC amplitudes following HFS (-0.74 ± 6.65 % increase from baseline: baseline 145.55 ± 48.67 pA; post-HFS: 135.42 ± 48.04 pA, P = 0.78, n = 8, paired Student's t-test, Fig 5.6 C and D). However, when $GABA_A$ receptors were blocked with picrotoxin, high-frequency stimulation of the internal capsule successfully induced LTP. Following HFS delivery, eEPSC amplitudes significantly increased compared to baseline increase from baseline (35.38 ± 11.57% p = 0.03, n = 6, paired Student's t-test, Fig 5.6 E and G), whilst not producing any change in paired pulse ratio (baseline 1.30 ± 0.14 PPR; post-HFS 1.11 ± 0.03 PPR, p = 0.63, n = 6, unpaired Student's t-test baseline versus post-LTP, Fig 5.6 H). demonstrating that blocking of GABAergic inhibition unmasks the capacity for synaptic strengthening at internal capsule-LA synapses (baseline: 227.49 ± 71.29 pA; post-HFS: 294.51 ± 93.82 pA). These findings demonstrate that strong presynaptic activation of the internal capsule to putative LA pyramidal neurons is sufficient to induce LTP when GABAergic transmission is reduced, confirming that this pathway possesses intrinsic plasticity capacity that is normally regulated by inhibitory gating.

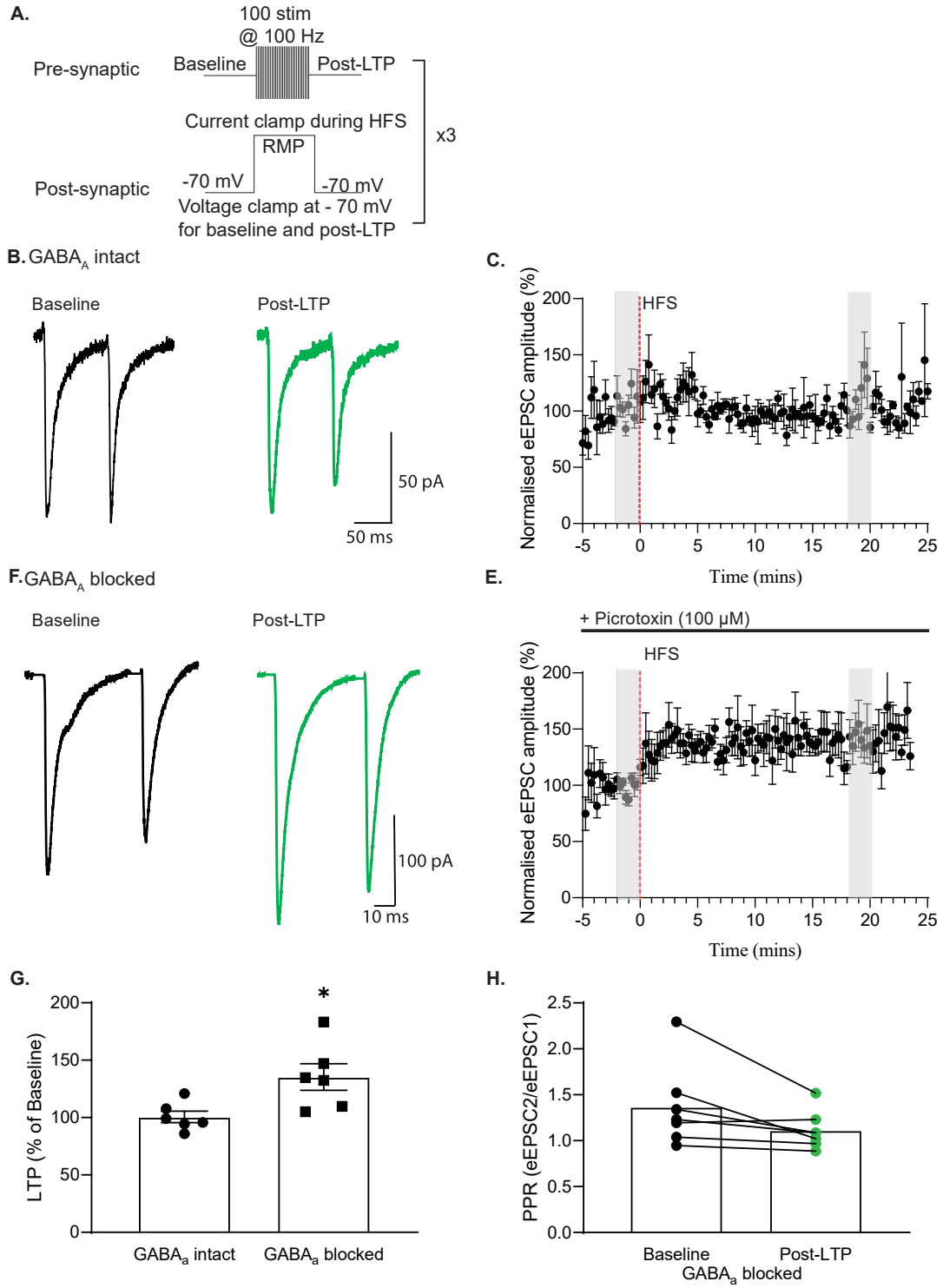

Figure 5.6. High-frequency stimulation induces LTP at internal capsule-LA synapses when GABA$_A$ receptors are blocked (A) Stimulation protocol. 100 electrical pulses were delivered at 100 Hz while the postsynaptic neuron was maintained in current-clamp mode at resting membrane potential. Evoked excitatory post-synaptic currents (eEPSCs) were recorded at -70 mV holding potential. (C-D) Representative traces and time from a putative LA pyramidal neuron showing no change in eEPSCs before and after HFS with GABA$_A$ signalling intact. (E-F) Representative traces and time from a putative LA pyramidal neuron showing increased eEPSCs after HFS with GABAa signalling blocked. (G) Graph showing normalised eEPSC as % of baseline when GABA$_A$ is blocked

and when $GABA_a$ is intact. Each induvial point represents a single neuron. Bars on graph represent mean ± SEM. Grey bars indicate where baseline and LTP effects were measured * P < 0.05 paired Student's t-test. (H) Graph showing paired pulse ratios during baseline and post LTP when $GABA_a$ was blocked. Each induvial point represents a single neuron. Bars on graph represent mean ± SEM

5.2.3 High-frequency stimulation of the internal capsule induces LTP onto putative interneurons

Having established that the internal capsule to LA pyramidal neuron input can undergo LTP when there is reduced GABAergic inhibition, I next investigated whether similar plasticity occurs at synapses onto LA interneurons. Using the same experimental approach as with pyramidal neurons, electrical stimulators were positioned in the internal capsule while recording from visually identified LA interneurons.

High frequency stimulation failed to induce LTP in interneurons when GABAergic inhibition remained intact, as eEPSC amplitudes shows no significant changes (6.47 ± 4.43% increase from baseline; baseline: 119.01 ± 23.98 pA; post-HFS: 127.53 ± 27.55 pA, P = 0.19, n = 5, paired Student's t-test, Fig 5.7 A and B). However, when $GABA_A$ receptors were blocked with picrotoxin (100 μM), the same high-frequency stimulation protocol successfully induced LTP in interneurons (61.57 ± 22.55% increase from baseline; baseline: 364.69 ± 136.23 pA; post-HFS: 426.59 ± 129.11 pA, P = 0.02, n = 6, paired Student's t-test, Fig 5.7 C and D), with no change in paired pulse ratio (baseline 1.30 ± 0.09 PPR; post-LTP 1.32 ± 0.11 PPR, p = 0.99, n = 5, unpaired Student's t-test baseline versus post-LTP, Fig 5.7 F). The level of potentiation onto interneurons was similar to that seen onto pyramidal neurons

(P = 0.15, unpaired Student's t-test, pyramidal neurons versus interneurons), suggesting that similar cellular mechanisms may underlie synaptic strengthening in both cell types. Together, these findings demonstrate that internal capsule input to both putative principal neurons and interneurons in the LA exhibit activity-dependent plasticity when inhibitory constraints are removed.

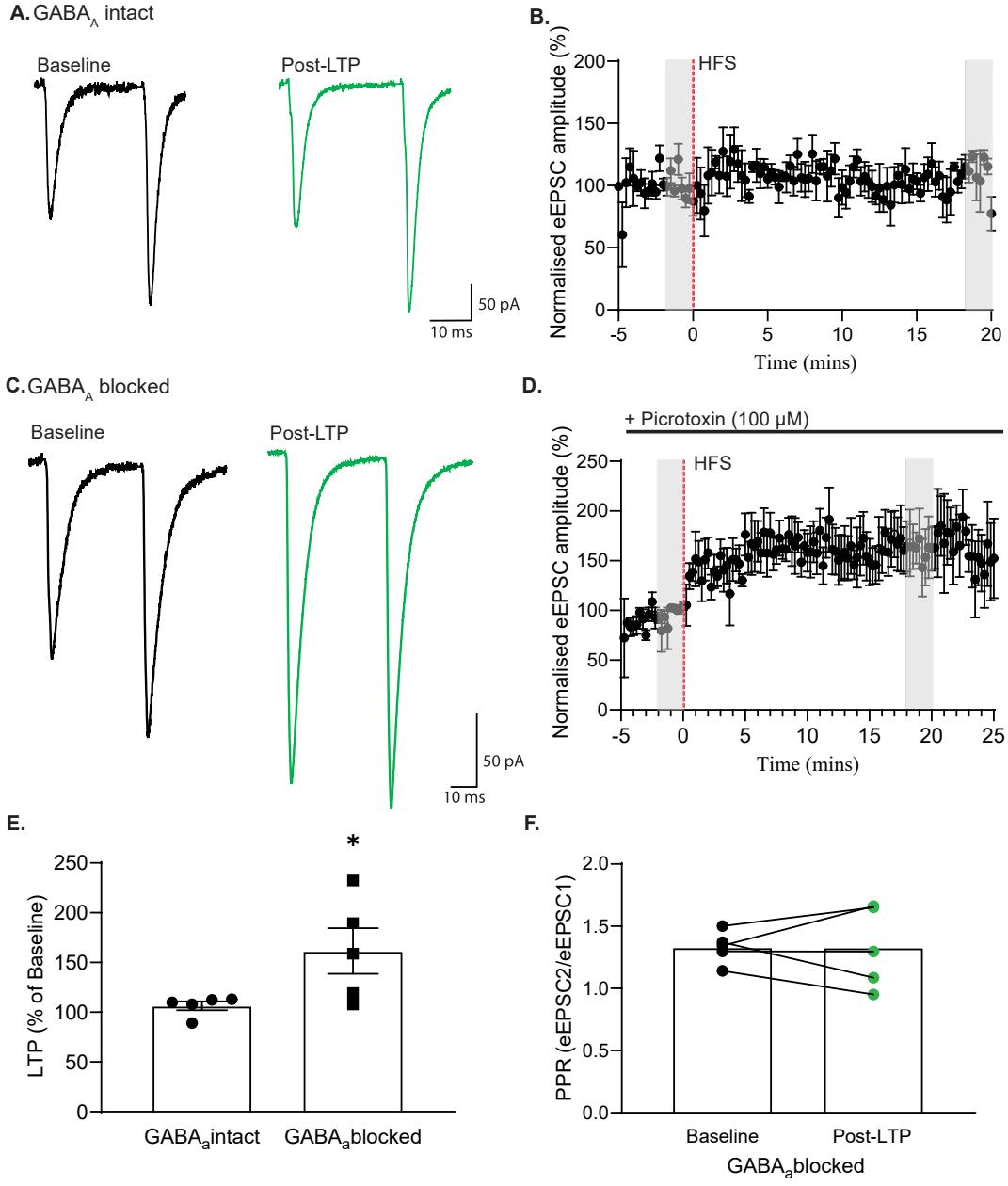

Figure 5.7. High-frequency stimulation induces LTP at LA interneurons when GABA$_A$ receptors are blocked (A-B) Representative traces and time from a putative LA

interneuron showing no change in eEPSCs before and after HFS with $GABA_A$ signalling intact. (C-D) Representative traces and time from a putative LA interneuron showing increased eEPSCs after HFS with $GABA_A$ signalling blocked. (E) Graph showing normalised eEPSC as % of baseline when $GABA_A$ is blocked and when $GABA_A$ is intact. (F) Graph showing paired pulse ratios during baseline and post LTP when $GABA_a$ was blocked. Each induvial point represents a single neuron. Bars on graph represent mean ± SEM. Grey bars indicate where baseline and LTP effects were measured. * $P < 0.05$ paired Student's t-test

5.3 Opioid modulation of synaptic plasticity

This section addresses aim 5.3: To determine if opioids modulate synaptic plasticity at the MGN to LA pathway

To address this, I will determine whether application of opioid receptor agonist alters LTD induction by stimulation of the internal capsule to LA synapse. I will also examine dopamine's effects on synaptic plasticity in this pathway to compare modulation by these different neurotransmitter systems.

5.3.1 Dopamine enable HFS-induced LTP at internal capsule-LA synapses

Previous studies have demonstrated that pairing internal capsule high-frequency stimulation with postsynaptic depolarisation can induce LTP in the presence of dopamine without the need to manipulate GABAergic transmission (Bissière et al., 2003). This is likely due to dopamine suppression of feedforward inhibition (Bissière et al., 2003), creating an environment where plasticity can be induced. Based on these findings, dopamine was initially selected as a positive control to validate the high-frequency stimulation.

To investigate dopamine's effects on plasticity, dopamine was present just during the high-frequency stimulation of the internal capsule whilst recording from putative LA pyramidal neurons voltage clamped at -70 mV, without picrotoxin. Dopamine itself did not significantly affect synaptic transmission when using electrical stimulation of the internal capsule (11.90 ± 6.66 % inhibition from baseline; baseline: 194.13 ± 46.83 pA; dopamine: 175.32 ± 52.36 pA, p = 0.29, n = 6, paired Student's t-test baseline versus dopamine, Fig 5.8 A-C). Following the stimulation protocol and subsequent dopamine washout, eEPSC amplitudes showed a sustained increase above baseline, 63.15 ± 23.72 % increase from baseline, p = 0.02, n = 6, paired Student's t-test baseline versus post-HFS, Fig 5.8 A-C), that persisted for at least 20 minutes, indicating successful LTP induction (baseline: 194.13 ± 46.83 pA; post-HFS; 291.09 ± 56.37 pA). These findings confirm previous findings (Bissière et al., 2003) that dopamine enables LTP induction at internal capsule-LA synapses using only presynaptic stimulations, without requiring pharmacological blockade of $GABA_A$ receptors. This suggests that dopamine may facilitate fear learning by creating conditions permissive for synaptic strengthening at the internal capsule-LA synapses, possibly through its actions on local inhibitory circuits. However, dopamine's exact role in facilitating synaptic plasticity was not tested in this thesis.

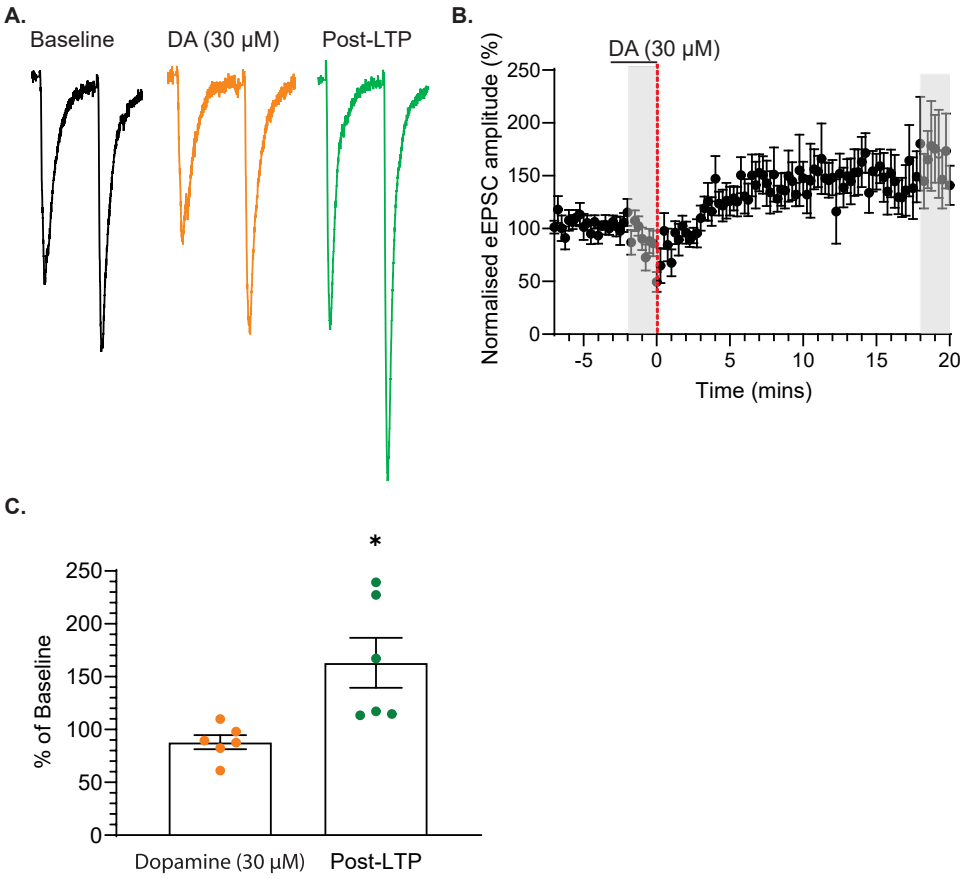

Figure 5.8. Dopamine facilitated HFS-induced long-term potentiation at the internal capsule-LA synapse without the need to block $GABA_A$ (A-B) Representative traces and time plot from a putative LA pyramidal neuron showing eEPSC increased after LTP protocol (C) Graph showing normalised eEPSC as % of baseline during dopamine (30 µM) application and post LTP. Each point on graphs represents a single neuron. Bars on graph reparents the mean ± SEM. Grey bars indicate where drug and LTP effects were measured. * $P < 0.05$ paired Student's t-test

5.3.2 Opioids facilitate HFS-induced LTP at the internal capsule-LA synapse

Given opioids established role in fear inhibition (Gavan P. McNally, 2009) and their demonstrated ability to suppress glutamate release from MGN terminals in the LA (Fig 3.6) (Gavan P. McNally, 2009), I had hypothesised that opioids may interfere with LTP induction. To test this prediction, these experiments utilised the maximum effective concentration of opioids that had previously shown robust inhibition of MGN terminals (Fig 3.6). Whole-cell patch clamp recording was performed onto putative LA pyramidal neurons voltage clamped

at -70 mV and without GABAA blockade. The same high-frequency stimulation protocol was employed as in the previous experiment, with opioids present during stimulation of the internal capsule.

Initial observations confirmed the expected effect, as opioids suppressed synaptic transmission at these synapses (21.71 ± 9.67 % inhibition from baseline; baseline: 273.83 ± 113.21 pA; met-enkephalin: 229.74 ± 95.84 pA, p = 0.02, n = 7, paired Student's t-test baseline versus met-enkephalin, Fig 5.9 A-C). However, the subsequent results revealed an unexpected outcome. Following the completion of the stimulation protocol and the washout of met-enkephalin, eEPSC amplitudes increased significantly above their baseline levels (42.60 ± 12.25 % increase from baseline, P = 0.01, n = 7, paired Student's t-test baseline versus pos-HFS, Fig 5.9 A-C). This increase demonstrated that LTP had been successfully induced, despite the synaptic suppression observed during the induction protocol (baseline: 273.83 ± 113.21 pA; post-HFS: 333.19 ± 112.09 pA).

To test that opioid-induced LTP was specifically mediated through MOR, experiments were repeated in the presence of the MOR antagonist CTAP. When CTAP was present throughout the experiment, met-enkephalin failed to inhibit eEPSC amplitude (4.63 ± 4.04% inhibition from baseline: baseline; 87.91 ± 12.67 pA; met-enkephalin; 82.72 ± 9.96 pA, p = 0.26, n = 6, paired Student's t-test baseline versus met-enkephalin Fig 5.8 D and E). Moreover, following HFS, no LTP was observed (1.31 ± 2.62% increase from baseline:

baseline; 87.91 ± 12.67 pA; post-HFS: 88.21 ± 11.35 pA, p = 0.87, n = 7, paired Student's t-test, Fig 5.8 D and E), demonstrating that MOR activation is necessary for this form of synaptic plasticity.

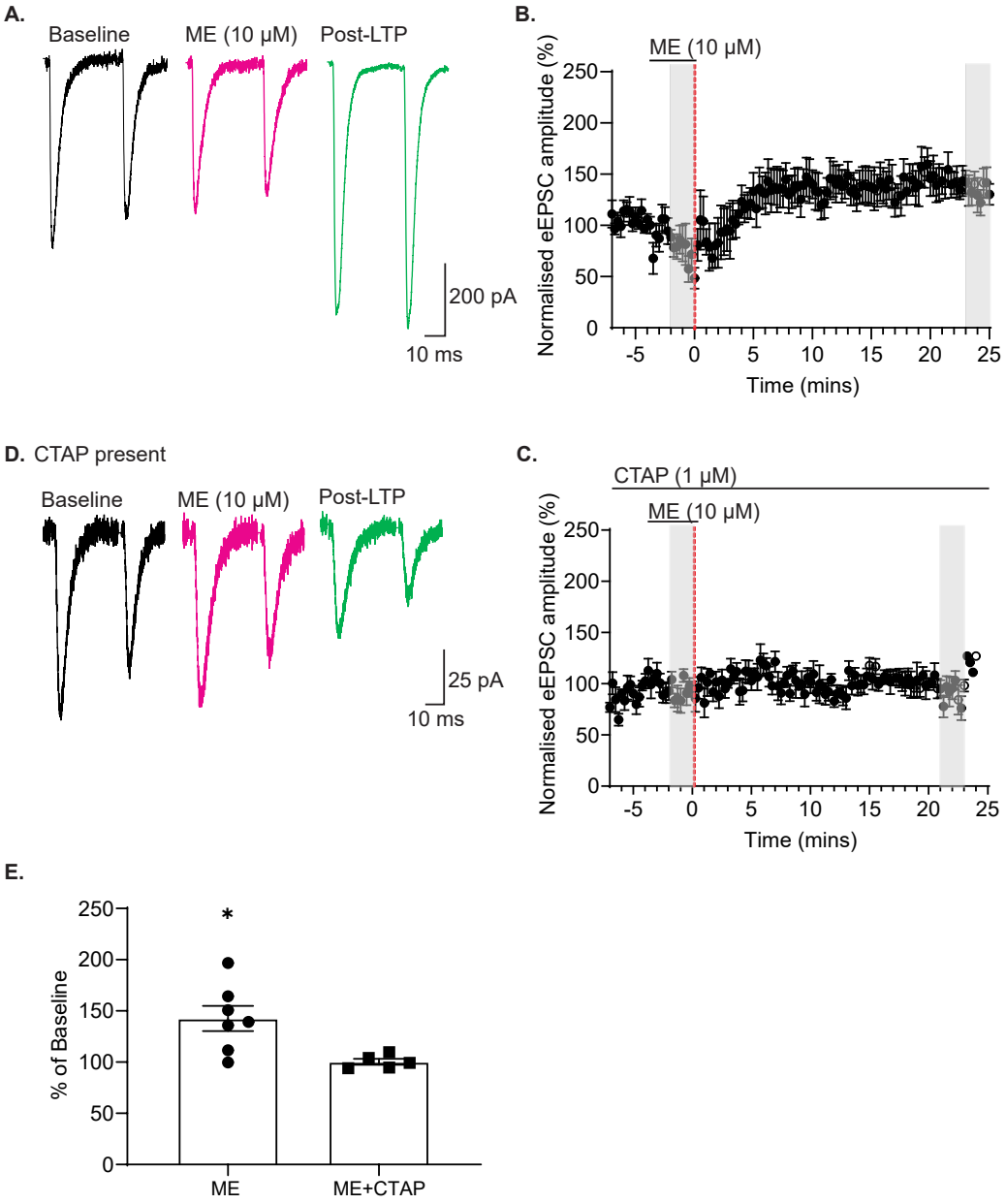

Figure 5.9. Opioids facilitated long-term potentiation at the internal capsule-LA through MOR activation (A-B) Representative traces and time plot from a putative LA pyramidal neuron showing eEPSC increased after LTP protocol (C-D) Representative traces and time plot from a putative LA pyramidal neuron showing eEPSC no change after LTP protocol when MOR was blocked by CTAP (1 μM) (C) Graph showing normalised eEPSC as % of baseline post LTP when MOR was active or blocked by CTAP. Each point on graphs represents a single neuron. Bars on graph reparents the mean ± SEM. Grey bars indicate where drug and LTP effects were measured. * P < 0.05 paired Student's t-test

This unexpected facilitation of LTP by opioids appears to contradict their proposed role as fear inhibitors, as they promote synaptic strengthening similarly to dopamine. However, the underlying mechanisms of opioid-induced LTP could potentially differ from dopamine-mediated plasticity. Since LTP at MGN-LA synapses induced by fear learning typically occurs through postsynaptic AMPA receptor insertion (Rogan et al., 1997), I conducted experiments to determine the specific mechanism of opioid-induced LTP. Initial baseline measurements of PPR and AMPA/NMDA ratios were obtained in picrotoxin to isolate glutamatergic currents. AMPA currents were recorded with cells held at -70 mV, while NMDA currents were measured at +40 mV (Fig 5.10 A and B), with NMDA amplitude measured 300 ms after electrical stimulation. PPR was assessed using paired-pulse stimulation with cells held at -70 mV. Using a separate set of slices, these same measurements were performed following opioid-induced LTP, which had been established in the absence of picrotoxin. No change in PPR was observed, providing no evidence for changes in presynaptic release probability (baseline 2.34 ± 0.45 PPR; post-HFS 1.77 ± 0.08 PPR, $p = 0.29$, $n = 7$, unpaired Student's t-test baseline versus post-HFS, Fig 5.10 C). Analysis of the AMPA/NMDA ratio revealed an increase following LTP induction (baseline 3.67 ± 0.49 AMPA/NMDA ratio; post-HFS 5.69 ± 0.85 AMPA/NMDA ratio, $p = 0.02$, $n = 7$, unpaired Student's t-test baseline versus post-HFS, Fig 5.10 D), suggesting enhanced AMPA receptor-mediated currents. This increase in AMPA/NMDA ratio following HFS indicates that opioid facilitated LTP likely results from increased postsynaptic AMPA receptor insertion into the membrane.

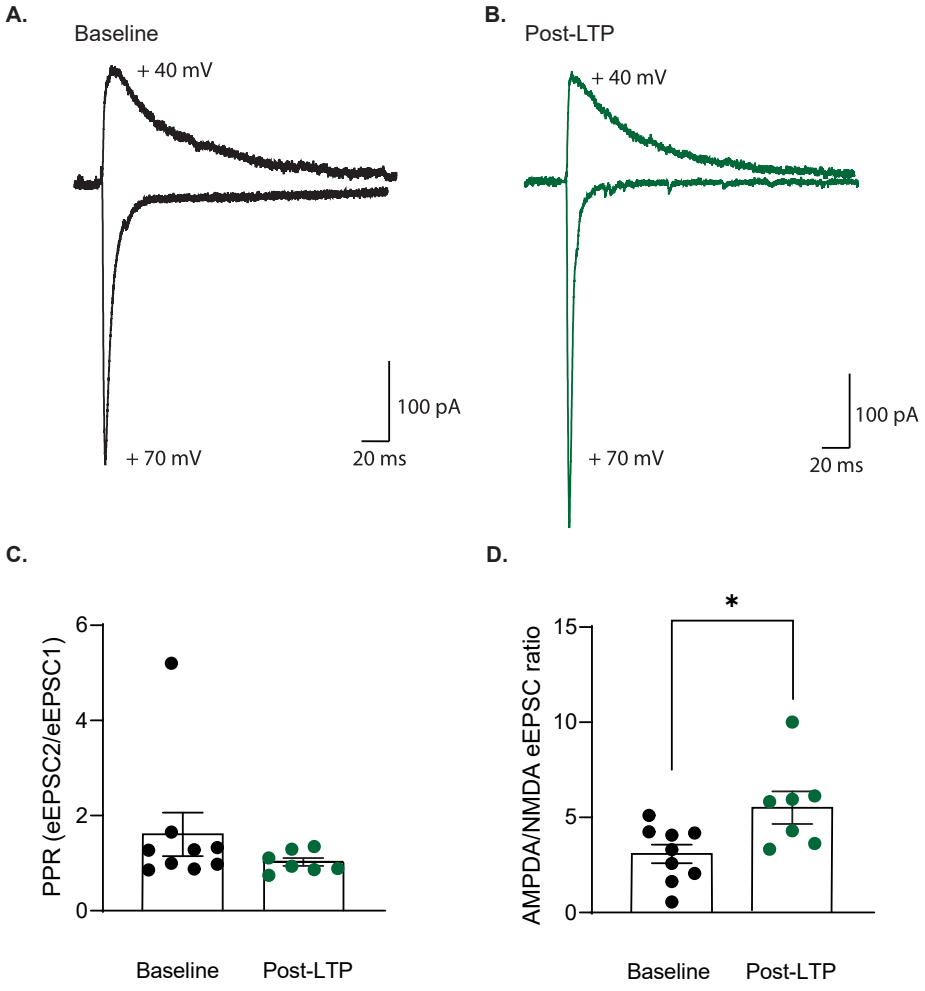

Figure 5.10. Met-enkephalin induced LTP results in increased AMPA. (A-B) Representative eEPSC traces of AMPA/NMDA ratio from putative LA pyramidal neurons during baseline and after LTP. (C) Graph showing AMP/NMDA ratios during baseline and post LTP (D) Graph showing paired pulse rations during baseline and post LTP. Each point on graph represents a single neuron. Bars on graph represent mean ± SEM

Further analysis investigated whether the level of opioid inhibition of glutamate release influenced the magnitude of LTP. If synaptic suppression constrained plasticity, a negative correlation would be expected between the degree of opioid-induced inhibition and LTP strength. However, correlation analysis revealed no significant relationship between these measures (R^2 = 0.02, Fig 5.7 I), indicating that the level of initial synaptic suppression does not predict or limit the extent of subsequent potentiation. These findings indicate that opioid facilitated LTP operates through mechanisms similar to those previously described for fear learning-induced (Rogan et al., 1997) and dopamine facilitated LTP (Bissière et al., 2003) at this synapse.

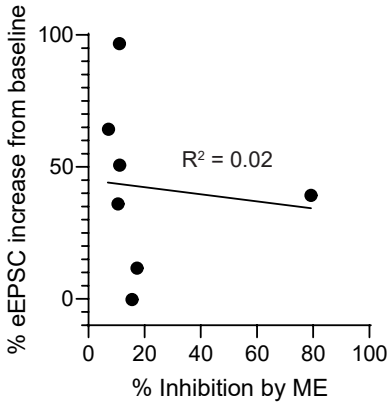

Figure 5.11. Correlation between met-enkephalin inhibition and LTP size. Met-enkephalin inhibition was plotted against the percentage of eEPSC increase due to LTP. No correlation was found. Each point represents a single neuron.

These results demonstrate that both dopamine and opioids enable LTP induction at internal capsule-LA synapses using presynaptic HFS alone. Despite opioids strong inhibition of glutamate release, which does not

correlate with LTP magnitude, the resulting potentiation shares similar postsynaptic expression mechanisms with fear learning-induced plasticity at this synapse. The ability of opioids to facilitate synaptic strengthening at this fear-encoding synapse presents an unexpected contrast to their established behavioural role in fear inhibition

5.4 Endogenous opioid modulate of synaptic plasticity

This section addresses aim 5.4: To determine if endogenous opioids modulate synaptic plasticity of the MGN to LA pathway

To address aim 5.4, To address this aim, I will induce endogenous opioid release through electrical stimulation of the ASt while monitoring internal capsule-LA synaptic responses during LTP induction protocols.

5.4.1 Endogenously released opioids facilitate LTP only when peptidase degradation is prevented

While exogenous application of met-enkephalin at a high concentration (10 μM) facilitated LTP induction, this high concentration across the slice likely doesn't reflect physiologically relevant conditions. To investigate the role of endogenously released opioids and plasticity under more physiologically relevant conditions, stimulating electrodes were positioned in the ASt to stimulate endogenous opioid release while recording from putative LA neurons (Fig 5.12 A). The ASt was electrically stimulated throughout the experiment using the moderate stimulus protocol confirmed to release endogenous opioids in chapter 3 and then the strength of the internal capsule-LA neuron synapse probed by stimulation of the internal capsule 200ms later (test pulse).

Electrical stimulation of the ASt during high-frequency stimulation failed to induce an increase in eEPSC amplitude (0.46 ± 9.66% increase from baseline; baseline: 147.57 ± 40.76 pA; post-HFS: 152.45 ± 45.37 pA, P = 0.66, n = 5, paired Student's t-test baseline versus post-HFS, Fig 5.12 A-C), consistent with opioids behaviourally established role in fear inhibition.

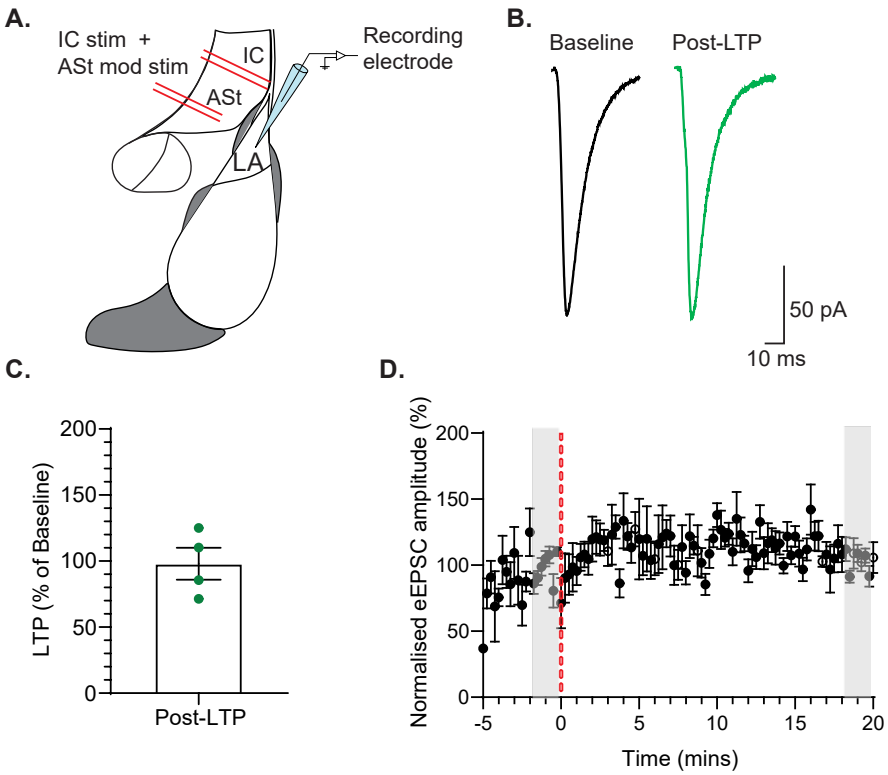

Figure 5.12. Endogenously released opioids do not induce LTP. (A) Cartoon diagram of a coronal amygdala indicating stimulating electrode placements in the ASt and the IC. Putative LA pyramidal neurons were recorded. (B) Representative trace from a putative LA pyramidal neuron showing no change in eEPSC after LTP during ASt moderate stimulations. (C) Graph showing normalised eEPSC as % of baseline after LTP. Each point on graph represents a single neuron. Bar on graph represents mean ± SEM (D) Normalised time plot showing normalised eEPSC amplitude. Grey bars indicate where baseline and LTP effects were measured.

I next examined whether preventing the degradation of endogenously released enkephalin could modify plasticity outcomes at internal capsule-LA synapses. To address this, I applied a cocktail of peptidase inhibitors (thiorphan 10 μM, Bestatin 10 μM, captopril 1 μM) throughout the experiment to help preserve released enkephalin in the synaptic environment.

When a cocktail of peptidase inhibitors was present ASt stimulation during HFS successfully induced LTP (53.31 ± 22.96% increase from baseline, P = 0.011, n = 10, paired Student's t-test baseline versus post-HFS, Fig 5.13 A and B). To determine whether this peptidase inhibitor enabled LTP was specifically mediated by opioids receptors, I applied the selective MOR antagonist CTAP (10 μM) throughout the recordings. Surprisingly, in the presence of peptidase inhibitors and the MOR antagonist CTAP ASt stimulation still produced a low but significant level of LTP not completely inhibited, with small but still significant LTP occurring (13.68 ± 5.10% increase from baseline; baseline: 230.84 ± 61.10 pA; post-HFS: 251.26 ± 58.67 pA, p = 0.04, n = 6, paired Student's t-test baseline versus post-HFS, Fig 5.13 C-E). This suggests that the plasticity observed with peptidase inhibition might be partially mediated by the protection of other non-MOR opioid peptides from degradation, rather than solely through elevated enkephalin signalling.

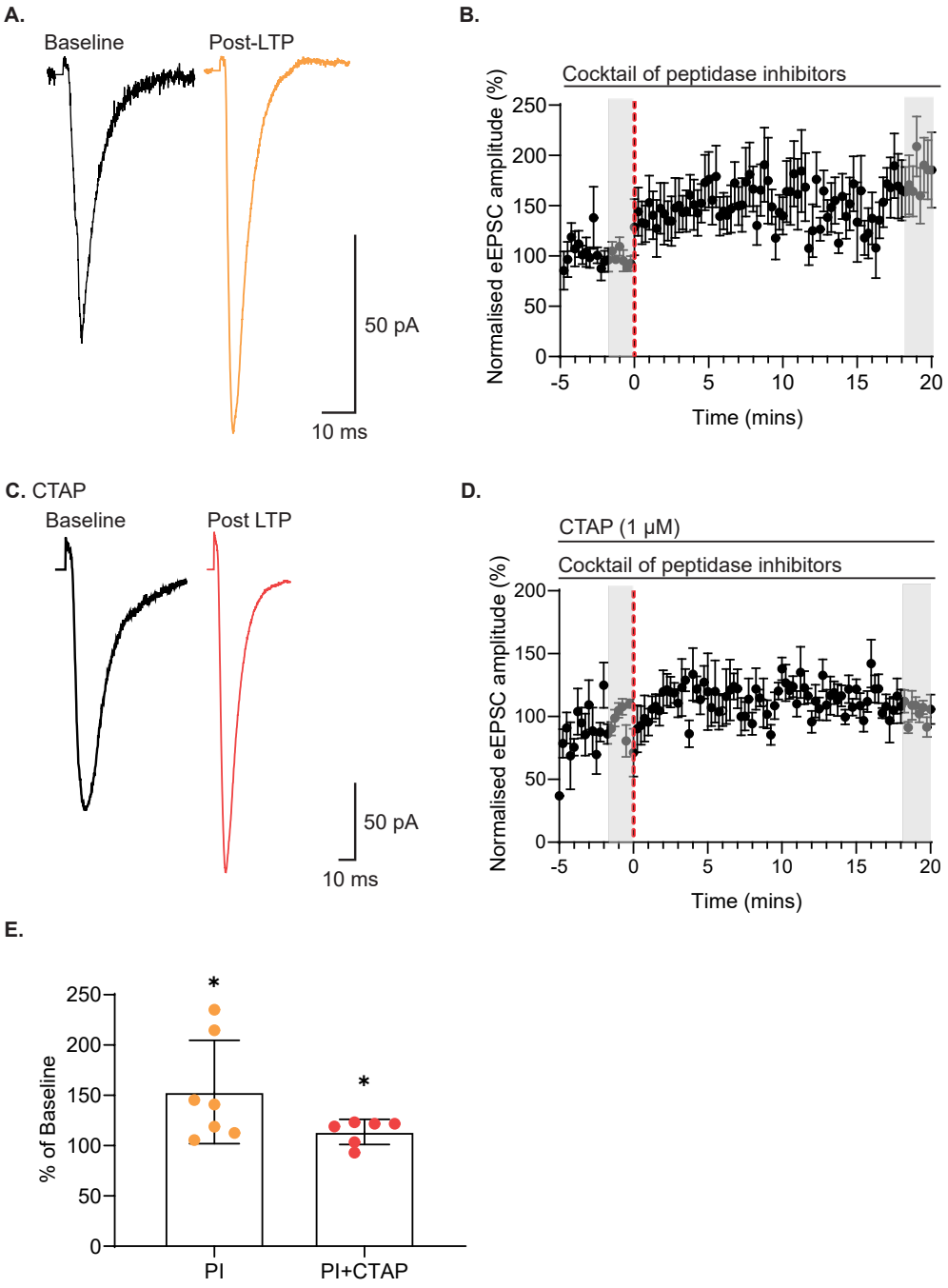

Figure 5.13. Protection of endogenously released peptides facilitated LTP (A-B) Representative traces and normalised time plot from a putative LA pyramidal neuron showing eEPSC increased after LTP protocol during peptidase inhibition (C-D) Representative traces and normalised time plot from a putative LA pyramidal neuron showing eEPSC increases after LTP protocol when MOR was blocked by CTAP (1 μM) and peptidase inhibitors was present Grey bars indicate where baseline and LTP effects were measured. (E) Graph showing normalised eEPSC as % of baseline post LTP when MOR was active or blocked by CTAP during peptidase inhibition. Each point on graphs represents a single neuron. Bars on graph reparents the mean ± SEM. * $P < 0.05$ paired Student's t-test

C. Discussions

This chapter investigated the mechanisms of synaptic plasticity at MGN-LA circuits and their modulation by opioids. Using a combination of optogenetic and electrical stimulation approaches, I examined the conditions under which LTP could be induced at the MGN-LA pathway. Three key findings emerged from these experiments. First, selective optogenetic stimulation of MGN terminals failed to induce LTP in LA neurons despite multiple induction protocols, including high-frequency stimulation alone, pairing stimulations with postsynaptic depolarisation, and spike timing-dependent plasticity. Second, electrical stimulation of the internal capsule, which carries MGN inputs along with other afferents (J. E. LeDoux et al., 1990), successfully induced LTP in both putative LA pyramidal neurons and interneurons, but only when GABAergic inhibition was inhibited. This demonstrates that feedforward inhibition normally constrains plasticity in this pathway. Third, both dopamine and MOR activation enabled LTP induction at internal capsule-LA synapses without requiring GABA receptor blockade. While exogenous application of met-enkephalin facilitated LTP through MOR activation, endogenously released opioids only enabled LTP when protected from degradation by peptidase inhibitors. These findings highlight the complex regulation of plasticity in fear circuits by inhibitory control and neuromodulators.

The inability to induce LTP at MGN-LA synapses using optogenetic stimulation across three different protocols was unexpected, especially considering previous studies have successfully induced LTP in this pathway using similar

protocols with electrical stimulation (Bissière et al., 2003). Despite testing multiple optogenetic LTP protocols, including high-frequency stimulation alone, paired with post-synaptic depolarisation and spike timing-dependent approached, none successfully induced plasticity as these synapses. In contrast, electrical stimulation of the internal capsule readily induced LTP, highlighting a fundamental difference between these stimulation methods. This discrepancy could arise from physiological factors. One possibility is that MGN inputs alone may be less susceptible to LTP than the suite of inputs activated by stimulation of the internal capsule (Papatheodoropoulos & Kouvaros, 2016), however, behavioural training and electrical stimulation both induce LTP at the MGN-LA synapse (Bissière et al., 2003; Kim & Cho, 2017), indicating that MGN terminals are capable of undergoing plasticity. Alternatively, even strong optogenetic activation of MGN inputs may only activate fewer connected cells compared to electrical stimulation, creating a difference in the strength of activation. This potentially reduced response raises an important question about whether stimulating MGN inputs alone provides sufficient excitatory drive for LTP. During fear learning, coincident activation of multiple pathways may be required for synaptic strengthening (Quirk et al., 1997; Ressler & Maren, 2019). However, the fact that LTP could not be induced even when LA neurons were directly depolarised or induced to fire actions potentials suggests that the primary limitation lies with presynaptic glutamate release rather than insufficient postsynaptic excitation. It is possible that rather than a property of the MGN-LA pathway it is a technical limitation of optogenetic stimulation that prevented LTP induction. The consistent inability to induce LTP, and the tendency toward long-term depression in some

recordings, may reflect fundamental limitations of the optogenetic approach rather than inherent properties of the synapse. While ChR2 can theoretically activate at high frequencies (Lin, 2011), its kinetic properties impose significant constraints on temporal precision above 15 Hz due to channel inactivation and slow off-rates during repetitive stimulation (Lin et al., 2009). Although many studies overcome these limitations through channel overexpression (Lin et al., 2009), the degree of depolarisation achieved during high-frequency stimulation may still be insufficient to drive the neurotransmitter release necessary for LTP induction. Additionally, viral expression patterns may not have infected all MGN inputs, reducing the overall synaptic drive compared to electrical stimulation. Future studies employing faster kinetic opsins such as ChIEF or ChrimsonR, which exhibits improved temporal precision during high-frequency stimulation (Lin, 2011), could more definitively investigate plasticity mechanisms at MGN-LA synapses.

In contrast to the limited connectivity observed with optogenetic stimulation of MGN terminals, I observed that electrical stimulation of the internal capsule produced reliable excitatory responses in 100% of both LA pyramidal neurons and interneurons. These responses displayed monosynaptic jitter values consistent with direct glutamatergic inputs. This discrepancy between optogenetic and electrical stimulation approaches raises important questions about pathway-specific connectivity and plasticity. The most likely explanation for this difference is that the internal capsule carries multiple afferent pathways to the LA (J. E. Ledoux et al., 1987) including not only MGN inputs, but also projections from various other cortical regions (J. E. Ledoux et al., 1987). By

stimulating this fibre bundle broader populations of input is likely recruited compared to selective activation of MGN terminals during optogenetic experiments. This recruitment of multiple pathways may create more favourable conditions for LTP induction by providing stronger excitatory drive.

The successful electrical induction of LTP at internal capsule-LA synapses confirms previous findings in this pathway but with an important distinction. My results demonstrate that presynaptic high-frequency stimulation alone is sufficient to induce LTP when inhibitory constraints are removed with picrotoxin. This adds to previous studies that typically employed pairing protocols combining presynaptic stimulation with postsynaptic depolarisation (Bissière et al., 2003). The ability to induce LTP with only presynaptic activation suggests that strong afferent inputs can provide sufficient postsynaptic depolarisation to trigger plasticity mechanisms. However, the broad nature of electrical stimulation makes it difficult to isolate pathway specific contributions to the observed plasticity. The successful induction of LTP could reflect strengthening of thalamic inputs, cortical inputs (J. E. Ledoux et al., 1987), or coordinated changes across multiple inputs, each potentially contributing differently to fear memory formation (Romanski & LeDoux, 1992).

Electrophysiological recordings revealed extensive connectivity from the internal capsule to LA interneurons, with all recorded interneurons forming a monosynaptic connection. This suggests strong feedforward inhibitory control in this circuit. While previous work has demonstrated internal capsule input

onto specific LA interneuron subtypes (Lucas et al., 2016),this data shows a more widespread connectivity across interneuron populations. This extensive inhibitory connectivity could explain why reducing GABAergic inhibition is typically necessary for LTP induction (Bissière et al., 2003) and suggests that afferent pathways though the internal capsule provide precise control of excitatory transmission through feedforward inhibition. A particularly interesting finding was that LTP could be induced not only in putative pyramidal neurons, but also in interneurons within the LA. While LTP at interneuron synapses has been previously demonstrated for specific interneuron populations and primarily with cortical stimulation (J. S. Polepalli, Sullivan, Yanagawa, & Sah, 2010), my results uniquely demonstrate plasticity at internal capsule inputs to LA interneurons. This plasticity across both neuronal types has important implication for circuit function during fear learning. As connections onto pyramidal neurons strengthen during fear conditioning, strengthening of connections onto interneurons would increase feedforward inhibition, potentially limiting the extent and duration of fear responses. This balanced plasticity might ensure that learned fear remained appropriately regulated and prevents uncontrolled excitation that could lead to pathological fear states.

Similar to previous studies (Bissière et al., 2003), I found that dopamine application enables LTP induction at this synapse even with GABAergic transmission intact. While I did not directly test the mechanism, previous work strongly suggests that dopamine permits LTP induction primarily through suppression of feedforward inhibition (Bissière et al., 2003). This disinhibitory

action creates a state where sensory information can more effectively drive synaptic strengthening, providing a cellular mechanism for dopamine's established role in facilitating fear learning (Lee et al., 2016). I had hypothesised that, in contrast to dopamine, opioids would limit LTP induction but in fact I found that met-enkephalin enabled LTP induction at internal capsule-LA synapses. This was surprising given opioid inhibition of fear learning (Gavan P. McNally, 2009). This LTP expression mechanism was similar to established forms of amygdala plasticity (Rogan et al., 1997), with evidence of AMPA receptor mediated strengthening. It is possible that opioids act, like dopamine, to reduce GABAergic inhibition and thus facilitate LTP. Like dopamine receptors opioid receptors are expressed in some amygdala interneurons (J. Zhang, Muller, & McDonald, 2015) and opioids and dopamine inhibit GABA release from intercalated neurons to a similar degree (~60% inhibition) (Gabrielle C. Gregoriou et al., 2019). This suggests that opioids, like dopamine (Bissière et al., 2003), might disinhibit principal neurons by suppressing feedforward GABAergic transmission, creating conditions permissive for LTP induction. To directly test if dopamine or opioids act to suppress feedforward inhibition, in future experiments, I will establish disynaptic responses by stimulating excitatory afferents that contact both projection neurons and interneurons. I will then test whether application of either dopamine or opioid agonists reduces the inhibitory component without effecting spontaneous inhibition. This will provide direct evidence on whether opioids and dopamine can suppress feedforward GABAergic inhibition

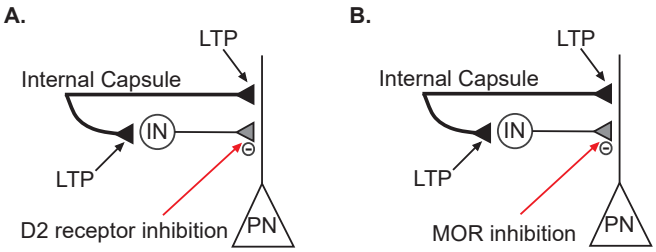

Figure 5.14. Dopamine and opioids facilitate LTP likely through inhibition of GABAergic transmission. (A) Dopamine D2 receptor activation suppresses feedforward inhibition decreasing GABA transmission onto projection neuron. (B) MOR activation likely also suppressed feedforward inhibition through the same mechanisms as D2 receptors. Figure adapted from Bissière et al (2003). PN – pyramidal neuron, IN – interneuron

The capacity of opioids to enable LTP at this synapse, which is thought to be important for allowing fear learning (Clugnet & LeDoux, 1990; Rich et al., 2019) appears at odds with opioids limiting fear learning. This apparent contradiction can potentially be explained through several considerations. First, the opioid inhibition of fear learning likely occurs at sites distinct from where we observed LTP facilitation. Opioids act at multiple locations within fear circuits (Faber & Sah, 2004; Gabrielle C. Gregoriou et al., 2019), including robust inhibition of sensory transmission at MGN-LA synapses as demonstrated in chapter 3. Additionally, in chapter 4 I showed opioid suppression of dopamine release in the amygdala, which represents another potent mechanism for fear inhibition, as dopamine is well-established to promote fear learning (Guarraci et al., 1999). The net behavioural effect of opioids likely reflects the integration of their actions across these multiple sites, with the inhibitory effects on sensory transmission and dopamine release potentially outweighing any LTP-enhancing effects at specific synapses.

Second, there are significant differences between exogenous opioid application and endogenous release patterns that may explain these seemingly contradictory findings. The application of saturating concentrations of met-enkephalin throughout the brain slice creates conditions that are radically different from the targeted, localised release. Of endogenous opioids. Bath application exposes all opioid receptors simultaneously to high concentrations for minutes at a time, while endogenous release from the ASt creates a more temporally and spatially restricted exposure with concentration gradients that diminish due to degradation. This may result in different opioid receptor combinations being activated, either different receptor subtypes or the same receptors in different cellular locations, leading to distinct downstream effects. The need for peptidase inhibition to enable endogenous opioid-mediated LTP supports this interpretation. By preventing degradation, peptidase inhibitors potentially extend the spatial reach and duration of endogenous opioid signals, pushing the response to more closely resemble the effects of bath-applied agonists.

This interpretation is further supported by findings using other neuromodulators. Both gastrin-releasing peptide and norepinephrine can similarly induce LTP under specific pharmacological conditions (Shumyatsky et al., 2002; Tully, Li, Tsvetkov, & Bolshakov, 2007). In the case of norepinephrine, LTP could only be induced when α-adrenoceptors were blocked, despite HPLC assays showing norepinephrine's presence in the amygdala during fear learning (Galvez, Mesches, & McGaugh, 1996). Under physiological conditions, norepinephrine would activate both α- and β-

adrenoceptors, suggesting that plasticity in vivo results from balanced activation of multiple signalling pathways rather than isolated receptor activation. This interpretation is further supported by my experiments examining endogenously released enkephalin, which failed to enable LTP unless protected from degradation by peptidase inhibitors (Fig 5.12). When peptidase inhibitors were present, stimulation of enkephalinergic inputs from the ASt enabled LTP induction, suggesting that endogenous opioid release can modulate synaptic plasticity under specific conditions. Interestingly, LTP could still be induced with peptidase inhibitors even when MORs were blocked with CTAP, suggesting that other neuropeptides protected by peptidase inhibition also contribute to synaptic plasticity. Several neuromodulator peptides including but not limited to, nociceptin, substance P (Hooper et al., 1985) and neurokinin (Marvizon et al., 2003), are susceptible to peptidase breakdown and could be protected under these conditions. Given that striatal MSNs also contain substance P (Blomeley, Kehoe, & Bracci, 2009), stimulation of the ASt likely triggers the release of multiple neuropeptides that can influence synaptic plasticity. These findings highlight the complex interplay between multiple peptide systems in regulating synaptic plasticity at amygdala synapses. To directly test if the nature of the non-selective electrical stimulation may be contributing to these unexpected results, in future experiments, I will use selective activation of MGN inputs to investigate if opioids can modulate plasticity specifically at this pathway.

This investigation into the mechanisms of synaptic plasticity at auditory thalamic to amygdala synapses reveal several key insights. The facilitation of

LTP by both dopamine and opioids despite their opposing effects on fear learning suggest these neuromodulators may influence difference aspects of the fear circuit. Particularly noteworthy was the finding that endogenous opioid mediated facilitation of LTP required protection from peptidase degradation, revealing peptidase activity as a critical regulatory mechanism that could adjust how different neuromodulators influences synaptic plasticity during various behavioural states. Future studies could employ faster kinetic opsins such as ChrimsonR or ChIEF to overcome the technical limitations encountered with ChR2. Together, these findings suggest a complex interplay between inhibitory control and neuromodulator systems in regulating synaptic plasticity at thalamo-amygdala synapses, with important implications for understanding the cellular mechanisms underlying fear learning and memory formation.

Chapter 6
General Discussion

This thesis investigates the role of endogenous opioid signalling in fear related circuits of the amygdala, examining how MGN inputs trigger opioid release from the ASt, how these opioids regulate fear learning in the LA, and the complex interactions between opioid and dopamine systems. Through a combination of electrophysiology, fibre photometry, and fluorescent imaging, these studies suggest that MGN terminals form functional glutamatergic synapses onto ASt neurons that can triggering enkephalin release. This enkephalin can act at multiple sites within the fear circuit, including on MGN terminals where it reduces glutamate release (chapter 3), VTA terminals where it suppresses dopamine release (chapter 4) on amygdala neurons themselves where it can modulate synaptic plasticity under specific conditions. These findings expand our understanding of how neuropeptides coordinate information flow within amygdala circuits, suggesting that endogenous opioids serve as important learning signals in fear circuits beyond their classical role in pain modulation

A. Amygdalo-striatal transition zone in fear learning

The functional connectivity of MGN inputs to the ASt reveals important insights into this understudied region. Previous anatomical studies have shown strong projections from the MGN to ASt (J. E. LeDoux et al., 1990), and my research adds additional electrophysiological evidence that supports these anatomical observations, with MGN inputs forming strong functional glutamatergic synapses onto all putative ASt MSNs. While recent optogenetic studies indicate that manipulating ASt MSNs can bidirectionally influence fear

learning, with D1 MSN inhibition reducing fear and D2 MSN inhibition enhancing it (Kintscher et al., 2023), these manipulations alone do not reveal how neurons usually participate in fear learning. The current findings demonstrate that the ASt potentially serves as a source of endogenous enkephalin release during fear learning. This enkephalin release, likely from D2 MSNs (Y. Wang et al., 2023), aligns with the increased fear observed when D2 neurons are inhibited (Kintscher et al., 2023). The relatively sparse ASt-LA GABAergic projections suggest that enkephalin signalling may represent the ASt's primary influence on fear circuits (C. Wang et al., 2002). By modulating synaptic transmission at MGN-LA terminals, VTA dopamine release, and potentially LA plasticity, ASt derived enkephalin can coordinate information flow across multiple fear related circuits. These findings suggest the ASt functions as a neuromodulator hub that regulates emotional learning through peptidergic signalling. Further experiments will utilise labelling of specific ASt neurons to identify their axonal projections and determine whether enkephalinergic MSNs directly project onto LA neurons, which would provide additional insights into how this peptidergic system influences fear learning circuits

B. Opioids as a fear-inhibiting neuropeptide

Previous behavioural studies have established that opioid receptor blockade enhances both first- and second-order fear conditioning (Michalscheck et al., 2021), suggesting that endogenous opioids act as fear-inhibiting molecules. The involvement of opioids in second-order conditioning, where learning

occurs without direct noxious stimulation, indicates that opioid signalling serves as a learning signal independent of pain processing. The current findings indicate that enkephalin is released during fear learning and provide multiple sites of action through which opioids might achieve this fear-inhibiting function. These sites of action include:

i. Inhibition of sensory input

The first mechanism through which opioids may inhibit fear learning is via direct suppression of sensory input to the lateral amygdala. Electrophysiological recordings demonstrate that met-enkephalin produces robust suppression of glutamate release at MGN-LA synapses through activation of presynaptic MORs (Fig 6.1). This finding is particularly significant as the MGN-LA pathway serves as the primary route for auditory information during fear conditioning. By reducing glutamate release at these synapses, enkephalin effectively attenuates the strength of incoming sensory signals that drive fear learning (Fig 6.1).

The anatomical and molecular evidence strongly supports this mechanism. The selective expression of MORs in the MGN (Alfred Mansour et al., 1994; Sharif & Hughes, 1989), with minimal expression of other opioid receptor subtypes, creates a system precisely tuned to regulate sensory transmission at its entry point into fear circuits. The presynaptic location of these receptors, suggested through changes in paired-pulse measurements, enables rapid modulation of synaptic transmission without requiring long-term cellular changes. This suppression of sensory input to the LA represents a direct

cellular mechanism for potential opioid mediated reduction of fear learning. To fully elucidate the role of opioid action on this pathway in fear learning, future experiments will utilise pathway specific knockdown of MORs in MGN neurons projecting to the LA. This approach will determine whether presynaptic inhibition of auditory thalamic inputs represents a necessary mechanism through which endogenous opioids regulate fear acquisition or if other sites of action contribute to this process.

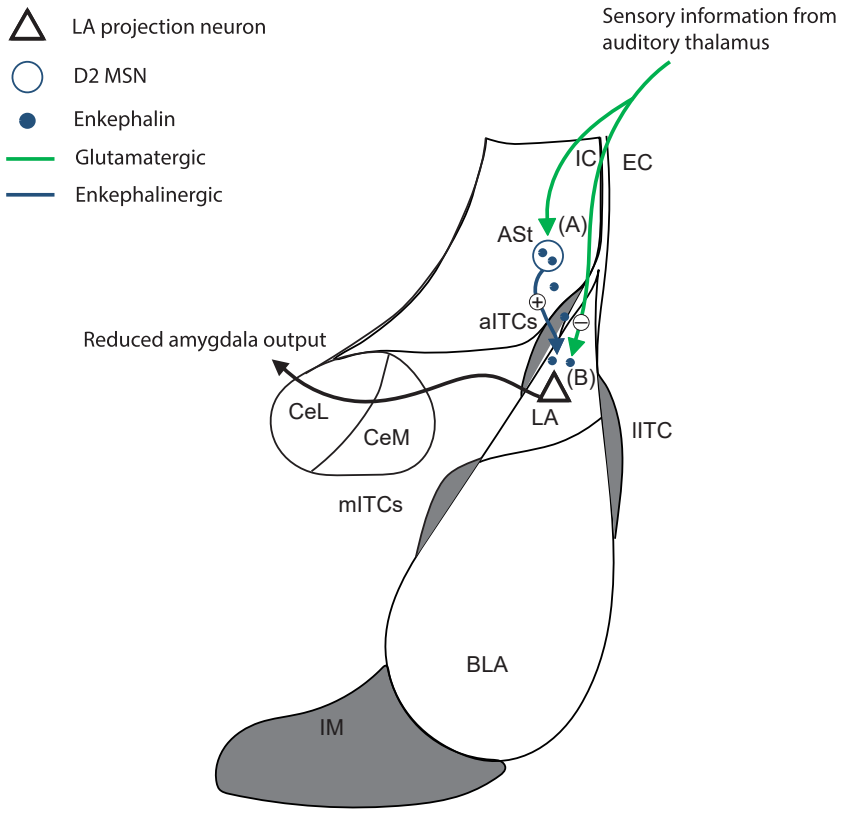

Figure 6.1. Opioid-mediated regulation of sensory input to the amygdala (A) During fear learning, sensory stimuli activate auditory thalamic projections to the amygdalo-striatal transition zone (ASt). This activation triggers enkephalin release from D2-expressing medium spiny neurons in the ASt, which release enkephalin both locally and into the lateral amygdala (LA). (B) The released enkephalin acts on auditory thalamic terminals, inhibiting glutamate release. This inhibition reduces sensory information flow to the LA, subsequently decreasing LA projection neuron activity.

ii. Regulation of dopamine-facilitated plasticity

A second mechanism through which opioids might regulate fear learning involves modulation of dopamine dependent plasticity in amygdala circuits (Fig 6.2). Previous work has established that dopamine plays a critical role in enabling fear learning likely by suppressing GABAergic inhibition in the LA, which allows the induction of synaptic plasticity at sensory inputs (Bissière et al., 2003). The current findings suggest a model where endogenous enkephalin release from the ASt could gate this dopamine dependent plasticity by reducing local dopamine release through activation of MORs on VTA terminals (Fig 6.2). This regulatory mechanism could be particularly important given the circuit organisation revealed in these studies. The predominantly dopaminergic nature of VTA-ASt projections (Jean-Francois Poulin et al., 2018; S. R. Taylor et al., 2014), combined with relatively sparse glutamatergic connectivity, suggests these inputs are specifically configured to modulate local circuit function rather than drive direct excitation. This organisation might allow precise control over the conditions that enable synaptic plasticity, with enkephalin serving as a brake on dopamine facilitated learning. By utilising the viral enkephalin knockdown strategy validated in this thesis as well as pathway specific receptors knockdowns, future experiment will investigate whether reducing enkephalin levels increases fear learning in behavioural studies, providing further evidence on the role of enkephalin as fear inhibiting.

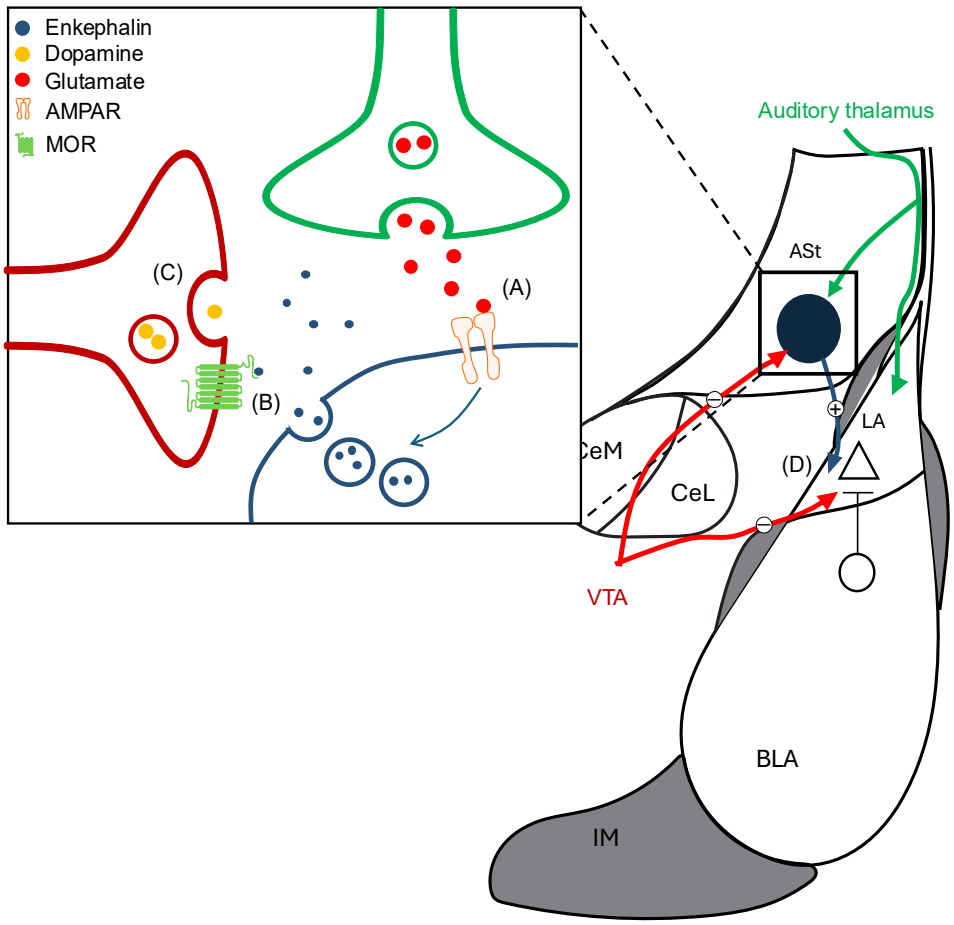

Figure 6.2. Enkephalin regulation of dopamine signalling in the amygdala circuit (A) Sensory-evoked glutamate release activates AMPA receptors on D2-expressing medium spiny neurons (MSNs) in the amygdalo-striatal transition zone (ASt). This activation triggers the local release of enkephalin from these neurons. (B) The released enkephalin acts through μ-opioid receptors (MOR), which are likely expressed on axon terminals from the ventral tegmental area (VTA) (C) Activation of MOR on VTA terminals leads to the inhibition of vesicular dopamine release .(D) Beyond its effects in the ASt, enkephalin may also act on dopaminergic terminals within the lateral amygdala (LA). This additional site of action could reduce long-term potentiation by preventing dopamine's typical role in suppressing GABAergic inhibition.

iii. Synaptic plasticity

A third mechanisms through which opioids may regulate fear learning involves their complex effects on synaptic plasticity. The initial hypothesis was that opioids would inhibit plasticity at fear related synapses, consistent with their role as fear inhibiting molecules (Gavan P. McNally, 2009). Surprisingly,

exogenous met-enkephalin application enabled LTP induction at internal capsule-LA synapses, with similar mechanisms of LTP induction as those previously established during fear learning (Bissière et al., 2003; Rogan et al., 1997). However, endogenously released enkephalin failed to produce this same facilitation under normal conditions. Therefore, endogenous opioids do not appear to promote plasticity under physiological conditions, suggesting their actions on fear learning likely occur through other mechanisms such as suppression of sensory transmission or modulation of dopamine release, rather than direct effects on synaptic strengthening. Only when protected from degradation by peptidase inhibitors could endogenously release enkephalin facilitate LTP induction, highlighting peptidase activity as a key control point in opioid signalling. This finding has significant implications as adenylyl cyclase signalling directly modulates peptidase activity (G. C. Gregoriou et al., 2020), creating a system where behavioural states can dynamically regulate opioid function. Exposure to substances such as alcohol or cocaine increases adenylyl cyclase/PKA signalling (Nestler, 2004), which could alter peptidase activity and consequently change how opioids influence fear circuits. While peptidase inhibitors are generally viewed as promoting endogenous opioid activity at their intended sites of action, such as enhancing analgesia during painful states (Murata et al., 2014; Shigeru et al., 2007), this research demonstrates that boosting endogenous opioid signalling may sometimes produce counterintuitive effects like facilitating synaptic plasticity in fear circuits. These activity dependent changes in peptidase function likely represent a mechanism through which different emotional states could alter how opioids influence synaptic plasticity, potentially shifting opioid function

from predominantly inhibitory to facilitatory under specific conditions. To fully elucidate potential effects of opioids on synaptic plasticity, future studies will utilise activity dependent tagging and investigate whether opioids actions in the amygdala can change recruitment of neurons into a memory engram.

iv. Enkephalin release

While optogenetic stimulation of MGN terminals in the ASt triggers robust enkephalin release in slice preparations, in behaving animals, enkephalin release was observed primarily in response to the foot shock during initial presentations, with minimal release to the tone alone. This observation provides important insights into the physiological conditions required for enkephalin release. Given the robust connectivity seen, the MGN-ASt circuit appears configured to release enkephalin in response to auditory information such as tone, yet during fear learning, it is the footshock rather than the tone that initially drives this release. This suggests that while MGN inputs can trigger enkephalin release, the level of activation produced by a tone alone may be insufficient to drive significant peptide release under normal physiological conditions. Therefore, this supports the proposal that *in vivo* it is the level of MGN activity that determines enkephalin release in the ASt. It is worth noting that the MGN itself undergoes plasticity during fear learning, with enhanced responses to specific tone frequencies (J. A. Taylor et al., 2021). As learning progresses, this MGN plasticity likely increases the strength of inputs to the ASt, potentially explaining why enkephalin release gradually transfers to the tone after conditioning. This delay in enkephalin release suggests a specific role in fear learning, rather than opioids preventing initial fear

acquisition, enkephalin may serve as a brake that prevents fear responses from becoming excessive or generalised. By allowing initial plasticity to occur before engaging inhibitory mechanisms, this system could permit adaptive fear learning while preventing pathological fear states.

C. Methodological advances

Recent advances in GPCR-based sensor technology have transformed our ability to monitor peptide release in real time, overcoming longstanding methodological barriers that have limited our understanding of peptidergic modulation in fear circuits (F. Sun et al., 2018). This research capitalised on novel biosensor technology, utilising both opioid and dopamine sensors to investigate interactions between these neuromodulator systems. The development and validation of targeted viral tools for manipulating peptide expression complemented these sensors by providing regional and molecular specificity. The effectiveness of these approaches provided additional evidence for the ASt as a primary source of enkephalin release and created new opportunities for investigating the causal role of specific peptide systems in regulating fear learning. The combination of these technologies created a powerful methodology for dissecting complex neuromodulator systems that was previously unattainable. By integrating fluorescent biosensors with electrophysiology, optogenetics, and behavioural assays, this research established a framework for simultaneously manipulating specific circuit connections, visualising resulting peptide release, and measuring functional consequences at cellular and behavioural levels, providing new insights into

how different inputs drive neuromodulator systems and how they can interact with each other in the amygdala. These technological advances extend beyond the specific findings of this thesis, establishing a template for investigating other neuromodulator systems in diverse brain regions and behavioural contexts.

D. Clinical implications and therapeutic potential

The identification of endogenous opioid signalling as a key regulator of fear learning has important implications for treating fear related disorders. The finding that opioids can suppress fear learning through multiple mechanisms suggests potential therapeutic strategies that target these pathways. Unlike exogenous opioids, which carry significant risk for addiction (Lutz & Kieffer, 2013), manipulating endogenous opioid signalling using peptidase inhibitors or positive allosteric modulators might provide more targeted approaches for treating anxiety and fear-related disorders.

The distinct temporal dynamics of opioid release during different phases of fear learning suggest that therapeutic interventions might be most effective when timed to specific stages of emotional learning. The parallel between opioid release patterns and prediction error signals also suggests that these systems might be particularly important for updating emotional memories, a process critical for extinction learning and exposure therapy (Raeder, Merz, Margraf, & Zlomuzica, 2020).

E. Concluding Remarks

This thesis provides evidence suggesting endogenous opioids may act as modulators of fear learning through multiple circuit mechanisms. The findings point to potential coordination between sensory, dopaminergic, and peptidergic systems in the regulation of emotional learning, though further research will be needed to fully understand these interactions. The implementation of novel biosensors and genetic tools has provided unprecedented insight into the dynamics of peptide signalling in behaving animals, while detailed circuit analysis has revealed multiple mechanisms through which these signals influence fear learning.

The demonstration that opioid signalling serves functions beyond pain modulation, particularly in regulating emotional learning, represents an important advance in our understanding of these circuits. The identification of multiple mechanisms through which opioids can influence fear learning, from direct suppression of sensory input to modulation of dopamine release and regulation of synaptic plasticity, highlights the sophisticated nature of peptidergic modulation in the brain.

This improved understanding of how endogenous opioids regulate fear circuits may provide new therapeutic approaches for treating fear related disorders while avoiding the addictive potential of exogenous opioids. Future studies building on these findings will likely reveal additional complexity in how peptide

systems regulate emotional learning and may lead to more effective treatments for anxiety and fear related disorders.

Chapter 7
Reference

Adolphs, R., Tranel, D., Damasio, H., & Damasio, A. R. (1995). Fear and the human amygdala. *J Neurosci, 15*(9), 5879-5891. doi:10.1523/jneurosci.15-09-05879.1995

Al-Hasani, R., Wong, J. T., Mabrouk, O. S., McCall, J. G., Schmitz, G. P., Porter-Stransky, K. A., . . . Bruchas, M. R. (2018). In vivo detection of optically-evoked opioid peptide release. *eLife, 7*. doi:10.7554/eLife.36520

Angulo, M. C., Rossier, J., & Audinat, E. (1999). Postsynaptic glutamate receptors and integrative properties of fast-spiking interneurons in the rat neocortex. *J Neurophysiol, 82*(3), 1295-1302. doi:10.1152/jn.1999.82.3.1295

Asan, E. (1998). The catecholaminergic innervation of the rat amygdala. *Adv Anat Embryol Cell Biol, 142*, 1-118. doi:10.1007/978-3-642-72085-7

Asede, D., Doddapaneni, D., Chavez, A., Okoh, J., Ali, S., Von-Walter, C., & Bolton, M. M. (2021). Apical intercalated cell cluster: A distinct sensory regulator in the amygdala. *Cell Reports, 35*(7), 109151. doi:https://doi.org/10.1016/j.celrep.2021.109151

Barbano, M. F., Wang, H. L., Zhang, S., Miranda-Barrientos, J., Estrin, D. J., Figueroa-González, A., . . . Morales, M. (2020). VTA Glutamatergic Neurons Mediate Innate Defensive Behaviors. *Neuron, 107*(2), 368-382.e368. doi:10.1016/j.neuron.2020.04.024

Basbaum, A. I., & Fields, H. L. (1984). Endogenous pain control systems: brainstem spinal pathways and endorphin circuitry. *Annual review of neuroscience, 7*, 309.

Bayer, H. M., & Glimcher, P. W. (2005). Midbrain dopamine neurons encode a quantitative reward prediction error signal. *Neuron, 47*(1), 129-141. doi:10.1016/j.neuron.2005.05.020

Bernard, J. F., Alden, M., & Besson, J. M. (1993). The organization of the efferent projections from the pontine parabrachial area to the amygdaloid complex: a Phaseolus vulgaris leucoagglutinin (PHA-L) study in the rat. *J Comp Neurol, 329*(2), 201-229. doi:10.1002/cne.903290205

Bernard, J. F., & Besson, J. M. (1990). The spino(trigemino)pontoamygdaloid pathway: electrophysiological evidence for an involvement in pain processes. *J Neurophysiol, 63*(3), 473-490. doi:10.1152/jn.1990.63.3.473

Bernard, J. F., Dallel, R., Raboisson, P., Villanueva, L., & Bars, D. L. (1995). Organization of the efferent projections from the spinal cervical enlargement to the parabrachial area and periaqueductal graye. A PHA‐L study in the rat. *Journal of Comparative Neurology, 353*(4), 480-505. doi:10.1002/cne.903530403

Beyeler, A., & Dabrowska, J. (2020). Neuronal diversity of the amygdala and the bed nucleus of the stria terminalis. *Handb Behav Neurosci, 26*, 63-100. doi:10.1016/b978-0-12-815134-1.00003-9

Beyeler, A., Namburi, P., Glober, G. F., Simonnet, C., Calhoon, G. G., Conyers, G. F., . . . Tye, K. M. (2016). Divergent Routing of Positive and Negative Information from the Amygdala during Memory Retrieval. *Neuron, 90*(2), 348-361. doi:10.1016/j.neuron.2016.03.004

Bi, G. Q., & Poo, M. M. (1998). Synaptic modifications in cultured hippocampal neurons: dependence on spike timing, synaptic strength, and postsynaptic cell type. *J Neurosci, 18*(24), 10464-10472. doi:10.1523/jneurosci.18-24-10464.1998

Bissière, S., Humeau, Y., & Lüthi, A. (2003). Dopamine gates LTP induction in lateral amygdala by suppressing feedforward inhibition. *Nature Neuroscience, 6*(6), 587-592. doi:10.1038/nn1058

Blackburn, J. R., & Phillips, A. G. (1990). Enhancement of freezing behaviour by metoclopramide: implications for neuroleptic-induced avoidance deficits. *Pharmacology, biochemistry and behavior, 35*(3), 685-691. doi:10.1016/0091-3057(90)90308-5

Blair, H. T., Sotres-Bayon, F., Moita, M. A. P., & Ledoux, J. E. (2005). The lateral amygdala processes the value of conditioned and unconditioned aversive stimuli. *Neuroscience, 133*(2), 561-569. doi:https://doi.org/10.1016/j.neuroscience.2005.02.043

Bliss, T. V., & Lomo, T. (1973). Long-lasting potentiation of synaptic transmission in the dentate area of the anaesthetized rabbit following stimulation of the perforant path. *The Journal of physiology, 232*(2), 331-356. doi:10.1113/jphysiol.1973.sp010273

Blomeley, C. P., Kehoe, L. A., & Bracci, E. (2009). Substance P mediates excitatory interactions between striatal projection neurons. *J Neurosci, 29*(15), 4953-4963. doi:10.1523/jneurosci.6020-08.2009

Bolles, R. C., & Fanselow, M. S. (1980). A perceptual-defensive-recuperative model of fear and pain. *Behavioral and Brain Sciences, 3*(2), 291-301. doi:10.1017/S0140525X0000491X

Bordi, F., & LeDoux, J. E. (1994). Response properties of single units in areas of rat auditory thalamus that project to the amygdala. II. Cells receiving convergent auditory and somatosensory inputs and cells antidromically activated by amygdala stimulation. *Exp Brain Res, 98*(2), 275-286. doi:10.1007/bf00228415

Borowski, T. B., & Kokkinidis, L. (1998). The effects of cocaine, amphetamine, and the dopamine D1 receptor agonist SKF 38393 on fear extinction as measured with potentiated startle: implications for psychomotor stimulant psychosis. *Behav Neurosci, 112*(4), 952-965. doi:10.1037//0735-7044.112.4.952

Bouton, M. E., & Bolles, R. C. (1980). Conditioned fear assessed by freezing and by the suppression of three different baselines. *Animal learning & behavior, 8*(3), 429-434.

Bramham, C. R., Milgram, N. W., & Srebro, B. (1991). Delta opioid receptor activation is required to induce LTP of synaptic transmission in the lateral perforant path in vivo. *Brain Res, 567*(1), 42-50. doi:10.1016/0006-8993(91)91433-2

Bramham, C. R., & Sarvey, J. M. (1996). Endogenous activation of mu and delta-1 opioid receptors is required for long-term potentiation induction in the lateral perforant path: dependence on GABAergic inhibition. *J Neurosci, 16*(24), 8123-8131. doi:10.1523/jneurosci.16-24-08123.1996

Brandão, M. L., & Coimbra, N. C. (2019). Understanding the role of dopamine in conditioned and unconditioned fear. *Rev Neurosci, 30*(3), 325-337. doi:10.1515/revneuro-2018-0023

Britt, J. P., & McGehee, D. S. (2008). Presynaptic opioid and nicotinic receptor modulation of dopamine overflow in the nucleus accumbens. *J Neurosci, 28*(7), 1672-1681. doi:10.1523/jneurosci.4275-07.2008

Bull, D. R., Bakhtiar, R., & Sheehan, M. J. (1991). Characterization of dopamine autoreceptors in the amygdala: A fast cyclic voltammetric study in vitro. *Neuroscience Letters, 134*(1), 41-44. doi:https://doi.org/10.1016/0304-3940(91)90504-M

Cai, J., & Tong, Q. (2022). Anatomy and Function of Ventral Tegmental Area Glutamate Neurons. *Front Neural Circuits, 16*, 867053. doi:10.3389/fncir.2022.867053

Cai, Y., & Ford, C. P. (2018). Dopamine Cells Differentially Regulate Striatal Cholinergic Transmission across Regions through Corelease of Dopamine and Glutamate. *Cell Rep, 25*(11), 3148-3157.e3143. doi:10.1016/j.celrep.2018.11.053

Calford, M. B., & Aitkin, L. M. (1983). Ascending projections to the medial geniculate body of the cat: evidence for multiple, parallel auditory pathways through thalamus. *J Neurosci, 3*(11), 2365-2380. doi:10.1523/jneurosci.03-11-02365.1983

Castro, D. C., Oswell, C. S., Zhang, E. T., Pedersen, C. E., Piantadosi, S. C., Rossi, M. A., . . . Bruchas, M. R. (2021). An endogenous opioid circuit determines state-dependent reward consumption. *Nature, 598*(7882), 646-651. doi:10.1038/s41586-021-04013-0

Chefer, V. I., Thompson, A. C., Zapata, A., & Shippenberg, T. S. (2009). Overview of Brain Microdialysis. *Current Protocols in Neuroscience, 47*(1), 7.1.1-7.1.28. doi:https://doi.org/10.1002/0471142301.ns0701s47

Cheng, D. T., Knight, D. C., Smith, C. N., Stein, E. A., & Helmstetter, F. J. (2003). Functional MRI of human amygdala activity during Pavlovian fear conditioning: stimulus processing versus response expression. *Behav Neurosci, 117*(1), 3-10. doi:10.1037//0735-7044.117.1.3

Clugnet, M. C., & LeDoux, J. E. (1990). Synaptic plasticity in fear conditioning circuits: induction of LTP in the lateral nucleus of the amygdala by stimulation of the medial geniculate body. *J Neurosci, 10*(8), 2818-2824. doi:10.1523/jneurosci.10-08-02818.1990

Cousens, G., & Otto, T. (1998). Both pre- and posttraining excitotoxic lesions of the basolateral amygdala abolish the expression of olfactory and contextual fear conditioning. *Behavioral Neuroscience, 112*(5), 1092-1103. doi:10.1037/0735-7044.112.5.1092

Davis, M. (1992). The role of the amygdala in conditioned fear. In *The amygdala: Neurobiological aspects of emotion, memory, and mental dysfunction.* (pp. 255-306). New York, NY, US: Wiley-Liss.

de Oliveira, A. R., Reimer, A. E., Macedo, C. E. A. d., Carvalho, M. C. d., Silva, M. A. d. S., & Brandão, M. L. (2011). Conditioned fear is modulated by D2 receptor pathway connecting the ventral tegmental area and basolateral amygdala. *Neurobiology of Learning and Memory, 95*(1), 37-45. doi:https://doi.org/10.1016/j.nlm.2010.10.005

de Souza Caetano, K. A., de Oliveira, A. R., & Brandão, M. L. (2013). Dopamine D2 receptors modulate the expression of contextual conditioned fear: role of the ventral tegmental area and the basolateral amygdala. *Behavioural Pharmacology, 24*(4).

DiFazio, L. E., Fanselow, M., & Sharpe, M. J. (2022). The effect of stress and reward on encoding future fear memories. *Behavioural Brain Research, 417*, 113587. doi:https://doi.org/10.1016/j.bbr.2021.113587

Dixon, D. M., & Traynor, J. R. (1990). Formation of [Leu5]enkephalin from dynorphin A(1-8) by rat central nervous tissue in vitro. *J Neurochem, 54*(4), 1379-1385. doi:10.1111/j.1471-4159.1990.tb01972.x

Dong, C., Gowrishankar, R., Jin, Y., He, X. J., Gupta, A., Wang, H., . . . Tian, L. (2024). Unlocking opioid neuropeptide dynamics with genetically encoded biosensors. *Nature Neuroscience, 27*(9), 1844-1857. doi:10.1038/s41593-024-01697-1

Doron, N. N., & Ledoux, J. E. (1999). Organization of projections to the lateral amygdala from auditory and visual areas of the thalamus in the rat. *J Comp Neurol, 412*(3), 383-409.

Doyle, M. W., & Andresen, M. C. (2001). Reliability of Monosynaptic Sensory Transmission in Brain Stem Neurons In Vitro. *Journal of Neurophysiology, 85*(5), 2213-2223. doi:10.1152/jn.2001.85.5.2213

Dudai, Y. (1989). *The neurobiology of memory: Concepts, findings, trends*. New York, NY, US: Oxford University Press.

Dunsmoor, J. E., & Paz, R. (2015). Fear Generalization and Anxiety: Behavioral and Neural Mechanisms. *Biological psychiatry (1969), 78*(5), 336-343. doi:10.1016/j.biopsych.2015.04.010

Duvarci, S., & Pare, D. (2014). Amygdala microcircuits controlling learned fear. *Neuron, 82*(5), 966-980. doi:10.1016/j.neuron.2014.04.042

Dymond, S., Dunsmoor, J. E., Vervliet, B., Roche, B., & Hermans, D. (2015). Fear Generalization in Humans: Systematic Review and Implications for Anxiety Disorder Research. *Behav Ther, 46*(5), 561-582. doi:10.1016/j.beth.2014.10.001

Egan, C. T., Herrick-Davis, K., & Teitler, M. (1998). Creation of a constitutively activated state of the 5-hydroxytryptamine2A receptor by site-directed mutagenesis: inverse agonist activity of antipsychotic drugs. *J Pharmacol Exp Ther, 286*(1), 85-90.

Eippert, F., Bingel, U., Schoell, E., Yacubian, J., & Büchel, C. (2008). Blockade of endogenous opioid neurotransmission enhances acquisition of conditioned fear in humans. *J Neurosci, 28*(21), 5465-5472. doi:10.1523/jneurosci.5336-07.2008

Faber, E. S. L., & Sah, P. (2004). Opioids Inhibit Lateral Amygdala Pyramidal Neurons by Enhancing a Dendritic Potassium Current. *The Journal of Neuroscience, 24*(12), 3031-3039. doi:10.1523/jneurosci.4496-03.2004

Fanselow, M. S. (1994). Neural organization of the defensive behavior system responsible for fear. *Psychon Bull Rev, 1*(4), 429-438. doi:10.3758/bf03210947

Fanselow, M. S. (1998). Pavlovian conditioning, negative feedback, and blocking: mechanisms that regulate association formation. *Neuron, 20*(4), 625-627. doi:10.1016/s0896-6273(00)81002-8

Fanselow, M. S., Calcagnetti, D. J., & Helmstetter, F. J. (1988). Peripheral versus intracerebroventricular administration of quaternary naltrexone and the enhancement of Pavlovian conditioning. *Brain Res, 444*(1), 147-152. doi:10.1016/0006-8993(88)90921-3

Fanselow, M. S., & Wassum, K. M. (2015). The Origins and Organization of Vertebrate Pavlovian Conditioning. *Cold Spring Harb Perspect Biol, 8*(1), a021717. doi:10.1101/cshperspect.a021717

Ford, C. P. (2014). The role of D2-autoreceptors in regulating dopamine neuron activity and transmission. *Neuroscience, 282*, 13-22. doi:10.1016/j.neuroscience.2014.01.025

Ford, C. P., Mark, G. P., & Williams, J. T. (2006). Properties and Opioid Inhibition of Mesolimbic Dopamine Neurons Vary according to Target Location. *The Journal of Neuroscience, 26*(10), 2788-2797. doi:10.1523/jneurosci.4331-05.2006

Gagnon, D., Petryszyn, S., Sanchez, M. G., Bories, C., Beaulieu, J. M., De Koninck, Y., . . . Parent, M. (2017). Striatal Neurons Expressing D1 and D2 Receptors are Morphologically Distinct and Differently Affected by Dopamine Denervation in Mice. *Scientific Reports, 7*(1), 41432. doi:10.1038/srep41432

Galvez, R., Mesches, M. H., & McGaugh, J. L. (1996). Norepinephrine Release in the Amygdala in Response to Footshock Stimulation. *Neurobiology of Learning and Memory, 66*(3), 253-257. doi:https://doi.org/10.1006/nlme.1996.0067

Goosens, K. A., Holt, W., & Maren, S. (2000). A role for amygdaloid PKA and PKC in the acquisition of long-term conditional fear memories in rats. *Behav Brain Res, 114*(1-2), 145-152. doi:10.1016/s0166-4328(00)00224-2

Greba, Q., & Kokkinidis, L. (2000). Peripheral and intraamygdalar administration of the dopamine D1 receptor antagonist SCH 23390 blocks fear-potentiated startle but not shock reactivity or the shock sensitization of acoustic startle. *Behav Neurosci, 114*(2), 262-272. doi:10.1037//0735-7044.114.2.262

Gregoriou, G. C., Kissiwaa, S. A., Patel, S. D., & Bagley, E. E. (2019). Dopamine and opioids inhibit synaptic outputs of the main island of the intercalated neurons of the amygdala. *European Journal of Neuroscience, 50*(3), 2065-2074. doi:https://doi.org/10.1111/ejn.14107

Gregoriou, G. C., Patel, S. D., Pyne, S., Winters, B. L., & Bagley, E. E. (2023). Opioid Withdrawal Abruptly Disrupts Amygdala Circuit Function by Reducing Peptide Actions. *J Neurosci, 43*(10), 1668-1681. doi:10.1523/jneurosci.1317-22.2022

Gregoriou, G. C., Patel, S. D., Winters, B. L., & Bagley, E. E. (2020). Neprilysin Controls the Synaptic Activity of Neuropeptides in the Intercalated Cells of the Amygdala. *Molecular Pharmacology, 98*(4), 454. doi:10.1124/mol.119.119370

Grover, L. M., & Yan, C. (1999). Blockade of GABAA receptors facilitates induction of NMDA receptor-independent long-term potentiation. *J Neurophysiol, 81*(6), 2814-2822. doi:10.1152/jn.1999.81.6.2814

Guarraci, F. A., Frohardt, R. J., & Kapp, B. S. (1999). Amygdaloid D1 dopamine receptor involvement in Pavlovian fear conditioning. *Brain Res, 827*(1-2), 28-40. doi:10.1016/s0006-8993(99)01291-3

Helmstetter, F. J., & Fanselow, M. S. (1987). Effects of naltrexone on learning and performance of conditional fear-induced freezing and opioid analgesia. *Physiology & Behavior, 39*(4), 501-505. doi:https://doi.org/10.1016/0031-9384(87)90380-5

Hiranuma, T., Kitamura, K., Taniguchi, T., Kobayashi, T., Tamaki, R., Kanai, M., . . . Oka, T. (1998). Effects of three peptidase inhibitors, amastatin, captopril and phosphoramidon, on the hydrolysis of [Met5]-enkephalin-Arg6-Phe7 and other opioid peptides. *Naunyn-Schmiedeberg's Archives of Pharmacology, 357*(3), 276-282. doi:10.1007/PL00005168

Hochgerner, H., Singh, S., Tibi, M., Lin, Z., Skarbianskis, N., Admati, I., . . . Zeisel, A. (2023). Neuronal types in the mouse amygdala and their transcriptional response to fear conditioning. *Nature Neuroscience, 26*(12), 2237-2249. doi:10.1038/s41593-023-01469-3

Hooper, N. M., Kenny, A. J., & Turner, A. J. (1985). The metabolism of neuropeptides. Neurokinin A (substance K) is a substrate for endopeptidase-24.11 but not for peptidyl dipeptidase A (angiotensin-converting enzyme). *Biochem J, 231*(2), 357-361. doi:10.1042/bj2310357

Hsu, D. T., Sanford, B. J., Meyers, K. K., Love, T. M., Hazlett, K. E., Walker, S. J., . . . Zubieta, J. K. (2015). It still hurts: altered endogenous opioid activity in the brain during social rejection and acceptance in major depressive disorder. *Mol Psychiatry, 20*(2), 193-200. doi:10.1038/mp.2014.185

Huang, Y. Y., & Kandel, E. R. (1998). Postsynaptic induction and PKA-dependent expression of LTP in the lateral amygdala. *Neuron, 21*(1), 169-178. doi:10.1016/s0896-6273(00)80524-3

Hui, K. S., Wang, Y. J., & Lajtha, A. (1983). Purification and characterization of an enkephalin aminopeptidase from rat brain membranes. *Biochemistry, 22*(5), 1062-1067. doi:10.1021/bi00274a010

Hull, C. L. (1943). Principles of behavior: an introduction to behavior theory.

Inoue, T., Izumi, T., Maki, Y., Muraki, I., & Koyama, T. (2000). Effect of the dopamine D(1/5) antagonist SCH 23390 on the acquisition of conditioned fear. *Pharmacology, biochemistry and behavior, 66*(3), 573-578. doi:10.1016/S0091-3057(00)00254-9

Inutsuka, A., Ino, D., & Onaka, T. (2021). Detection of neuropeptides in vivo and open questions for current and upcoming fluorescent sensors for neuropeptides. *Peptides, 136*, 170456. doi:https://doi.org/10.1016/j.peptides.2020.170456

Janak, P. H., & Tye, K. M. (2015). From circuits to behaviour in the amygdala. *Nature, 517*(7534), 284-292. doi:10.1038/nature14188

Keiflin, R., & Janak, P. H. (2015). Dopamine Prediction Errors in Reward Learning and Addiction: From Theory to Neural Circuitry. *Neuron, 88*(2), 247-263. doi:10.1016/j.neuron.2015.08.037

Kile, B. M., Walsh, P. L., McElligott, Z. A., Bucher, E. S., Guillot, T. S., Salahpour, A., . . . Wightman, R. M. (2012). Optimizing the Temporal Resolution of Fast-Scan Cyclic Voltammetry. *ACS Chem Neurosci, 3*(4), 285-292. doi:10.1021/cn200119u

Kim, W. B., & Cho, J. H. (2017). Encoding of Discriminative Fear Memory by Input-Specific LTP in the Amygdala. *Neuron, 95*(5), 1129-1146.e1125. doi:10.1016/j.neuron.2017.08.004

Kintscher, M., Kochubey, O., & Schneggenburger, R. (2023). A striatal circuit balances learned fear in the presence and absence of sensory cues. *eLife, 12*, e75703. doi:10.7554/eLife.75703

Klapoetke, N. C., Murata, Y., Kim, S. S., Pulver, S. R., Birdsey-Benson, A., Cho, Y. K., . . . Boyden, E. S. (2014). Independent optical excitation of distinct neural populations. *Nat Methods, 11*(3), 338-346. doi:10.1038/nmeth.2836

Kröner, S., Rosenkranz, J. A., Grace, A. A., & Barrionuevo, G. (2005). Dopamine Modulates Excitability of Basolateral Amygdala Neurons In Vitro. *Journal of Neurophysiology, 93*(3), 1598-1610. doi:10.1152/jn.00843.2004

Kwon, J. T., Nakajima, R., Kim, H. S., Jeong, Y., Augustine, G. J., & Han, J. H. (2014). Optogenetic activation of presynaptic inputs in lateral amygdala forms associative fear memory. *Learning & memory (Cold Spring Harbor, N.Y.), 21*(11), 627-633. doi:10.1101/lm.035816.114

Lanuza, E., Moncho-Bogani, J., & Ledoux, J. E. (2008). Unconditioned stimulus pathways to the amygdala: effects of lesions of the posterior intralaminar thalamus on foot-shock-induced c-Fos expression in the subdivisions of the lateral amygdala. *Neuroscience, 155*(3), 959-968. doi:10.1016/j.neuroscience.2008.06.028

Lappin, J. M., Reeves, S. J., Mehta, M. A., Egerton, A., Coulson, M., & Grasby, P. M. (2008). Dopamine Release in the Human Striatum: Motor and Cognitive Tasks Revisited. *Journal of Cerebral Blood Flow & Metabolism, 29*(3), 554-564. doi:10.1038/jcbfm.2008.146

Le Merrer, J., Becker, J. A., Befort, K., & Kieffer, B. L. (2009). Reward processing by the opioid system in the brain. *Physiol Rev, 89*(4), 1379-1412. doi:10.1152/physrev.00005.2009

Le Roy, C., Laboureyras, E., Gavello-Baudy, S., Chateauraynaud, J., Laulin, J.-P., & Simonnet, G. (2011). Endogenous Opioids Released During Non-Nociceptive Environmental Stress Induce Latent Pain Sensitization Via a NMDA-Dependent Process. *The journal of pain, 12*(10), 1069-1079. doi:https://doi.org/10.1016/j.jpain.2011.04.011

LeDoux, J. (2003). The Emotional Brain, Fear, and the Amygdala. *Cellular and Molecular Neurobiology, 23*(4-5), 727-738. doi:10.1023/A:1025048802629

LeDoux, J. E. (2014). Coming to terms with fear. *Proc Natl Acad Sci U S A, 111*(8), 2871-2878. doi:10.1073/pnas.1400335111

LeDoux, J. E., Farb, C., & Ruggiero, D. A. (1990). Topographic organization of neurons in the acoustic thalamus that project to the amygdala. *J Neurosci, 10*(4), 1043-1054. doi:10.1523/jneurosci.10-04-01043.1990

Ledoux, J. E., Ruggiero, D. A., Forest, R., Stornetta, R., & Reis, D. J. (1987). Topographic organization of convergent projections to the thalamus from the inferior colliculus and spinal cord in the rat. *J Comp Neurol, 264*(1), 123-146. doi:10.1002/cne.902640110

Lee, J. H., Lee, S., & Kim, J.-H. (2016). Amygdala Circuits for Fear Memory: A Key Role for Dopamine Regulation. *The Neuroscientist, 23*(5), 542-553. doi:10.1177/1073858416679936

Leppla, C. A., Keyes, L. R., Glober, G., Matthews, G. A., Batra, K., Jay, M., . . . Tye, K. M. (2023). Thalamus sends information about arousal but not valence to the amygdala. *Psychopharmacology (Berl), 240*(3), 477-499. doi:10.1007/s00213-022-06284-5

Li, X. F., Phillips, R., & LeDoux, J. E. (1995). NMDA and non-NMDA receptors contribute to synaptic transmission between the medial geniculate body

and the lateral nucleus of the amygdala. *Exp Brain Res, 105*(1), 87-100. doi:10.1007/bf00242185
Lim, S. A., Kang, U. J., & McGehee, D. S. (2014). Striatal cholinergic interneuron regulation and circuit effects. *Front Synaptic Neurosci, 6*, 22. doi:10.3389/fnsyn.2014.00022
Lin, J. Y. (2011). A user's guide to channelrhodopsin variants: features, limitations and future developments. *Exp Physiol, 96*(1), 19-25. doi:10.1113/expphysiol.2009.051961
Lin, J. Y., Lin, M. Z., Steinbach, P., & Tsien, R. Y. (2009). Characterization of engineered channelrhodopsin variants with improved properties and kinetics. *Biophys J, 96*(5), 1803-1814. doi:10.1016/j.bpj.2008.11.034
Linke, R., Braune, G., & Schwegler, H. (2000). Differential projection of the posterior paralaminar thalamic nuclei to the amygdaloid complex in the rat. *Exp Brain Res, 134*(4), 520-532. doi:10.1007/s002210000475
Lisman, J., & Spruston, N. (2005). Postsynaptic depolarization requirements for LTP and LTD: a critique of spike timing-dependent plasticity. *Nat Neurosci, 8*(7), 839-841. doi:10.1038/nn0705-839
Lledo, P. M., Homburger, V., Bockaert, J., & Vincent, J. D. (1992). Differential G protein-mediated coupling of D2 dopamine receptors to K+ and Ca2+ currents in rat anterior pituitary cells. *Neuron, 8*(3), 455-463. doi:https://doi.org/10.1016/0896-6273(92)90273-G
Lorétan, K., Bissière, S., & Lüthi, A. (2004). Dopaminergic modulation of spontaneous inhibitory network activity in the lateral amygdala. *Neuropharmacology, 47*(5), 631-639. doi:10.1016/j.neuropharm.2004.07.015
Love, T. M., Stohler, C. S., & Zubieta, J. K. (2009). Positron emission tomography measures of endogenous opioid neurotransmission and impulsiveness traits in humans. *Arch Gen Psychiatry, 66*(10), 1124-1134. doi:10.1001/archgenpsychiatry.2009.134
Lucas, E. K., Jegarl, A. M., Morishita, H., & Clem, R. L. (2016). Multimodal and Site-Specific Plasticity of Amygdala Parvalbumin Interneurons after Fear Learning. *Neuron, 91*(3), 629-643. doi:10.1016/j.neuron.2016.06.032
Ludwig, M., Apps, D., Menzies, J., Patel, J. C., & Rice, M. E. (2016). Dendritic Release of Neurotransmitters. *Compr Physiol, 7*(1), 235-252. doi:10.1002/cphy.c160007
Lüscher, C., & Malenka, R. C. (2012). NMDA receptor-dependent long-term potentiation and long-term depression (LTP/LTD). *Cold Spring Harb Perspect Biol, 4*(6). doi:10.1101/cshperspect.a005710
Lutz, P. E., & Kieffer, B. L. (2013). Opioid receptors: distinct roles in mood disorders. *Trends Neurosci, 36*(3), 195-206. doi:10.1016/j.tins.2012.11.002
Maltais, S., Côté, S., Drolet, G., & Falardeau, P. (2000). Cellular colocalization of dopamine D1 mRNA and D2 receptor in rat brain using a D2 dopamine receptor specific polyclonal antibody. *Progress in Neuro-Psychopharmacology and Biological Psychiatry, 24*(7), 1127-1149. doi:https://doi.org/10.1016/S0278-5846(00)00125-1
Mansour, A., Fox, C. A., Burke, S., Meng, F., Thompson, R. C., Akil, H., & Watson, S. J. (1994). Mu, delta, and kappa opioid receptor mRNA expression in the rat CNS: An in situ hybridization study. *Journal of*

Comparative Neurology, 350(3), 412-438. doi:https://doi.org/10.1002/cne.903500307
Mansour, A., Meador-Woodruff, J. H., Bunzow, J. R., Civelli, O., Akil, H., & Watson, S. J. (1990). Localization of dopamine D2 receptor mRNA and D1 and D2 receptor binding in the rat brain and pituitary: an in situ hybridization- receptor autoradiographic analysis. *The Journal of Neuroscience, 10*(8), 2587-2600. doi:10.1523/jneurosci.10-08-02587.1990
Maren, S. (1999). Neurotoxic Basolateral Amygdala Lesions Impair Learning and Memory But Not the Performance of Conditional Fear in Rats. *The Journal of Neuroscience, 19*(19), 8696. doi:10.1523/JNEUROSCI.19-19-08696.1999
Maren, S., & Fanselow, M. S. (1996). The amygdala and fear conditioning: has the nut been cracked? *Neuron, 16*(2), 237-240. doi:10.1016/s0896-6273(00)80041-0
Marvizon, J. C., Wang, X., Lao, L. J., & Song, B. (2003). Effect of peptidases on the ability of exogenous and endogenous neurokinins to produce neurokinin 1 receptor internalization in the rat spinal cord. *British journal of pharmacology, 140*(8), 1389-1398. doi:10.1038/sj.bjp.0705578
Massopust, L. C., Hauge, D. H., Ferneding, J. C., Doubek, W. G., & Taylor, J. J. (1985). Projection systems and terminal localization of dorsal column afferents: an autoradiographic and horseradish peroxidase study in the rat. *J Comp Neurol, 237*(4), 533-544. doi:10.1002/cne.902370409
McKernan, M. G., & Shinnick-Gallagher, P. (1997). Fear conditioning induces a lasting potentiation of synaptic currents in vitro. *Nature, 390*(6660), 607-611. doi:10.1038/37605
McNally, G. P. (2009). The roles of endogenous opioids in fear learning. *International Journal of Comparative Psychology, 22*(3), 153-169.
McNally, G. P., & Cole, S. (2006). Opioid receptors in the midbrain periaqueductal gray regulate prediction errors during Pavlovian fear conditioning. *Behavioral Neuroscience, 120*(2), 313-323. doi:10.1037/0735-7044.120.2.313
McNally, G. P., & Westbrook, R. F. (2003). Opioid receptors regulate the extinction of Pavlovian fear conditioning. *Behav Neurosci, 117*(6), 1292-1301. doi:10.1037/0735-7044.117.6.1292
Michalscheck, R. M. L., Leidl, D. M., Westbrook, R. F., & Holmes, N. M. (2021). The Opioid Receptor Antagonist Naloxone Enhances First-Order Fear Conditioning, Second-Order Fear Conditioning and Sensory Preconditioning in Rats. *Front Behav Neurosci, 15*. doi:10.3389/fnbeh.2021.771767
Miguez, G., Laborda, M. A., & Miller, R. R. (2014). Classical conditioning and pain: Conditioned analgesia and hyperalgesia. *Acta Psychologica, 145*, 10-20. doi:https://doi.org/10.1016/j.actpsy.2013.10.009
Mills, F., Lee, C. R., Howe, J. R., Li, H., Shao, S., Keisler, M. N., . . . Tye, K. M. (2022). Amygdalostriatal transition zone neurons encode sustained valence to direct conditioned behaviors. *bioRxiv*, 2022.2010.2028.514263. doi:10.1101/2022.10.28.514263
Mingote, S., Chuhma, N., Kusnoor, S. V., Field, B., Deutch, A. Y., & Rayport, S. (2015). Functional Connectome Analysis of Dopamine Neuron

Glutamatergic Connections in Forebrain Regions. *J Neurosci, 35*(49), 16259-16271. doi:10.1523/jneurosci.1674-15.2015

Mitchell, J. M., O'Neil, J. P., Janabi, M., Marks, S. M., Jagust, W. J., & Fields, H. L. (2012). Alcohol consumption induces endogenous opioid release in the human orbitofrontal cortex and nucleus accumbens. *Sci Transl Med, 4*(116), 116ra116. doi:10.1126/scitranslmed.3002902

Morris, J. S., Frith, C. D., Perrett, D. I., Rowland, D., Young, A. W., Calder, A. J., & Dolan, R. J. (1996). A differential neural response in the human amygdala to fearful and happy facial expressions. *Nature, 383*(6603), 812-815. doi:10.1038/383812a0

Morrow, B. A., Elsworth, J. D., & Roth, R. H. (1996). Tyrosine enhances behavioral and mesocorticolimbic dopaminergic responses to aversive conditioning. *Synapse (New York, N.Y.), 22*(2), 100-105. doi:10.1002/(SICI)1098-2396(199602)22:2<100::AID-SYN2>3.0.CO;2-H

Muller, J. F., Mascagni, F., & McDonald, A. J. (2009). Dopaminergic innervation of pyramidal cells in the rat basolateral amygdala. *Brain Structure and Function, 213*(3), 275-288. doi:10.1007/s00429-008-0196-y

Murata, T., Yoshikawa, M., Watanabe, M., Takahashi, S., Kawaguchi, M., Kobayashi, H., & Suzuki, T. (2014). Potentiation of [Met5]enkephalin-induced antinociception by mixture of three peptidase inhibitors in rat. *Journal of Anesthesia, 28*(5), 708-715. doi:10.1007/s00540-014-1819-5

Nabavi, S., Fox, R., Proulx, C. D., Lin, J. Y., Tsien, R. Y., & Malinow, R. (2014). Engineering a memory with LTD and LTP. *Nature, 511*(7509), 348-352. doi:10.1038/nature13294

Nader, K., & LeDoux, J. (1999). The Dopaminergic Modulation of Fear: Quinpirole Impairs the Recall of Emotional Memories in Rats. *Behavioral Neuroscience, 113*(1), 152-165. doi:10.1037/0735-7044.113.1.152

Nair-Roberts, R. G., Chatelain-Badie, S. D., Benson, E., White-Cooper, H., Bolam, J. P., & Ungless, M. A. (2008). Stereological estimates of dopaminergic, GABAergic and glutamatergic neurons in the ventral tegmental area, substantia nigra and retrorubral field in the rat. *Neuroscience, 152*(4), 1024-1031. doi:10.1016/j.neuroscience.2008.01.046

Nestler, E. J. (2004). Historical review: Molecular and cellular mechanisms of opiate and cocaine addiction. *Trends Pharmacol Sci, 25*(4), 210-218. doi:10.1016/j.tips.2004.02.005

Nieoullon, A., & Coquerel, A. (2003). Dopamine: a key regulator to adapt action, emotion, motivation and cognition. *Current opinion in neurology, 16 Suppl 2*(2), S3-S9. doi:10.1097/00019052-200312002-00002

Papatheodoropoulos, C., & Kouvaros, S. (2016). High-frequency stimulation-induced synaptic potentiation in dorsal and ventral CA1 hippocampal synapses: the involvement of NMDA receptors, mGluR5, and (L-type) voltage-gated calcium channels. *Learning & memory (Cold Spring Harbor, N.Y.), 23*(9), 460-464. doi:10.1101/lm.042531.116

Paré, D., Royer, S., Smith, Y., & Lang, E. J. (2003). Contextual inhibitory gating of impulse traffic in the intra-amygdaloid network. *Ann N Y Acad Sci, 985*, 78-91. doi:10.1111/j.1749-6632.2003.tb07073.x

Pavlov, I. P. (1927). *Conditioned reflexes: an investigation of the physiological activity of the cerebral cortex*. Oxford, England: Oxford Univ. Press.

Pickel, V. M., Joh, T. H., & Reis, D. J. (1975). Ultrastructural localization of tyrosine hydroxylase in noradrenergic neurons of brain. *Proc Natl Acad Sci U S A, 72*(2), 659-663. doi:10.1073/pnas.72.2.659

Pinard, C. R., Muller, J. F., Mascagni, F., & McDonald, A. J. (2008). Dopaminergic innervation of interneurons in the rat basolateral amygdala. *Neuroscience, 157*(4), 850-863. doi:10.1016/j.neuroscience.2008.09.043

Polepalli, J. S., Gooch, H., & Sah, P. (2020). Diversity of interneurons in the lateral and basal amygdala. *npj Science of Learning, 5*(1), 10. doi:10.1038/s41539-020-0071-z

Polepalli, J. S., Sullivan, R. K., Yanagawa, Y., & Sah, P. (2010). A specific class of interneuron mediates inhibitory plasticity in the lateral amygdala. *J Neurosci, 30*(44), 14619-14629. doi:10.1523/jneurosci.3252-10.2010

Poulin, J.-F., Caronia, G., Hofer, C., Cui, Q., Helm, B., Ramakrishnan, C., . . . Awatramani, R. (2018). Mapping projections of molecularly defined dopamine neuron subtypes using intersectional genetic approaches. *Nature Neuroscience, 21*(9), 1260-1271. doi:10.1038/s41593-018-0203-4

Poulin, J.-F., Chevalier, B., Laforest, S., & Drolet, G. (2006). Enkephalinergic afferents of the centromedial amygdala in the rat. *Journal of Comparative Neurology, 496*(6), 859-876. doi:https://doi.org/10.1002/cne.20956

Qian, T., Wang, H., Wang, P., Geng, L., Mei, L., Osakada, T., . . . Li, Y. (2023). A genetically encoded sensor measures temporal oxytocin release from different neuronal compartments. *Nature Biotechnology, 41*(7), 944-957. doi:10.1038/s41587-022-01561-2

Qian, T., Wang, H., Xia, X., & Li, Y. (2023). Current and emerging methods for probing neuropeptide transmission. *Current Opinion in Neurobiology, 81*, 102751. doi:https://doi.org/10.1016/j.conb.2023.102751

Quirk, G. J., Armony, J. L., & LeDoux, J. E. (1997). Fear Conditioning Enhances Different Temporal Components of Tone-Evoked Spike Trains in Auditory Cortex and Lateral Amygdala. *Neuron, 19*(3), 613-624. doi:10.1016/S0896-6273(00)80375-X

Radley, J. J., Farb, C. R., He, Y., Janssen, W. G., Rodrigues, S. M., Johnson, L. R., . . . Morrison, J. H. (2007). Distribution of NMDA and AMPA receptor subunits at thalamo-amygdaloid dendritic spines. *Brain Res, 1134*(1), 87-94. doi:10.1016/j.brainres.2006.11.045

Raeder, F., Merz, C. J., Margraf, J., & Zlomuzica, A. (2020). The association between fear extinction, the ability to accomplish exposure and exposure therapy outcome in specific phobia. *Scientific Reports, 10*(1), 4288. doi:10.1038/s41598-020-61004-3

Rangel-Barajas, C., Boehm, S. L., 2nd, & Logrip, M. L. (2021). Altered excitatory transmission in striatal neurons after chronic ethanol consumption in selectively bred crossed high alcohol-preferring mice.

Neuropharmacology, 190, 108564. doi:10.1016/j.neuropharm.2021.108564
Rappleye, M., Gordon-Fennel, A., Castro, D. C., Matarasso, A. K., Zamorano, C. A., Stine, C., . . . Berndt, A. (2022). Opto-MASS: a high-throughput engineering platform for genetically encoded fluorescent sensors enabling all-optical in vivo detection of monoamines and opioids. *bioRxiv*, 2022.2006.2001.494241. doi:10.1101/2022.06.01.494241
Rescorla, R. A. (1973). Effects of US habituation following conditioning. *Journal of comparative and physiological psychology, 82*(1), 137.
Ressler, R. L., & Maren, S. (2019). Synaptic encoding of fear memories in the amygdala. *Curr Opin Neurobiol, 54*, 54-59. doi:10.1016/j.conb.2018.08.012
Rich, M. T., Huang, Y. H., & Torregrossa, M. M. (2019). Plasticity at Thalamo-amygdala Synapses Regulates Cocaine-Cue Memory Formation and Extinction. *Cell Reports, 26*(4), 1010-1020.e1015. doi:https://doi.org/10.1016/j.celrep.2018.12.105
Riley, B., Gould, E., Lloyd, J., Hallum, L. E., Vlajkovic, S., Todd, K., & Freestone, P. S. (2024). Dopamine transmission in the tail striatum: Regional variation and contribution of dopamine clearance mechanisms. *Journal of Neurochemistry, 168*(3), 251-268. doi:https://doi.org/10.1111/jnc.16052
Robinson, D. L., Hermans, A., Seipel, A. T., & Wightman, R. M. (2008). Monitoring rapid chemical communication in the brain. *Chem Rev, 108*(7), 2554-2584. doi:10.1021/cr068081q
Rogan, M. T., Stäubli, U. V., & LeDoux, J. E. (1997). AMPA receptor facilitation accelerates fear learning without altering the level of conditioned fear acquired. *J Neurosci, 17*(15), 5928-5935. doi:10.1523/jneurosci.17-15-05928.1997
Romanski, L. M., Clugnet, M. C., Bordi, F., & LeDoux, J. E. (1993). Somatosensory and auditory convergence in the lateral nucleus of the amygdala. *Behav Neurosci, 107*(3), 444-450. doi:10.1037//0735-7044.107.3.444
Romanski, L. M., & LeDoux, J. E. (1992). Equipotentiality of thalamo-amygdala and thalamo-cortico-amygdala circuits in auditory fear conditioning. *J Neurosci, 12*(11), 4501-4509. doi:10.1523/jneurosci.12-11-04501.1992
Root, D. H., Mejias-Aponte, C. A., Qi, J., & Morales, M. (2014). Role of glutamatergic projections from ventral tegmental area to lateral habenula in aversive conditioning. *J Neurosci, 34*(42), 13906-13910. doi:10.1523/jneurosci.2029-14.2014
Rouiller, E. M., & de Ribaupierre, F. (1985). Origin of afferents to physiologically defined regions of the medial geniculate body of the cat: ventral and dorsal divisions. *Hear Res, 19*(2), 97-114. doi:10.1016/0378-5955(85)90114-5
Rumpel, S., LeDoux, J., Zador, A., & Malinow, R. (2005). Postsynaptic receptor trafficking underlying a form of associative learning. *Science, 308*(5718), 83-88. doi:10.1126/science.1103944
Sah, P., Faber, E. S., Lopez De Armentia, M., & Power, J. (2003). The amygdaloid complex: anatomy and physiology. *Physiol Rev, 83*(3), 803-834. doi:10.1152/physrev.00002.2003

Schafe, G. E., & LeDoux, J. E. (2000). Memory consolidation of auditory pavlovian fear conditioning requires protein synthesis and protein kinase A in the amygdala. *J Neurosci, 20*(18), Rc96. doi:10.1523/JNEUROSCI.20-18-j0003.2000

Schindelin, J., Arganda-Carreras, I., Frise, E., Kaynig, V., Longair, M., Pietzsch, T., . . . Cardona, A. (2012). Fiji: an open-source platform for biological-image analysis. *Nat Methods, 9*(7), 676-682. doi:10.1038/nmeth.2019

Schultz, W. (1998). Predictive reward signal of dopamine neurons. *J Neurophysiol, 80*(1), 1-27. doi:10.1152/jn.1998.80.1.1

Schultz, W. (2016). Dopamine reward prediction error coding. *Dialogues Clin Neurosci, 18*(1), 23-32. doi:10.31887/DCNS.2016.18.1/wschultz

Schultz, W., Apicella, P., & Ljungberg, T. (1993). Responses of monkey dopamine neurons to reward and conditioned stimuli during successive steps of learning a delayed response task. *J Neurosci, 13*(3), 900-913. doi:10.1523/jneurosci.13-03-00900.1993

Schwartz, J.-C. (1983). Metabolism of enkephalins and the inactivating neuropeptidase concept. *Trends in Neurosciences, 6*, 45-48. doi:10.1016/0166-2236(83)90023-1

Scott, S. K., Young, A. W., Calder, A. J., Hellawell, D. J., Aggleton, J. P., & Johnson, M. (1997). Impaired auditory recognition of fear and anger following bilateral amygdala lesions. *Nature, 385*(6613), 254-257. doi:10.1038/385254a0

Sharif, N. A., & Hughes, J. (1989). Discrete mapping of brain mu and delta opioid receptors using selective peptides: Quantitative autoradiography, species differences and comparison with kappa receptors. *Peptides, 10*(3), 499-522. doi:https://doi.org/10.1016/0196-9781(89)90135-6

Shi, C., & Davis, M. (1999). Pain pathways involved in fear conditioning measured with fear-potentiated startle: lesion studies. *J Neurosci, 19*(1), 420-430. doi:10.1523/jneurosci.19-01-00420.1999

Shigeru, T., Xing Lu, J., Kenya, K., Masanobu, Y., Hiroyuki, K., & Tetsuo, O. (2007). The Enhancing Effects of Peptidase Inhibitors on the Antinociceptive Action of [Met5]Enkephalin-Arg6-Phe7 in Rats. *Journal of Pharmacological Sciences, 105*(1), 117-121. doi:10.1254/jphs.FP0070922

Shouval, H. Z., Wang, S. S., & Wittenberg, G. M. (2010). Spike Timing Dependent Plasticity: A Consequence of More Fundamental Learning Rules. *Frontiers in Computational Neuroscience, 4*. doi:10.3389/fncom.2010.00019

Shumyatsky, G. P., Tsvetkov, E., Malleret, G., Vronskaya, S., Hatton, M., Hampton, L., . . . Bolshakov, V. Y. (2002). Identification of a Signaling Network in Lateral Nucleus of Amygdala Important for Inhibiting Memory Specifically Related to Learned Fear. *Cell, 111*(6), 905-918. doi:10.1016/S0092-8674(02)01116-9

Spruston, N. (2008). Pyramidal neurons: dendritic structure and synaptic integration. *Nature Reviews Neuroscience, 9*(3), 206-221. doi:10.1038/nrn2286

Spruston, N., Jaffe, D. B., Williams, S. H., & Johnston, D. (1993). Voltage- and space-clamp errors associated with the measurement of

electrotonically remote synaptic events. *J Neurophysiol, 70*(2), 781-802. doi:10.1152/jn.1993.70.2.781

Sun, F., Zeng, J., Jing, M., Zhou, J., Feng, J., Owen, S. F., . . . Li, Y. (2018). A Genetically Encoded Fluorescent Sensor Enables Rapid and Specific Detection of Dopamine in Flies, Fish, and Mice. *Cell, 174*(2), 481-496.e419. doi:10.1016/j.cell.2018.06.042

Sun, Y., Gooch, H., & Sah, P. (2020). Fear conditioning and the basolateral amygdala. *F1000Res, 9*. doi:10.12688/f1000research.21201.1

Tang, W., Kochubey, O., Kintscher, M., & Schneggenburger, R. (2020). A VTA to Basal Amygdala Dopamine Projection Contributes to Signal Salient Somatosensory Events during Fear Learning. *J Neurosci, 40*(20), 3969-3980. doi:10.1523/jneurosci.1796-19.2020

Taylor, J. A., Hasegawa, M., Benoit, C. M., Freire, J. A., Theodore, M., Ganea, D. A., . . . Gründemann, J. (2021). Single cell plasticity and population coding stability in auditory thalamus upon associative learning. *Nature Communications, 12*(1), 2438. doi:10.1038/s41467-021-22421-8

Taylor, S. R., Badurek, S., Dileone, R. J., Nashmi, R., Minichiello, L., & Picciotto, M. R. (2014). GABAergic and glutamatergic efferents of the mouse ventral tegmental area. *J Comp Neurol, 522*(14), 3308-3334. doi:10.1002/cne.23603

Terman, G. W., Wagner, J. J., & Chavkin, C. (1994). Kappa opioids inhibit induction of long-term potentiation in the dentate gyrus of the guinea pig hippocampus. *J Neurosci, 14*(8), 4740-4747. doi:10.1523/jneurosci.14-08-04740.1994

Thompson, S. J., Pitcher, M. H., Stone, L. S., Tarum, F., Niu, G., Chen, X., . . . Bushnell, M. C. (2018). Chronic neuropathic pain reduces opioid receptor availability with associated anhedonia in rat. *Pain, 159*(9), 1856-1866. doi:10.1097/j.pain.0000000000001282

Tully, K., Li, Y., Tsvetkov, E., & Bolshakov, V. Y. (2007). Norepinephrine enables the induction of associative long-term potentiation at thalamo-amygdala synapses. *Proceedings of the National Academy of Sciences, 104*(35), 14146-14150. doi:doi:10.1073/pnas.0704621104

Uwano, T., Nishijo, H., Ono, T., & Tamura, R. (1995). Neuronal responsiveness to various sensory stimuli, and associative learning in the rat amygdala. *Neuroscience, 68*(2), 339-361. doi:10.1016/0306-4522(95)00125-3

Valverde, O., Fournié-Zaluski, M.-C., Roques, B. P., & Maldonado, R. (1996). Similar involvement of several brain areas in the antinociception of endogenous and exogenous opioids. *European Journal of Pharmacology, 312*(1), 15-25. doi:https://doi.org/10.1016/0014-2999(96)00437-2

Vaughan, C. W., Ingram, S. L., Connor, M. A., & Christie, M. J. (1997). How opioids inhibit GABA-mediated neurotransmission. *Nature, 390*(6660), 611-614. doi:10.1038/37610

Waksman, G., Hamel, E., Delay-Goyet, P., & Roques, B. P. (1986). Neuronal localization of the neutral endopeptidase 'enkephalinase' in rat brain revealed by lesions and autoradiography. *Embo j, 5*(12), 3163-3166. doi:10.1002/j.1460-2075.1986.tb04624.x

Wang, C., Kang-Park, M. H., Wilson, W. A., & Moore, S. D. (2002). Properties of the pathways from the lateral amygdal nucleus to basolateral nucleus

and amygdalostriatal transition area. *J Neurophysiol, 87*(5), 2593-2601. doi:10.1152/jn.2002.87.5.2593

Wang, Y., Krabbe, S., Eddison, M., Henry, F. E., Fleishman, G., Lemire, A. L., . . . Sternson, S. M. (2023). Multimodal mapping of cell types and projections in the central nucleus of the amygdala. *eLife, 12*, e84262. doi:10.7554/eLife.84262

Weeber, E. J., Atkins, C. M., Selcher, J. C., Varga, A. W., Mirnikjoo, B., Paylor, R., . . . Sweatt, J. D. (2000). A role for the beta isoform of protein kinase C in fear conditioning. *J Neurosci, 20*(16), 5906-5914. doi:10.1523/jneurosci.20-16-05906.2000

Weinberger, N. M. (2011). The medial geniculate, not the amygdala, as the root of auditory fear conditioning. *Hearing research, 274*(1-2), 61-74. doi:10.1016/j.heares.2010.03.093

Weisskopf, M. G., Bauer, E. P., & LeDoux, J. E. (1999). L-Type Voltage-Gated Calcium Channels Mediate NMDA-Independent Associative Long-Term Potentiation at Thalamic Input Synapses to the Amygdala. *The Journal of Neuroscience, 19*(23), 10512-10519. doi:10.1523/jneurosci.19-23-10512.1999

Weisskopf, M. G., Zalutsky, R. A., & Nicoll, R. A. (1993). The opioid peptide dynorphin mediates heterosynaptic depression of hippocampal mossy fibre synapses and modulates long-term potentiation. *Nature, 362*(6419), 423-427. doi:10.1038/362423a0

Westbrook, R. F., Greeley, J. D., Nabke, C. P., & Swinbourne, A. L. (1991). Aversive conditioning in the rat: effects of a benzodiazepine and of an opioid agonist and antagonist on conditioned hypoalgesia and fear. *J Exp Psychol Anim Behav Process, 17*(3), 219-230. doi:10.1037//0097-7403.17.3.219

Williams, J. T., Christie, M. J., & Manzoni, O. (2001). Cellular and Synaptic Adaptations Mediating Opioid Dependence. *Physiological Reviews, 81*(1), 299-343. doi:10.1152/physrev.2001.81.1.299

Winters, B. L., Gregoriou, G. C., Kissiwaa, S. A., Wells, O. A., Medagoda, D. I., Hermes, S. M., . . . Bagley, E. E. (2017). Endogenous opioids regulate moment-to-moment neuronal communication and excitability. *Nature Communications, 8*(1), 14611. doi:10.1038/ncomms14611

Woodson, W., Farb, C. R., & Ledoux, J. E. (2000). Afferents from the auditory thalamus synapse on inhibitory interneurons in the lateral nucleus of the amygdala. *Synapse, 38*(2), 124-137. doi:10.1002/1098-2396(200011)38:2<124::Aid-syn3>3.0.Co;2-n

Yau, J. O.-Y., Chaichim, C., Power, J. M., & McNally, G. P. (2021). The Roles of Basolateral Amygdala Parvalbumin Neurons in Fear Learning. *The Journal of Neuroscience, 41*(44), 9223. doi:10.1523/JNEUROSCI.2461-20.2021

Yau, J. O., Chaichim, C., Power, J. M., & McNally, G. P. (2021). The Roles of Basolateral Amygdala Parvalbumin Neurons in Fear Learning. *J Neurosci, 41*(44), 9223-9234. doi:10.1523/jneurosci.2461-20.2021

Yu, K., Ahrens, S., Zhang, X., Schiff, H., Ramakrishnan, C., Fenno, L., . . . Li, B. (2017). The central amygdala controls learning in the lateral amygdala. *Nat Neurosci, 20*(12), 1680-1685. doi:10.1038/s41593-017-0009-9

Zhang, J., & McDonald, A. J. (2016). Light and electron microscopic analysis of enkephalin-like immunoreactivity in the basolateral amygdala, including evidence for convergence of enkephalin-containing axon terminals and norepinephrine transporter-containing axon terminals onto common targets. *Brain research, 1636*, 62-73. doi:https://doi.org/10.1016/j.brainres.2016.01.045

Zhang, J., Muller, J. F., & McDonald, A. J. (2015). Mu opioid receptor localization in the basolateral amygdala: An ultrastructural analysis. *Neuroscience, 303*, 352-363. doi:10.1016/j.neuroscience.2015.07.002

Zhou, F. M., Wilson, C. J., & Dani, J. A. (2002). Cholinergic interneuron characteristics and nicotinic properties in the striatum. *J Neurobiol, 53*(4), 590-605. doi:10.1002/neu.10150